DTIC/TR-98-1 AD-A338212

The DTIC Review

HYBRID & ELECTRIC VEHICLES

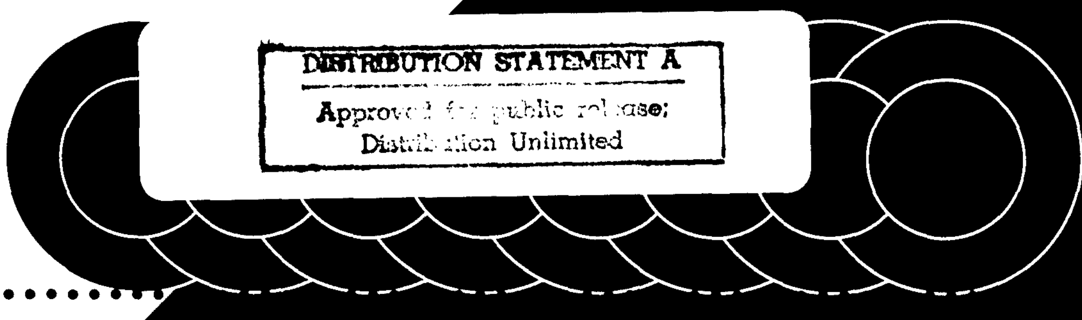

Vol. 4, No. 1
June 1998

REPORT DOCUMENTATION PAGE

Form Approved
OMB No. 074-0188

1. AGENCY USE ONLY (Leave blank)	2. REPORT DATE	3. REPORT TYPE AND DATES COVERED
	June 1998	Final

4. TITLE AND SUBTITLE
The DTIC Review
Hybrid and Electric Vehicles
Volume 4 No. 1

5. FUNDING NUMBERS

6. AUTHOR(S)

Christian M. Cupp, Editor
Phyllis Levine, Compiler

7. PERFORMING ORGANIZATION NAME(S) AND ADDRESS(ES)

Defense Technical Information Center
DTIC -BRR, Suite 0944
8725 John J. Kingman Rd
Ft. Belvoir, VA 22060-6218

8. PERFORMING ORGANIZATION REPORT NUMBER
DTIC/TR-98/1

9. SPONSORING / MONITORING AGENCY NAME(S) AND ADDRESS(ES)

Defense Technical Information Center
DTIC -BRR, Suite 0944
8725 John J. Kingman Rd
Ft. Belvoir, VA 22060-6218

10. SPONSORING / MONITORING AGENCY REPORT NUMBER

11. SUPPLEMENTARY NOTES
This publication is published irregularly by the Defense Technical Information Center

12a. DISTRIBUTION / AVAILABILITY STATEMENT
A - Approved for public release; distribution unlimited.

12b. DISTRIBUTION CODE
Statement A

13. ABSTRACT ***(Maximum 200 Words)***
"Hybrid" vehicles combine the best of gasoline, electricity and energy storage systems. Government and industry research and development programs are working on the multimillion dollar program to develop a fleet of experimental hybrid vehicles. The DARPA Electric and Hybrid Vehicle Technology program is pursuing research, development and demonstrations of technologies for electric and hybrid vehicles that address military missions, modernization and cost mitigation.

The hybrid technology is equally important to both military and industry. Environmental regulations motivate both to find alternatives to the traditional vehicle. In an effort to comply with these strict regulations research efforts focus on building engines with high efficiency and low exhaust emission. In addition to improving air quality, it is also desirable to build inexpensive, reliable, long lasting, and compact vehicles. Formidable technological barriers exist however, to achieving performance cost and reliability.

14. SUBJECT TERMS
HEV (Hybrid Electric Vehicle), Hybrid vehicles, Auxiliary Power Units
Units, Hybrid Electric Vehicles Electric Vehicles

15. NUMBER OF PAGES

16. PRICE CODE

17. SECURITY CLASSIFICATION OF REPORT	18. SECURITY CLASSIFICATION OF THIS PAGE	19. SECURITY CLASSIFICATION OF ABSTRACT	20. LIMITATION OF ABSTRACT
UNCLASSIFIED	UNCLASSIFIED	UNCLASSIFIED	UL

The DTIC Review

Hybrid and Electric Vehicles

AD-A338212

Vol. 4, No. 1
June 1998

FOREWORD

Electric and hybrid electric drivetrains provide compelling advantages for future tactical and combat vehicles. Electric and hybrid vehicle research and development is focused on higher efficiency, improved acceleration and maneuverability and reduced thermal and acoustic signatures.

This edition of *The DTIC Review* features an overview of technology development in the area of electric and hybrid vehicles. The technologies are being demonstrated in both commercial and military models.

The editorial staff hope you find this effort of value and appreciate you comments.

Kurt N. Molholm
Administrator

TABLE OF CONTENTS

INTRODUCTION

"Hybrid" vehicles combine the best of gasoline, electricity and energy storage systems. Government and industry research and development programs are working on this multimillion dollar program to develop a fleet of experimental hybrid vehicles. The DARPA Electric and Hybrid Vehicle Technology program is pursuing research, development and demonstrations of technologies for electric and hybrid vehicles that address military missions, modernization and cost mitigation.

DARPA works with seven regional consortia. Consortium participants include military laboratories, bases, state and local governments large and small defense contractors, well-established and startup manufacturers of vehicles and components, electric and gas utilities, public interest groups and universities.

For the military, the hybrid electric vehicle would be used for administrative-tactical wheeled vehicle or combat tracked vehicle applications. Performance, fuel efficiency, low-heat, low noise are critical objectives in the military combat environment and high demand situations.

The hybrid technology is equally important to both military and industry. Environmental regulations motivate both to find alternatives to the traditional vehicle. In an effort to comply with these strict regulations, research efforts focus on building engines with high efficiency and low exhaust emission. In addition to improving air quality, it is also desirable to build inexpensive, reliable, long lasting, and compact vehicles. Formidable technological barriers exist however, to achieving performance cost and reliability.

This issue of the DTIC Review addresses the use and production of hybrid/electronic vehicle technology and prototype demonstrations essential for the future military and commercial systems. Hybrid vehicle development, whether it is batteries, flywheels, fuel cells, or other electric concepts and systems are most deserving of further study and investigation.

The selected documents and bibliography are a representation of the information available on hybrid electronic vehicles from DTIC's extensive collection this topic. Additional references, including electronic resources, can be found at the end of the volume. In-depth literature searches may be requested by contacting the Reference and Retrieval Services Branch at the Defense Technical Information Center:
(703) 767-8274/DSN 427-8274; FAX (703) 767-9070; E-mail bibs@dtic.mil

DOCUMENT 1

Development of a Natural Gas-Powered APU for a Hybrid Electric S-10 Pickup Truck

AD-A333298

December 1997

TACOM Research Development and Engineering Center
Warren, MI

AD A333298

DEVELOPMENT OF A NATURAL GAS-POWERED APU FOR A HYBRID ELECTRIC S-10 PICKUP TRUCK

FINAL INTERIM REPORT
TFLRF No. 315

By
Daniel J. Podnar
William K. Capshaw
U.S. Army TARDEC Fuels and Lubricants Research Facility (SwRI)
Southwest Research Institute
San Antonio, Texas

prepared for

Defense Advanced Research Projects Agency
3701 N. Fairfax Drive
Arlington, Virginia 22203-1714

Under Contract to
U.S. Army TARDEC
Petroleum and Water Business Area
Warren, Michigan 58397

Contract No. DAAK70-92-C-0059

Approved for public release; distribution unlimited

December 1997

Disclaimers

DTIC Availability Notice

Disposition Instructions

REPORT DOCUMENTATION PAGE

Form Approved
OMB No. 0704-0188

1. AGENCY USE ONLY (Leave blank)

2. REPORT DATE
October 1997

3. REPORT TYPE AND DATES COVERED
Interim
May 1994-April 1995

4. TITLE AND SUBTITLE
Development of a Natural Gas-Powered APU for a Hybrid Electric S-10 Pickup Truck

5. FUNDING NUMBERS
DAAK70-92-C-0059; WD 22

6. AUTHOR(S)
Podnar, Daniel J. And Capshaw, William K.

7. PERFORMING ORGANIZATION NAME(S) AND ADDRESS(ES)
U.S. Army TARDEC Fuels and Lubricants Research Facility (SwRI)
Southwest Research Institute
P.O. Drawer 28510
San Antonio, Texas 78228-0510

8. PERFORMING ORGANIZATION REPORT NUMBER
TFLRF No. 315

9. SPONSORING/MONITORING AGENCY NAME(S) AND ADDRESS(ES)
U. S. Army TARDEC
Petroleum and Water Business Area
Warren, Michigan 58397-5000

10. SPONSORING/MONITORING AGENCY REPORT NUMBER

11. SUPPLEMENTARY NOTES

12a. DISTRIBUTION/AVAILABILITY STATEMENT
Approved for public release; distribution unlimited

12b. DISTRIBUTION CODE

13. ABSTRACT (Maximum 200 words)
A natural gas-fueled Auxiliary Power Unit (APU) was developed for use in a hybrid electric vehicle. The project involved conversion and development of the powerplant from gasoline to natural gas operation, application of an engine control system, application of a three-way catalyst system, development of an APU controller, and integration and testing of the APU in the laboratory and vehicle environment. The project was divided into three phases: (1) engine development, (2) APU control system development, and (3) APU integration/testing. The resultant APU was integrated into a hybrid electric utility truck for use as a range extender in a series hybrid configuration. The project resulted in an APU configuration producing ultra-low emissions levels while achieving high efficiency due to implementation of a unique APU operating strategy.

14. SUBJECT TERMS

hybrid electric vehicle	auxiliary power unit	compressed natural gas
natural gas engine	electronic engine control	electronic APU control

15. NUMBER OF PAGES
79

16. PRICE CODE

17. SECURITY CLASSIFICATION OF REPORT	18. SECURITY CLASSIFICATION OF THIS PAGE	19. SECURITY CLASSIFICATION OF ABSTRACT	20. LIMITATION OF ABSTRACT
Unclassified	Unclassified	Unclassified	

EXECUTIVE SUMMARY

The purpose of this project was to develop a natural gas-fueled Auxiliary Power Unit (APU) for use in a hybrid electric vehicle. The project involved conversion and development of the natural gas engine, application of an engine control system, application of a three-way catalyst system, development of an APU controller, and integration and testing of the APU in the laboratory and vehicle environment. The project was divided into three phases: (1) engine development, (2) APU control system development, and (3) APU integration/testing.

The first phase involved a multi-step development process aimed at providing a natural gas engine with maximum performance and efficiency while minimizing engine-out exhaust emissions. This work included the application of an electronic control system to provide dedicated fuel and ignition timing control. A closed-loop adaptive fuel control system, utilizing feedback from an Exhaust Gas Oxygen (EGO) sensor in conjunction with a speed-density algorithm was employed. Work also included optimization of spark timing and compression ratio, as well as an intake manifold and fuel system design to insure that a uniform homogeneous air-fuel mixture was distributed to both cylinders. A three-way exhaust catalyst was applied to the engine in order to dramatically reduce exhaust emissions. The catalyst used was effective in simultaneously removing in excess of 95 percent of total hydrocarbons (THC), over 98 percent of carbon monoxide (CO), and roughly 99 percent of oxides of nitrogen (NO_x) over the APU operating conditions. The final package delivered is a state-of-the-art low emissions natural gas APU power plant.

The second phase of the project involved design, development, and application of a prototype APU control system which provided the energy management and battery charging profile for the vehicle. The APU controller was based on a personal computer (PC) platform and provided control of the engine operating conditions via engine throttle and generator control, battery state of charge calculation, closed loop battery charging current control, and control of the engine start and stop functions. The controller was also capable of controlling an electrically-heated catalyst (EHC) system which was investigated during the project.

The third phase of the project concentrated on integration and testing of the APU system in both the laboratory environment as well as on the actual vehicle. Stand-alone APU testing was accomplished in the laboratory through the use of a battery pack and resistive load bank to simulate the load of the vehicle traction motor. The APU was also installed in the S-10 vehicle and stand-alone tested using a battery pack.

TABLE OF CONTENTS

Section **Page**

LIST OF ILLUSTRATIONS

LIST OF ILLUSTRATIONS (Cont'd)

1.0 BACKGROUND

1.1 Objective

The technical objective of this work was to develop, integrate, and test a natural gas-powered auxiliary power unit (APU) for a hybrid electric vehicle application. The specific technical objectives for the APU were to achieve very low emissions levels, high efficiency, and allow extended vehicle range over an electric vehicle. Vehicle emissions below CARB ULEV (0.04 g/mile NMOG, 1.7 g/mile CO, 0.2 g/mile NO_x) levels were desired, while engine efficiency and vehicle range were to be maximized. This report describes the engine selection, and development process, as well as the APU and APU controller development, integration, and testing performed.

1.2 Technical Background

Southwest Research Institute (SwRI) has converted many diesel engine models to operate with natural gas in a lean-burn combustion mode. Exhaust emissions have been far lower than their diesel counterparts[(1,2)*]. SwRI has typically developed these engines to produce oxides of nitrogen (NO_x) emissions of less than 2.5 g/hp-hr. While achieving these NO_x levels, non-methane hydrocarbons (NMHC) emissions have been near or less than 1 g/hp-hr while total hydrocarbons (THC) have been in the 4 to 6 g/hp-hr range. These emissions are "engine-out," that is, they do not rely on a catalyst. These lean-burn combustion engines are more efficient than stoichiometric combustion engines but do not lend themselves to the extremely low emissions possible with effective three-way catalyst-equipped engines.

The use of an automotive three-way catalyst can provide exhaust emissions levels far below those of lean-burn combustion engines. However, for a three-way catalyst to operate at peak efficiency, the engine must operate very near stoichiometric equivalence ratios. The methodology of three-way catalyst operation is well documented in the literature for gasoline engines.[(3)] There is also literature documenting the use of three-way catalysts with natural gas fuel.[(4,5)] Natural gas engines with three-way catalysts operate very much like their gasoline counterparts with one notable exception. While gasoline engines must operate about stoichiometric conditions, natural gas engines, (equipped with three-way catalysts), operate at an equivalence ratio slightly rich of stoichiometry in order to generate sufficient carbon monoxide (CO) to allow complete NO_x reduction in the catalyst.[(6)] The window of peak conversion for both NO_x and HC emissions is narrower for natural gas than for gasoline. This requires even greater control of equivalence ratio when using natural gas fuel.

1.3 APU Duty-Cycle

APUs in series hybrid electric vehicles typically operate in a limited and well defined speed and load range. This application required the engine to run between 1500 and 3600 rpm and essentially only at wide open throttle (WOT). This allowed the engine to be finely tuned for peak efficiency and power while maintaining minimum exhaust emissions at these operating points. Furthermore, the APU control strategy chosen was such that the APU would operate in "quasi

* Superscript numbers refer to references listed at the end of this report.

steady-state," i.e., relatively slow changes to engine operating conditions were made, and therefore rapid transients would not be encountered. This would result in even lower emissions levels and potentially increased efficiency.

1.4 Target Hybrid Vehicle

The vehicle for which the APU was developed was a Chevrolet S-10 pickup truck. The conventional drive train was removed from the vehicle and replaced with an electric drive system by Solar Car Corp. (a vehicle converter). The vehicle was equipped with 20 - 12 Volt lead acid batteries for which the APU provided the charging power.

Solar Car Corp. ceased operation in 1996. The vehicle integration, at the time of this report, is being completed by the Florida Solar Energy Center.

2.0 TECHNICAL DISCUSSION

2.1 Engine Development

Development of the engine for the APU included an engine selection process, engine baselining on gasoline, conversion to operation on compressed natural gas (CNG), and performance and emissions testing. As part of the engine development process, engine modeling and simulation was conducted in order to aid in the performance development of the engine. The details of the engine development process are described in this section.

2.1.1 Engine Selection

A set of engine selection criteria were agreed upon by SwRI, DARPA, and the vehicle integrator, Solar Car Corp. It was concluded that the engine must be produced within the United States, produce about 20 kW, and fit within the S-10 pickup electric vehicle space requirements. Due to the limited space requirements and consideration for keeping the engine weight to a minimum, only air-cooled utility engines met the requirements. All of the US manufactured water-cooled engines were too large and heavy for this application. The largest air-cooled utility engine made in the US is the new Kohler Command Series product line. This engine is shown in Figure 1.

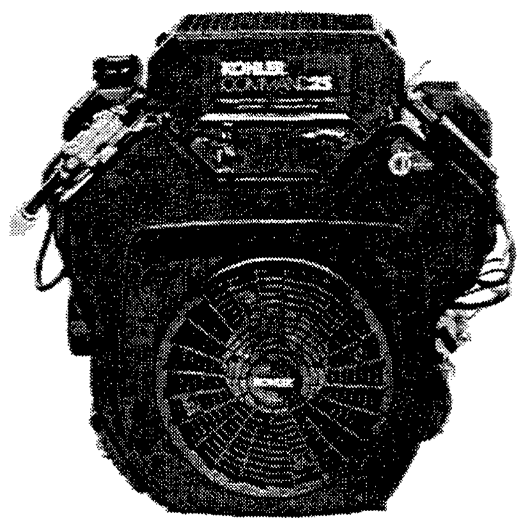

FIGURE 1. STOCK KOHLER CH-25 ENGINE

The largest of the Kohler Command series engines is the CH25 which displaces 44 cubic inches (0.721 liters). The engine is rated at 25 hp (18.6 kW) at 3600 rpm. The Kohler CH22 is slightly smaller at 38 cubic inches (0.625 liters) and rated 22 hp (16.4 kW) at 3600 rpm. The CH22 utilizes a cast iron cylinder liner whereas the CH25, with a larger bore size, does not. In the CH25 engine, the piston operates on the parent aluminum of the block. Both of these engines were performance tested at SwRI on gasoline fuel. The maximum dyno power produced by the engines were very similar. Due to the small differences in power output, it was determined that the CH22 engine with the smaller bore and iron liner would be used in order to maximize engine durability.

2.1.2 Engine Baseline Tests

During the engine baseline tests, two Kohler engines, CH25 and CH22, were operated in their stock configuration at SwRI. The baseline tests resulted in a set of performance data for which the natural gas engine could be compared. The Kohler CH25 and CH22 engines were instrumented to measure relevant parameters such as temperatures, pressures, and fuel flow and were coupled to an eddy current dynamometer, as shown in Figure 2. The engines were operated on gasoline to determine baseline performance, efficiency, cylinder pressure, and emissions data. This mapping provided a basic understanding of power, fuel consumption, volumetric efficiency, emissions, and acoustic noise.

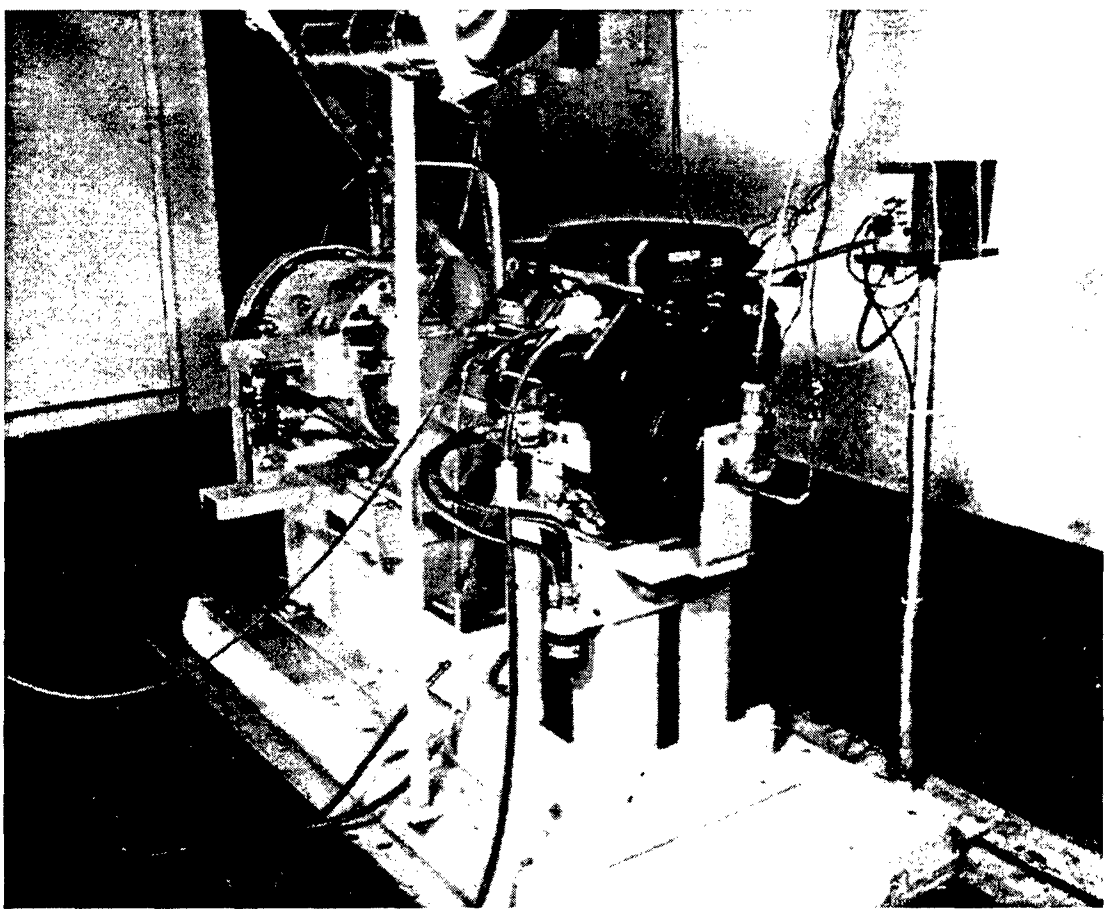

FIGURE 2. CH-22 ENGINE INSTALLED ON TEST STAND

Baseline data for the CH25 and CH22 engines at WOT conditions are shown in Figures 3 and 4, respectively. It should be noted that the WOT torque curves measured at SwRI for each of the baseline engines was less (up to 18 percent less for the CH25, and up to 11 percent less for the CH22) than that advertised by Kohler. This is possibly due to differences in parasitic loads, such as the cooling fan, between the SwRI data and the manufacturer's data.

2.1.3 CNG Conversion

A stock Kohler CH22 engine was converted to operate on compressed natural gas (CNG). The conversion process included numerous engine modifications as well as engine control system modifications. The details of the conversion process are described in the following paragraphs.

2.1.3.1 Engine Control System Application

As part of the CNG conversion process, the stock gasoline carburetor and ignition system were replaced with an electronic control system obtained from Mesa Environmental. This system, referred to as GEM (Gas Engine Management), allowed the engine to be operated near stoichiometric air-fuel ratios with complete control of ignition timing. A speed/density calculation was utilized for open-loop fueling calculations, with a closed-loop adaptive learn algorithm based on information from an exhaust gas oxygen (EGO) sensor to allow very accurate control of equivalence ratio around the stoichiometric point. The GEM system utilized a single gasoline-type fuel injector for metering of the CNG to a centralized fuel injection ring located immediately above the throttle body. The fuel injector operated as a critical flow orifice utilizing the opening time, (or injector pulse width), as the means of modulating the metered fuel flow rate. In order to compensate for fuel density changes upstream of the injector, natural gas pressure and temperature measurements were also incorporated into the fuel metering block of the GEM system.

In addition to fuel control, the GEM system also provided control of the spark ignition timing and ignition coil dwell functions. This was provided through a distributorless ignition system which utilized ignition coil driver circuits integrated into the GEM unit, along with production Ford ignition coils. Thus, the spark timing and coil dwell time could be accurately controlled to any value desired.

2.1.3.2 Intake Modifications

The stock intake system for the Kohler CH22 and CH25 engines is a compact design incorporating minimal length from the air cleaner, through the carburetor, throttle body, and intake manifold. Since increasing the maximum power output of the engine was of primary concern, engine simulation and experimental evaluations were conducted to investigate the sensitivity of engine power output to the intake system length. As part of this investigation, SwRI's engine cycle simulation, called Virtual Indicated Performance of Reciprocating Engines (VIPRE), was used. Details of the overall simulation study are contained in the Engine Modeling section of this report. The simulation predicted significant power increases could be realized through modification or "tuning" of the intake system length. The results from the simulation are shown in Figure 5. As can be seen from the data, the simulation predicted a large increase in power output when the intake runner length was set at roughly 0.5m. Based on the simulation results, a "snorkel"- type intake

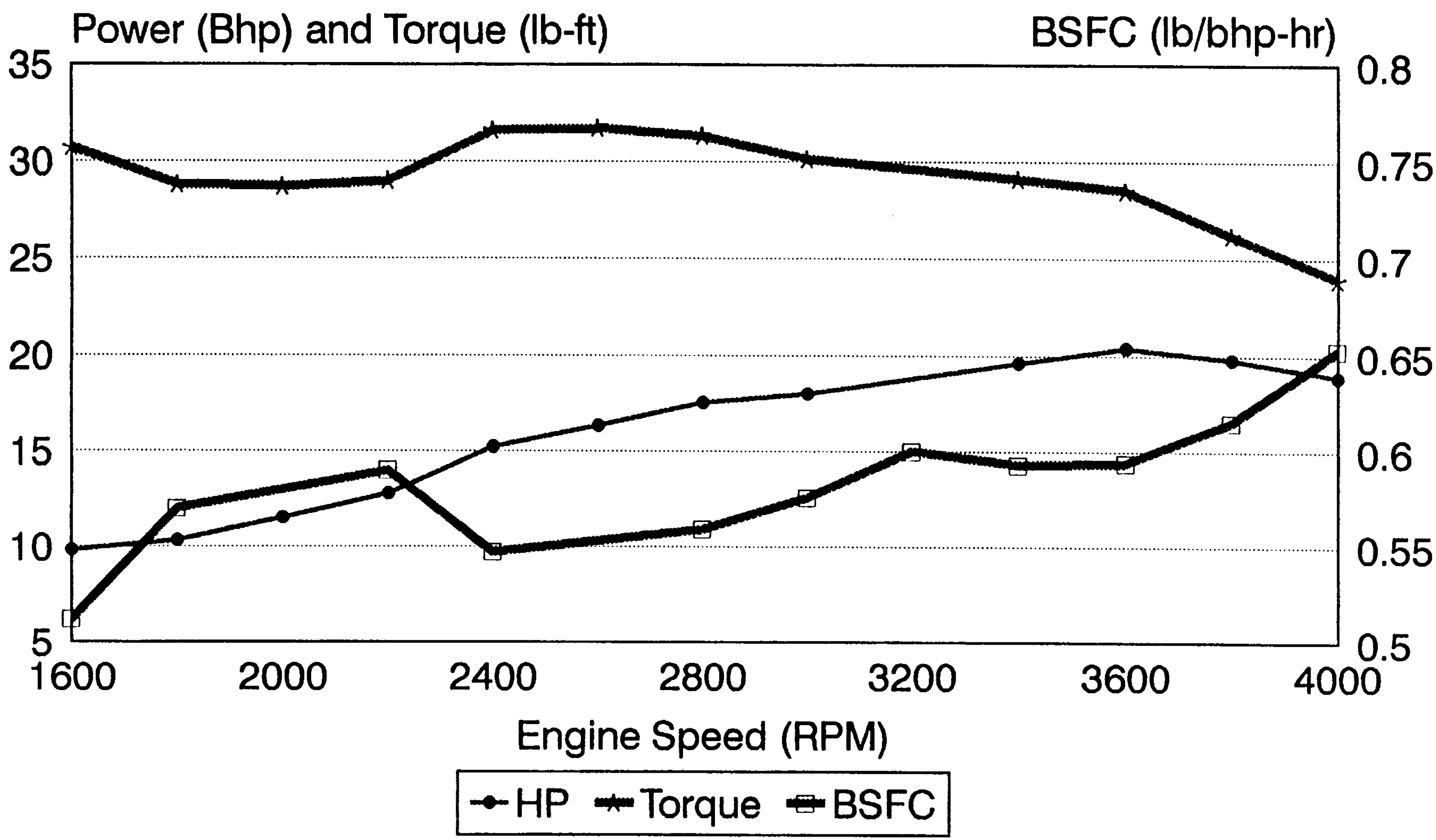

FIGURE 3. BASELINE CH-25 PERFORMANCE

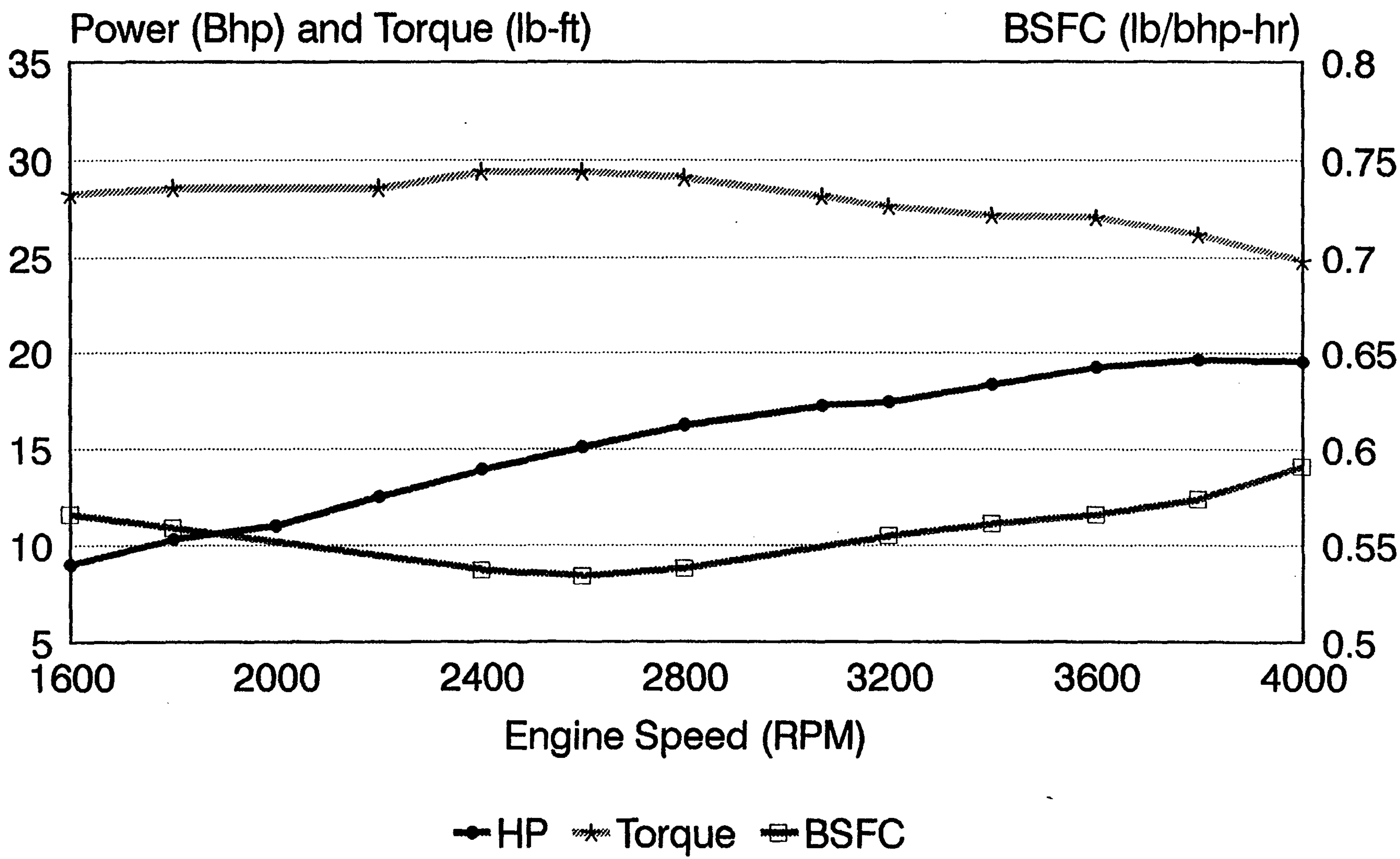

FIGURE 4. BASELINE CH-22 PERFORMANCE

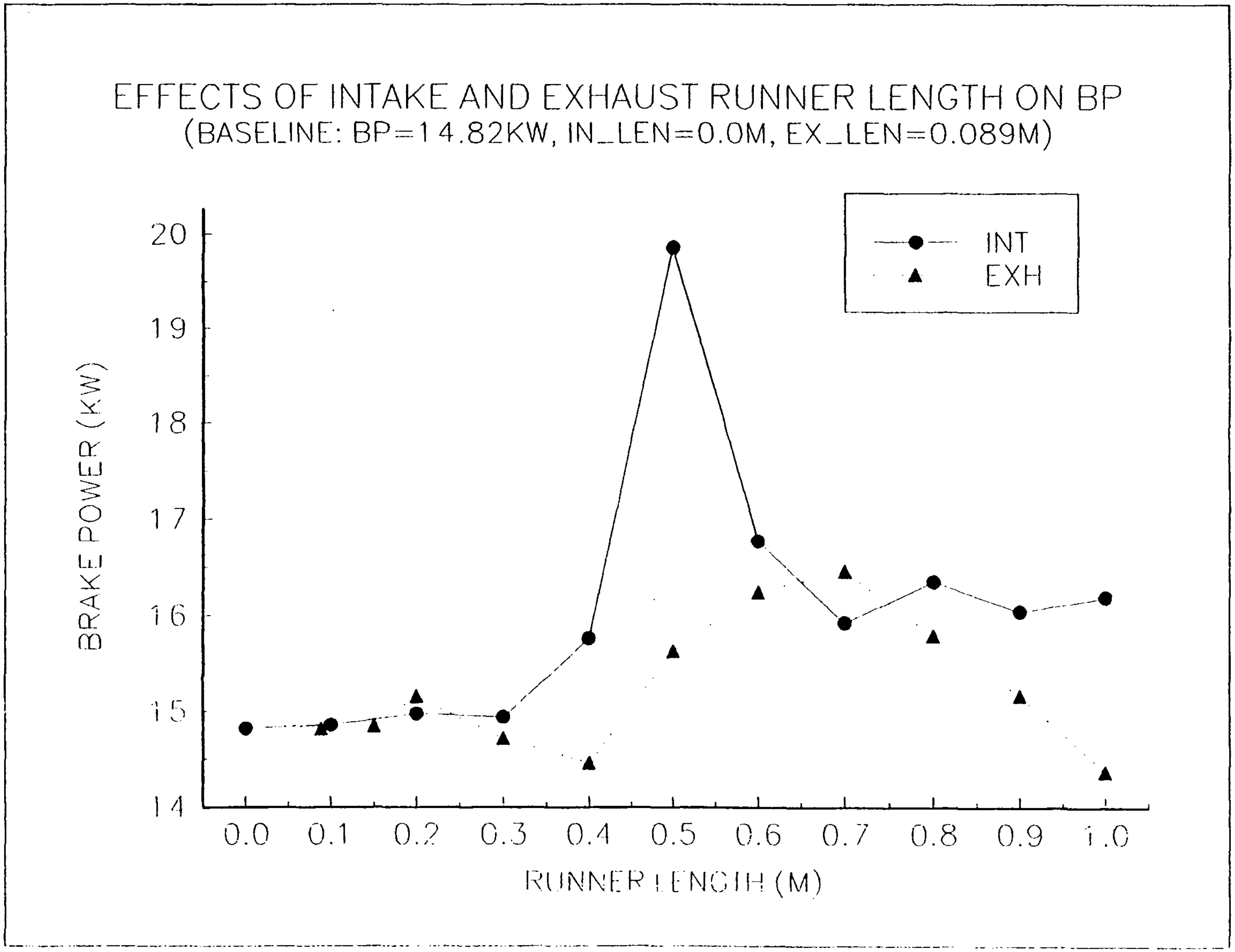

FIGURE 5. SIMULATED EFFECTS OF RUNNER LENGTH ON ENGINE POWER

system was fabricated for the engine. The snorkel attached to the engine throttle body and was made up of a long length of piping, of which the length was adjusted. Experimental data was gathered to quantify the maximum power output from the engine as a function of the intake snorkel length. This data is shown in Figure 6. As can be seen from the data, the significant power increase predicted by the simulation was not achieved in the engine tests. Problems with the simulation were later found and corrected by SwRI as a result of this effort.

2.1.3.3 Fuel Introduction

The key to providing low emissions from a catalyst-equipped natural gas engine is good equivalence ratio control to each cylinder. It is important to operate as close to the optimum equivalence ratio as possible to maintain catalyst efficiency. In order to accomplish this, a homogeneous fuel-air charge must be maintained in each cylinder. In addition, each cylinder should operate at the same fuel-air equivalence ratio. Two basic fuel introduction schemes were tried, central point fuel injection and port fuel injection, with multiple variations on both.

2.1.3.3.1 Central Point Fuel Injection

The first fuel delivery method tried was to admit the fuel from a tubular ring inside of the air filter above the throttle. The ring was made from 1/4 inch copper tubing and contained a series of spray holes around the inside diameter and top of the ring. This is shown in Figure 7. The holes on top of the ring are .042 inches (1.07 mm) in diameter spaced about 1 (25 mm) inch apart. The holes on the inside of the ring are .111 inches (2.82 mm) in diameter.

A second ring was made from 1/4 inch stainless steel tubing and contained 15 holes, each with a diameter of .052 inch (1.32 mm), spaced about 1 inch apart around the top of the ring. This is shown in Figure 8.

Both ring configurations were tested on the engine. The second ring, with larger diameter holes was found to give better performance in terms of the quality of the EGO sensor signal in the exhaust. Improved homogeneity of the charge mixture was found to produce an improved EGO sensor signal (i.e., free of noise or high frequency switching content) during closed-loop engine operation. During the development process, it was later found that the best configuration for the fuel metering ring was to reduce the number of holes by as much as 50 percent. The improvement can likely be attributed to an increase in natural gas flow velocity at the ring holes and thus increased penetration into the intake air stream.

In addition to the fuel admission rings previously described, several other mixing device designs were investigated on the engine. Among the designs tested was a "spray bar," which was simply an open ended piece of 1/4 inch tubing angled into the intake air stream. Also, a "shower head"-type device was fabricated and tested. The shower head fuel mixer consisted of a fitting placed onto the end of the tubing with small holes drilled into the fitting to allow the natural gas to escape into the air stream. Both of these mixer designs proved to be inferior to the spray ring approach, which was finally chosen as the preferred method of fuel-air mixing.

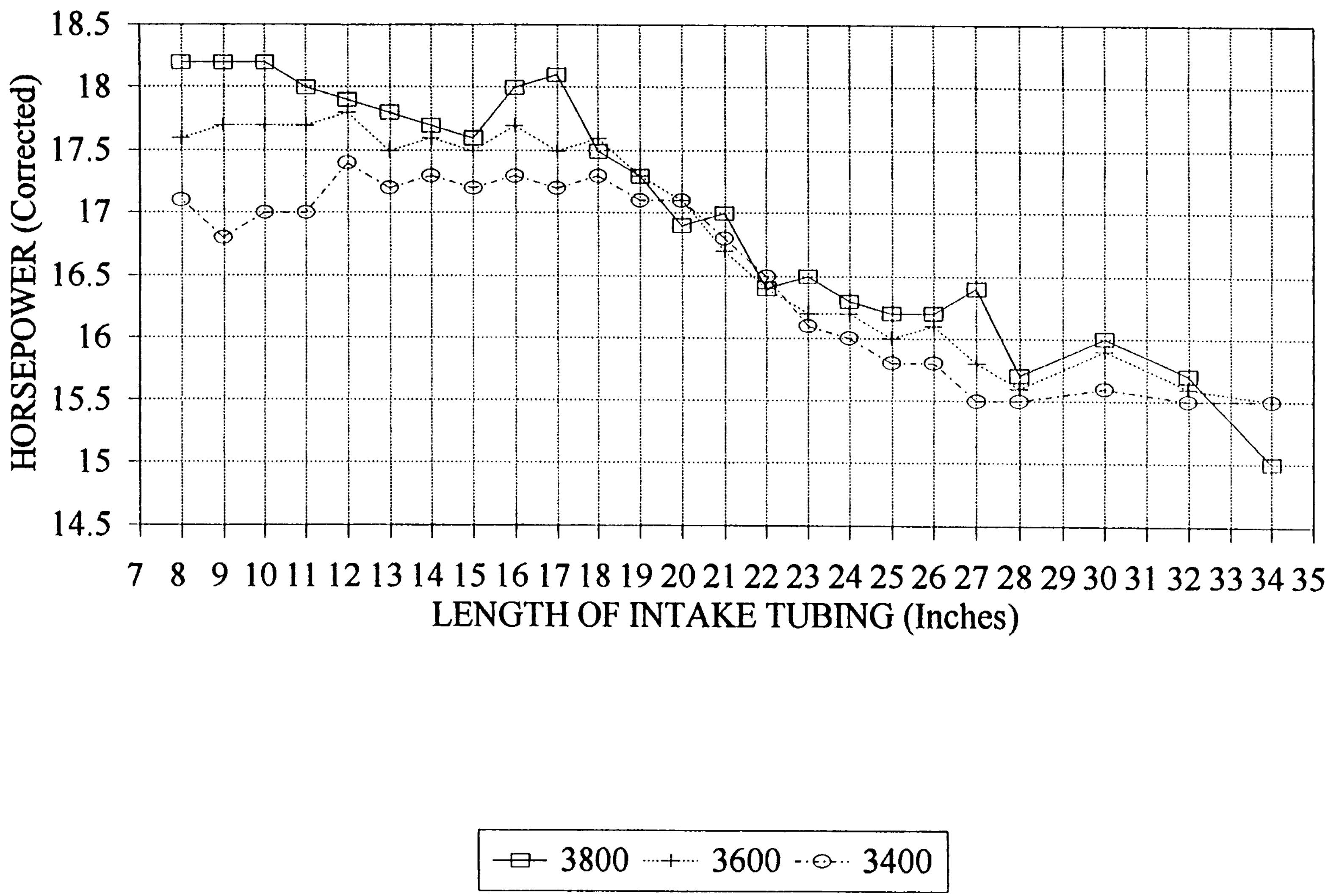

FIGURE 6. HORSEPOWER COMPARISON TREND DUE TO INTAKE LENGTH ADJUSTMENT

FIGURE 7. COPPER TUBING FUEL SPRAY RING

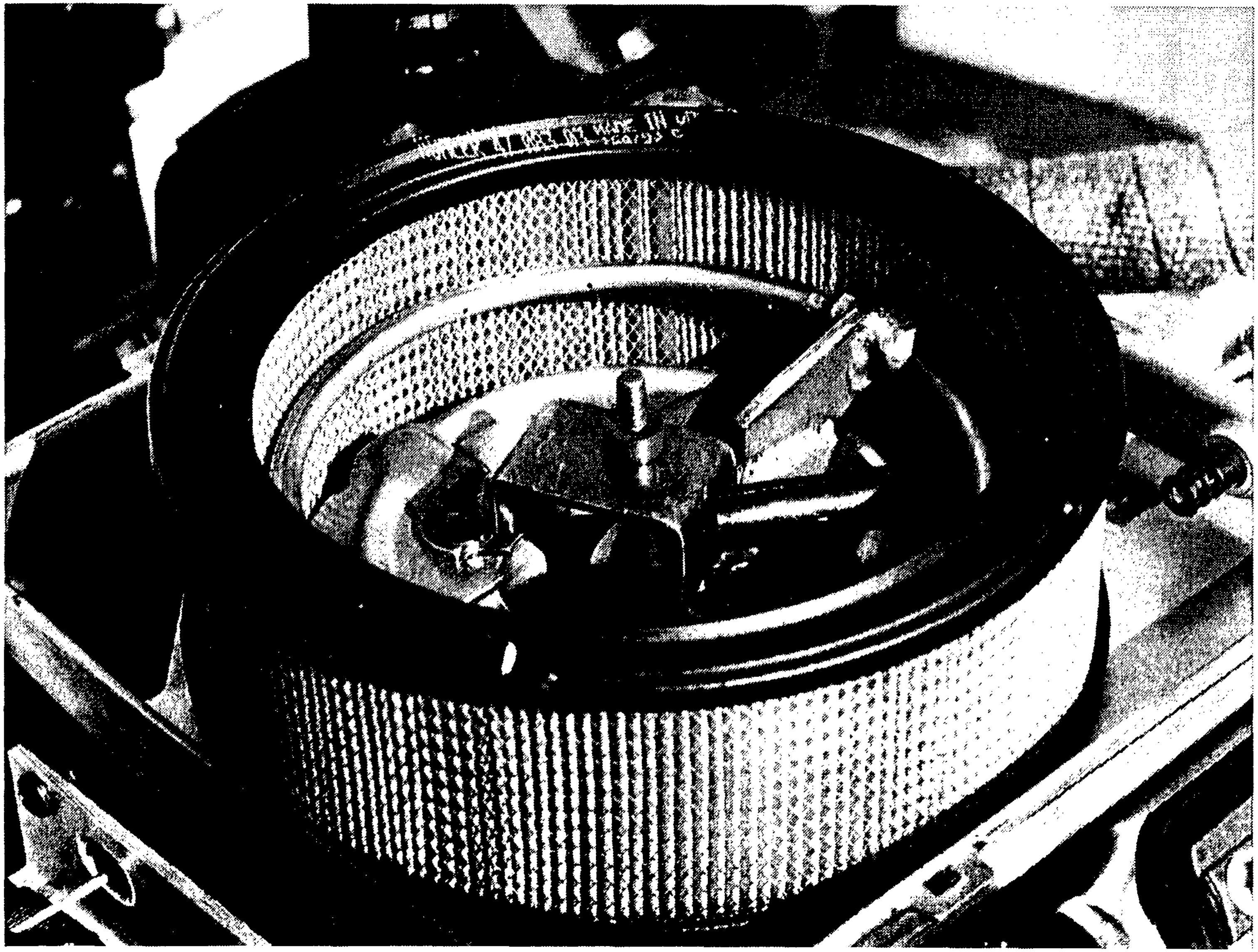

FIGURE 8. UPGRADED STAINLESS STEEL FUEL SPRAY RING

2.1.3.3.2 Port Fuel Injection

With the objective of maximizing the engine's power output, a port injection fueling system was designed, fabricated, and tested on the engine. It was hoped that port fuel injection, when combined with a properly tuned intake system, would allow higher power levels to be achieved. The port injection system utilized separate injectors located in the intake manifold (roughly 2 inches away from the respective intake port). Natural gas at roughly 120 psig, from the fuel regulator, was supplied to each injector via individual fuel lines. An illustration of the port injection system installation on the engine is shown in Figure 9.

Results from port fuel injection engine testing are shown in Figure 10. As was previously stated, the objective of the testing was to achieve increased engine power output. As can be seen from the data, this objective was not met. The likely reason for the reduced performance is that there was inadequate mixing of the fuel-air charge in the cylinder. This is a common problem among port-injected natural gas engines. Thus, since the fuel-air charge in the cylinder was non-homogeneous, or stratified, incomplete and inefficient combustion was taking place within the cylinder. Given the objective of the test and the results of the engine testing performed, port injection was not considered to be an adequate approach for the engine. Therefore, central fuel injection, using the fuel mixing ring previously described, was the strategy which was finalized upon.

2.1.3.4 Cylinder Head/Intake Manifold/Throttle Body Modifications

Since maximum power output from the engine was limited only by the amount of airflow which the engine could pump through it, modifications were made in order to reduce flow restrictions on the intake side of the engine. Namely, three major modifications were made to the engine: (1) cylinder head machining or "porting," (2) intake manifold smoothing, and (3) throttle body diameter increases.

The cylinder heads on the Kohler Command 22 engine feature typical die-cast intake and exhaust ports. These ports have runners which intersect at a 90 degree angle (which is preferred for simplicity in the die-casting setup), and the resulting transition area is very abrupt. The zero short side radius of these ports results in a very large recirculation zone which inhibits air flow, particularly at high lifts. Since this engine would be operated with a gaseous fuel which displaces much more volume than the equivalent mass of liquid fuel, port restriction was a major concern. SwRI has vast experience with intake and exhaust port testing, design, and evaluation, and was positioned well to improve on flow performance of the Kohler heads. The intake and exhaust ports were flow tested on the SwRI flow bench to determine baseline performance.

The intake port was modified by adding a small radius to the short side of the port runner. A larger radius would have been even more beneficial, but there was limited room available for modification. It would have also been desirable to fill the transition area on the long side of the port to create a large radius, but this option was not exercised due to time constraints. The simple modification to the short side of the port resulted in approximately 10 percent improvement in flow at medium to high valve lifts as shown in Figure 11. This is a significant flow improvement, particularly if a revised camshaft profile is considered. Figure 11 shows volumetric flowrate in SCFM vs. non-dimensional valve lift.

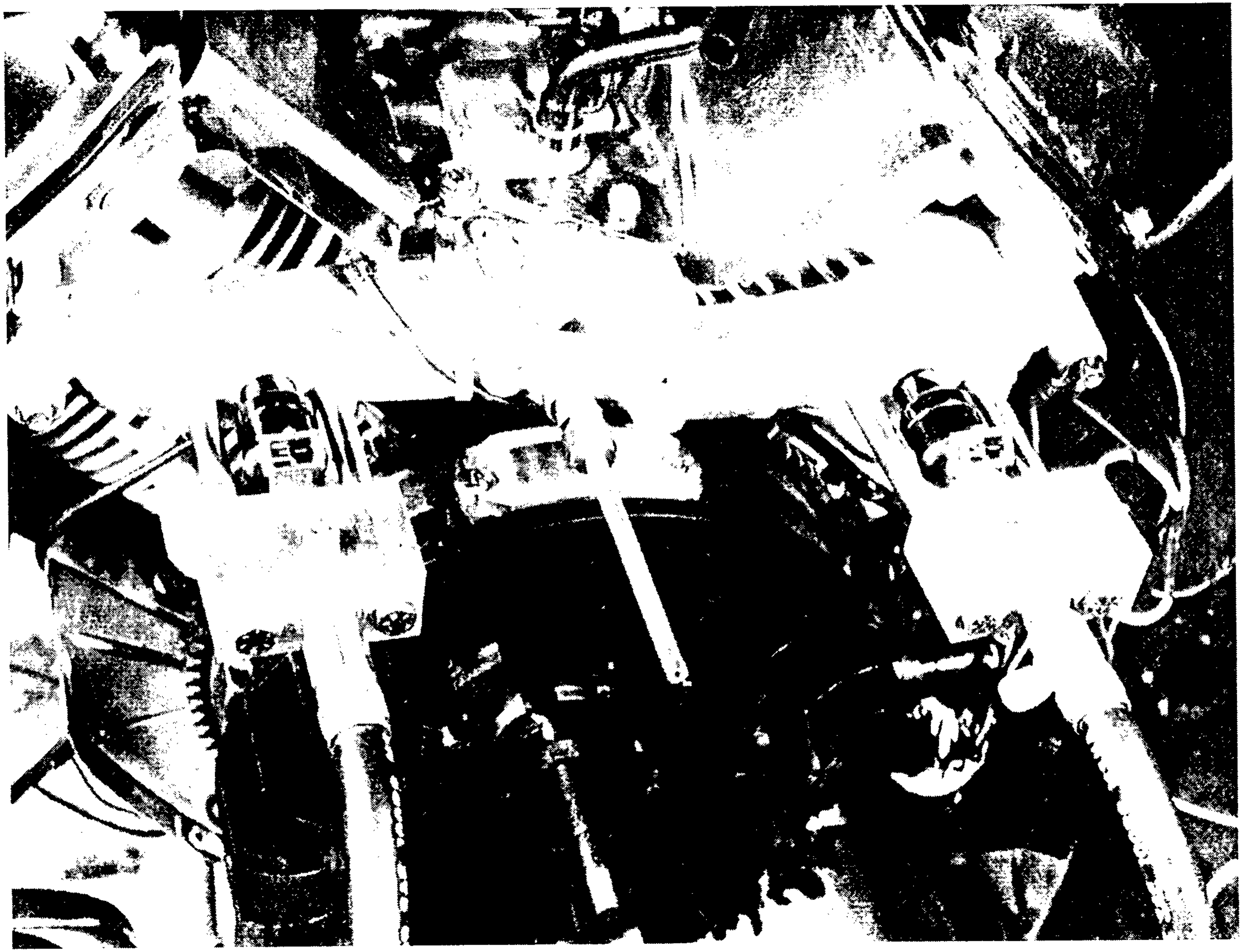

FIGURE 9. PORT INJECTION HARDWARE

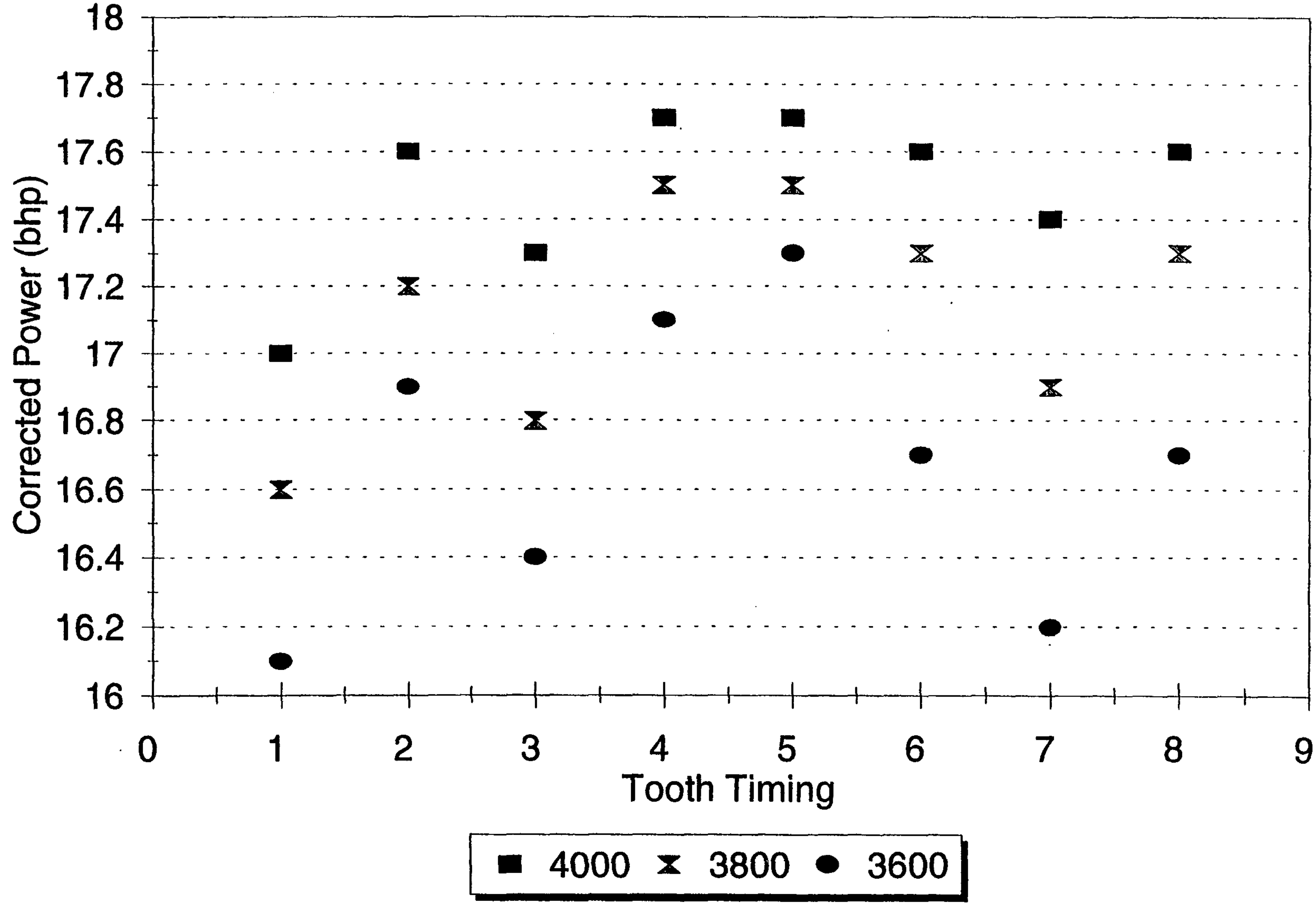

FIGURE 10. PORT INJECTION, MAXIMUM POWER VS. INJECTION TIMING

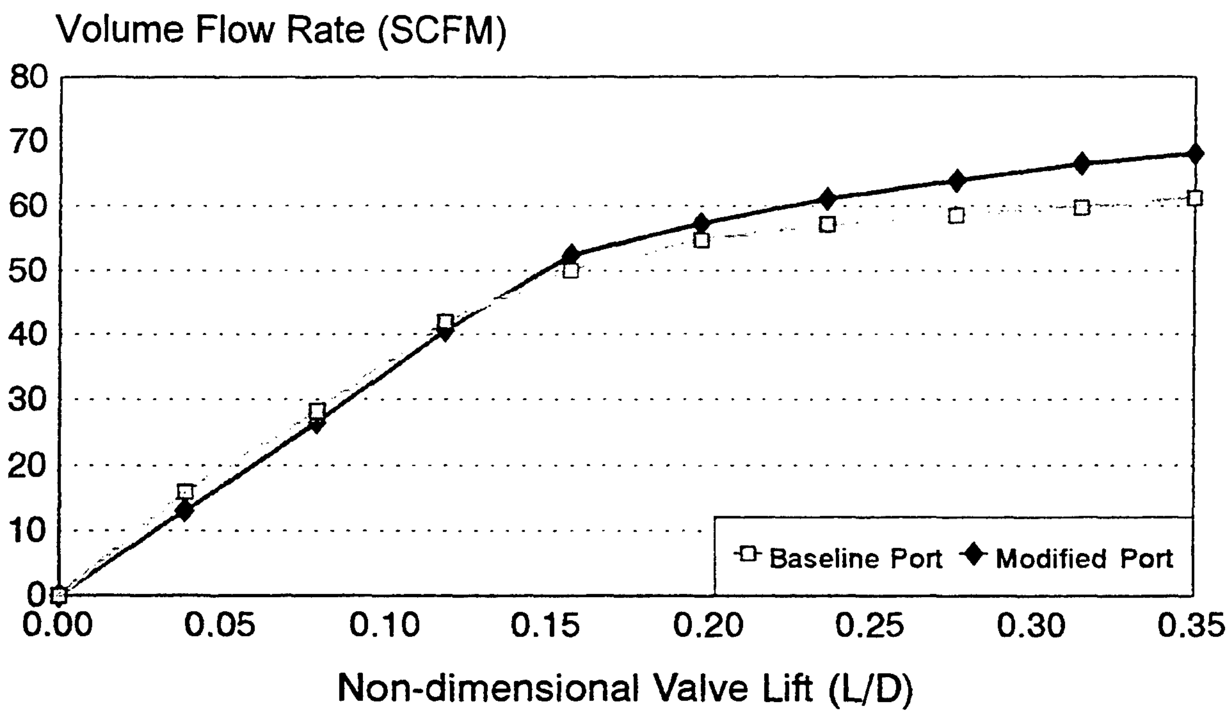

FIGURE 11. CH-22 INTAKE PORT FLOW COMPARISON

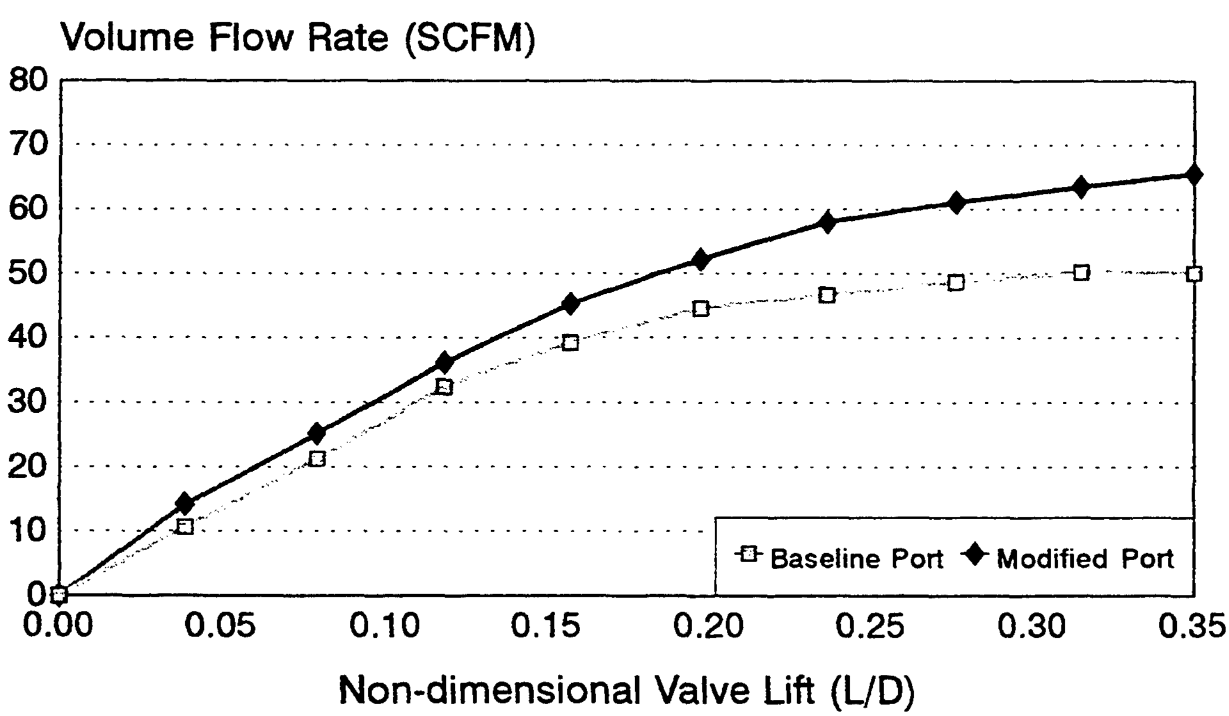

FIGURE 12. CH-22 EXHAUST PORT FLOW COMPARISON

The exhaust port was modified by increasing the available flow area in the transition between the horizontal and vertical runners. Material was removed, and the transition was made as smooth as possible. The port surfaces were lightly polished to improve flow and reduce heat transfer within the exhaust port. The exhaust port was re-tested, as shown in Figure 12, resulting in significant flow improvements at all valve lifts. At high lifts, flow increased by approximately 25 percent. These relatively simple modifications resulted in measurable improvements in volumetric efficiency and power density.

2.1.3.5 Piston Modifications

Methane has a much higher octane rating, or knock resistance, than gasoline. Common natural gas blends contain about 90-95 percent methane and have octane numbers over 130. This compared to typical gasoline blends with octane numbers under 90. This means that higher compression ratios can be tolerated when operating on natural gas. It is advantageous to raise the compression ratio since the result is increased power and efficiency. The Kohler CH22 has a compression ratio of 8:1 in stock form. Natural aspirated spark ignition engines have been run at compression ratios in excess of 15:1.

It was determined that overall engine efficiency could be improved through the use of a higher compression ratio, which was allowed due to the higher octane rating of compressed natural gas. The production Kohler Command 22 piston has a relatively deep dish and slightly negative deck height. SwRI estimated that an increase in compression ratio in the area of 10:1 up to 14:1 would provide significant improvements in efficiency and power density.

To keep prototype design and fabrication time to a minimum, it was determined that a suitable existing piston design be modified for use with the Kohler engine. Such a piston was found available in blank form from Arias Pistons for the Yamaha FJ1200 motorcycle engine. This was a forged piston design, which provided superior strength compared to the cast Kohler production piston, with a small increase in mass. The pistons were ordered from Arias through consultant Glenn O'Neal, who machined the ring grooves to match the production Kohler piston rings. Arias provided the pistons with ½" additional crown height to facilitate machining of any required piston dome at a later date. The piston ring depth was raised slightly compared to the production piston in order to reduce the dead volume above the top ring. This was intended to help reduce trapped hydrocarbon emissions. The wrist pin bores in the piston were sized to match the Kohler connecting rods, and a high strength, lightweight wrist pin was obtained to work with the pistons. The wrist pins were retained by circlips in this design.

For a 10:1 compression ratio, SwRI milled the pistons flat with a zero deck height. Since a higher 14:1 compression ratio was also desired for testing, a domed piston was also designed. The dome outlined the shape of the combustion chamber, with a radiused transition to the piston deck surface. The final 14:1 dome design was made in 3-D CAD, and transferred to Mastercam for CNC toolpath generation. A three axis CNC controlled milling machine in the SwRI machine shop was used to cut the domes first into wax for verification, and then into the prototype pistons. The underside of the pistons were machined in the wrist pin boss areas to match the weight between the 10:1 and 14:1 piston sets.

Both the flat-top and domed pistons were tested in the engine, without any problems. The increased loading on the pistons due to the higher compression ratios did result in failure of a stock Kohler connecting rod, but this was later rectified through an SwRI redesign of the rod. The high compression ratio pistons made a significant contribution towards power and efficiency goals for the project.

Figure 13 shows the performance of the engine operating with increased compression ratio. This is the final power data (i.e., maximum power output on CNG). An illustration of the thermal efficiency levels achieved with the final engine concept is shown in Figure 14. The figure shows thermal efficiency using lower heating value over the engine's entire operating range. Note the data in the figure also represents the flow improvements from the cylinder head modifications.

2.1.3.6 Connecting Rod Modifications

During the course of engine testing, a catastrophic engine failure was experienced. Upon investigation, it was found that a connecting rod failure was experienced near the wrist pin. Based on force calculations performed by SwRI, it was determined that the increased forces on the connecting rod, associated with the increased compression ratio, were the likely cause of the failure. This conclusion was supported by a second failure of a similar engine. Given this, it was decided that a new connecting rod be designed to withstand the increased compression forces of the modified CNG engine. The upgraded connecting rods were designed, fabricated, and tested at SwRI and found to solve the problem. The upgraded connecting rod is shown in Figures 15 and 16. Details of the upgraded connecting rod design are contained in the following paragraphs.

As previously noted, shortly after installation of the high compression ratio pistons, the Kohler engine experienced failure of a stock connecting rod. Analysis of the failure showed that the upper end of the rod beam split vertically, starting from the base of the wrist pin bore in the small end of the rod. It was determined that a combination of increased loading from the high compression ratio pistons and inadequate lubrication of the wrist pin bore with the stock connecting rod design were responsible for failure. The other connecting rod in the same engine was also analyzed and found to have galling of the wrist pin bore, indicating that failure of the second rod would have happened shortly thereafter.

Based on this analysis, SwRI decided to redesign the connecting rods in the engine for improved strength and durability under higher load conditions. Since the production connecting rod was made of cast aluminum and was relatively light, the new design needed to increase strength with minimal increase in mass. It was determined that 6061-T6 aluminum had the best combination of strength to weight ratio, cost, and machinability for the new rod design. 7075 aluminum alloy was originally considered until it was realized that the high oil sump temperatures in this air-cooled engine resulted in lower strength properties of the 7075 alloy at elevated temperatures compared to the 6061 alloy. Titanium was also considered, but was regarded as too expensive and difficult to machine for this application.

The bottom end (or main journal end) of the new connecting rod design was basically left the same as the original design, with some material removed in less critical areas for weight savings. The beam of the rod was redesigned to take advantage of the superior strength of the 6061-T6 alloy (as compared to the stock cast material), particularly in the direction where bending stresses were

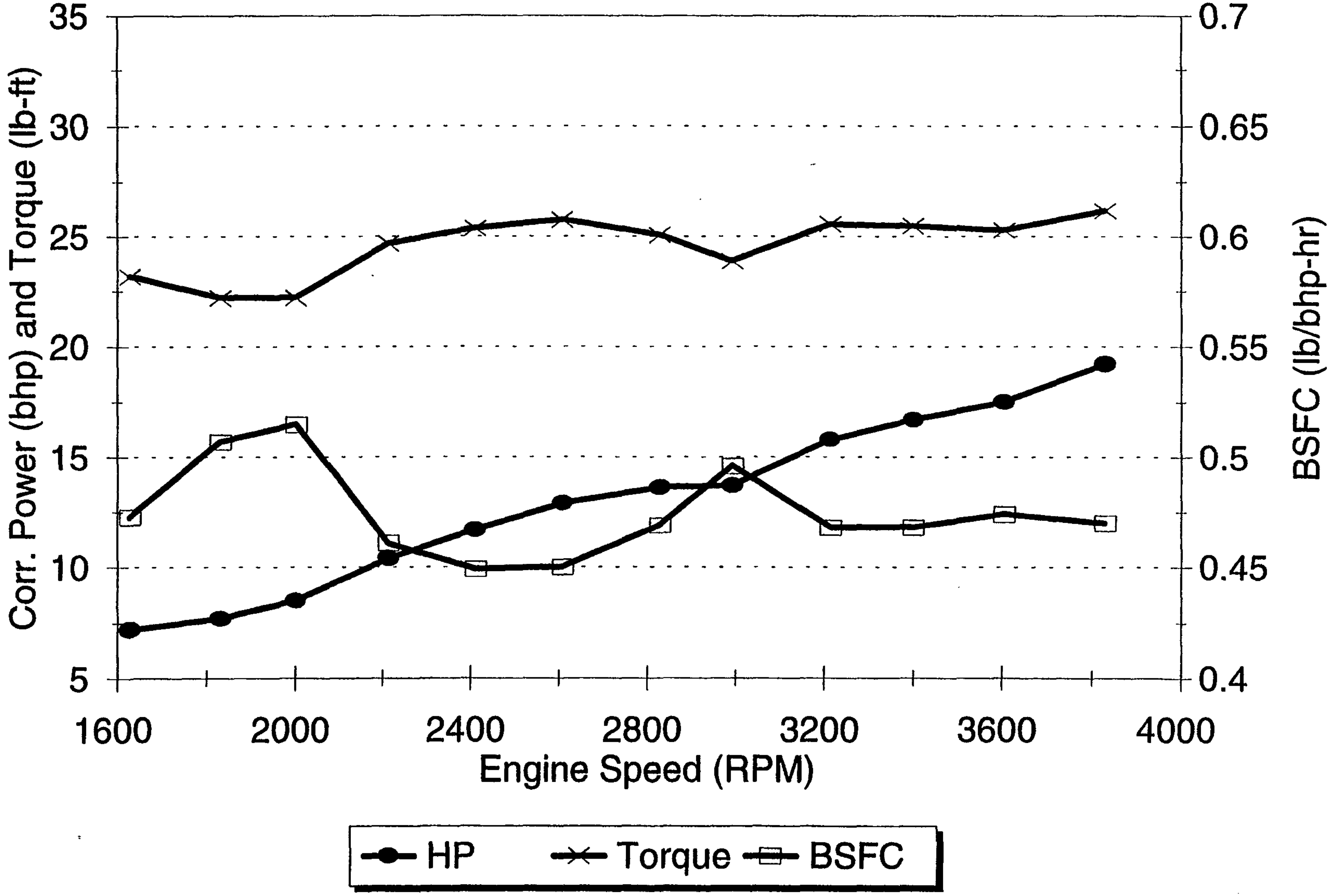

FIGURE 13. CH-22 NG ENGINE PERFORMANCE, 12:1 CR/PORTED HEADS

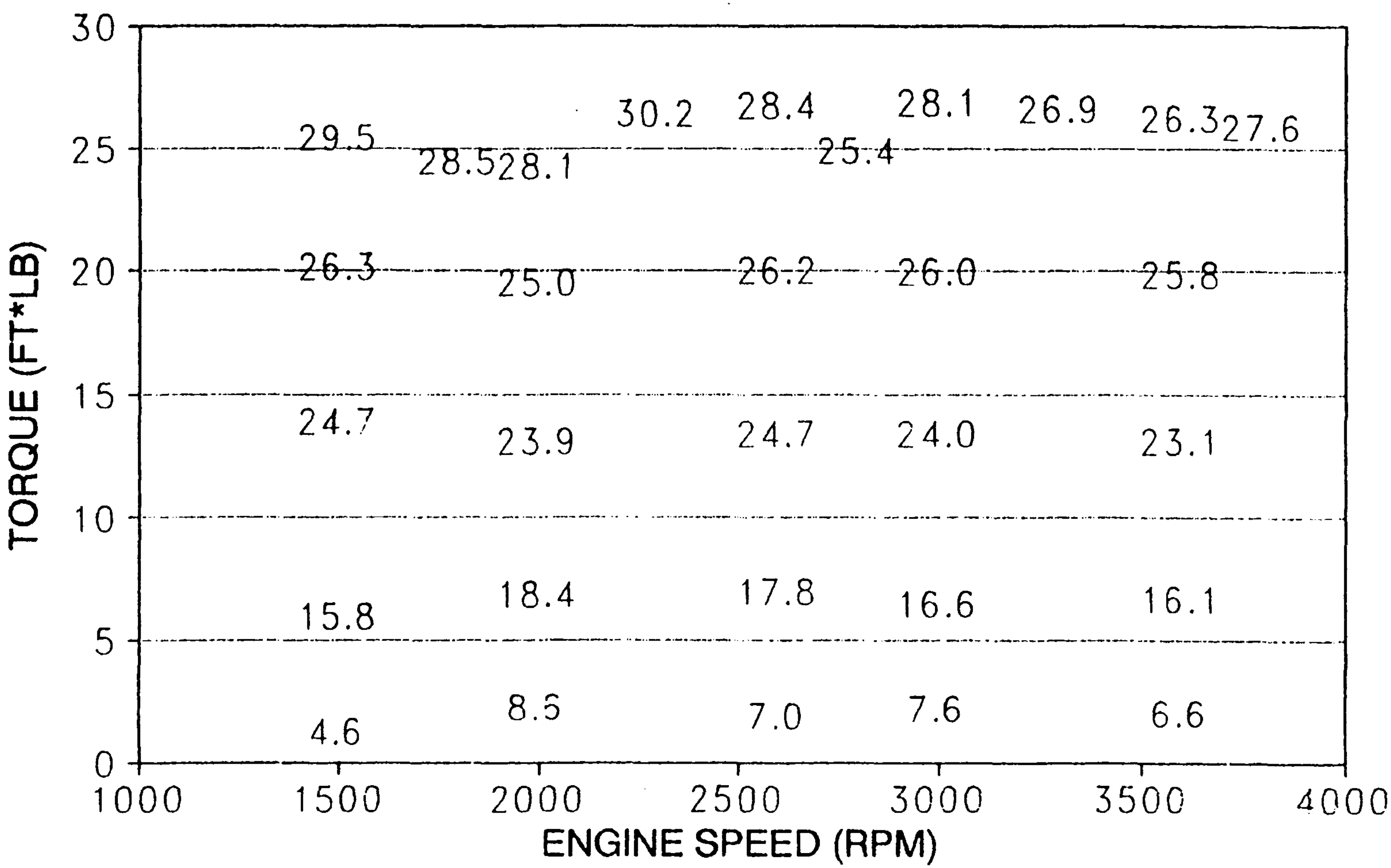

FIGURE 14. FINAL ENGINE THERMAL EFFICIENCY MAP WITH MIRATECH CATALYST

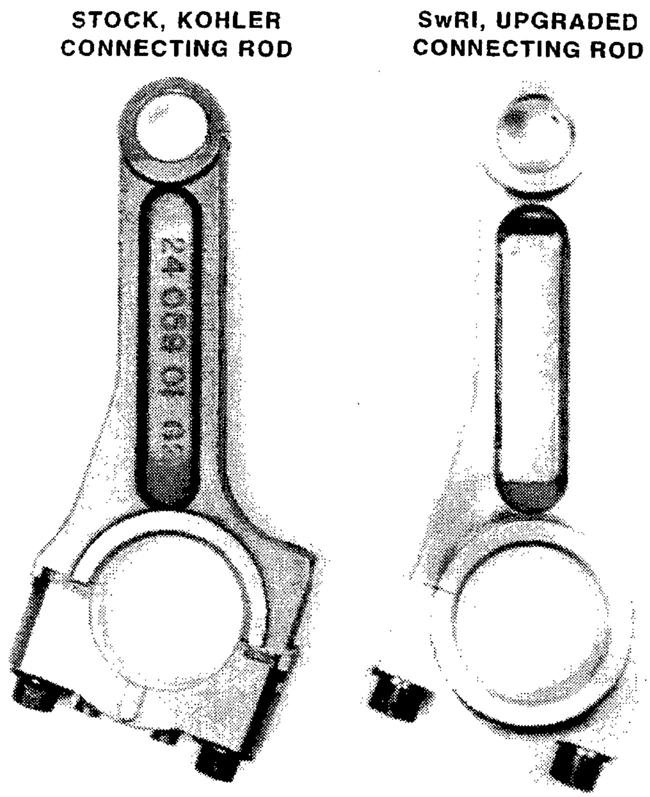

FIGURE 15. KOHLER ENGINE CONNECTING RODS, STOCK VS. SwRI DESIGN

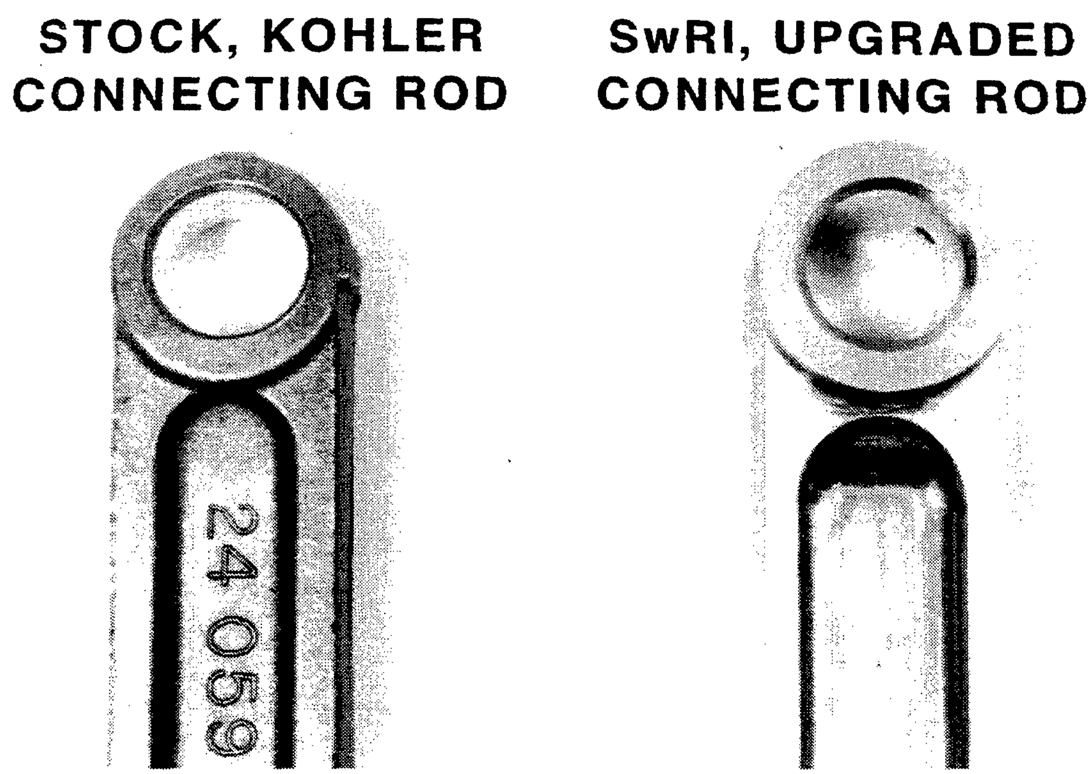

FIGURE 16. CLOSE-UP VIEW OF CONNECTING ROD COMPARISON

greatest. The small end, or wrist pin end of the rod was completely redesigned with additional surface area in the wrist pin bore for increased load capacity. The upper end of the connecting rod was not tapered like the original design, which allowed for the addition of a second oil hole over the stock design. This was done to improve lubrication through the wrist pin bore of the connecting rod.

After the design was completed, the connecting rods were machined from a billet of 6061-T6 aluminum. Steel dowel pins were added for alignment of the connecting rod cap, along with grade 8 fasteners. The cap was installed on the rod for final boring of the main journal. Both ends of the rods were finish honed to the appropriate size. The upper end oil holes were chamfered to enhance oil retention in the wrist pin area.

The resulting connecting rod weighed within 5% of the stock cast rod, with much improved strength and upper end lubrication characteristics. The prototype pistons were machined in the wrist pin area to allow for extra clearance of the wider wrist pin boss of the new connecting rods. After an initial run-in period with the new connecting rods, the rods were removed and examined, and no galling or preliminary indications of failure were found. The connecting rods were re-installed, and testing resumed without any additional connecting rod failures.

2.1.4 CNG Engine Performance/Emissions Testing

SwRI contacted catalyst suppliers to select an appropriate three-way catalyst for the test engine. A sample catalyst was obtained from Johnson Matthey. This catalyst was equipped with a heating coil for electrical pre-heating of the catalyst for rapid light-off during cold starting conditions. The catalyst was installed on the test engine and mapped for emissions. Catalyst conversion efficiency for NO_x, CO, and THC emissions was measured over a range of operating conditions and fuel-air equivalence ratios near stoichiometry. The pre- and post-catalyst emissions, at full-load conditions, are shown in Figures 17 through 19. Note that post-catalyst emissions are shown with and without the electrically-heated catalyst (EHC).

Close attention was paid to catalyst light-off temperature. In order to minimize vehicle emissions, it is important to insure proper catalyst performance at any engine operating condition used during vehicle operation. Furthermore, it is also important that the catalyst become effective (i.e., catalyst light-off) quickly upon engine startup. For this reason, the Johnson Matthey catalyst was equipped with an electrically-heated element. The intent was to only use the heater element during and shortly after engine start up. For emissions testing, catalyst conversion efficiency was measured both with and without the heating element active. Small improvements in catalyst efficiency were measured with electrical power applied to the heater.

As can be seen from the data, the conversion efficiencies measured from the Johnson Matthey catalyst were less than desirable. Expected conversion efficiencies from a "good" catalyst were hoped to be in upwards of 95 percent conversion of CO and NO_x, and 90 percent conversion of THC. Since the conversion efficiencies of the Johnson Matthey catalyst were found to be well below these levels, a catalyst from a second supplier was sought.

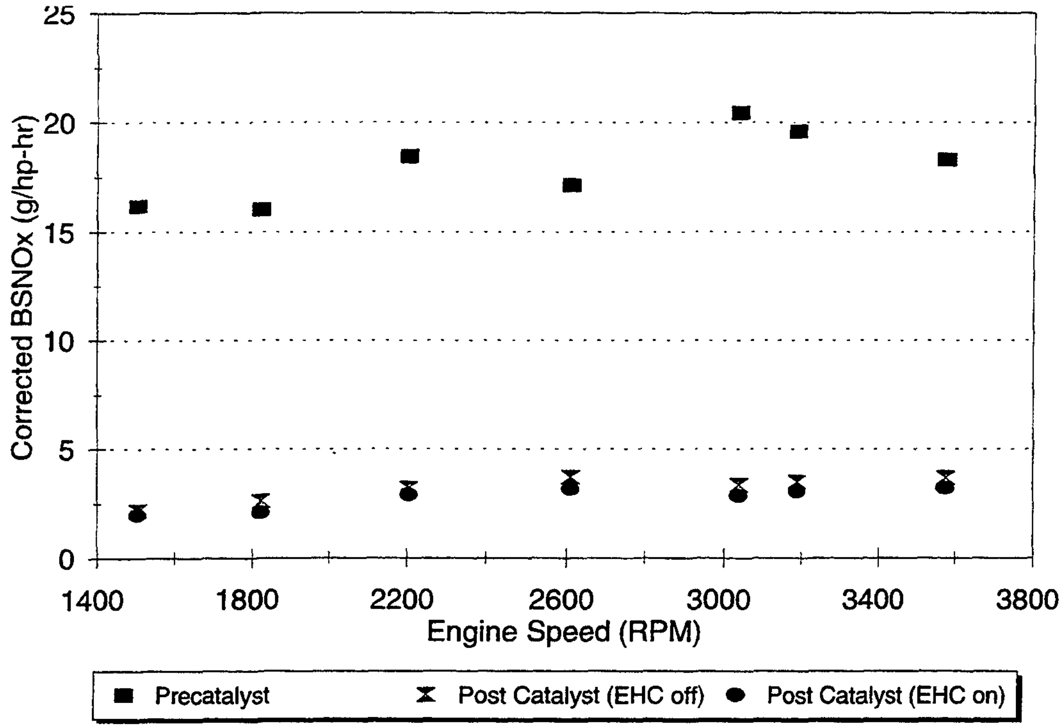

FIGURE 17. WOT NO_x EMISSIONS, JOHNSON MATTHEY CATALYST

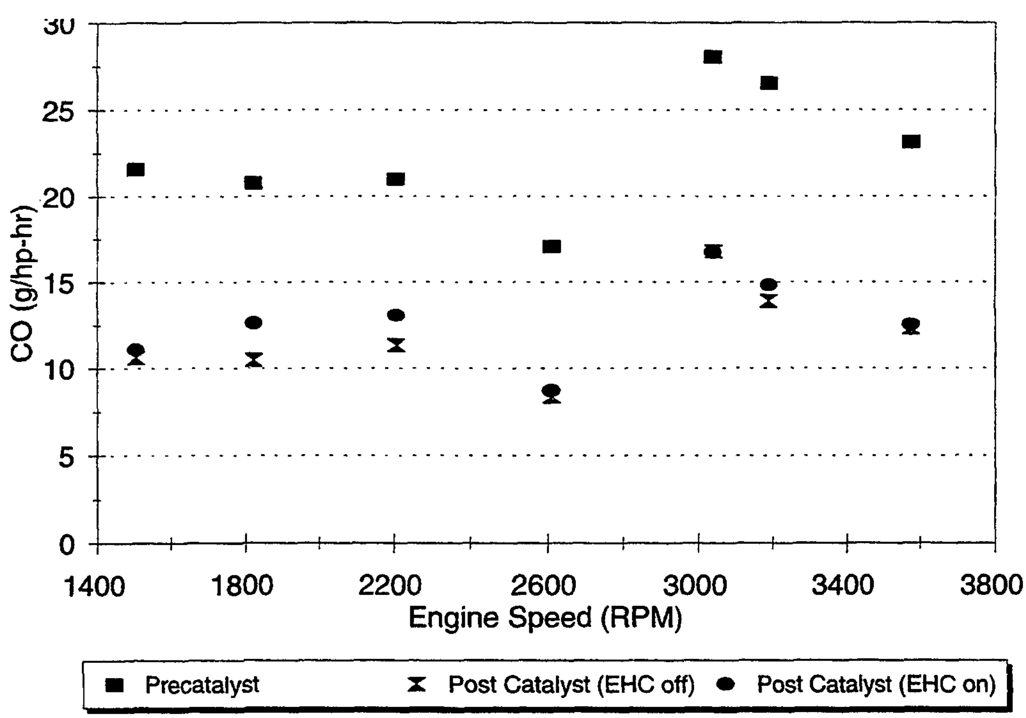

FIGURE 18. WOT CO EMISSIONS, JOHNSON MATTHEY CATALYST

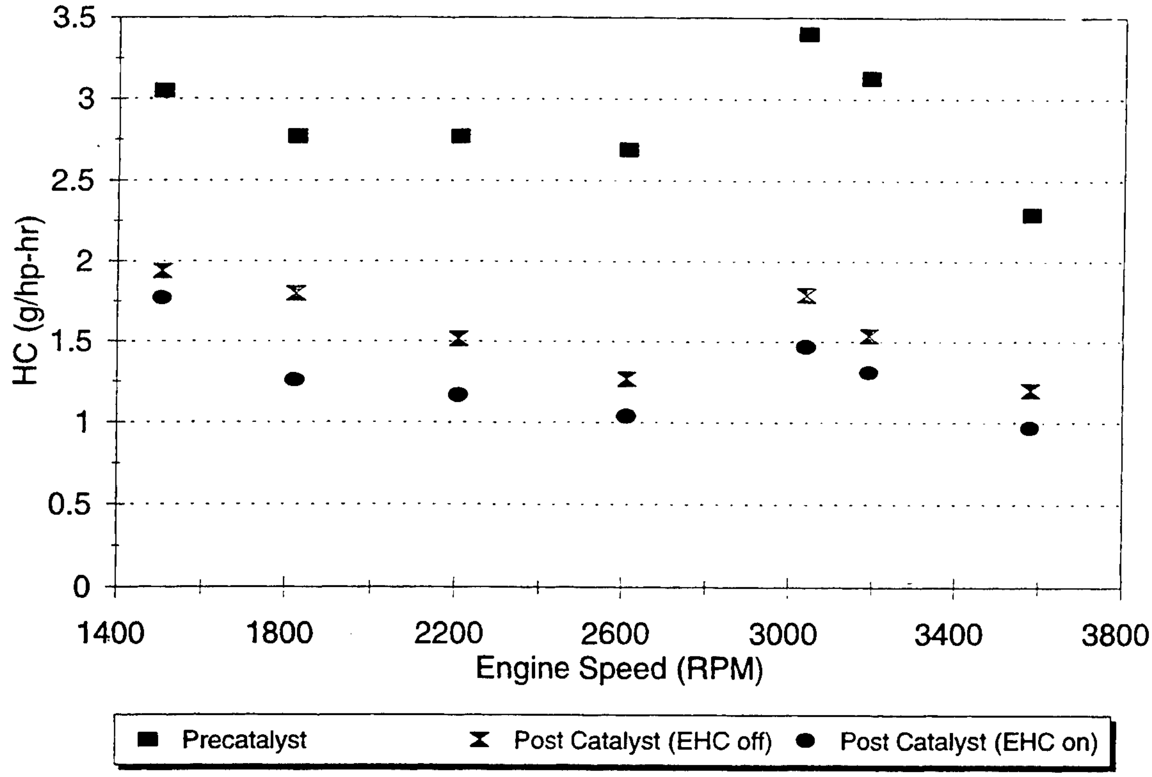

FIGURE 19. WOT HC EMISSIONS, JOHNSON MATTHEY CATALYST

A sample catalyst from Miratech was secured for testing on the engine. Miratech had supplied catalysts for another natural gas engine project at SwRI. Very high conversion efficiencies were measured for the Miratech catalyst used on that project. The Miratech catalyst was not equipped with an electrical heating element. This was not considered to be major obstacle considering that the initial focus would be on achieving increased catalyst conversion efficiencies under hot conditions.

The Miratech catalyst was emissions tested on the engine at SwRI under the same operating conditions and equivalence ratios evaluated during the previous catalyst testing. The conversion efficiencies, engine-out, and catalyst-out NO_x, CO, and THC emissions are shown in Figures 20 through 28. As can be seen from the data, extremely high conversion efficiencies were achieved using the Miratech catalyst at virtually every engine condition tested. Conversion efficiency of THC was found to be the lowest at low speed, light-load operation. This is due to the reduced exhaust temperatures at those low power conditions. NO_x conversion was also found to be above 99 percent at all conditions except those near idle. CO conversion was found to be above 97 percent at all conditions tested, and roughly 99 percent at most operating conditions. Catalyst-out emissions were found to be at or below equivalent zero emissions or Best Available Control Technology (BACT) levels as specified by the South Coast Air Quality Management District (SCAQMD). Catalyst degradation as a function of time was not measured, although the catalyst accumulated over 20 hours of operation prior to final emissions testing.

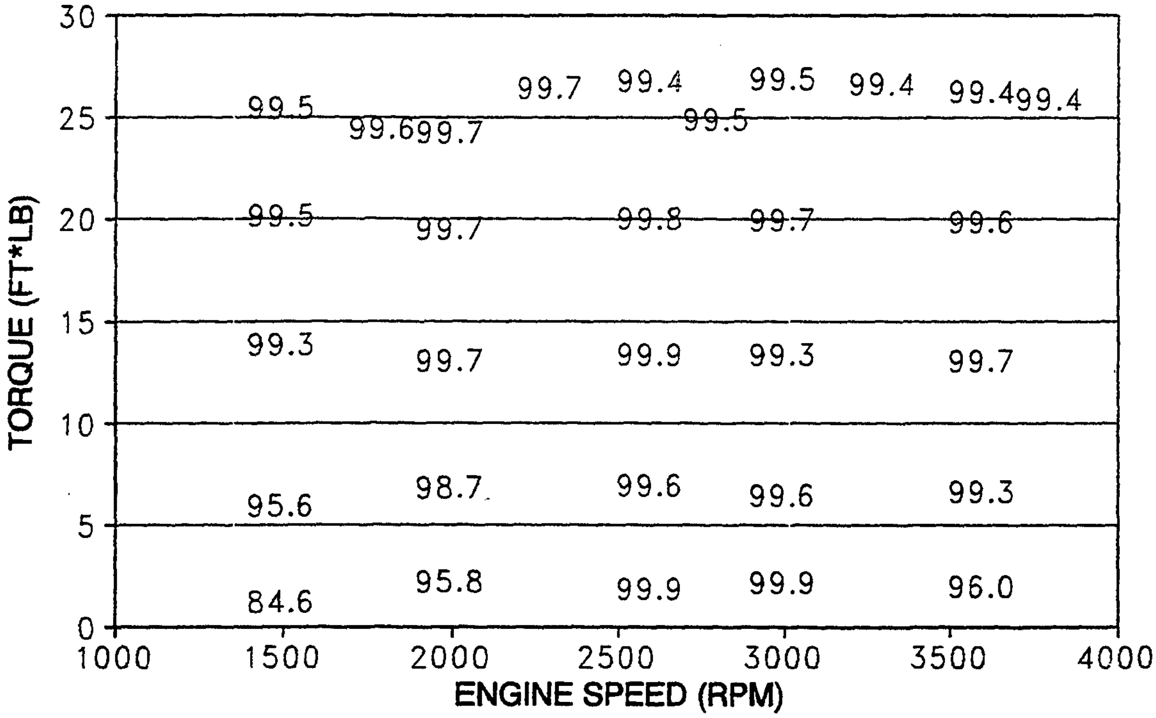

FIGURE 20. NO_x CONVERSION EFFICIENCY (%), MIRATECH CATALYST

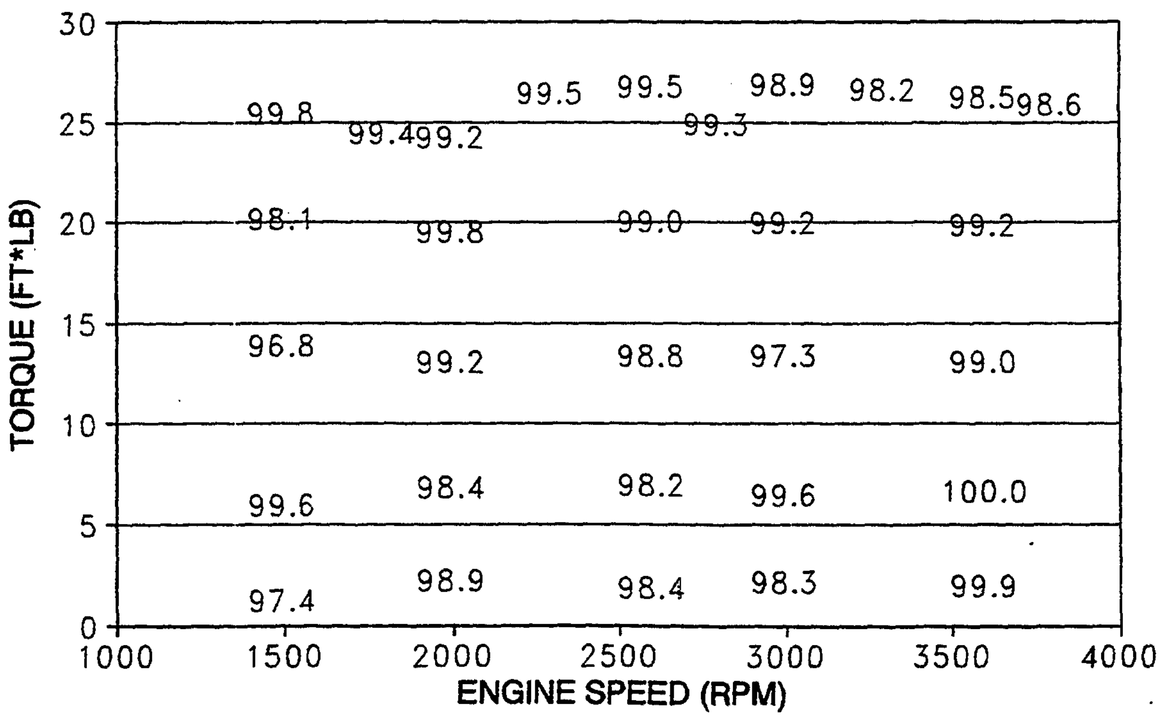

FIGURE 21. CO CONVERSION EFFICIENCY (%), MIRATECH CATALYST

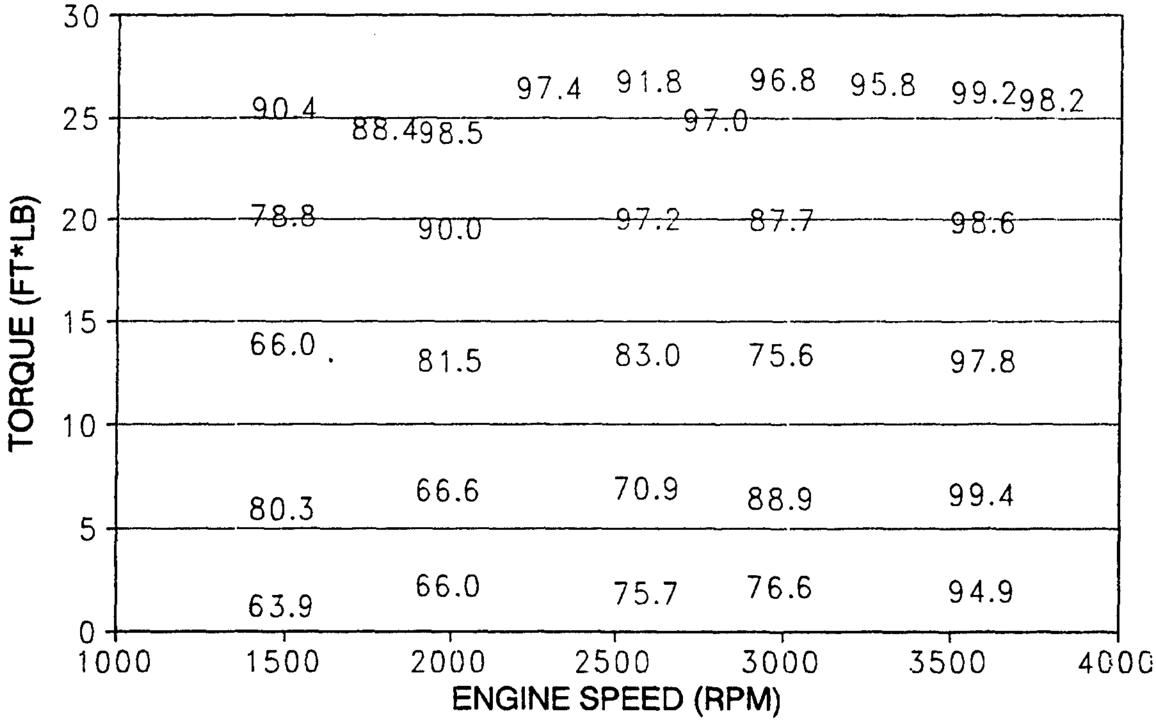

FIGURE 22. HC CONVERSION EFFICIENCY (%), MIRATECH CATALYST

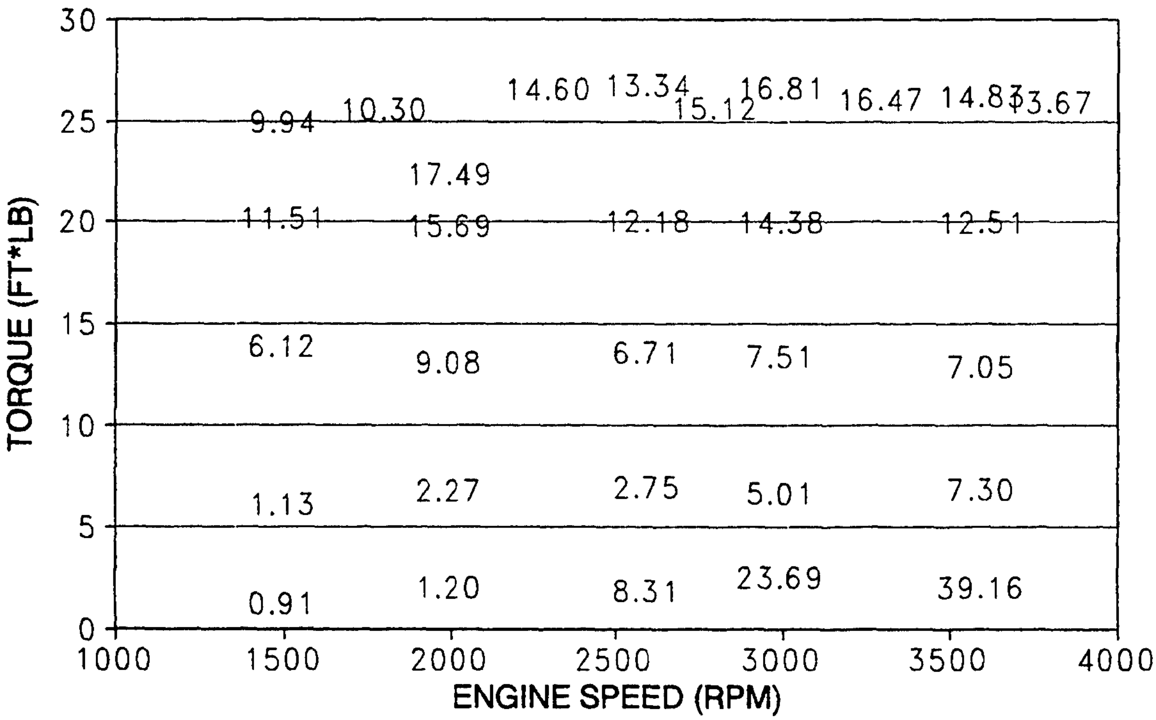

FIGURE 23. PRE-CATALYST BSNO$_x$ (G/BHP-HR), MIRATECH CATALYST

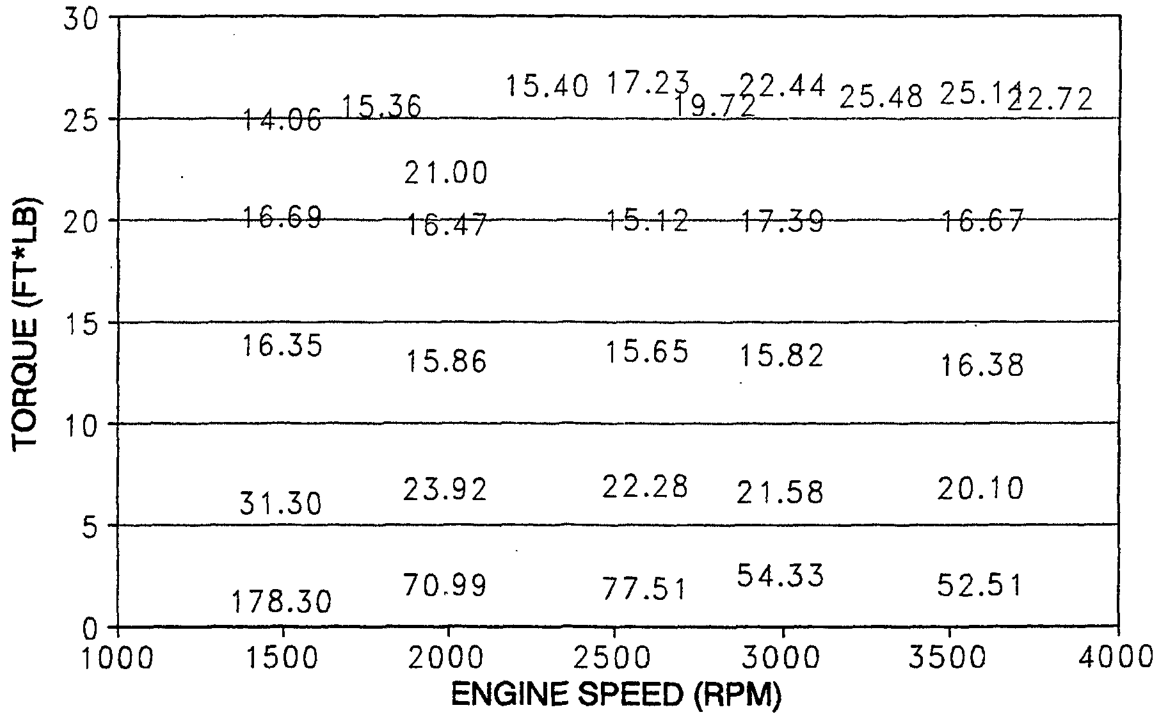

FIGURE 24. PRE-CATALYST BSCO (G/BHP-HR), MIRATECH CATALYST

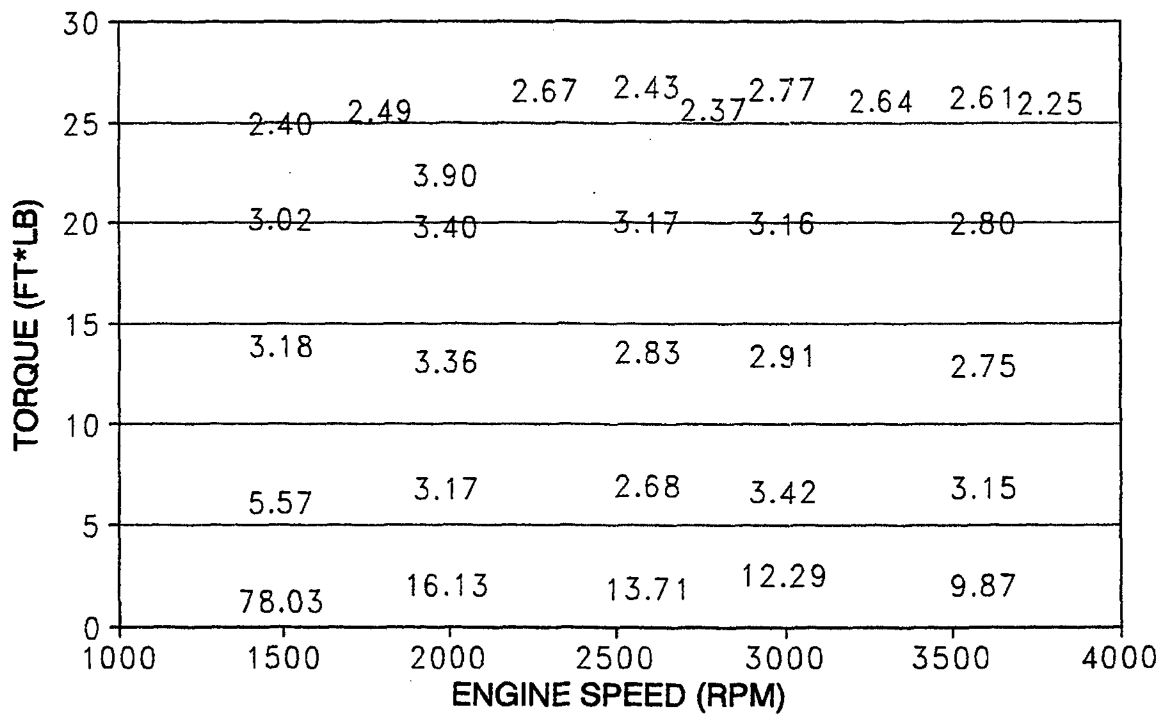

FIGURE 25. PRE-CATALYST BSHC (G/BHP-HR), MIRATECH CATALYST

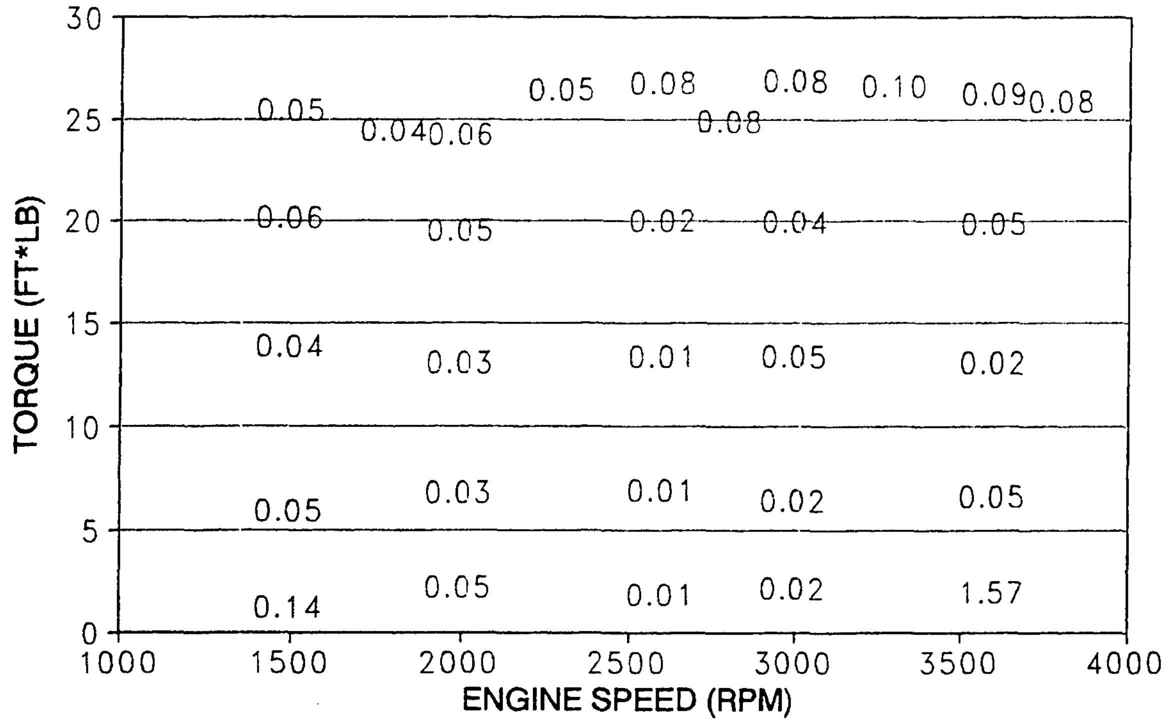

FIGURE 26. POST-CATALYST $BSNO_x$ (G/BHP-HR), MIRATECH CATALYST

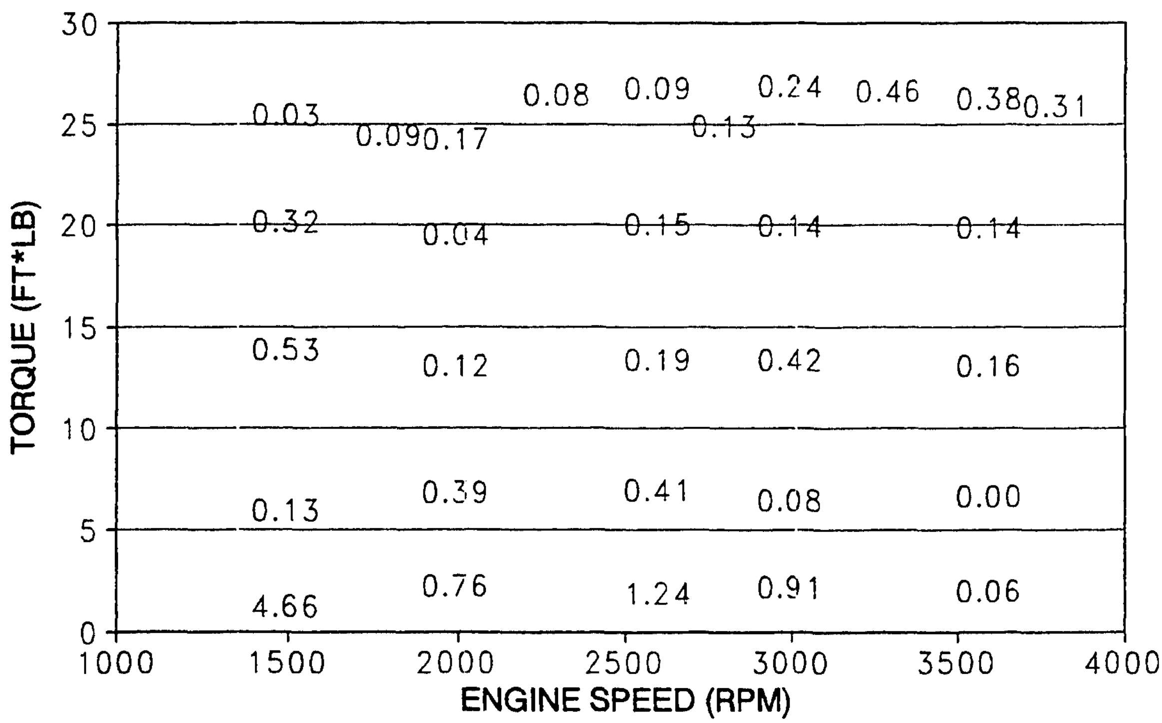

FIGURE 27. POST-CATALYST BSCO (G/BHP-HR), MIRATECH CATALYST

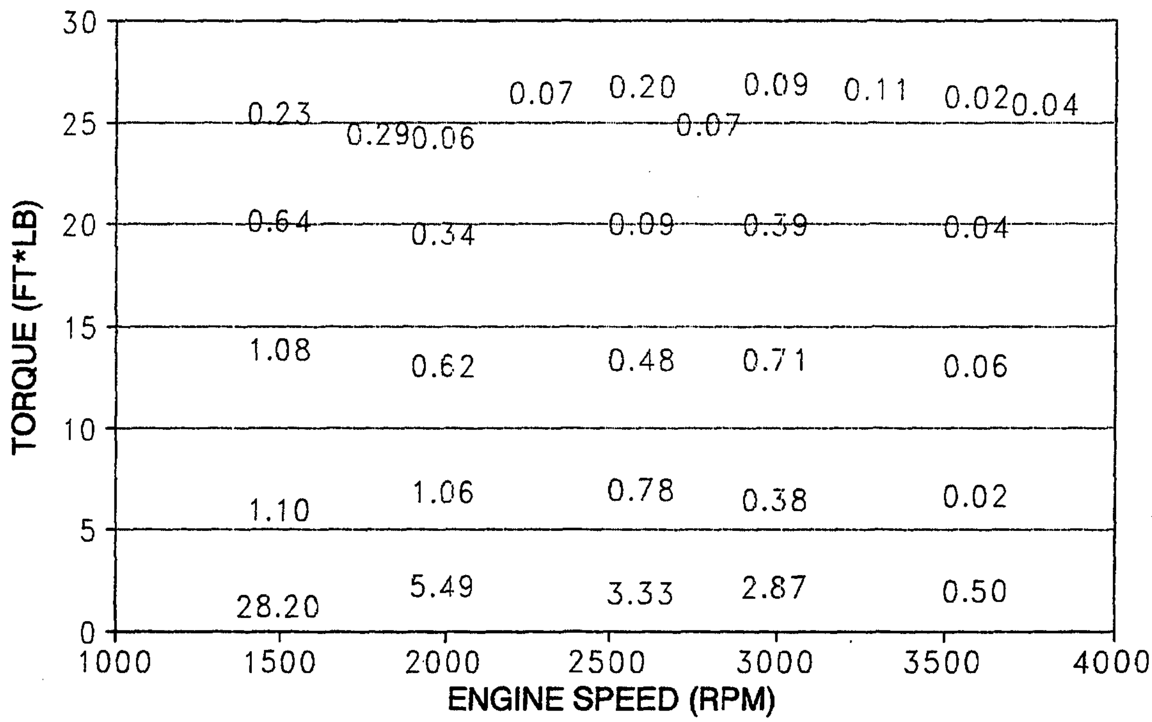

FIGURE 28. POST-CATALYST BSHC (G/BHP-HR), MIRATECH CATALYST

2.1.5 Engine Modeling

An engine modeling effort was undertaken to aid in the task of increasing engine power output. SwRI's VIPRE cycle simulation software was used in the modeling effort. Details of the engine modeling effort are described in Appendix A of this report.

2.1.6 Engine Acoustic Testing

Engine acoustic noise was believed to be an important issue in the vehicle application of the APU. During the engine development process, engine acoustic testing was performed to quantify the acoustic signature of the engine at various operating conditions and physical locations. The results of the acoustic testing were used to help select a suitable muffler for the engine to reduce engine exhaust noise. The details of the engine acoustic testing are contained in Appendix B.

2.2 APU Control System Development

As part of the APU system which SwRI was tasked to deliver on the project, an APU control system was necessary to provide control of the engine operating point and control the battery charging profile. SwRI designed and constructed a PC-based APU/Energy Management control system to accomplish these functions. The SwRI-developed controller was a design based on its Rapid Prototyping Electronic Control System (RPECS) platform. The RPECS is a highly flexible PC-based prototyping tool used for real-time control in a variety of applications from engine and powertrain control to test cell control and many others.

The APU control system was developed and tested with all other APU components at SwRI. The APU control system was shipped to Solar Car Corporation, along with the remainder of the APU hardware. It was installed in the vehicle and successfully stand alone tested on the S-10 pickup at Solar Car in April 1995.

2.2.1 Control Functions

The SwRI APU controller was designed to provide numerous control functions as related to the APU components and battery pack. Fundamentally, the APU controller provided control of the APU operating point through manipulation of the engine throttle and control of the generator output via the voltage boost unit. The APU controller also computed the state of charge of the battery pack and adjusted the charging current accordingly to maintain adequate charging of the batteries on the vehicle. In addition, the APU controller was responsible for the engine start and stop functions, as well as control of the electrically-heated catalyst (EHC) heater function. The EHC function was not ultimately used since the final catalyst configuration was not electrically heated.

2.2.2 Controller Hardware Platform

As previously noted, the APU controller platform was based on an industrial PC. The controller utilized a commercially available 486 66MHz CPU card, with a 1.44 MB solid state RAM disk emulator as the primary memory device. The controller utilized commercially available data acquisition and control cards, as well as a commercial watchdog timer board for protection. The controller enclosure for the APU controller is shown in Figure 29. In order to provide the necessary signal conditioning and driver circuitry for interfacing with the APU hardware, a custom interface enclosure was designed and constructed by SwRI. Electrical power for the control system, on the vehicle, was provided via a 500 Watt inverter through a single 12 VDC connection.

2.2.3 Control Software/Algorithm Descriptions

The APU control software was written in C language and executed in the MS DOS environment. The control software was written to utilize floating point arithmetic in order to allow modifications to be made to the algorithms with minimum development time. The 486 processor capably executed all control equations in a time-based interrupt driven routine operating at 100 Hz. Because the system was built around the existing SwRI RPECS platform, built-in functions such as real-time plotting and datalogging were easily integrated into the control system. A detailed description of the APU control algorithms is contained in the following paragraphs.

The APU controller's most fundamental function was to control the power output of the APU. APU power output was modulated in accordance with the average power needed at the traction motor in conjunction with the desired charging current (which was dependent on the state of charge of the batteries). The battery state of charge calculation was based on an integration of power into and out of the battery pack. The state of charge calculation also had a reset function at no-load conditions based on the no-load battery voltage level. This function would reset the power integration periodically to eliminate the accumulation of error from inaccurately modeled or neglected effects.

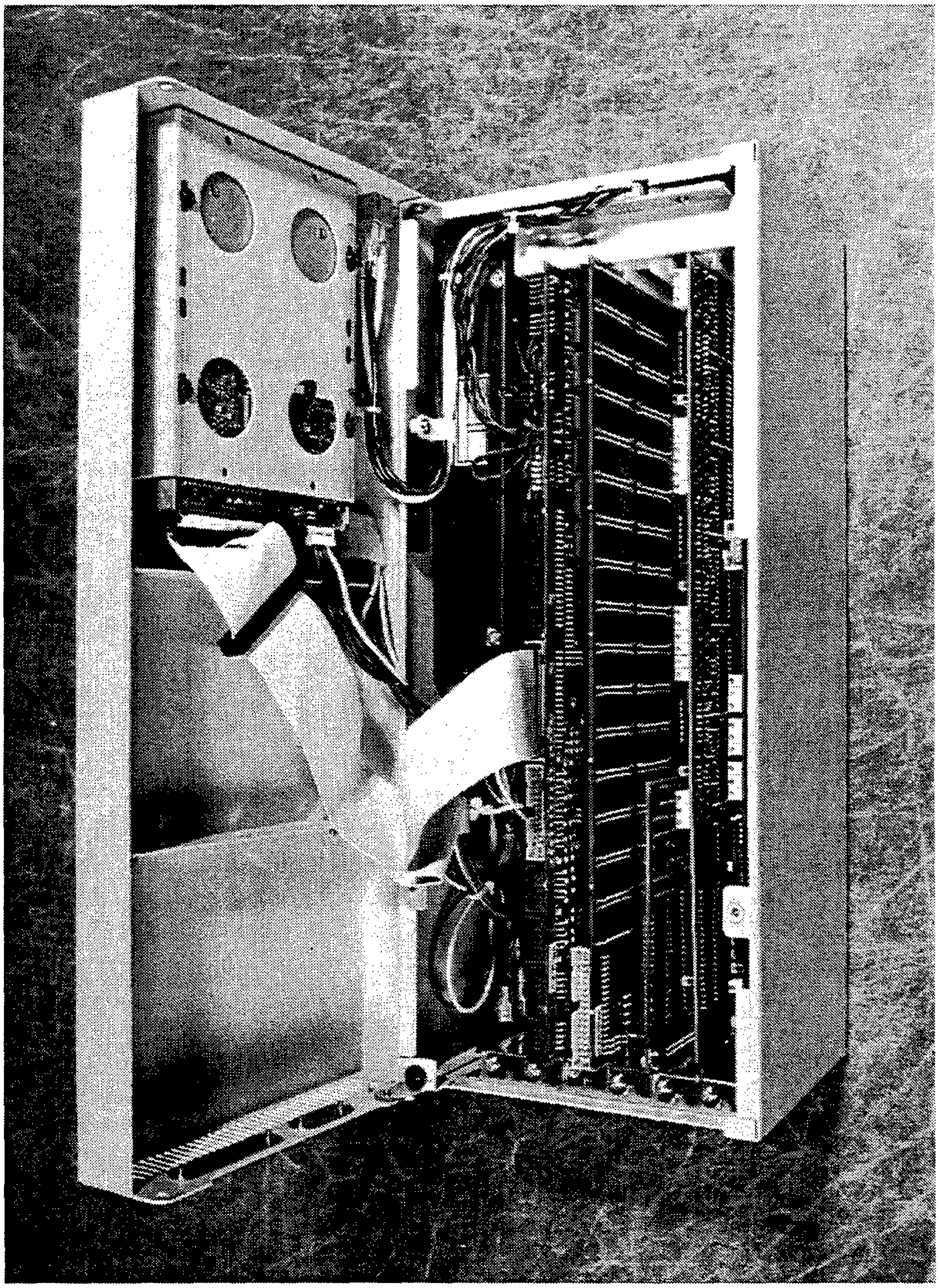

FIGURE 29. PROTOTYPE APU CONTROLLER

Given the desired APU power output, the engine speed and throttle set point were computed via a programmable engine operation trajectory. The engine operation trajectory was calibrated to maximize the APU efficiency at all operating conditions. Thus, for the Kohler engine/Fisher generator pair, the maximum APU efficiency trajectory was found to correspond directly with the maximum thermal efficiency trajectory for the engine. Since the Kohler engine was a throttled SI engine, the maximum thermal efficiency was produced along the wide open throttle (WOT) torque curve of the engine. Therefore, the engine operation trajectory programmed into the APU controller entailed transitioning the engine to the wide open throttle point at the lowest engine speed (i.e., 1500 RPM), and running the engine at WOT up to the maximum power point of the engine (i.e., 3800 RPM). In turn, if the desired power output from the APU was set above roughly 4 kW, the engine was always operated at WOT. Only when the desired APU power output was less than 4 kW was the engine operated at a less efficient, part-throttle condition. This approach was anticipated to provide the benefits of both maximum vehicle fuel economy and minimum vehicle emissions.

Having computed the desired engine speed and throttle position, the APU controller first provided the necessary signal to the throttle actuator in order to achieve the desired action. The engine throttle actuator was driven with a standard pulse width modulated (PWM) signal of a variable duty cycle. In order to achieve the desired engine speed, the APU controller utilized information from an engine speed sensor for feedback control. In order to control engine speed, the APU controller modulated the load applied to the engine via the generator. The generator control was provided through a voltage boost controller provided by SuperPower Inc. Through manipulation of the voltage boost controller, the output voltage of the generator and thus the load could be controlled. The APU power control functions, including the state of charge calculation function, are shown in block diagram form in Figure 30.

In addition to the APU power output control function and energy management functions, the APU controller also provided control of the engine start and stop functions. The engine start control was accomplished by controlling the stock starter motor on the Kohler engine. The APU did not have the ability to start the engine via motoring from the generator. Engine stop was accomplished through control of the 12 VDC power available to the engine control system. Also, in order to accommodate the EHC, the APU controller was also capable of controlling a relay to energize the heater on the EHC for pre-heating prior to engine start. This function was ultimately not necessary since the final catalyst was not electrically heated.

In conjunction with the control functions and algorithms previously described, the APU controller also had a limited set of diagnostics designed into it. Out of range diagnostics for each of the sensors used by the APU controller were implemented to detect and react to sensor failures. Furthermore, system level diagnostics and protections were built into the APU controller to detect and prevent APU operation that could damage the unit, (i.e., engine protection diagnostics). The diagnostic functions of the APU were designed to be sufficient to prevent operation that could cause permanent damage to the unit and also could provide valuable information for diagnosing problems should they occur.

2.3 APU Integration/Testing

The components which made up the APU system for the S-10 vehicle, i.e., the engine, generator, engine controller, APU controller, and voltage boost controller were integrated and stand

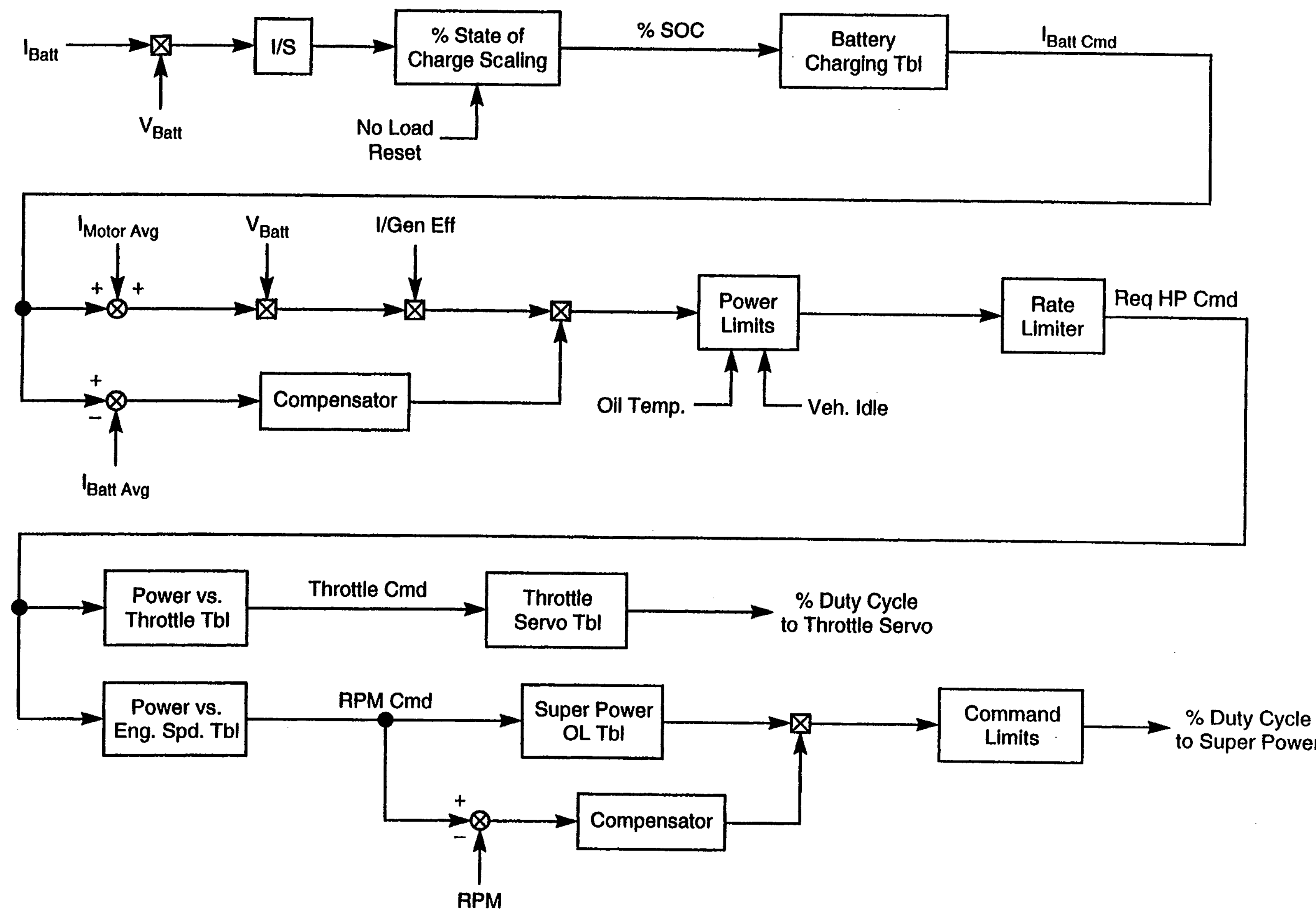

FIGURE 30. APU CONTROL STRATEGY BLOCK DIAGRAM

alone tested both at SwRI before shipment and at Solar Car after initial installation on the vehicle. The performance of the system was found to be satisfactory in each environment. Since the drive motor system for the S-10 vehicle was not delivered before the end of this project, the APU has not been tested in a completely integrated vehicle environment.

2.3.1 Laboratory Environment

Prior to shipment of the APU to Solar Car, the components were integrated together and tested in the laboratory environment at SwRI. For purposes of this testing, a battery pack consisting of 20-12V lead acid batteries, and a resistive load bank were used to simulate the vehicle battery pack and drive system load, respectively. Various load step transients were used to simulate the changing load of the drive system in order to test the response and stability of the APU controller and all APU subsystems. Performance of the APU system was found to be quite favorable in all aspects including APU efficiency, response, and stability. Upon completion of the APU testing at SwRI, the APU system was shipped to Solar Car for vehicle installation.

2.3.2 Vehicle Environment

The APU system was initially installed in the S-10 vehicle by Solar Car personnel. Initially, the engine/generator, along with the engine control system, was installed at the rear of the vehicle underneath the bed of the truck. This was done since it was believed that inadequate space was available in the engine compartment due to the location of other vehicle components. The APU controller was installed in the cab behind the passenger's seat. The voltage boost controller was installed in the engine compartment. Photographs of the initial vehicle installation of the APU hardware at Solar Car are included in Figures 31 and 32.

In order to verify the performance of the APU system, once integrated into the vehicle, SwRI personnel went to Solar Car to debug the vehicle installation and test the APU under similar conditions to those at SwRI. Testing of the APU system at Solar Car involved charging into a charge depleted battery pack, as no resistive load bank was available at their facility. The final APU stand alone testing was completed at Solar Car and the APU performance was found acceptable.

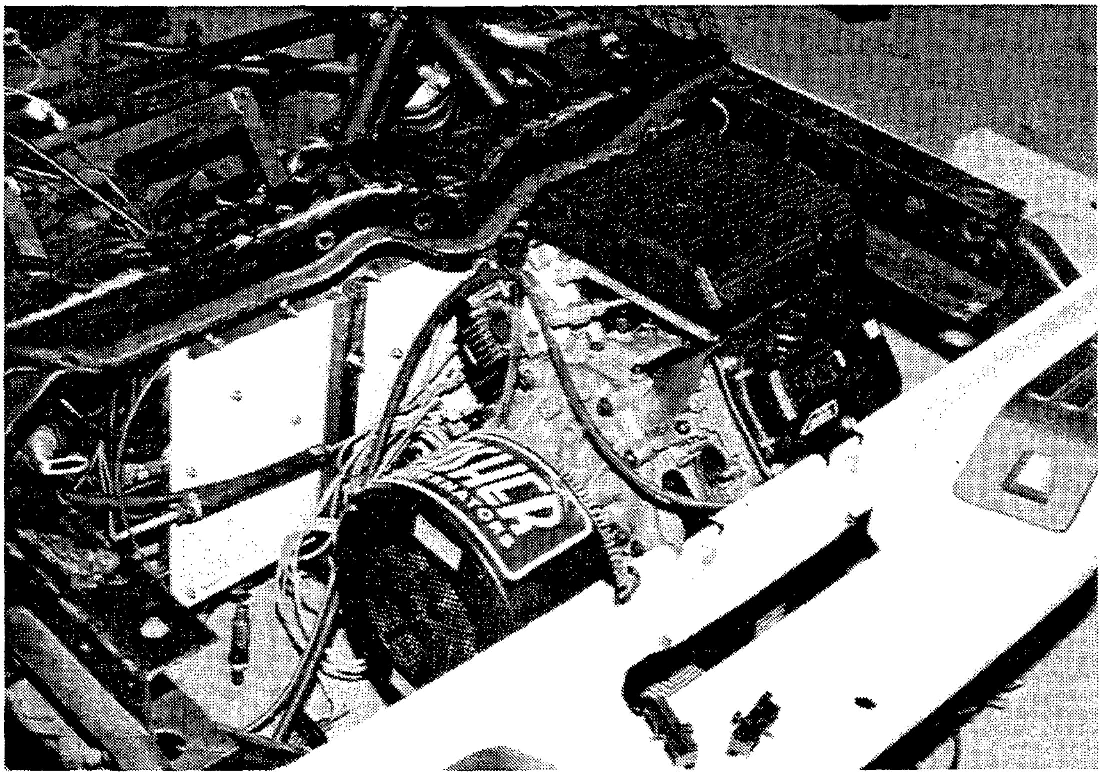

FIGURE 31. SwRI APU INSTALLED IN S-10 VEHICLE (REAR MOUNT)

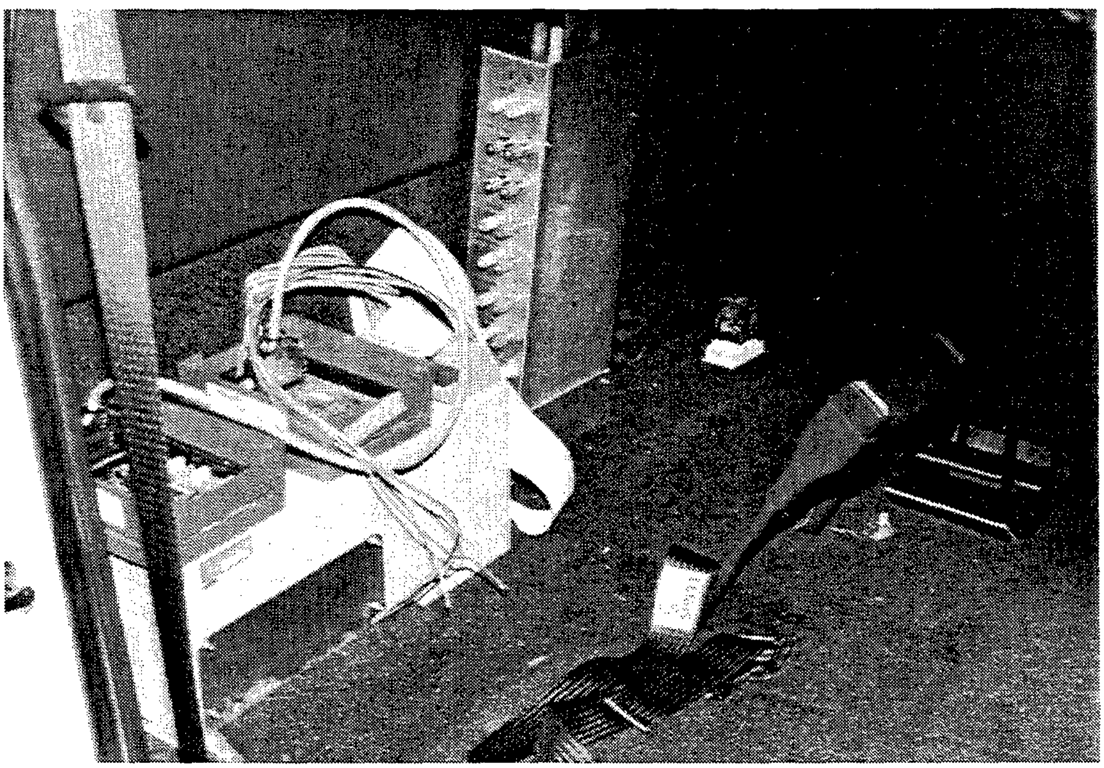

FIGURE 32. PROTOTYPE APU CONTROLLER HARDWARE IN S-10 VEHICLE

3.0 SUMMARY

A natural gas-powered APU was developed and integrated into an S-10 hybrid electric vehicle. The APU utilized a modified Kohler CH-22 engine, a Fisher permanent magnet generator, and appropriate control and power electronics to produce a regulated DC output suitable for charging a battery pack from a range of roughly 100 VDC to 300 VDC. Maximum electrical power output from the APU was approximately 13 kW.

The engine for the APU was developed and optimized for operation on natural gas and utilized an electronic engine control system for enhancement of the performance and emissions characteristics of the engine. Engine thermal efficiency levels, as high as 30 percent (using lower heating value), were measured from the final engine configuration. Extremely low emissions levels, (i.e., at or below those levels deemed by CARB as Equivalent Zero Emissions Vehicle), were achieved from the engine using a three-way catalyst system from Miratech, paired with a precisely calibrated fuel control system. In addition, maximum engine power output essentially equal to the original gasoline engine configuration was achieved using natural gas fuel.

A prototype APU control system was developed by SwRI for energy management, battery charging profile management, and control of APU power output. The prototype controller was designed around a personal computer platform for maximum flexibility in control algorithm development, control system calibration, and sensor and actuator flexibility. The resultant APU controller, along with its signal conditioning electronics, was integrated into the vehicle cab area unobtrusively, behind the passenger's seat.

4.0 RECOMMENDATIONS

The APU was successfully developed for the project. The APU delivered adequate power output, with high efficiency, and ultra-low emissions. However, in order to improve and bring the concept into commercial viability, SwRI has the following recommendations.

First, an alternative engine should be considered. The primary consideration for the APU development was to achieve higher power output. Originally, a 16 kW APU was thought necessary for the vehicle in order to achieve a target vehicle cruise speed of 65 mph. Given this and assuming a 90 percent efficiency level for the generator and boost regulator electronics, the necessary power output from the engine was about 24 hp. None of the Kohler engines tested at SwRI, (including the CH25 gasoline engine), produced above 21 hp. By starting out with an under-powered engine, it was necessary to push the base engine to its limits, (and occasionally beyond its limits), in terms of compression ratio and flow increases. Furthermore, the Kohler CH22 and CH25 engines are not designed for the high-duty cycle operation needed for this APU application. As a result of these factors, the durability of the engine in this application is less than desirable. Also, in order to minimize the acoustic noise from the engine and to simplify the vehicle installation requirements, a water-cooled engine would be better suited for the APU application.

Secondly, in order to vastly improve the installation of all the electronic subsystems on the vehicle, the electronics subsystems should be integrated into a single package. On the S-10, the engine control system, APU control system, and boost regulator are all separate electronic subsystems. Each of these systems has its own space and electrical power requirements. These subsystems should be integrated together into a single hardened electronic subsystem. This same concept could be carried through to include the drive motor control system. This approach would likely result in the most cost effective approach as well. A closely related topic to integrating the electronic subsystems is to utilize a field controllable generator. Utilizing a generator of this type would eliminate the need for the large and costly boost regulator controller. The boost regulator controller could be substituted for a simple rectifier/regulator circuit.

Lastly, in order to achieve extremely low (EZEV) driving cycle emissions, it would be necessary to incorporate some type of cold start emissions reduction technology, such as an EHC or thermal reactor type system. A rapid catalyst light-off will be necessary since engine emissions during and immediately after startup will comprise a significant portion of the cycle emissions. Either of the above mentioned technologies could be readily tailored for the APU application.

REFERENCES

1. *The 3rd Biennial International Conference & Exhibition on Natural Gas Vehicles,* Proceedings, Part II, Göteborg, Sweden, September 24, 1992, pp. 322.

2. Meyer, R. C., D. P. Meyers, S. M. Shahed, and V. K. Duggal, "Development of a Heavy-Duty On-Highway Natural Gas-Fueled Engine," SAE Paper No.922362.

3. Heywood, J. B., *Internal Combustion Engine Fundamentals,* McGraw Hill, 1988, pp. 655.

4. Weaver, Christopher, S., "Natural Gas Vehicles - A Review of the State of the Art," SAE Paper No. 892133, September 1989.

5. Klimstra, Jacob, "Catalytic Converters for Natural Gas Fueled Engines -- A Measurement and Control Problem," SAE Paper No. 872165, November 1987.

6. White, Jeff, "Low Emission Catalysts for Natural Gas Engines," GRI Topical Report GETA 91-09, SwRI Project No. 03-3178, August 1991.

APPENDIX A

REPORT ON VIPRE SIMULATIONS FOR KOHLER V2 ENGINE

VIPRE SIMULATIONS FOR KOHLER V2 ENGINE

In this report, parametric studies on the intake runner and exhaust runner lengths, the air cleaner volume and valve timing were carried out using VIPRE (Virtual Indicated Performance of Reciprocating Engines) code. VIPRE is a full-cycle simulation designed for engine performance prediction/analysis. VIPRE's calculations showed that the increase of the intake runner length to 0.5m could increase power by 34 percent, while experiments indicated that there was no improvement on power. A study was carried out to understand this contradictory result. It was found that the reason for the erroneous results could be traced to the simplified model used in VIPRE where a characteristic method was employed to solve gas dynamics in the piping system. This method is not capable of directly predicting the pressure loss due to a bend or an elbow, and junction, which is critical to affect tuning. In order to model the pressure loss due to elbows, special provisions are required. In this study, a restriction with a diameter of 0.014m and length of 0.02m was imposed between the intake manifold and the intake port to model the pressure loss due to the elbow in the intake manifold. As a result, it was found that "tuning" was not seen at the intake runner length of 0.5m. This suggests that the strong tuning effect originally found by VIPRE is not correct due to its limitation to model the elbow pressure loss. On the other hand, this suggests that improving the elbow shape could reduce the pressure loss, yielding some power improvement.

1.0 Technical Approach

VIPRE is a suite of engine cycle simulation code that was developed for prediction of engine performance and fuel economy. The techniques are based on the first principles of thermodynamics and gas dynamics. The characteristics method is used for the piping system, while relatively simple submodels are employed for combustion, heat transfer, charge motion and mixing for the engine. Due to its simplicity of characteristics, this method is not able to predict pressure losses due to a bend, or T-junction, nor does it model heat transfer in the piping system. However, previous experience shows that, if it is used judiciously, it can help to reduce the scope of testing and development required to achieve design goals.

The approach taken to perform the parametric study was first to construct a baseline engine model at 3600 rpm. The intake, exhaust, and engine geometry were provided by SwRI personnel while the cam profile and valve timing were provided by Kohler. Valve flow coefficients were not identified. Therefore, the flow coefficients of a similar engine were used. The air cleaner was modeled as a volume, and an orifice was used to model the pressure loss across the air cleaner. Due to a lack of pressure measurements at the air cleaner, this orifice diameter was varied in order to match experimental data. However, once the simulated result was correlated to actual engine data, the parametric studies were then carried out.

2.0 Simulated Results

In this section, no restriction was imposed at the connection between the intake manifold and the intake port. Actual engine data was matched as closely as possible.

2.1 Baseline Model Simulation

Table 1 lists performance comparison data between the baseline simulation and actual measurements. Note that the results predicted by VIPRE agree well with the actual engine data.

TABLE 1. COMPARISON BETWEEN DATA AND VIPRE SIMULATION

Source	Brake Power (kW)	Air Flow (kg/s)
Engine Data	13.80	0.0164
Simulation Result	13.57	0.0168

In view of the above comparison, parametric studies were performed. Parametric studies of valve timing, air cleaner volume, and exhaust and intake runner length were then performed, respectively. It should be pointed out that a compression ratio of 8:1 was used for the above baseline model and the valve timing simulations, while a compression ratio of 12:1 was used for the remaining parametric studies.

2.2 Parametric Studies

2.2.1 Valve Timing Optimization

Valve timing optimization consisted of varying the intake and exhaust opening and closing timings. Whenever one timing event was varied, all other timings remained fixed. Table 2 through 5 list the results of the simulation.

TABLE 2. INTAKE VALVE CLOSING (IVC)*

IVC	Brake Power (kW)	Air Flow (kg/s)
Baseline (270 ATDC)	13.57	0.0168
220	12.98	0.0161
230	13.43	0.0165
240	13.68	0.0168
250	13.80	0.0169
260	13.76	0.0169
280	13.55	0.0164
285	12.98	0.0161
*Values are CAD with respect to TDC at the beginning of the intake stroke.		

TABLE 3. INTAKE VALVE OPENING (IVO)

IVO	Brake Power (kW)	Air Flow (kg/s)
Baseline (-41 BTDC)	13.57	0.0168
-11	13.28	0.0167
-21	13.47	0.0169
-31	13.56	0.0169
-51	13.55	0.0170
-61	12.81	0.0161
-71	12.75	0.0161

TABLE 4. EXHAUST VALVE OPENING (EVO)*

EVO	Brake Power (kW)	Air Flow (kg/s)
Baseline (-249)	13.57	0.0168
-219	12.89	0.0163
-229	13.20	0.0165
-239	13.43	0.0166
-259	13.61	0.0164
-269	13.50	0.0167
-279	13.43	0.0168
* Angles are CAD with respect to TDC at the beginning of the intake stroke (TDC).		

TABLE 5. EXHAUST VALVE CLOSING (ECV)

EVC	Brake Power (kW)	Air Flow (kg/s)
Baseline (72)	13.57	0.0168
42	13.43	0.0166
52	13.51	0.0167
62	13.59	0.0168
82	13.46	0.0166
92	13.30	0.0164
102	12.90	0.0160

From the preceding tables, it is shown that power increases were predicted with IVC at 250 CAD ATDC. The baseline values for all other events were found to be nearly optimal.

2.2.2 *Air Cleaner Volume*

Table 6 shows the results of the parametric study on the air cleaner volume. The volume was varied from 0.0008 m^3 to 0.004 m^3 (piston displacement is 0.000312 m^3). The basic trend is that the increase of the volume is accompanied with an increase of power.

TABLE 6. OPTIMIZATION OF AIR CLEANER VOLUME

Air Cleaner Volume (m^3)	Brake Power (kW)	Air Flow (kg/s)
Baseline (0.001 m^3)	14.82	0.01670
0.0008	14.94	0.01675
0.0015	15.27	0.01702
0.0025	15.78	0.01736
0.0035	16.15	0.01754
0.0040	16.23	0.01755

2.2.3 *Exhaust Runner Length*

The exhaust runner length was varied from 0.15m to 0.60m. It was found that with an exhaust runner length of 0.7m, power was increased from 14.82 kW to 16.45 kW. The results are shown in Table 7.

TABLE 7. PARAMETRIC STUDY ON EXHAUST RUNNER LENGTH

Exhaust Runner Length (m)	Brake Power (kW)	Air Flow (kg/s)
Baseline (0.089m)	14.82	0.01670
0.15	14.85	0.01670
0.20	15.16	0.01696
0.30	14.72	0.01659
0.40	14.46	0.01636
0.50	15.63	0.01745
0.60	16.24	0.01800
0.70	16.45	0.01814
0.80	15.79	0.01753
0.90	15.17	0.01689
1.00	14.37	0.01609

2.2.4 Intake Runner Length

The simulations show that power can be increased to 19.85 kW if the intake runner length was set at 0.5m. This represents a 34 percent improvement compared to the baseline model (14.82 kW). Table 8 lists the predicted results.

TABLE 8. PARAMETRIC STUDY FOR INTAKE RUNNER LENGTH

Intake Runner Length (m)	Brake Power (kW)	Air Flow (kg/s)
Baseline (0.00m)	14.82	0.01670
0.10	14.86	0.01668
0.20	14.98	0.01682
0.30	14.94	0.01684
0.40	15.76	0.01769
0.50	19.85	0.02195
0.60	16.77	0.01856
0.70	15.92	0.01790
0.80	16.35	0.01710
0.90	16.04	0.01684
1.00	16.19	0.01701

An engine experiment immediately followed based on the runner length VIPRE suggested. However, the experiment did not show any significant power improvement. In order to understand the source of error in the simulation, another study was conducted. Details of this study are provided in the next section.

3.0 Discussion and Comments on VIPRE

Three possible sources of error were identified in setting up the VIPRE model for the Kohler engine. The first was that the orifice of the air cleaner was incorrectly modeled. The second may have been the incorrect use of the valve flow coefficients. The third could be linked to the sharp elbow in the intake manifold going to the intake ports. This was not directly modeled by VIPRE.

Due to the nature of the one-dimensional model, the only way to model the pressure loss across the air cleaner is to use an orifice. A parametric study was carried out by varying the orifice diameter. The results show that varying the orifice diameter changes the magnitude of tuning, but peak power was still seen in the intake runner length around 0.5m, suggesting that this orifice was not the reason for the tuning.

The intake port contains a very sharp corner, which should cause a noticeable pressure loss. The valve flow coefficient used for the Kohler engine was from another engine. However, the flow behavior of the Kohler engine could be quite different due to the sharp corner. To understand this effect, the flow coefficients were varied from -100 percent to +100 percent. Interestingly, the strong tuning at the length of 0.5m was still found, although power was changed noticeably.

It was noticed that the orifice, representing the air cleaner, and the sharp corner of the intake port were located at the ends of the intake system. The above results indicate that the variation of the end conditions only change wave magnitude. This resulted in a change of power magnitude, but did not change the wave pattern in the intake system. This means that the compression or expansion wave still remains the same type during valve opening or closing, regardless of the variation of the end conditions. Therefore, the only components that would cause the wave pattern to change must be located in the middle of the intake system.

By carefully checking the intake manifold, a sharp elbow in the outlet of the manifold was discovered. Due to model limitations, VIPRE can not directly model the pressure loss across the bend or elbow without special treatment. In order to model this pressure loss, a restriction with a diameter varying from 0.010m to 0.014m and a length of 0.02m was imposed at the location between the intake manifold and the intake port. Figure 1 shows the VIPRE simulation results. It is clear that this restriction changes the wave pattern significantly, resulting in tuning disappearance around the intake runner length of 0.5m. This finding was consistent with that found in the engine experiments.

Two conclusions can be drawn from this study. First, VIPRE does require special provisions in order to handle the pressure loss across sharp elbows. This can be accomplished by imposing a restriction around this location. Secondly, the elbow on the actual engine should be redesigned to reduce the pressure loss.

Report prepared by:

Houshun Zhang
Senior Research Engineer
Department of Engine Design
Tel: (210) 522-5290
Fax: (210) 522-4673

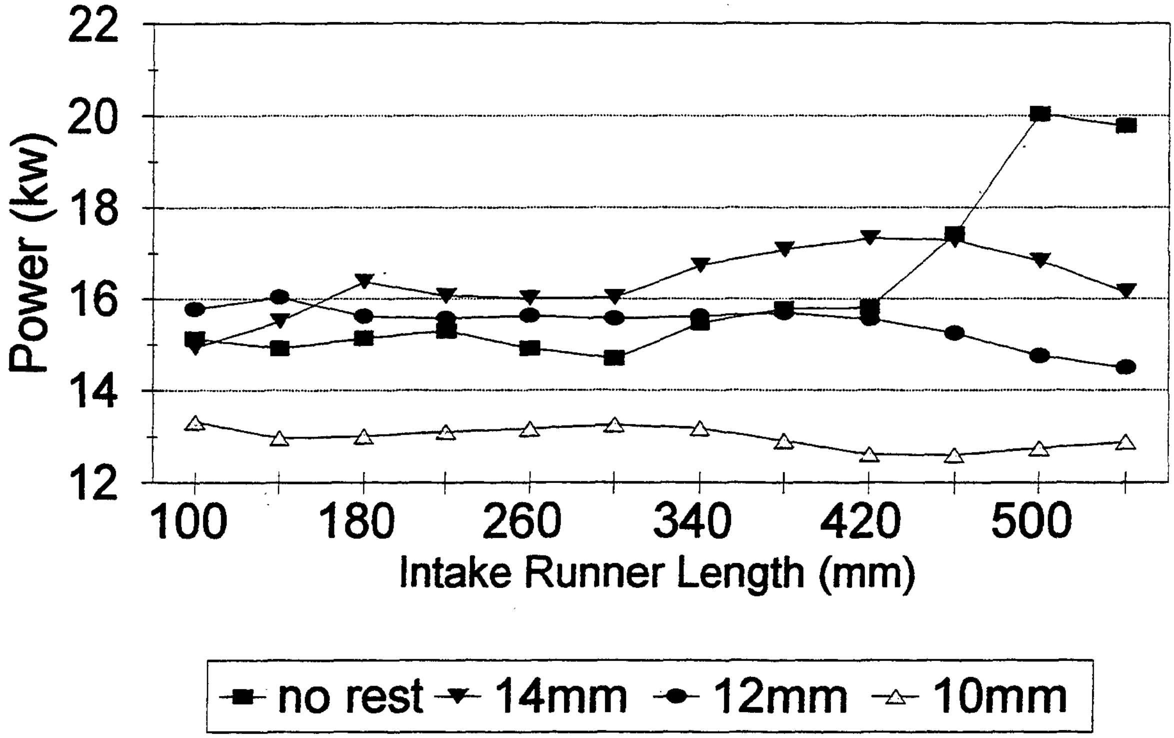

FIGURE 1. EFFECT OF ELBOW RESTRICTION ON TUNING

APPENDIX B

REPORT ON ACOUSTIC SURVEY OF THE SwRI/KOHLER COMMAND 22 NATURAL GAS ENGINE

ACOUSTIC SURVEY OF THE SwRI/KOHLER COMMAND 22 NATURAL GAS ENGINE

Acoustic Test Setup

An acoustic survey was performed on a Kohler Command 22 natural gas engine while it was operating in an engine test cell. Figure 1 shows the test setup. The engine test cell is not an ideal location for acoustic measurements due to the highly reflective walls and confined spaces. Acoustic intensity measurements were taken so as to reduce the problems associated with the poor environment. Acoustic intensity is a vector quantity and thus indicates direction of acoustic energy flow as well as amplitude. However, acoustic intensity measurements can be severely compromised in a reflective environment due to standing wave interference.

The equipment used (as shown in Figure 2) included a Rockland System/90 spectral analyzer with built-in A-weighting acoustic filters, an intensity probe with two opposing ½-inch pressure microphones separated by a 16 mm spacer, and a battery power supply for the microphones. The choice of the microphone size and spacer dimension provided accurate measurements in the frequency range of 100 Hz to 3,150 Hz with reduced accuracy beyond this range. The analyzer was triggered off the engine rpm so that sound levels not synchronous with the engine operation would be reduced.

The Kohler Engine was operated at three constant speeds: 3600 rpm, 2600 rpm, and 1600 rpm. The acoustic survey was performed on November 15, 1994. The condition of the engine on this date was recorded by the engine operator. The engine was operated continuously while all of the measurements were completed at each speed. Each side of the engine was identified as follows: front towards the blower (Figure 3), right side towards the solenoid (Figure 4), left side towards the cooling fins (Figure 5), back towards the drive shaft (Figure 6), and top towards the top cover. The plastic cover was removed from the blower throughout the testing.

Acoustic Measurements: Sound Pressure Levels

A-Weighted sound pressure level (SPL) measurements were taken at each engine operating speed to determine general acoustic trends. Four measurements were made at each speed: (1) one meter in front, (2) one meter from the right side, (3) one meter from the left side, and (4) ½ meter from the top. The back and bottom of the engine were inaccessible for acoustic measurements.

Figures 7 through 9 show the SPL results over the frequency range of 0 to 10,000 Hz for each of the 1600 rpm, 2600 rpm and 3600 rpm operating speeds, respectively. The general trends of the data are similar for each operating speed:

- High amplitudes at lower frequencies associated with engine firing orders,
- Large increase in SPL near 2,600 Hz, possibly due to a structural resonance,
- Overall decrease in SPL with increasing frequency above 3,000 Hz.

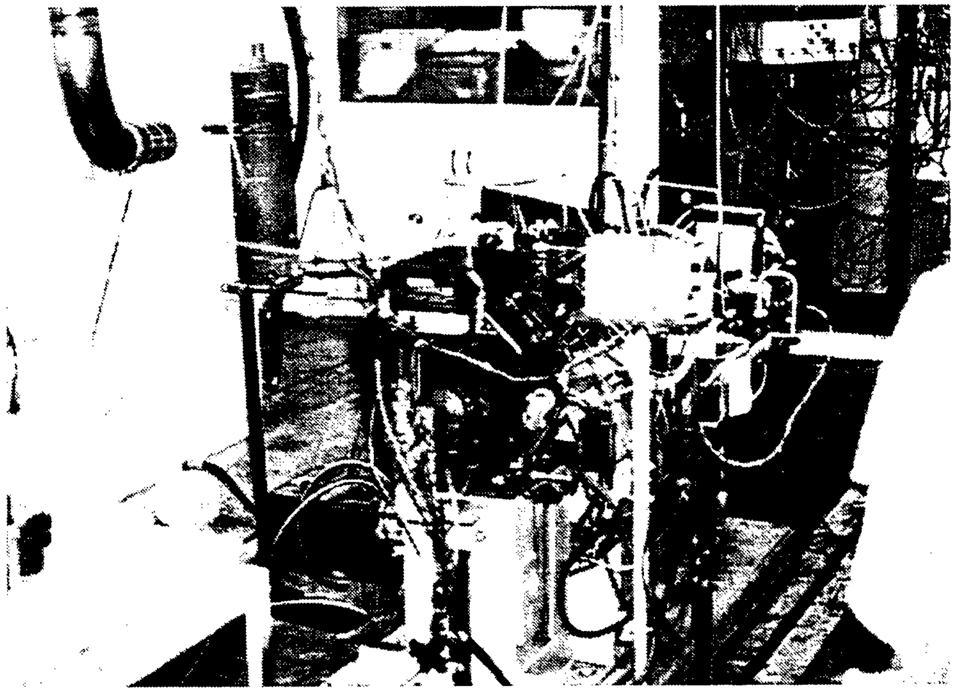

FIGURE 1. ACOUSTIC TEST SETUP

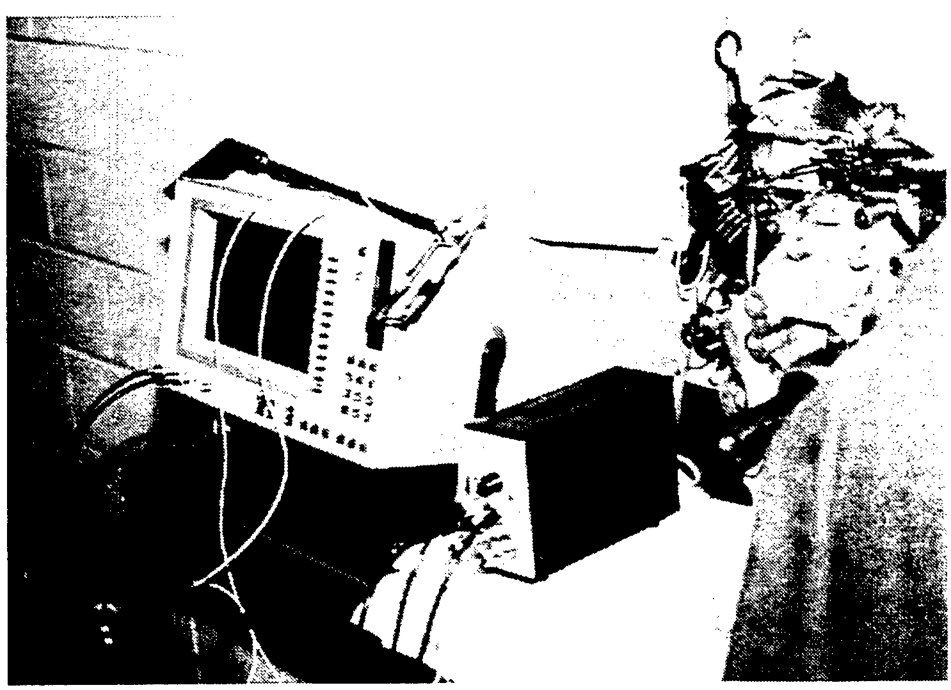

FIGURE 2. ACOUSTIC INTENSITY EQUIPMENT

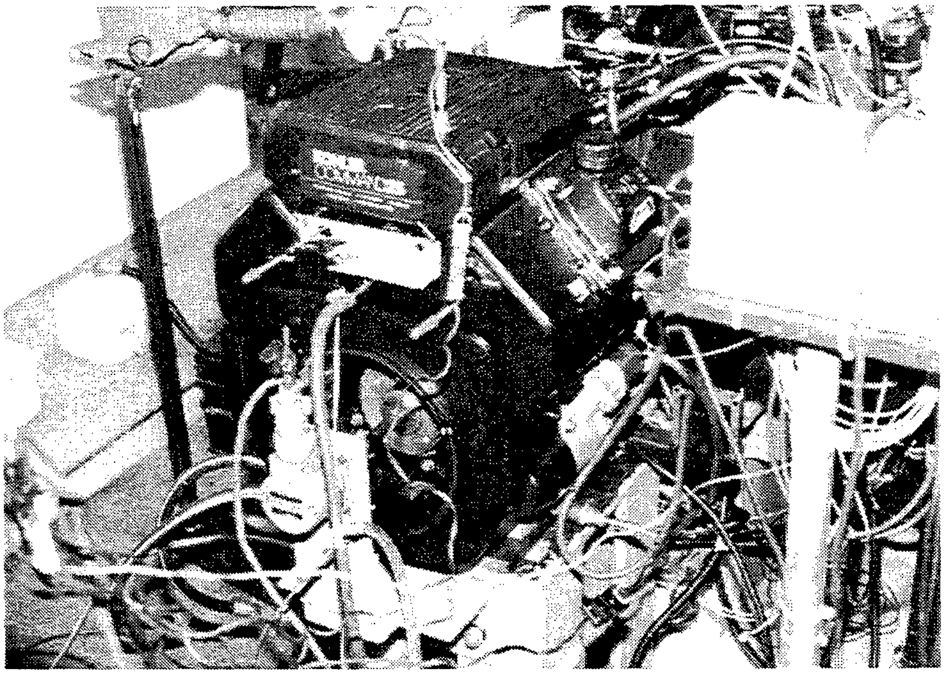

FIGURE 3. FRONT OF ENGINE

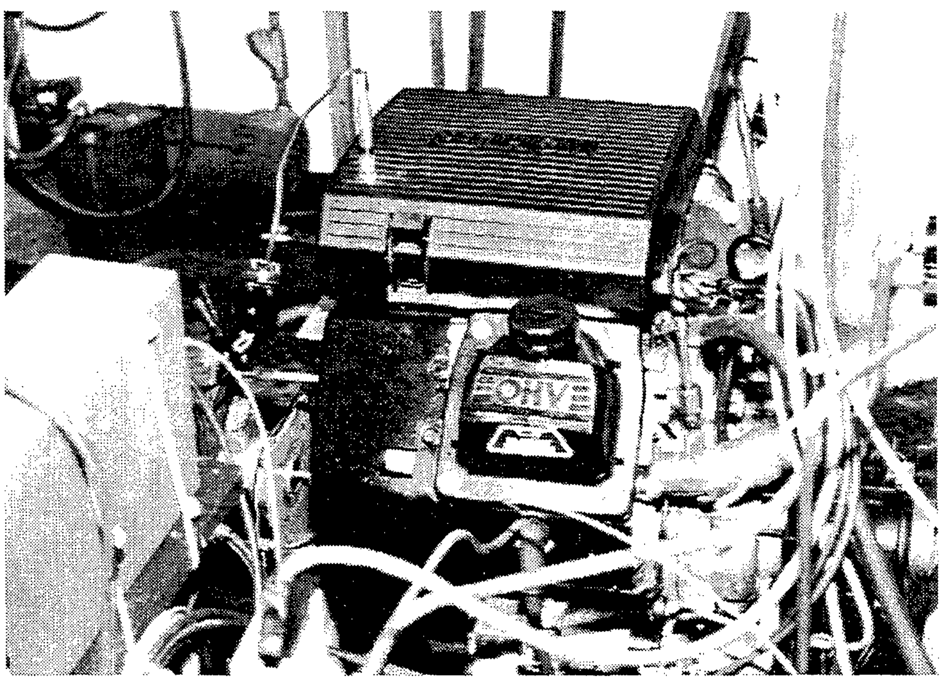

FIGURE 4. RIGHT SIDE OF ENGINE

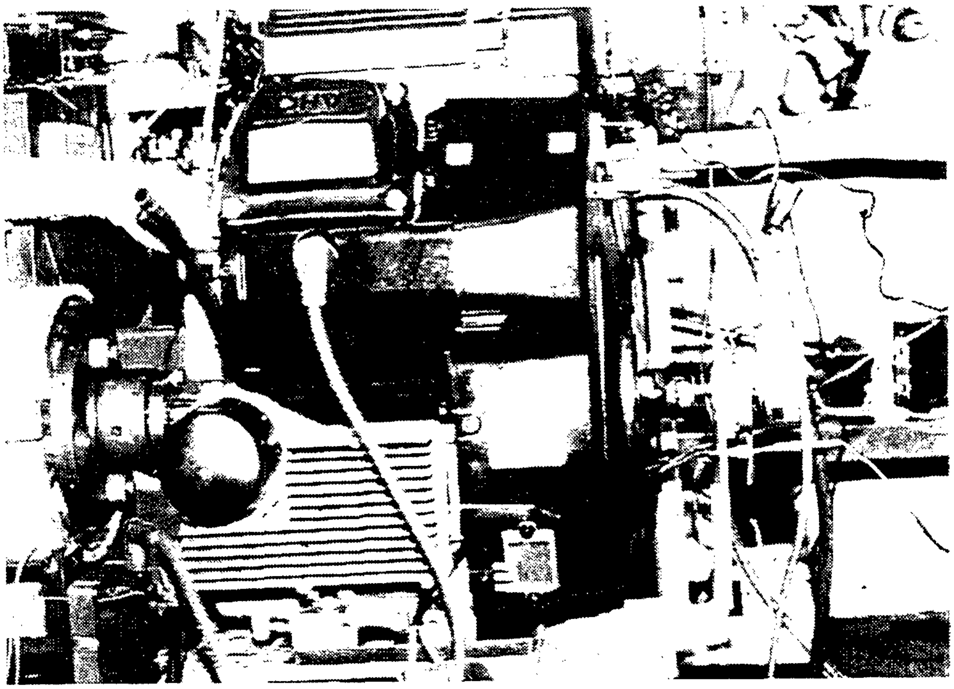

FIGURE 5. LEFT SIDE OF ENGINE

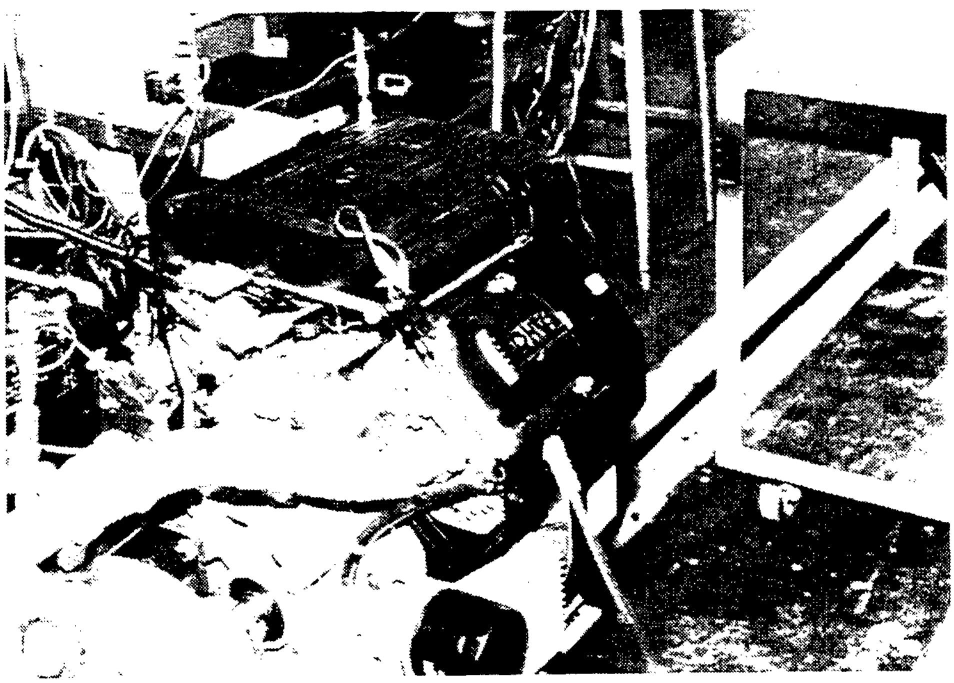

FIGURE 6. BACK OF ENGINE

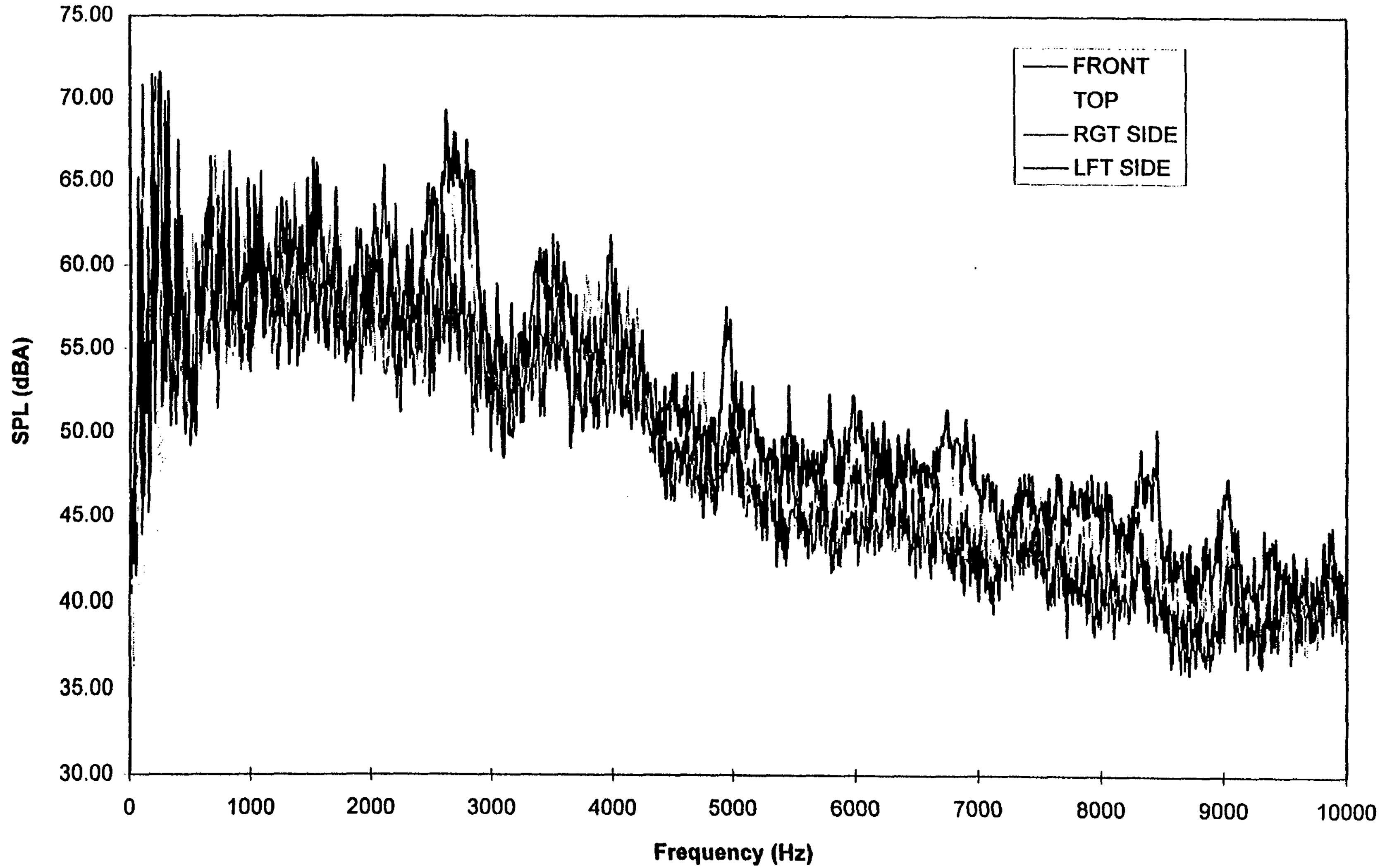

FIGURE 7. SPL MEASUREMENTS AT 1600 RPM

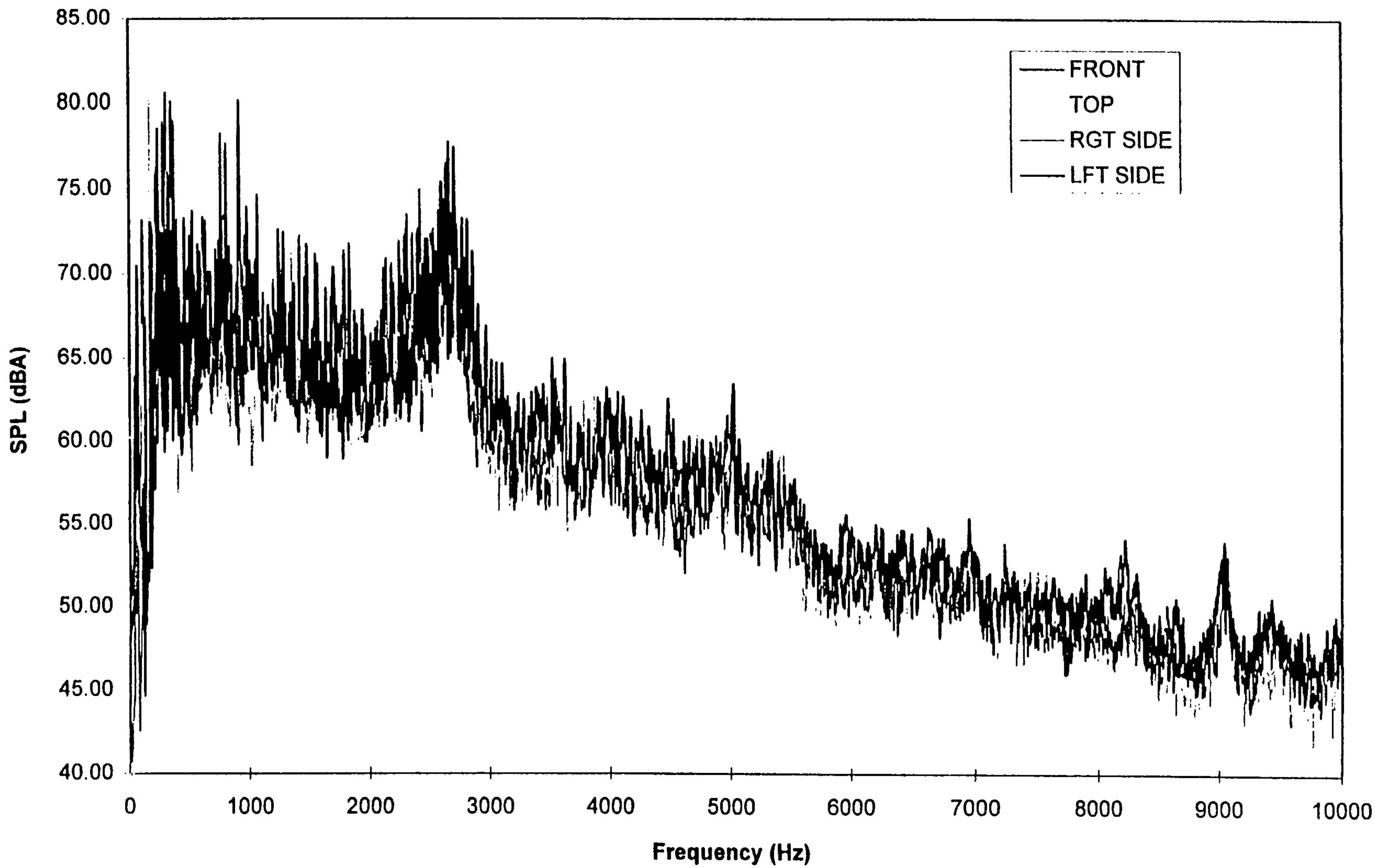

FIGURE 8. SPL MEASUREMENTS AT 2600 RPM

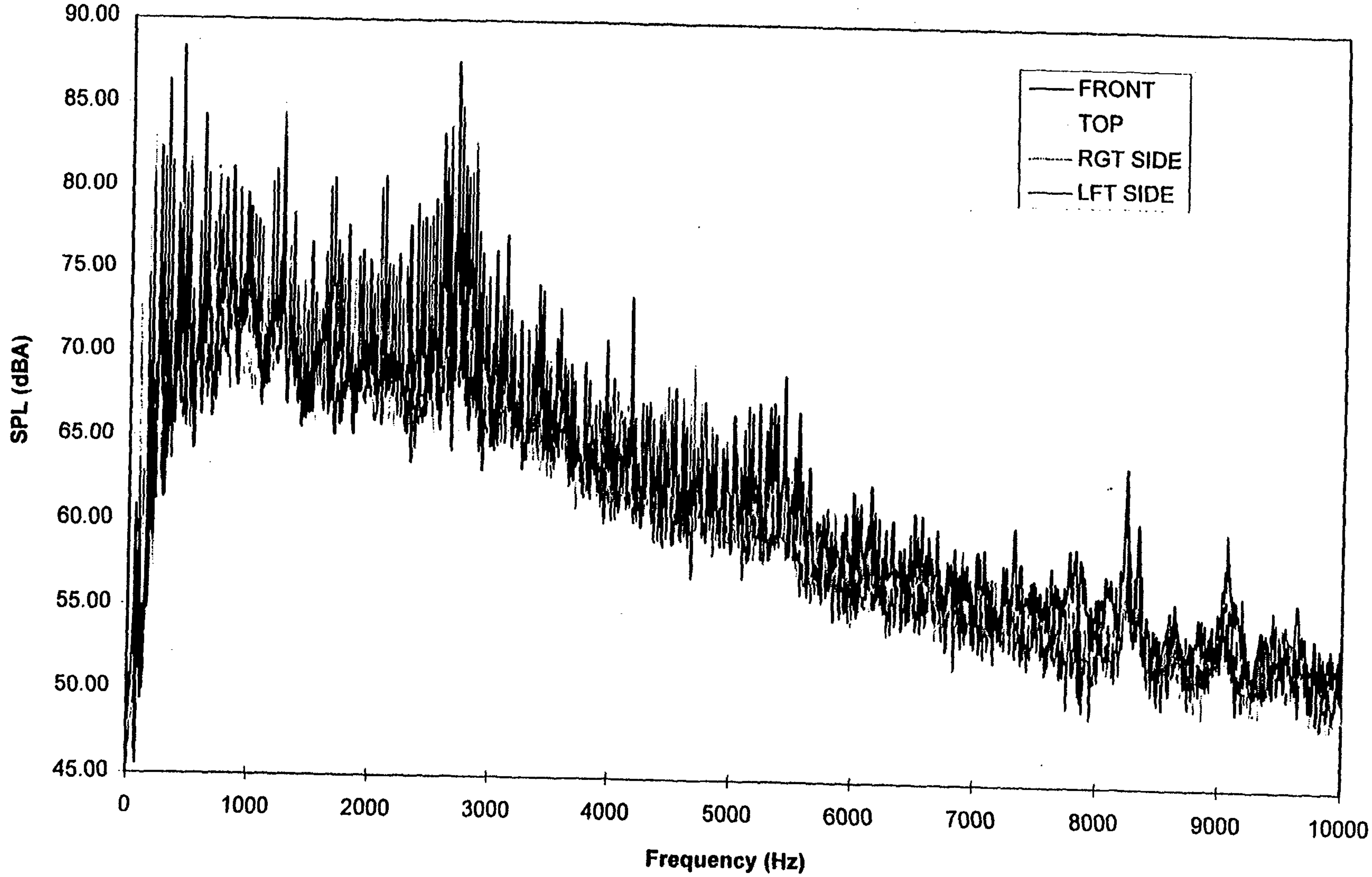

FIGURE 9. SPL MEASUREMENTS AT 3600 RPM

Figures 10 through 12 show the SPL measurements through 3,000 Hz since this frequency range dominates the overall sound emission. Beside the high SPL amplitudes below 500 Hz and near 2,600 Hz, significant peaks occur near 800 Hz at 2600 rpm and near 1,250 Hz at 3600 rpm. Thus, there are a number of potential noise sources that must be addressed to begin reduction of overall noise levels.

The overall SPL levels at each measurement position are listed in Table 1. Again, the test conditions were less than ideal and thus these levels should be used for relative comparison between engines operated in the same environment. Note that the levels at each engine speed are relatively constant at each position. This indicates that the SPL measured is diffuse rather direct and thus dependent on the acoustic environment.

TABLE 1. OVERALL SPL AT EACH MEASUREMENT POSITION*

Measurement Position	Overall SPL (dBA) 1600 rpm	Overall SPL (dBA) 2600 rpm	Overall SPL (dBA) 3600 rpm
Front	86.6	95.0	100.3
Top	87.5	94.5	99.9
Right Side	86.1	94.7	100.2
Left Side	89.1	94.9	100.8
Average	87.5	94.8	100.3
* To be used for relative comparisons only, not for absolute levels			

The conclusions from the SPL survey are:

- Low frequency noise, below 500 Hz, is a significant source of the overall SPL. Noise abatement through sound absorption or transmission loss may be limited in this low frequency range.

- A large increase in noise occurs between 2,500 and 3,000 Hz. This frequency range is consistent for all engine operating speeds which may indicate a structural resonance.

- Since the dominant frequency range is less than 3,150 Hz, a 16 mm spacer and ½-inch microphone combination are adequate for acoustic intensity measurements.

Acoustic Measurements: Sound Intensity Measurements

The sound intensity measurements were performed by mapping a grid over the surface of the engine effectively dividing the engine into grid areas. The intensity measurements were then spatially averaged over each grid area at a distance approximately six inches from the surface. Table 2 lists each grid area and the figure in which each area is shown. The photographs indicated in this table are of a non-operating engine similar to the one used for the acoustic survey. Note that the back of the engine was inaccessible thus only a small area at the back of the top cover was surveyed. Figure 13 is a schematic layout of the acoustic intensity survey grid areas.

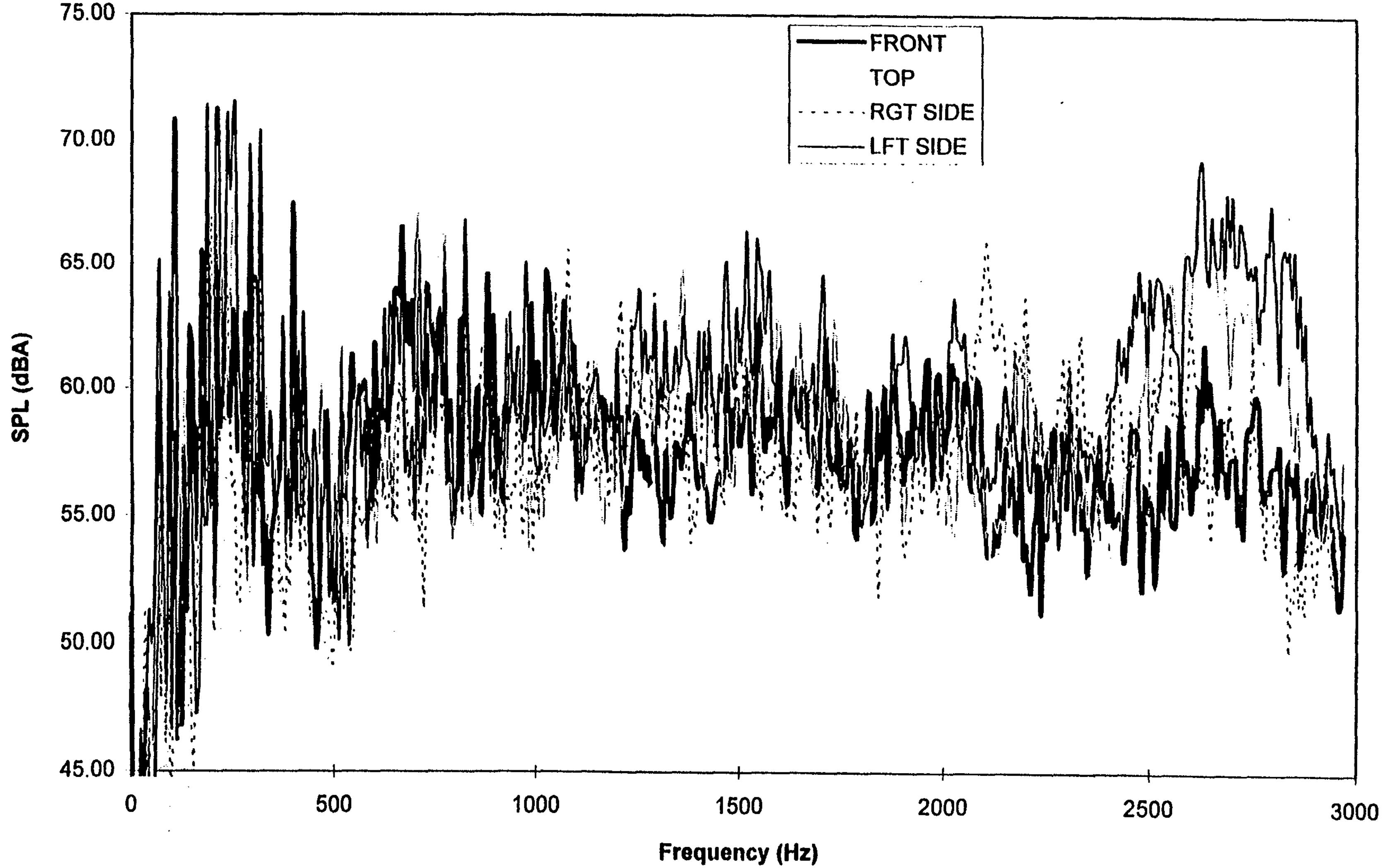

FIGURE 10. SPL MEASUREMENTS AT 1600 RPM (0-3000 Hz)

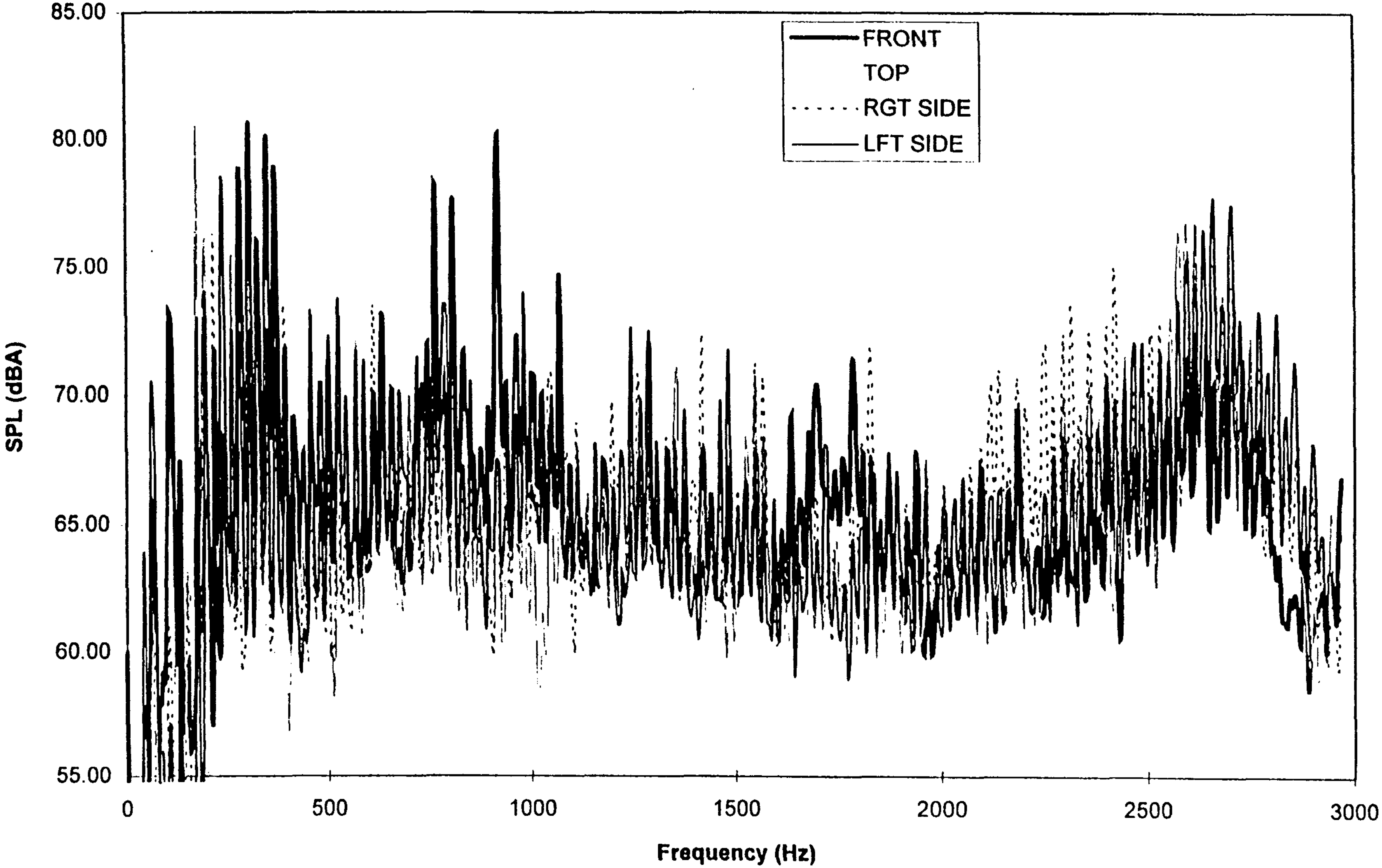

FIGURE 11. SPL MEASUREMENTS AT 2600 RPM (0-3000 Hz)

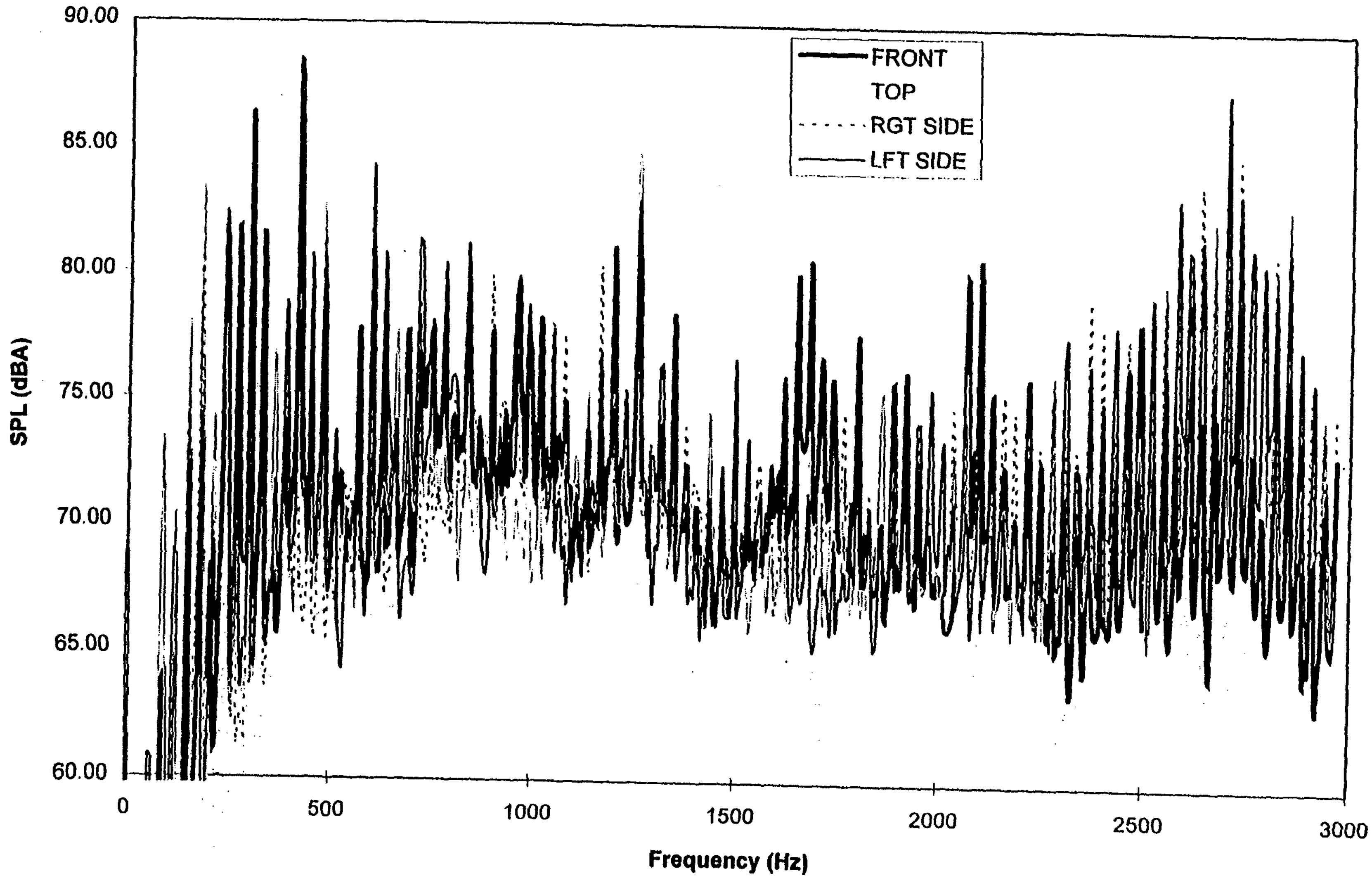

FIGURE 12. SPL MEASUREMENTS AT 3600 RPM (0-3000 Hz)

TABLE 2. ACOUSTIC INTENSITY GRID AREA IDENTIFICATION

Grid No.	Grid Area Identification	Dimensions	Area (in^2)	Figure No.
1	Top Cover Top	9" x 10"	90	14
2	Top Cover Front	9" x 4"	36	14
3	Left Side Top	7" x 10"	70	15
4	Left Side Middle	4" x 10"	40	15
5	Left Side Bottom	7" x 12"	84	15
6	Front Upper Left	6" x 6"	36	14
7	Front Center	12" x 12"	144	14
8	Front Upper Right	6" x 6"	36	14
9	Right Side Top	7" x 10"	70	14
10	Right Side Middle	4" x 10"	40	14
11	Right Side Bottom	7" x 12"	84	14
12	Top Cover Back	9" x 4"	36	16

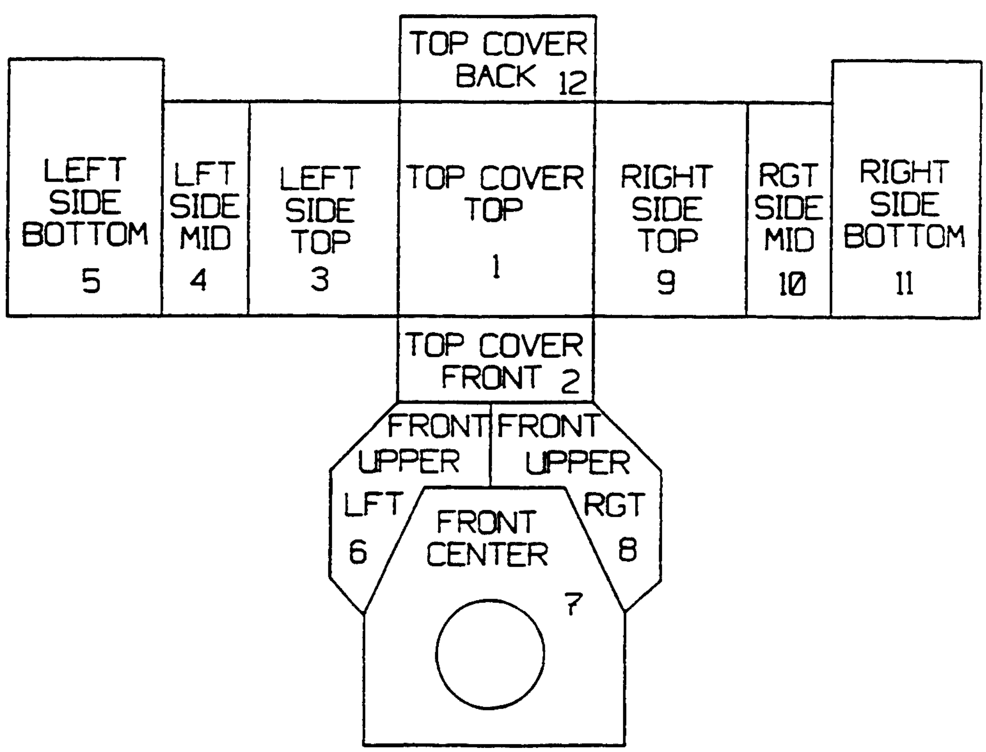

FIGURE 13. ACOUSTIC INTENSITY GRID AREAS, SCHEMATIC LAYOUT

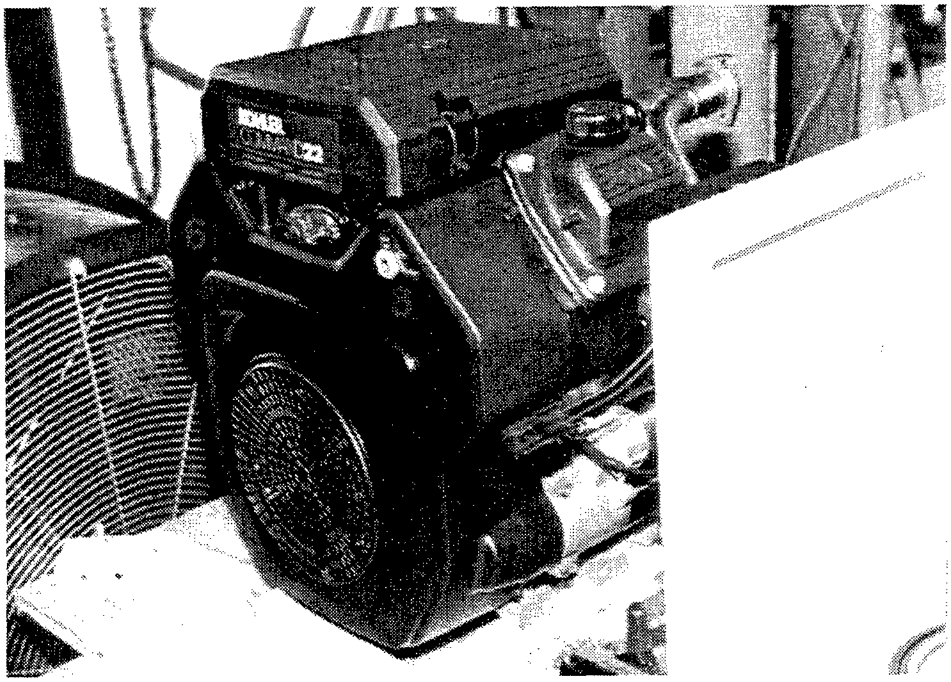

FIGURE 14. ACOUSTIC INTENSITY GRID AREAS,
FRONT AND RIGHT SIDE OF ENGINE

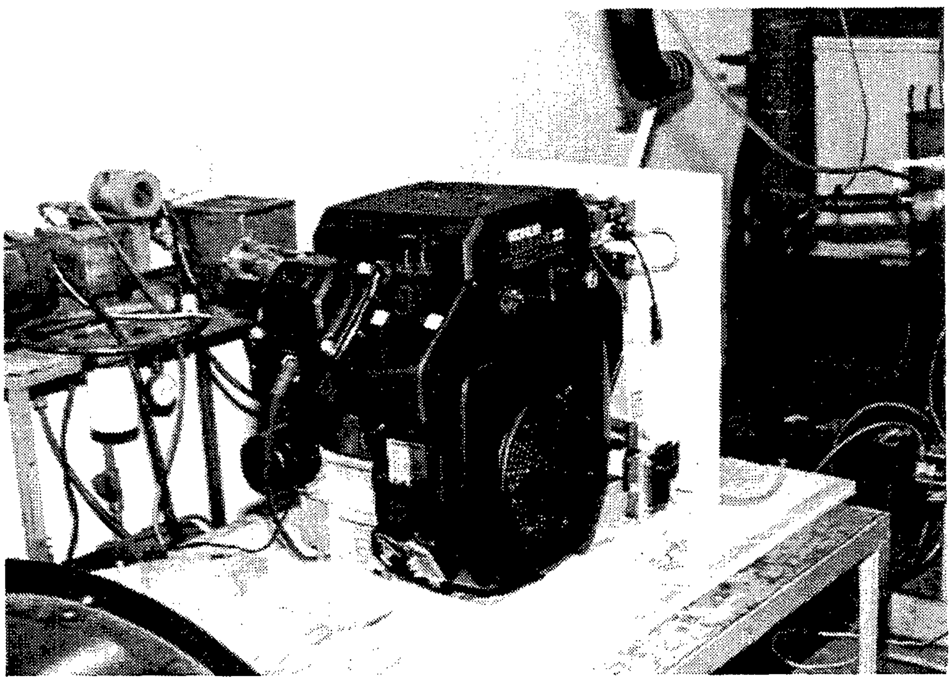

FIGURE 15. ACOUSTIC INTENSITY GRID AREAS, LEFT SIDE OF ENGINE

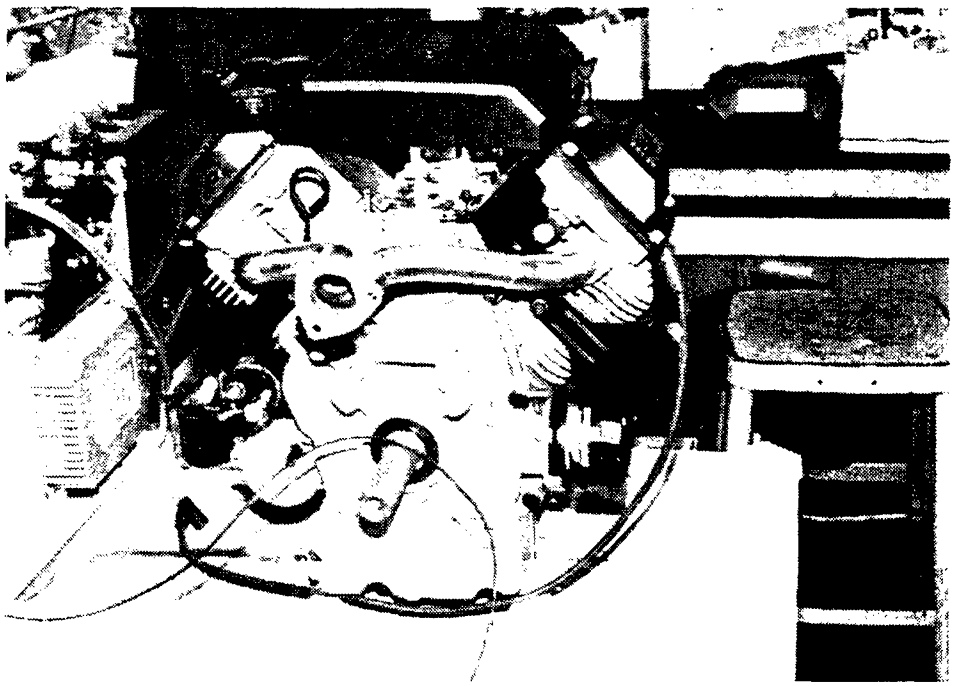

FIGURE 16. ACOUSTIC INTENSITY GRID AREA, BACK OF ENGINE

In addition to the twelve measurements indicated, an intensity survey at 3600 rpm was also conducted on the major components of the engine exhaust system (header, catalytic converter, tail pipe, and muffler). This data is not presented here since these noise sources are not typical of the actual prototype exhaust system. Preliminary results showed that the exhaust system is not a major noise source since the acoustic intensity data showed the noise radiating towards the exhaust components rather than away from them.

The overall sound power radiating from each surface was calculated from the intensity data and is presented in Figures 17 through 19 for each engine rpm. These figures show at a glance where the major noise sources are. Data is not shown where the intensity measurements were negative.

Figures 20 through 22 show the ⅓ octave sound power levels for each grid area at the three engine speeds, respectively. The ⅓ octave band centered at 2,500 Hz is clearly a dominant noise band. Figure 23 through 25 show the sound power levels in the 2,500 Hz band for each grid area. The largest sound power levels lie along the side-to-side axis. This indicates that at this frequency the engine may be rocking side-to-side on the engine support structure. If this were the case, the 2,500 Hz band would not be associated with engine operation but with mounting conditions. A modal survey was beyond the present level of effort.

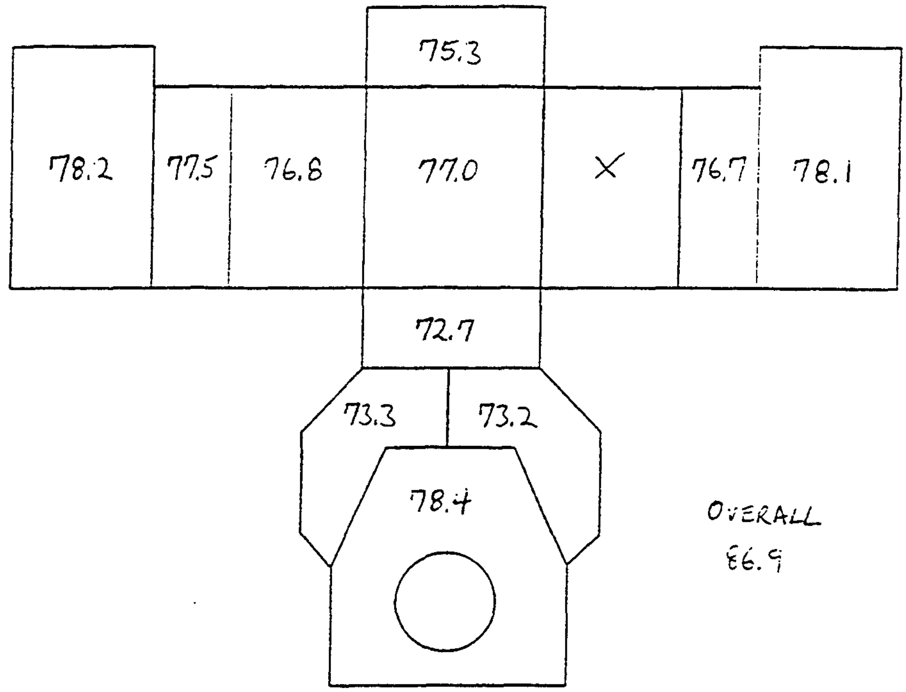

FIGURE 17. OVERALL SOUND POWER LEVEL (dBA), 1600 RPM, 100-3150 Hz

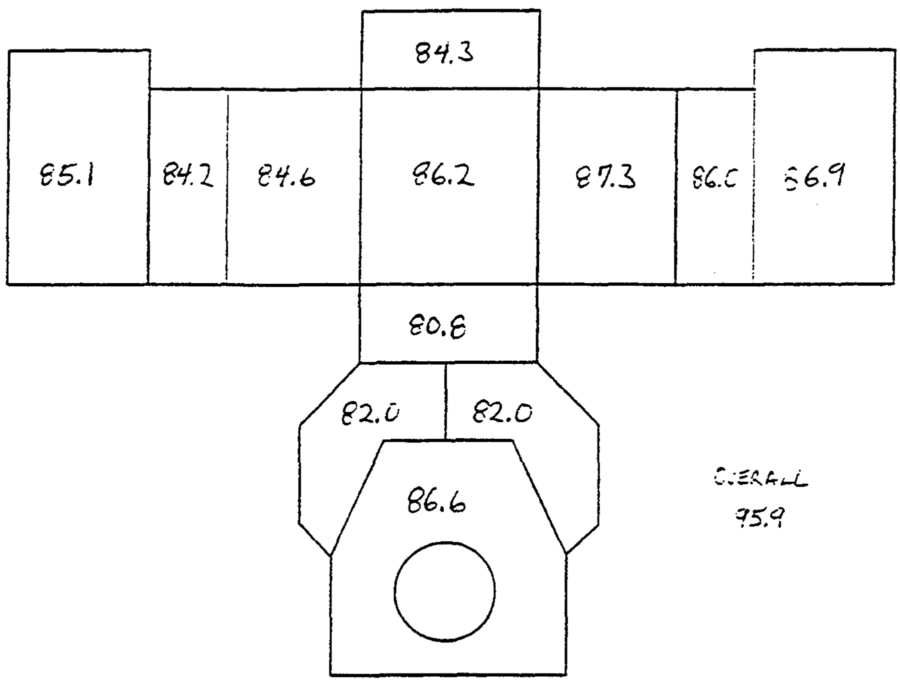

FIGURE 18. OVERALL SOUND POWER LEVEL (dBA), 2600 RPM, 100-3150 Hz

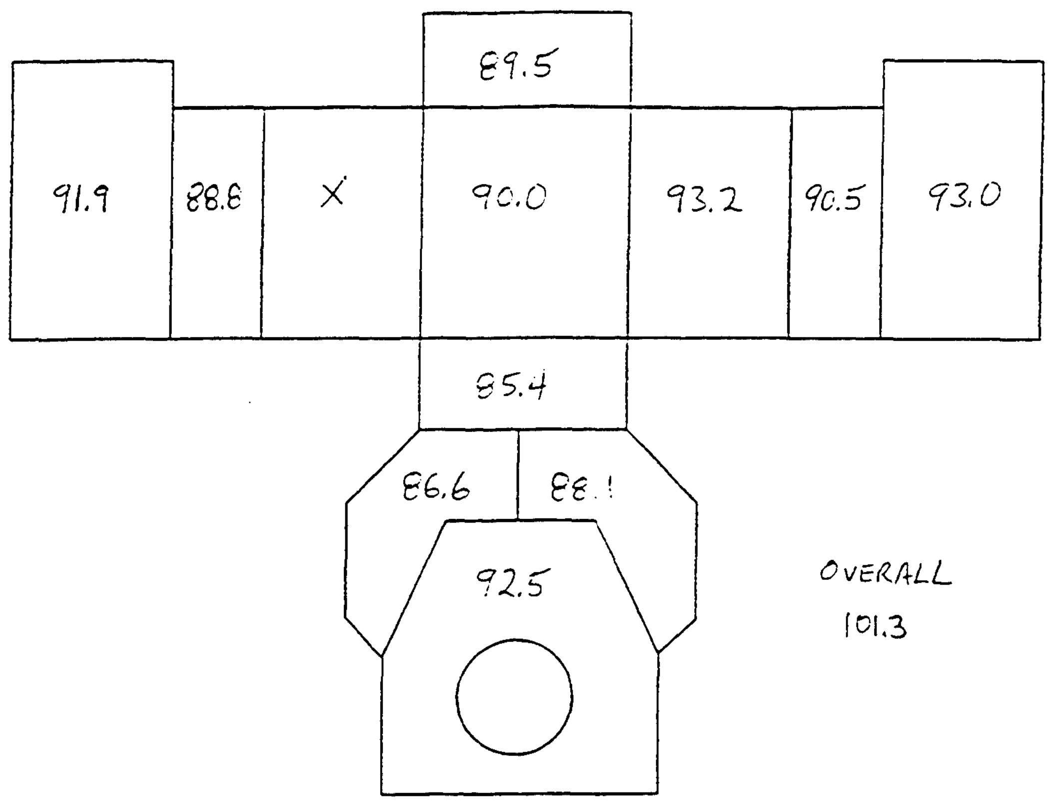

FIGURE 19. OVERALL SOUND POWER (dBA), 3600 RPM, 100-3150 Hz

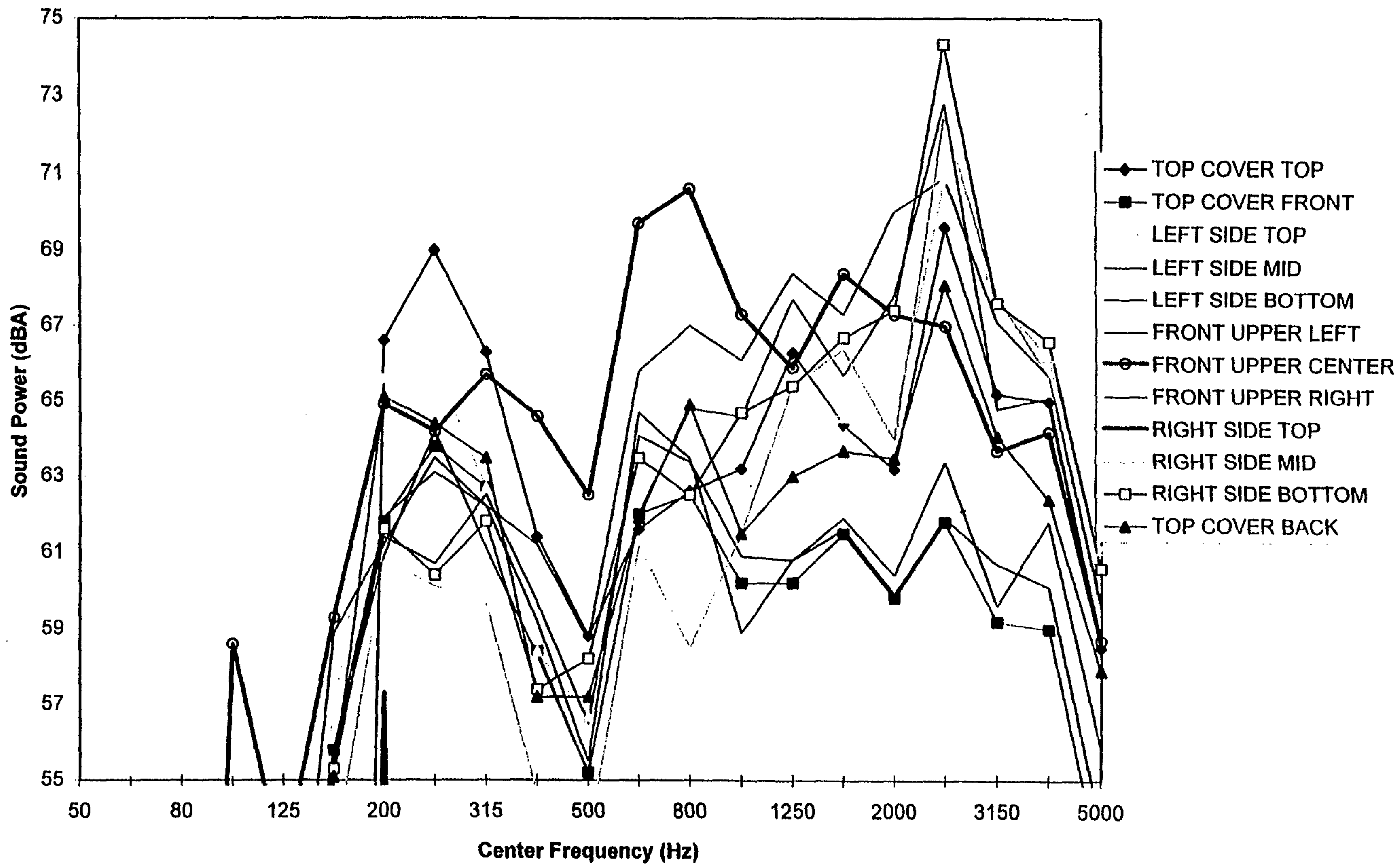

FIGURE 20. THIRD OCTAVE SOUND POWER LEVELS, 1600 RPM

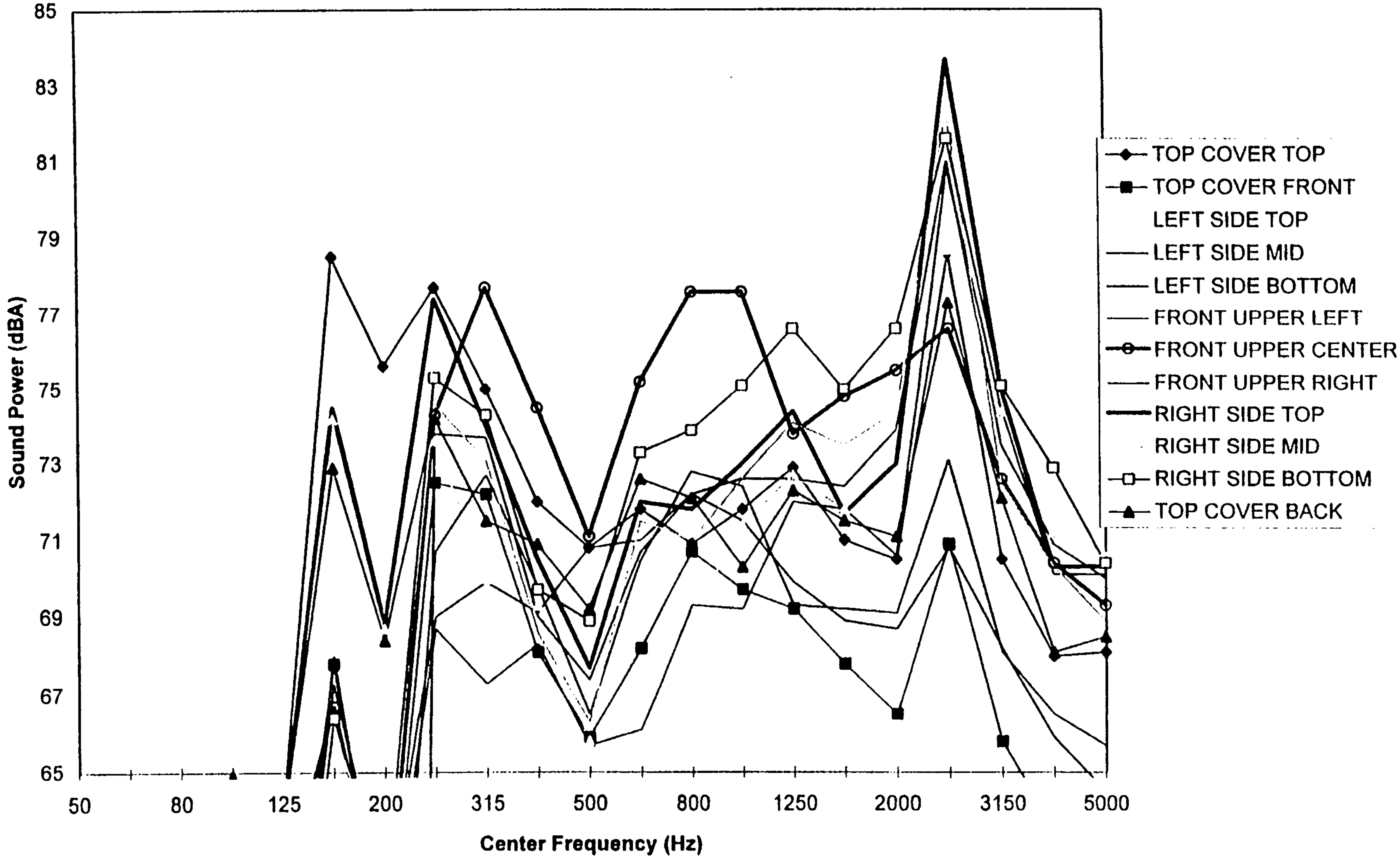

FIGURE 21. THIRD OCTAVE SOUND POWER LEVELS, 2600 RPM

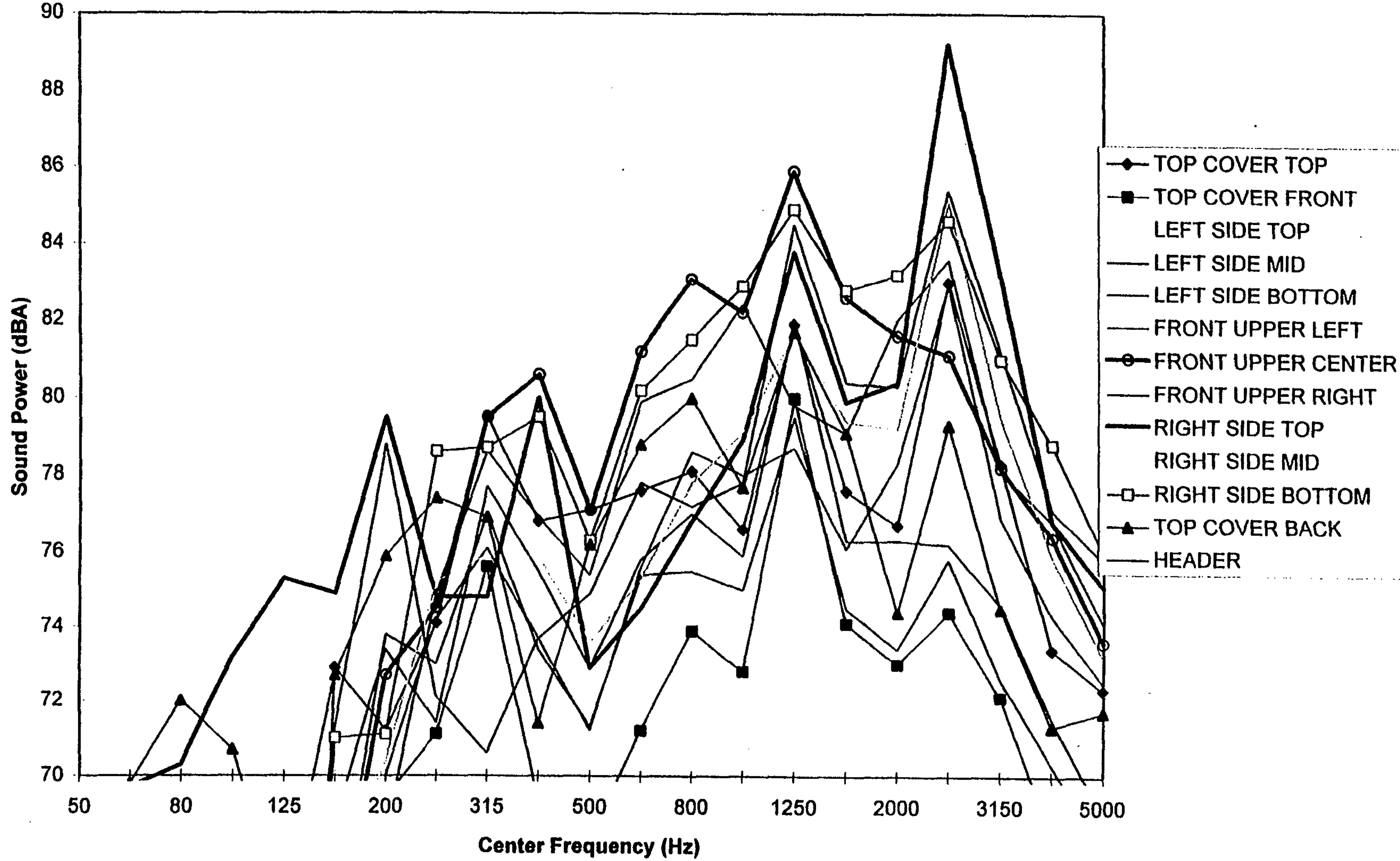

FIGURE 22. THIRD OCTAVE SOUND POWER LEVELS, 3600 RPM

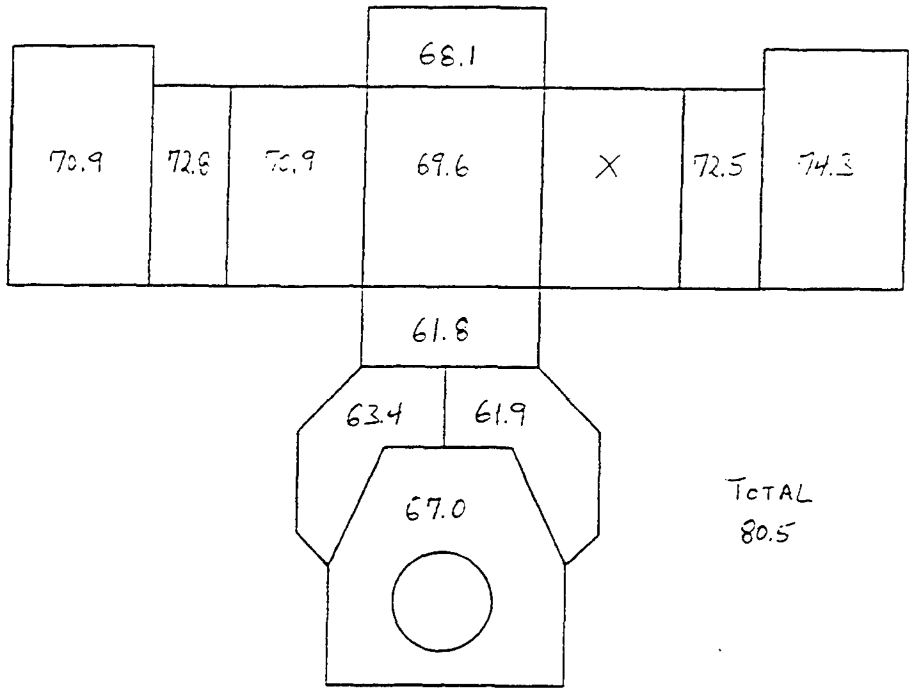

FIGURE 23. ⅓ OCTAVE SOUND POWER LEVEL (dBA), 1600 RPM, 2500 Hz

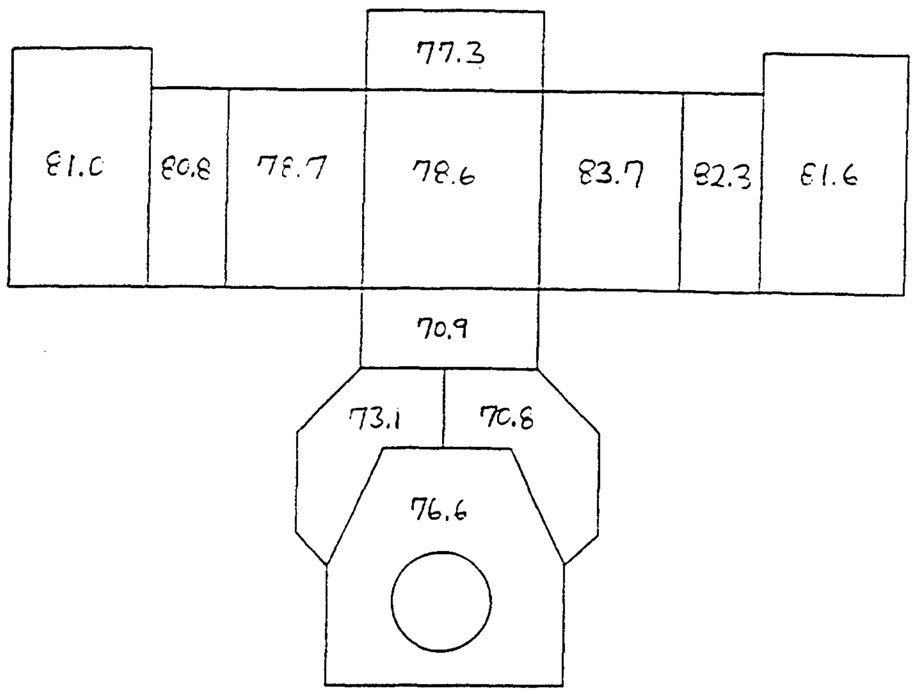

FIGURE 24. ⅓ OCTAVE SOUND POWER LEVEL, 2600 RPM, 2500 Hz

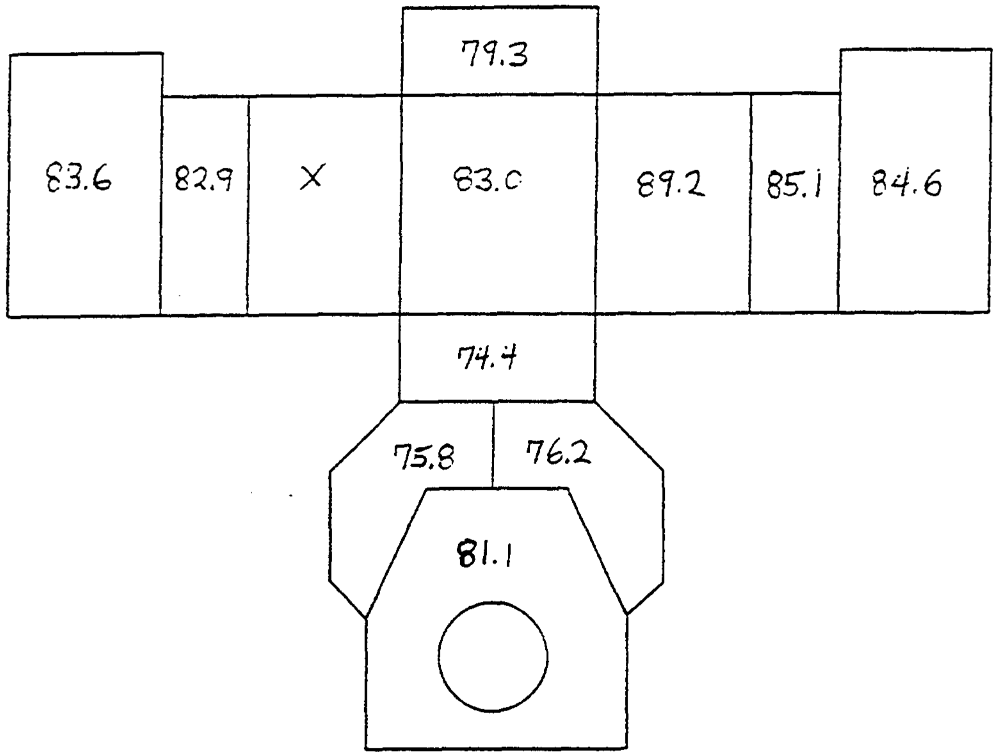

FIGURE 25. ⅓ OCTAVE SOUND POWER LEVEL, 3600 RPM, 2500 Hz

To concentrate on the lower frequency noise radiation, sound power levels were calculated for the frequency bands from 125 to 1,600 Hz. Figures 26 through 28 show the overall sound power levels radiating from each grid area at each engine speed. Figures 29 through 31 are the corresponding ⅓ octave sound power results. The following are results obtained from this lower frequency survey:

- At a glance, the front upper center grid area is dominant in the 500 to 1000 Hz range. This grid area includes the engine fan which is a likely noise source. As the engine rpm increases, the aerodynamic noise associated with the fan becomes less significant.

- The top cover is a dominant noise source at frequencies below 400 Hz for the lower engine speeds indicating a potential induction noise source. The top, sides, and back of the top cover all radiate significant noise at the 1600 and 2600 rpm engine speeds.

- At the 3600 rpm engine speed, the sound power radiation is dominated by the 1,250 Hz ⅓ octave band. Most of the grid areas have a peak in this frequency range. Narrow band analysis indicates that a single resonance peak is present at 1,260 Hz, the 21st order of the fundamental 3,600 rpm (60 Hz) operating speed. A modal survey may indicate whether this peak is another mounting resonance or an engine structural resonance.

- Other than the front upper center position (where the turbine fan is located) and the 1,260 Hz resonance, significant noise radiators at 3600 rpm are the bottom grid areas of the engine on the left and right sides.

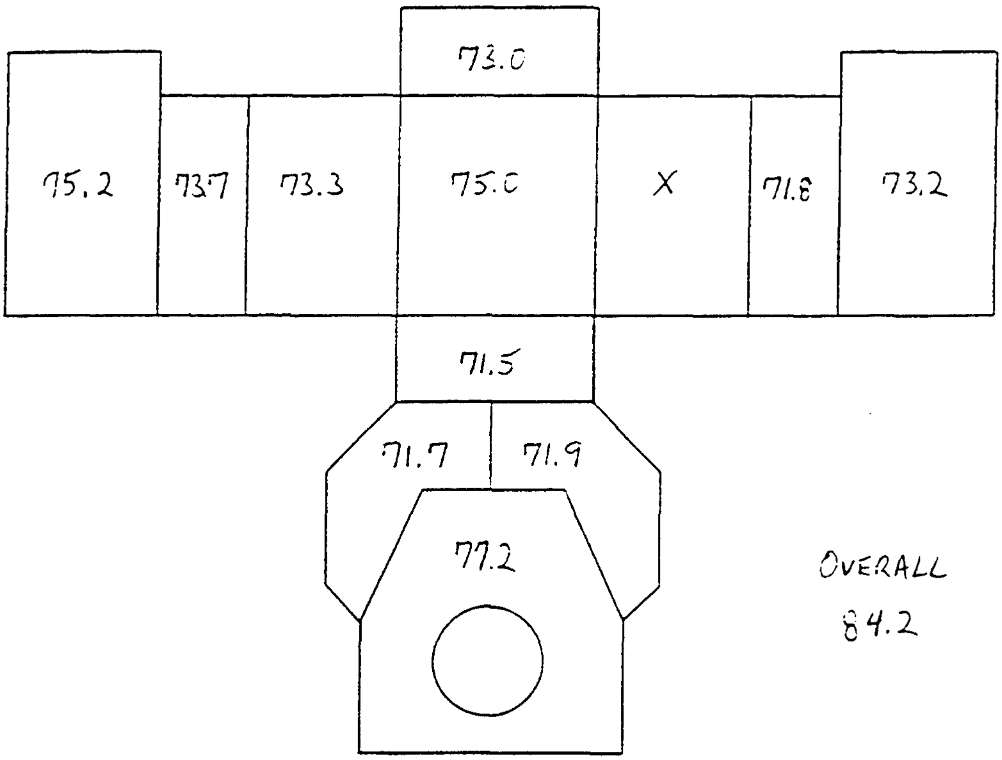

FIGURE 26. OVERALL SOUND POWER LEVEL (dBA), 1600 RPM, 125-1600 Hz

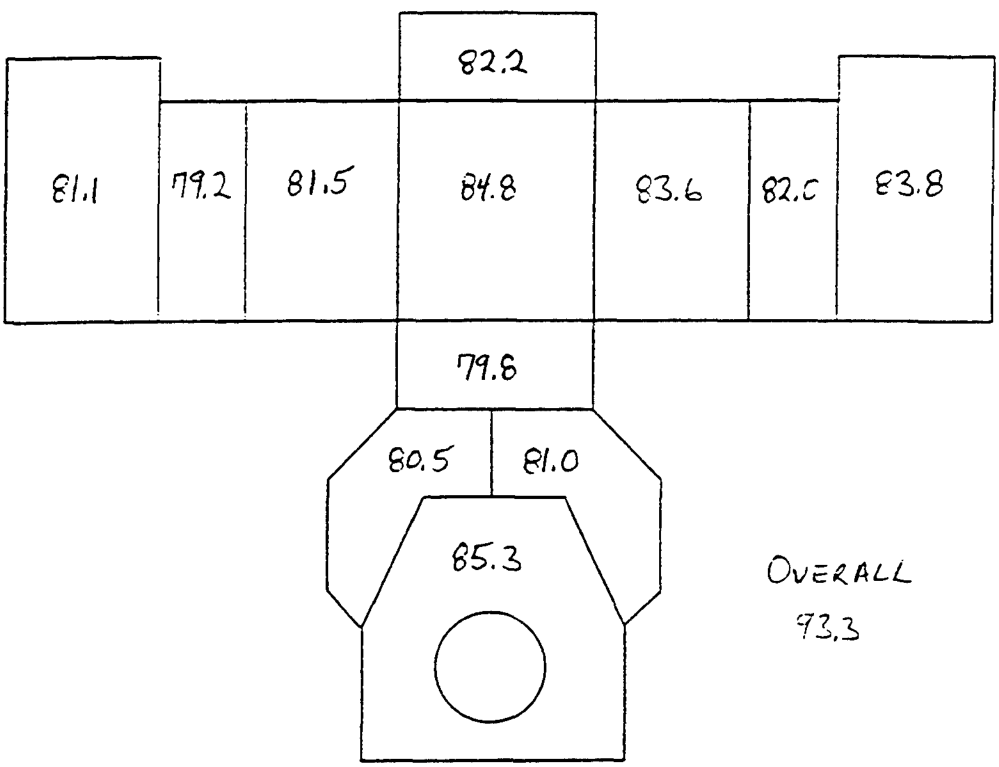

FIGURE 27. OVERALL SOUND POWER LEVEL (dBA), 2600 RPM, 125-1600 Hz

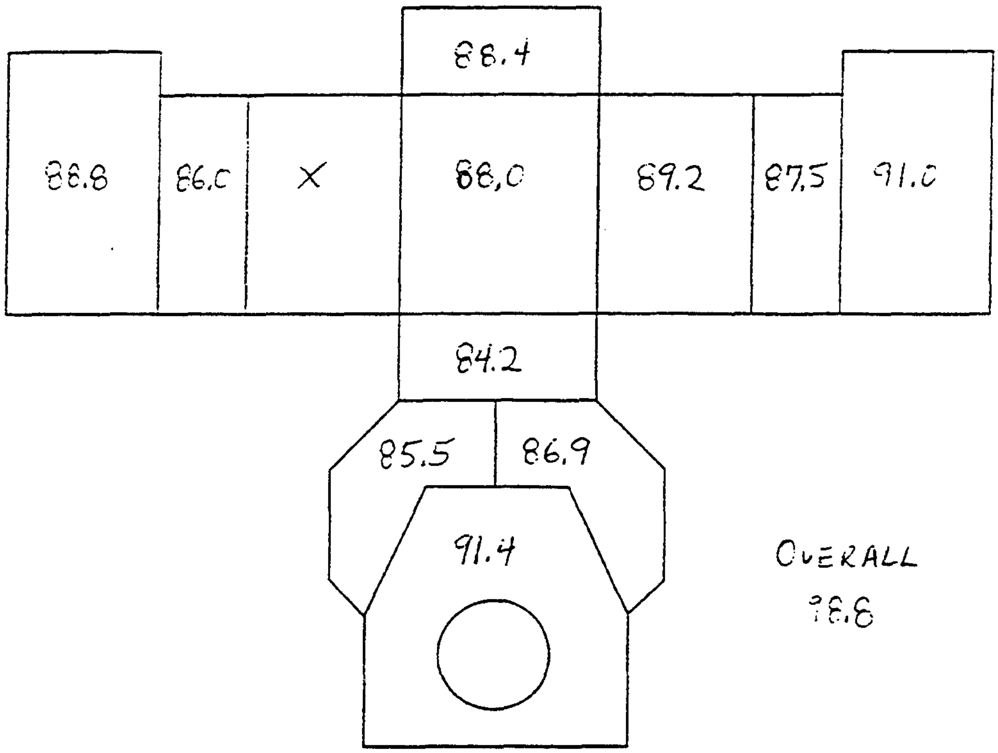

FIGURE 28. OVERALL SOUND POWER LEVEL (dBA), 3600 RPM, 125-1600 Hz

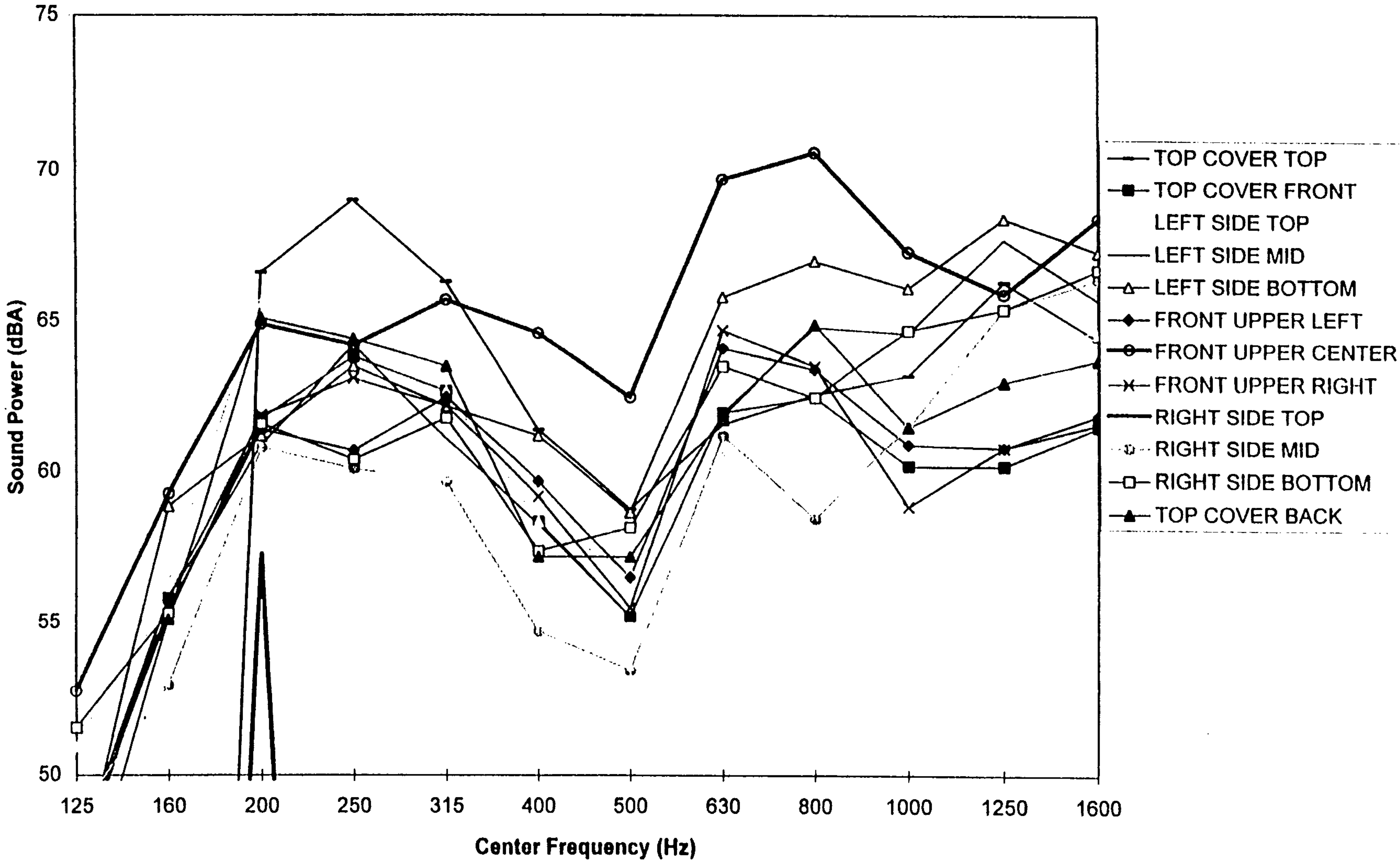

FIGURE 29. THIRD OCTAVE SOUND POWER LEVELS, 1600 RPM

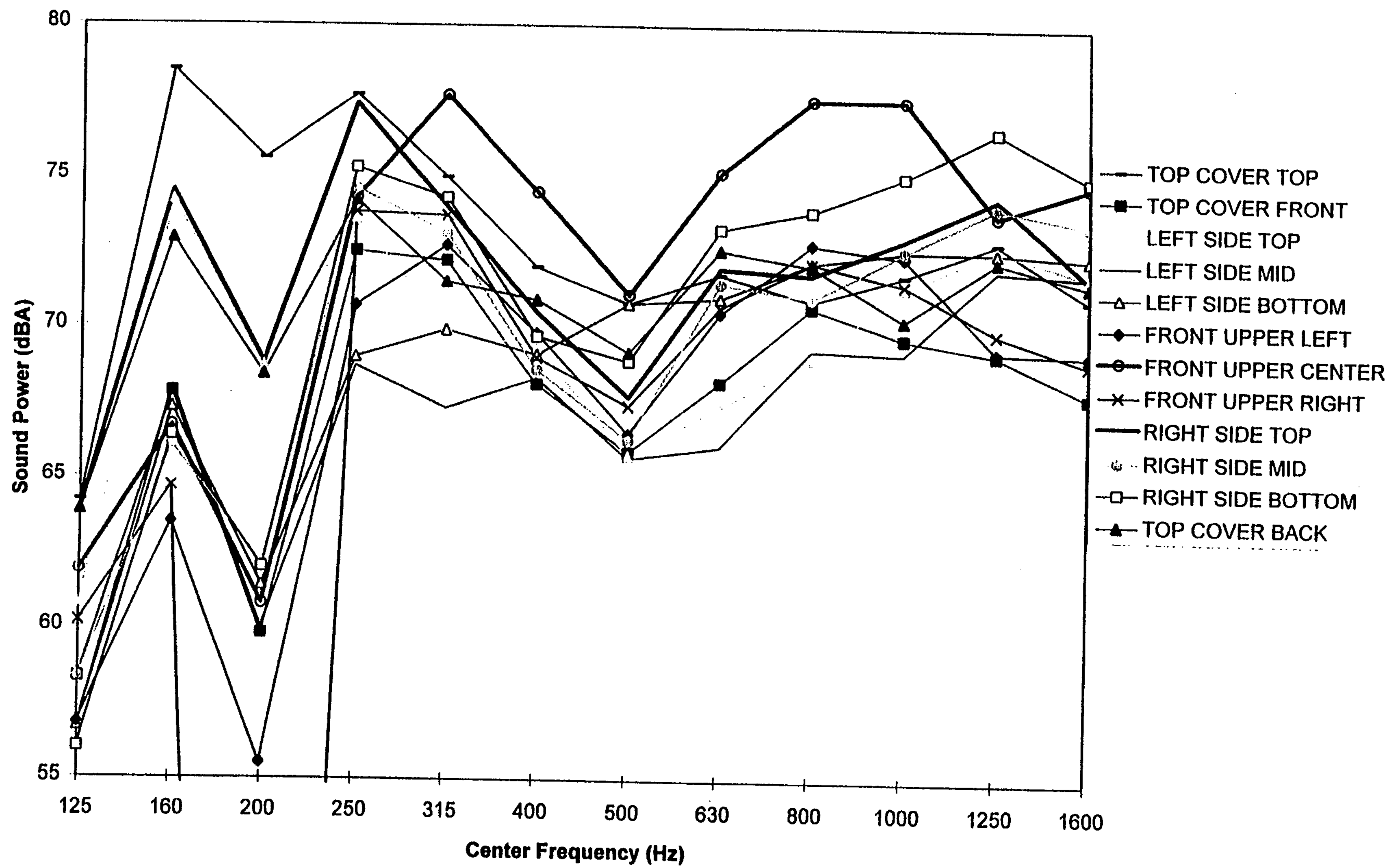

FIGURE 30. THIRD OCTAVE SOUND POWER LEVELS, 2600 RPM

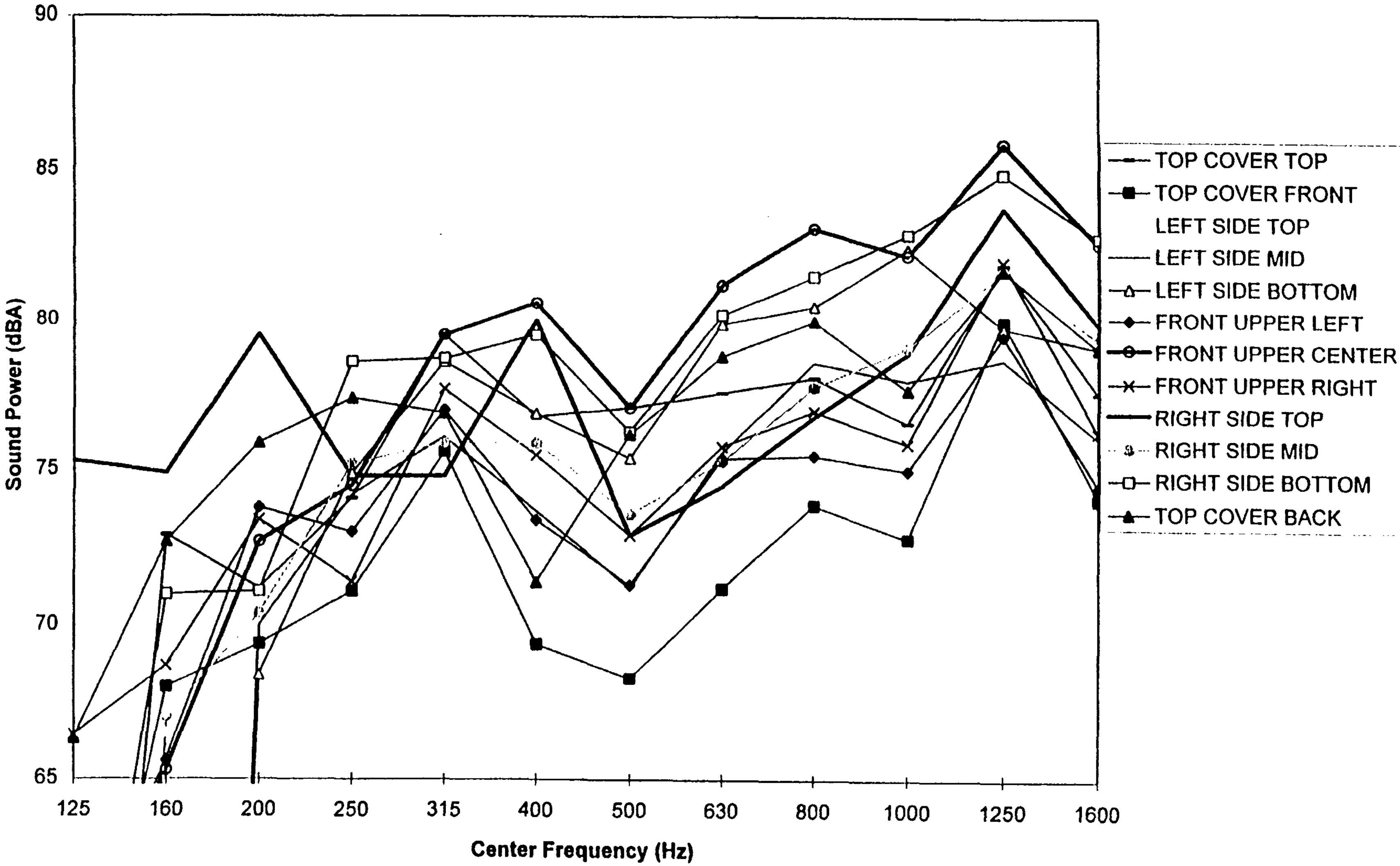

FIGURE 31. THIRD OCTAVE SOUND POWER LEVELS, 3600 RPM

From sound power level measurements, sound pressure levels (SPL) may be predicted. Assuming a spherically radiating body, predicted SPL at 1.0 meters from the engine were calculated. Table 3 lists these predicted SPL results from the sound power measurements and the measured SPL obtained directly in the test cell. The measured SPL are high by about 7 dBA over the predicted levels (for the 100-3150 Hz range).

TABLE 3. SOUND POWER PREDICTED SPL AND MEASURED SPL AT 1 METER

Engine Speed (rpm)	Average SPL Measured in Cell (0-5000 Hz)	Predicted SPL from Sound Power (100-3150 Hz)	Predicted SPL from Sound Power (125-1600 Hz)
1600	87.5 dBA	79.9 dBA	76.2 dBA
2600	94.8 dBA	87.9 dBA	85.3 dBA
3600	100.3 dBA	93.3 dBA	90.8 dBA

Conclusions and Recommendations

From this initial acoustic survey, the following conclusions and recommendations are drawn:

- The high noise levels measured in the higher frequency range may be associated with support structure vibration. A modal survey can determine if support structure resonances were contributing to the noise emission.

- Noise generated in the lower end of the frequency spectrum is of major importance due to expected lower level of absorption and noise transmission loss possible from an insulated enclosure.

- At the lower engine speeds, the top cover noise radiation (possibly generated from induction noise) could be of concern requiring improved induction system noise control.

- The blower cover may require noise control treatment with an additional filter element used in conjunction with the protective screen.

- The engine noise levels obtained at 1.0 meters as predicted from the measured sound power levels are not extremely high. Depending on the acoustic propagation of the engine enclosure, additional noise control development may not be necessary.

- The engine test cell is not an ideal location for acoustic measurements and the engine support structure is not an installed configuration for the engine. Absolute sound levels can only be determined with an end-use supported engine installed in a proper acoustic environment.

Report prepared by:

Douglas J. Fox
Research Engineer
Mechanical & Fluids Engineering Division
Tel: (210) 522-2920; Fax: (210) 522-5122

Dr. James F. Unruh, P.E.
Institute Engineer
Mechanical & Fluids Engineering Division
Tel: (210) 522-2344; Fax: (210) 522-5122

Fuels Distribution List

Department of Defense

DEFENSE TECH INFO CTR 12
ATTN: DTIC OCC
8725 JOHN J KINGMAN RD
STE 0944
FT BELVOIR VA 22060-6218

ODUSD
ATTN: (L) MRM 1
PETROLEUM STAFF ANALYST
PENTAGON
WASHINGTON DC 20301-8000

ODUSD
ATTN: (ES) CI 1
400 ARMY NAVY DR
STE 206
ARLINGTON VA 22202

HQ USEUCOM
ATTN: ECJU L1J 1
UNIT 30400 BOX 1000
APO AE 09128-4209

US CINCPAC
ATTN: J422 BOX 64020 1
CAMP H M SMITH
HI 96861-4020

JOAP TSC 1
BLDG 780
NAVAL AIR STA
PENSACOLA FL 32508-5300

DIR DLA
ATTN: DLA MMSLP 1
8725 JOHN J KINGMAN RD
STE 2533
FT BELVOIR VA 22060-6221

CDR
DEFENSE FUEL SUPPLY CTR
ATTN: DFSC I (C MARTIN) 1
DFSC IT (R GRAY) 1
DFSC IQ (L OPPENHEIM) 1
8725 JOHN J KINGMAN RD
STE 2941
FT BELVOIR VA 22060-6222

DIR
DEFENSE ADV RSCH PROJ AGENCY
ATTN: ARPA/ASTO 1
3701 N FAIRFAX DR
ARLINGTON VA 22203-1714

Department of the Army

HQDA
ATTN: DALO TSE 1
DALO SM 1
500 PENTAGON
WASHINGTON DC 20310-0500

SARDA
ATTN: SARD TT 1
PENTAGON
WASHINGTON DC 20310-0103

CDR AMC
ATTN: AMCRD S 1
AMCRD E 1
AMCRD IT 1
AMCEN A 1
AMCLG M 1
AMXLS H 1
5001 EISENHOWER AVE
ALEXANDRIA VA 22333-0001

U.S. ARMY TACOM
TARDEC PETR. & WTR. BUS. AREA
ATTN AMSTA TR-D/210 (L. VILLHAHERMOSA)10
AMSTA TR-D/210 (T. BAGWELL) 1
WARREN, MI 48397-5000

CDR ARMY TACOM
ATTN: AMSTA IM LMM 1
AMSTA IM LMB 1
AMSTA IM LMT 1
AMSTA TR NAC MS 002 1
AMSTA TR R MS 202 1
AMSTA TR D MS 201A 1
AMSTA TR M 1
AMSTA TR R MS 121 (C RAFFA) 1
AMSTA TR R MS 158 (D HERRERA) 1
AMSTA TR R MS 121 (R MUNT) 1
AMCPM ATP MS 271 1
AMSTA TR E MS 203 1
AMSTA TR K 1
AMSTA IM KP 1
AMSTA IM MM 1
AMSTA IM MT 1
AMSTA IM MC 1
AMSTA IM GTL 1
AMSTA CL NG 1
USMC LNO 1
AMCPM LAV 1
AMCPM M113 1
AMCPM CCE 1
WARREN MI 48397-5000

Department of the Army

PROG EXEC OFFICER ARMORED SYS MODERNIZATION ATTN: SFAE ASM S	1
SFAE ASM H	1
SFAE ASM AB	1
SFAE ASM BV	1
SFAE ASM CV	1
SFAE ASM AG	1
CDR TACOM WARREN MI 48397-5000	
PROG EXEC OFFICER ARMORED SYS MODERNIZATION ATTN: SFAE FAS AL	1
SFAE FAS PAL	1
PICATINNY ARSENAL NJ 07806-5000	
PROG EXEC OFFICER TACTICAL WHEELED VEHICLES ATTN: SFAE TWV TVSP	1
SFAE TWV FMTV	1
SFAE TWV PLS	1
CDR TACOM WARREN MI 48397-5000	
PROG EXEC OFFICER ARMAMENTS ATTN: SFAE AR HIP	1
SFAE AR TMA	1
PICATINNY ARSENAL NJ 07806-5000	
PROG MGR UNMANNED GROUND VEH ATTN: AMCPM UG	1
REDSTONE ARSENAL AL 35898-8060	
DIR ARMY RSCH LAB ATTN: AMSRL PB P	1
2800 POWDER MILL RD ADELPHIA MD 20783-1145	
VEHICLE PROPULSION DIR ATTN: AMSRL VP (MS 77 12)	1
NASA LEWIS RSCH CTR 21000 BROOKPARK RD CLEVELAND OH 44135	
CDR AMSAA ATTN: AMXSY CM	1
AMXSY L	1
APG MD 21005-5071	
CDR ARO ATTN: AMXRO EN (D MANN)	1
RSCH TRIANGLE PK NC 27709-2211	
CDR AEC ATTN: SFIM AEC ECC (T ECCLES)	1
APG MD 21010-5401	
CDR ARMY ATCOM ATTN: AMSAT I WM	1
AMSAT I ME (L HEPLER)	1
AMSAT I LA (V SALISBURY)	1
AMSAT R EP (V EDWARD)	1
4300 GOODFELLOW BLVD ST LOUIS MO 63120-1798	
CDR ARMY SOLDIER SPT CMD ATTN: SATNC US (J SIEGEL)	1
SATNC UE	1
NATICK MA 01760-5018	
CDR ARMY ARDEC ATTN: AMSTA AR EDE S	1
PICATINNY ARSENAL NJ 07808-5000	
CDR ARMY WATERVLIET ARSN ATTN: SARWY RDD	1
WATERVLIET NY 12189	
CDR APC ATTN: SATPC L	1
SATPC Q	1
NEW CUMBERLAND PA 17070-5005	
CDR ARMY LEA ATTN: LOEA PL	1
NEW CUMBERLAND PA 17070-5007	
CDR ARMY TECOM ATTN: AMSTE TA R	1
AMSTE TC D	1
AMSTE EQ	1
APG MD 21005-5006	
PROJ MGR MOBILE ELEC PWR ATTN: AMCPM MEP T	1
AMCPM MEP L	1
7798 CISSNA RD STE 200 SPRINGFIELD VA 22150-3199	
CDR ARMY COLD REGION TEST CTR ATTN: STECR TM	1
STECR LG	1
APO AP 96508-7850	
ARMY COMBINED ARMS SPT CMD ATTN: ATCL MS FT LEE VA 23801-6000	

Department of the Army

CDR
ARMY BIOMED RSCH DEV LAB
ATTN: SGRD UBZ A 1
FT DETRICK MD 21702-5010

CDR FORSCOM
ATTN: AFLG TRS 1
FT MCPHERSON GA 30330-6000

CDR TRADOC
ATTN: ATCD SL 5 1
INGALLS RD BLDG 163
FT MONROE VA 23651-5194

CDR ARMY ARMOR CTR
ATTN: ATSB CD ML 1
ATSB TSM T 1
FT KNOX KY 40121-5000

CDR ARMY QM SCHOOL
ATTN: ATSM PWD 1
FT LEE VA 23001-5000

CDR ARMY FIELD ARTY SCH
ATTN: ATSF CD 1
FT SILL OK 73503

CDR ARMY TRANS SCHOOL
ATTN: ATSP CD MS 1
FT EUSTIS VA 23604-5000

CDR ARMY INF SCHOOL
ATTN: ATSH CD 1
ATSH AT 1
FT BENNING GA 31905-5000

CDR ARMY AVIA CTR
ATTN: ATZQ DOL M 1
FT RUCKER AL 36362-5115

CDR ARMY ENGR SCHOOL
ATTN: ATSE CD 1
FT LEONARD WOOD
MO 65473-5000

CDR 49TH QM GROUP
ATTN: AFFL GC 1
FT LEE VA 23801-5119

CDR ARMY SAFETY CTR
ATTN: CSSC PMG 1
CSSC SPS 1
FT RUCKER AL 36362-5363

CDR ARMY ABERDEEN TEST CTR
ATTN: STEAC EN 1
STEAC LI 1
STEAC AE 1
STEAC AA 1
APG MD 21005-5059

CDR ARMY YPG
ATTN: STEYP MT TL M 1
YUMA AZ 85365-9130

CDR ARMY CERL
ATTN: CECER EN 1
P O BOX 9005
CHAMPAIGN IL 61826-9005

DIR 1
AMC FAST PROGRAM
10101 GRIDLEY RD STE 104
FT BELVOIR VA 22060-5818

CDR I CORPS AND FT LEWIS
ATTN: AFZH CSS 1
FT LEWIS WA 98433-5000

CDR
RED RIVER ARMY DEPOT
ATTN: SDSRR M 1
SDSRR Q 1
TEXARKANA TX 75501-5000

PS MAGAZINE DIV
ATTN: AMXLS PS 1
DIR LOGSA
REDSTONE ARSENAL AL 35898-7466

CDR 6TH ID (L)
ATTN: APUR LG M 1
1060 GAFFNEY RD
FT WAINWRIGHT AK 99703

CDR ARMY ORDN CTR
ATTN: ATSL CD CS 1
APG MD 21005

Department of the Navy

OFC CHIEF NAVAL OPER
ATTN: DR A ROBERTS (N420) 1
2000 NAVY PENTAGON
WASHINGTON DC 20350-2000

CDR
NAVAL AIR WARFARE CTR
ATTN: CODE PE33 AJD 1
P O BOX 7176
TRENTON NJ 08628-0176

CDR
NAVAL SEA SYSTEMS CMD
ATTN: SEA 03M3 1
2531 JEFFERSON DAVIS HWY
ARLINGTON VA 22242-5160

CDR
NAVAL SURFACE WARFARE CTR
ATTN: CODE 63 1
CODE 632 1
CODE 859 1
3A LEGGETT CIRCLE
ANNAPOLIS MD 21402-5067

CDR
NAVAL RSCH LABORATORY
ATTN: CODE 6181 1
WASHINGTON DC 20375-5342

CDR 1
NAVAL PETROLEUM OFFICE
8725 JOHN J KINGMAN RD
STE 3719
FT BELVOIR VA 22060-6224

CDR
NAVAL AIR SYSTEMS CMD
ATTN: AIR 4.4.5 (D MEARNS) 1
1421 JEFFERSON DAVIS HWY
ARLINGTON VA 22243-5360

Department of the Navy/U.S. Marine Corps

HQ USMC
ATTN: LPP 1
WASHINGTON DC 20380-0001

PROG MGR COMBAT SER SPT 1
MARINE CORPS SYS CMD
2033 BARNETT AVE STE 315
QUANTICO VA 22134-5080

PROG MGR GROUND WEAPONS 1
MARINE CORPS SYS CMD
2033 BARNETT AVE
QUANTICO VA 22134-5080
PROG MGR ENGR SYS 1
MARINE CORPS SYS CMD
2033 BARNETT AVE
QUANTICO VA 22134-5080

CDR
MARINE CORPS SYS CMD
ATTN: SSE 1
2030 BARNETT AVE STE 315
QUANTICO VA 22134-5010

CDR
BLOUNT ISLAND CMD
ATTN: CODE 922/1 1
5880 CHANNEL VIEW BLVD
JACKSONVILLE FL 32226-3404

CDR
ATTN: CODE 837 1
814 RADFORD BLVD
ALBANY GA 31704-1128

CDR 1
2ND MARINE DIV
PSC BOX 20090
CAMP LEJEUNNE
NC 28542-0090

CDR 1
FMFPAC G4
BOX 64118
CAMP H M SMITH
HI 96861-4118

Department of the Air Force

HQ USAF/LGSF
ATTN: FUELS POLICY 1
1030 AIR FORCE PENTAGON
WASHINGTON DC 20330-1030

HQ USAF/LGTV
ATTN: VEH EQUIP/FACILITY 1
1030 AIR FORCE PENTAGON
WASHINGTON DC 20330-1030

SA ALC/SFT 1
1014 BILLY MITCHELL BLVD STE 1
KELLY AFB TX 78241-5603

SA ALC/LDPG
ATTN: D ELLIOTT 1
580 PERRIN BLDG 329
KELLY AFB TX 78241-6439

AIR FORCE WRIGHT LAB
ATTN: WL/POS 1
WL/POSF 1
1790 LOOP RD N
WRIGHT PATTERSON AFB
OH 45433-7103

AIR FORCE MEEP MGMT OFC 1
OL ZC AFMC LSO/LOT PM
201 BISCAYNE DR
BLDG 613 STE 2
ENGLIN AFB FL 32542-5303

WR ALC/LVRS 1
225 OCMULGEE CT
ROBINS AFB
GA 31098-1647

Other Federal Agencies

NASA
LEWIS RESEARCH CENTER 1
CLEVELAND OH 44135

RAYMOND P. ANDERSON, PH.D., MANAGER 1
FUELS & ENGINE TESTING
BDM-OKLAHOMA, INC.
220 N. VIRGINIA
BARTLESVILLE OK 74003

EPA
AIR POLLUTION CONTROL 1
2565 PLYMOUTH RD
ANN ARBOR MI 48105

DOT
FAA
AWS 110 1
800 INDEPENDENCE AVE SW
WASHINGTON DC 20590

DOCUMENT 2

Development of Auxiliary Power Units for Electric Hybrid Vehicles

AD-A325918

June 1997

Southwest Research Institute
San Antonio, TX

AD A325918

DEVELOPMENT OF AUXILIARY POWER UNITS FOR ELECTRIC HYBRID VEHICLES

INTERIM REPORT
TFLRF No. 302

By

E.C. Owens
J. Steiber
U.S. Army TARDEC Fuels and Lubricants Research Facility (SwRI)
Southwest Research Institute
San Antonio, Texas

Under Contract to

U.S. Army TARDEC
Mobility Technology Center–Belvoir
Fort Belvoir, Virginia

Prepared for

Defense Advanced Research Projects Agency
3701 N. Fairfax Drive
Arlington, Virginia 22203-1714

Contract No. DAAK70-92-C-0059

Approved for public release; distribution unlimited

June 1997

Disclaimers

DTIC Availability Notice

Disposition Instructions

REPORT DOCUMENTATION PAGE

Form Approved
OMB No. 0704-0188

1. AGENCY USE ONLY (Leave blank)	2. REPORT DATE	3. REPORT TYPE AND DATES COVERED
	June 1997	Interim July 1993 to February 1994

4. TITLE AND SUBTITLE

Development of Auxiliary Power Units for Electric Hybrid Vehicles

5. FUNDING NUMBERS

DAAK70-92-C-0059; WD 20

6. AUTHOR(S)

Owens, Edwin C. and Steiber, Joe

7. PERFORMING ORGANIZATION NAME(S) AND ADDRESS(ES)

U.S. Army TARDEC Fuels and Lubricants Research Facility (SwRI)
Southwest Research Institute
P.O. Drawer 28510
San Antonio, Texas 78228-0510

8. PERFORMING ORGANIZATION REPORT NUMBER

TFLRF No. 302

9. SPONSORING/MONITORING AGENCY NAME(S) AND ADDRESS(ES)

Advanced Research Projects Agency
3701 N. Fairfax Drive
Arlington, Virginia 22203-1714

Department of the Army
Mobility Technology Center-Belvoir
10115 Gridley Road, Suite 128
Ft. Belvoir, Virginia 22060-5843

10. SPONSORING/MONITORING AGENCY REPORT NUMBER

11. SUPPLEMENTARY NOTES

12a. DISTRIBUTION/AVAILABILITY STATEMENT

Approved for public release; distribution unlimited

12b. DISTRIBUTION CODE

13. ABSTRACT (Maximum 200 words)

Electric drive is being considered for a wide variety of urban vehicles. Larger urban commercial vehicles (such as shuttle and transit buses), various delivery and service vehicles (such as panel and step vans), and garbage trucks and school buses are particularly well-suited for this type of propulsion system due to their relatively short operating routes, operation and maintenance from central sites. Furthermore, these vehicles contribute a proportionately large amount to metropolitan air pollution by virtue of their continuous operation in those areas. Thus, reductions of emissions from these vehicles can have a large impact on urban air quality. It is, therefore, a necessity to develop auxiliary power units (APUs) that minimize emissions and in addition, increase range of electric vehicles. This report focuses on the first phase study of the development of APUs for large, eletric drive commercial vehicles, intended primarily for metropolitan applications. This paper (1) summarizes the differences between available mobile APUs and Electric Vehicle APU requirements, (2) describes the major components in APUs, and (3) discusses APU integration issues. During this phase, three potential APU manufacturers were identified and selected for development of prototype units at 25-kW and 50-kW power levels.

14. SUBJECT TERMS

Auxiliary Power Units, Series Hybrid Vehicles, APU components, APU integration, APU design, APU requirements, APU costs, HEV costs, HEV requirements

15. NUMBER OF PAGES

35

16. PRICE CODE

17. SECURITY CLASSIFICATION OF REPORT	18. SECURITY CLASSIFICATION OF THIS PAGE	19. SECURITY CLASSIFICATION OF ABSTRACT	20. LIMITATION OF ABSTRACT
Unclassified	Unclassified	Unclassified	

EXECUTIVE SUMMARY

Problem: APUs are used with electric drives to form hybrid vehicles, primarily because of inadequate energy storage capabilities with current battery technology. APUs allow the vehicles to operate for greater distances than batteries or other energy storage devices alone and can provide greater vehicle operating flexibility as vehicle use profiles change. At the present time, commercially available gensets are not adequately designed for vehicular application. As a result, there is a need to develop APUs specifically for hybrid electric vehicles.

Objective: The objective of this project was to design, build, and test APUs utilizing natural gas engine technologies for large, electric hybrid, commercial vehicle applications. The first phase (corresponding to this report) included the review of available technological options for APU components such as alternating current (AC) generator configurations, heat engine types, and APU control algorithms as well as some of the issues and concerns regarding the integration of APUs into a pure electric vehicle.

Importance of Project: Electric drive is being considered for a wide variety of urban vehicles. Larger urban commercial vehicles (such as shuttle and transit buses), various delivery and service vehicles (such as panel and step vans), and garbage trucks and school buses are particularly well-suited for this type of propulsion system due to their relatively short operating routes, operation and maintenance from central sites. Furthermore, these vehicles contribute a proportionately large amount to metropolitan air pollution by virtue of their continuous operation in those areas. Thus, reductions of emissions from these vehicles can have a disproportionately large impact on urban air quality. It is, therefore, a necessity to develop auxiliary power units (APUs) that minimize emissions and in addition, increase range of electric vehicles.

Technical Approach: The first phase of this project focuses on the development of auxiliary power units (APUs) for large, electric drive commercial vehicles, intended primarily for metropolitan applications. Such APU would be incorporated in a series hybrid vehicle configuration where the vehicle propulsion is accomplished solely through electric motor drives. This project does not consider the parallel configuration since it does not incorporate an APU as a stand-alone unit. Several APU technologies were researched. Then, several manufacturers were contacted, evaluated, and selected for procurement.

Accomplishments: This paper (1) summarizes the differences between available mobile APUs and Electric Vehicle APU requirements, (2) describes the major components in APUs, and (3) discusses the major issues associated with integration of an APU into a vehicle. During this phase, three potential APU manufacturers were identified and selected for development of prototype units at 25-kW and 50-kW power levels.

Military Impact: Availability of APU component technologies, weight, size, cost, performance, safety and reliability are as important in military vehicles as in commercial. Electric drive also provides a low-heat, low-noise signature option for military vehicles. Consequently, issues associated with APU development for commercial hybrid vehicles are readily transferable to military applications. In a military combat environment, however, component vulnerability issues must be considered as well. Nevertheless, the results of this research study can be valuable in military APU development. While it is generally expected to see component specifications in military system to extend the envelope of commercially-feasible practices, it would not be unrealistic for some military APU requirements to be relaxed in order to increase vehicle performance (by allowing greater emissions) and increase survivability (by compromising fuel-efficient operating conditions) during critical high-demand scenarios.

FOREWORD/ACKNOWLEDGEMENTS

This work was performed by the U.S. Army TARDEC Fuels and Lubricants Research Facility (TFLRF) located at Southwest Research Institute (SwRI), San Antonio, TX, during the period July 1993 to February 1994. Funding was provided by the Defense Advanced Research Projects Agency (DARPA), Arlington, VA, under Contract No. DAAK70-92-C-0059 with the U.S. Army TARDEC, Mobility Technology Center-Belvoir (MTCB). Mr. T.C. Bowen (AMSTA-RBFF) of MTCB served as the contracting officer's representative, Mr. M.E. LePera (AMSTA-RBF) served as the project technical monitor, and Major Richard Cope served as the DARPA project monitor.

The authors would like to acknowledge the assistance provided by Mr. J.W. Pryor and Ms. M.M. Clark of the TFLRF editorial group.

TABLE OF CONTENTS

LIST OF ILLUSTRATIONS

LIST OF TABLES

I. INTRODUCTION

Electric drive is being considered for a wide variety of urban vehicles. Larger urban commercial vehicles (such as shuttle and transit buses), various delivery and service vehicles (such as panel and step vans), and garbage trucks and school buses are particularly well-suited for this type of propulsion system due to their relatively short operating routes, operation and maintenance from central sites. Furthermore, these vehicles contribute a proportionately large amount to metropolitan air pollution by virtue of their continuous operation in those areas. Thus, reductions of emissions from these vehicles can have a large impact on urban air quality.

This paper focuses on a first-phase study of the development of auxiliary power units (APUs) for large, electric drive commercial vehicles, intended primarily for metropolitan applications. Such APU would be incorporated in a series hybrid-vehicle configuration where the vehicle propulsion is accomplished solely through electric motor drives. This document does not consider the parallel configuration since it does not incorporate an APU as a stand-alone unit. Rather, parallel hybrid designs require load sharing between the electric and engine drivelines.

II. OBJECTIVE

The objective of this project was to design, build, and test APUs utilizing natural gas engine technologies for large, electric hybrid, commercial vehicle applications. The first phase (corresponding to this report) included the review of available technological options for APU components (such as alternating current (AC) generator configurations, heat engine types, and APU control algorithms) as well as some of the issues and concerns regarding the integration of APUs into a pure electric vehicle. During this phase, three potential APU manufacturers were identified and selected for development of prototype units at 25-kW and 50-kW power levels.

III. APPROACH

APUs are used with electric drives to form hybrid vehicles, primarily because of inadequate energy storage capabilities with current battery technology. APUs allow the vehicles to operate for greater distances than batteries or other energy storage devices alone and can provide greater vehicle operating flexibility as vehicle-use profiles change. Although an APU will increase local emissions compared to an all-electric vehicle, emissions should be significantly less than a comparable conventional, internal combustion engine (ICE) vehicle.

An APU consists of a heat engine driving an electrical generator, which in turn supplies additional electrical energy to supplement the battery or other on-board storage devices. A general schematic is shown in Fig. 1. The engine is one of the main components of an APU, and its selection has the largest impact on overall APU efficiency and operating flexibility. Connected to the engine is a

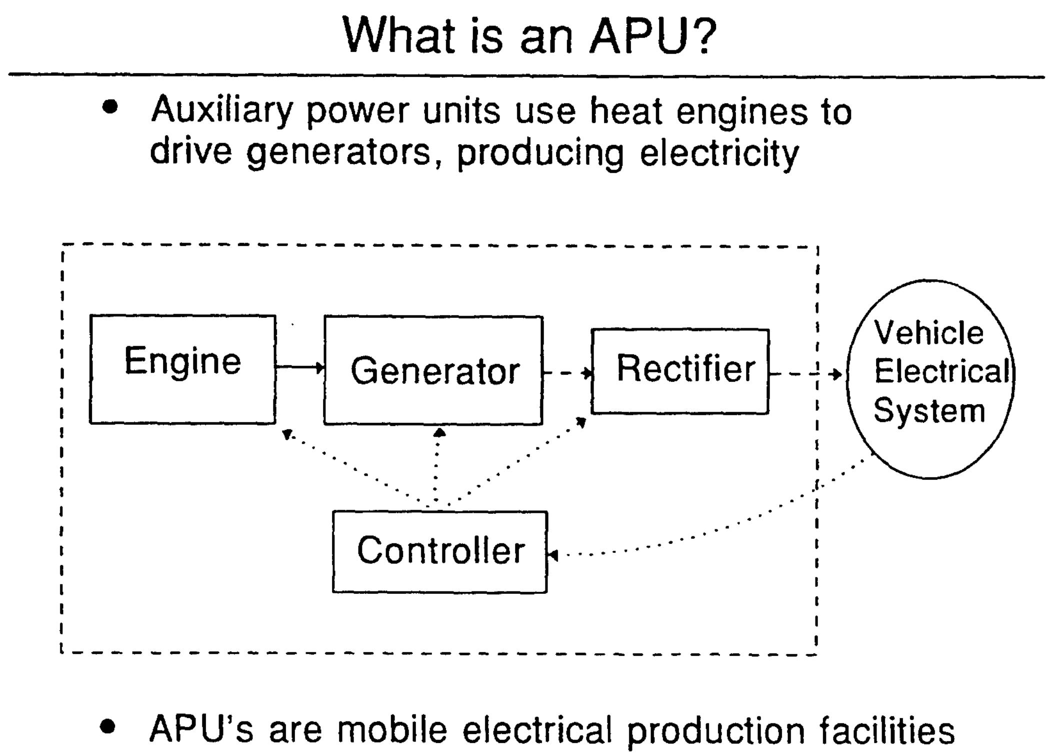

Figure 1. **Auxiliary power unit configuration**

generator that can be chosen from a variety of technologies and can have a substantial impact on the APU size, weight, and cost. Associated with the generator is a power-conversion device. This could be a simple diode rectifier and filter for conversion from AC to direct current (DC) or a more complex system, such as an IGBT inverter, for rectifying and controlling the output voltage independent of the generator voltage. Finally, the APU must be connected to, and controlled by, the vehicle through some control interface unit.

IV. ELECTRIC HYBRID VEHICLE APU REQUIREMENT DIFFERENCES FROM AVAILABLE MOBILE APU

The requirements for vehicle APUs are different from conventional mobile generator sets (gensets) in a number of ways. Non-vehicle gensets place less emphasis on minimizing size and weight. The relationship between weight and power is illustrated in Fig. 2a, which summarizes data from a survey of commercial generator sets. With commercial units, size minimization in particular may be sacrificed to avoid maintenance compromises, and there is little financial incentive for weight reductions other than reductions in the cost of raw materials. There is a general trend to lower cost with increasing power output, as seen in Fig. 2b.

The most significant difference between available commercial gensets and hybrid vehicle APUs is the genset requirement for precise regulation of output voltage and frequency. This regulation is needed to satisfy the electrical requirements of equipment intended for operation from the electrical power grid. The constant frequency requirement is met on these units by tight control of engine speed, usually at 1,800 or 3,600 rpm. Voltage is controlled by varying generator-field excitation current in a field-generating coil within the unit. Variations in output power are accommodated by variations in engine load at the controlled speed.

This requirement for frequency control is eliminated in an hybrid vehicle APU, where the power is usually delivered to the vehicle as direct current. As a result, engine speed can vary, providing an additional degree of freedom in APU design, which can have a substantial impact on engine efficiency in some operating modes.

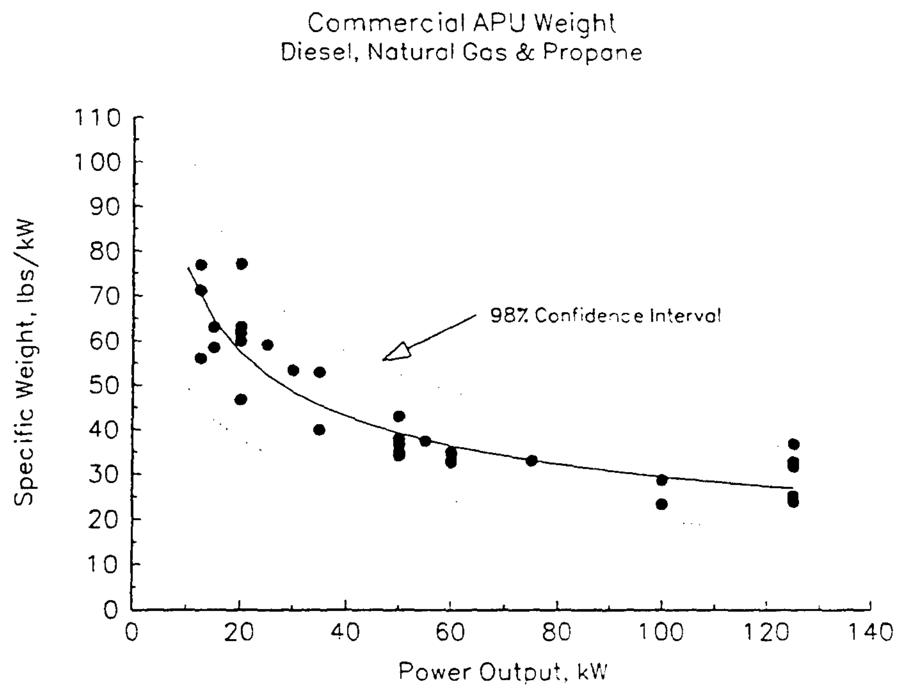

a. Specific weight vs. power

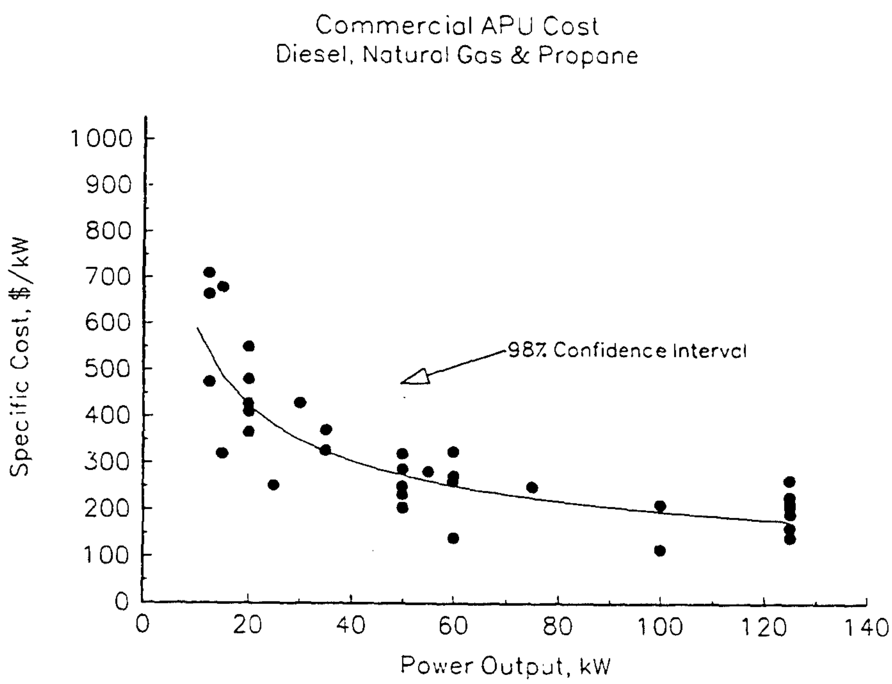

b. Specific cost vs. power

Figure 2. <u>Commercial APU weight and cost relationships</u>

APUs are being considered for use in two somewhat distinct types of vehicle applications. The simplest application will be referred to as range extension, in which the APU maximum continuous power is less than the vehicle average power requirement for the operating mode. In this configuration, the vehicle begins the operating day with a fully charged battery pack that discharges throughout the operation. The APU is started when the battery has depleted to some level and it operates continuously at peak power, supplying electricity to supplement the battery pack, thus slowing the battery discharge rate. Optimally, at the end of the day, the battery pack's available charge is depleted and the APU fuel exhausted as the vehicle returns to the service center to be refueled and recharged for the next day. Because of the need to balance vehicle energy storage with operating route requirements, this operation requires that the vehicle be designed with knowledge of the driving route. APU size is minimized, as is on-board fuel consumption. Electrical grid power consumption is maximized, and in the absence of opportunity charging, battery charging would likely occur during non-peak hours.

The other operating mode is state-of-charge (SOC) maintenance. In this application, the APU is larger and provides enough power to meet the average vehicle power demands over the driving cycle. On average, the stored energy in the vehicle does not fall below a specific level, hence the term "charge maintenance." The higher APU power output results in more on-board fuel consumption and increased local emissions, but provides more vehicle operating flexibility. Also, reducing large variations in SOC can greatly extend battery life for many battery designs.

In the sections that follow, APU component options and aspects of APU design will be discussed in greater detail. These system-control strategy options and the resulting impacts on vehicle performance and system design will be shown to play a key role in the selection of APUs.

V. APU COMPONENTS

A. Heat Engines

Heat engines for APUs were reviewed by the U.S. Department of Energy (DOE) during 1984 (Fig. 3). Various alternatives were ranked by power, efficiency, cost, size and weight, and were based on projections of then-current engine technology.(1) Some ten years later, some of the projections, most notably specific fuel consumption, appear overly optimistic.

Each of these engine types have advantages and shortcomings for APU applications, depending on how the APU is applied in the vehicle. TABLE 1 summarizes many of the characteristics of the various engine options.

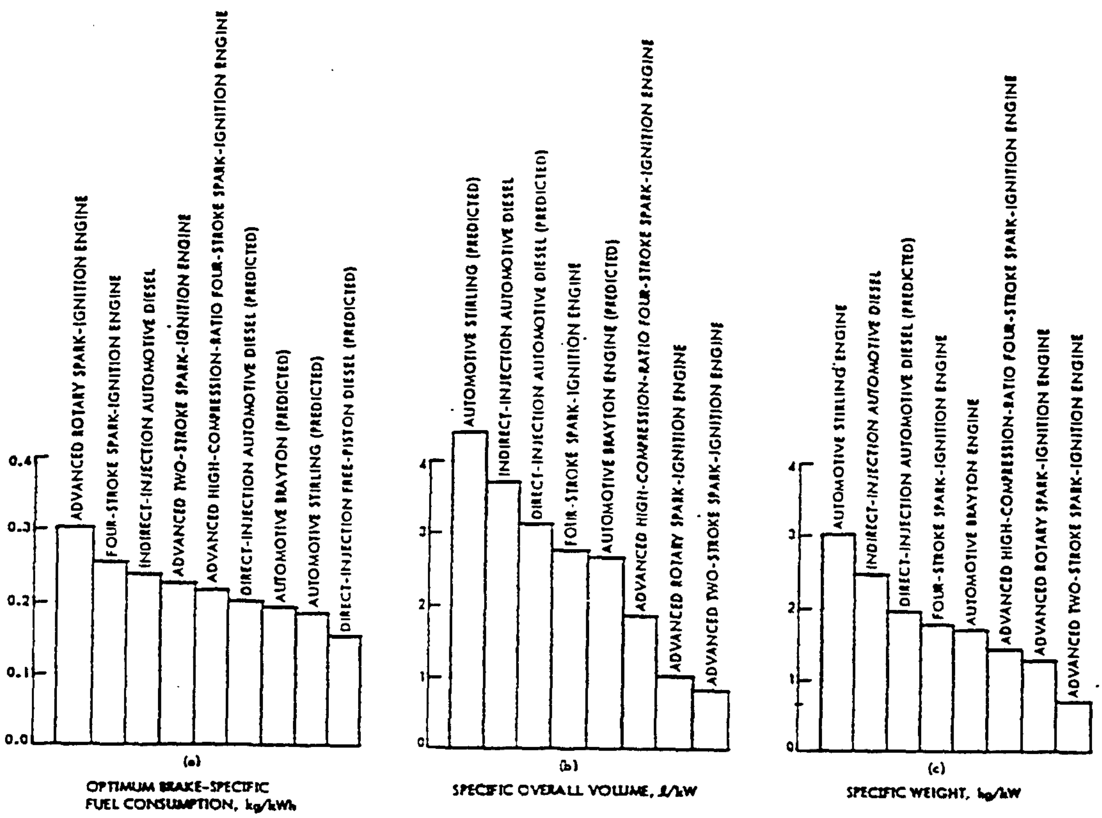

Figure 3. <u>Comparison of automotive heat engine parameters</u> (2)

* Underscored numbers in parentheses refer to the list of references at the end of this report.

TABLE 1. Some Advantages and Disadvantages of Heat Engines

Engine Type	Advantages	Disadvantages
Diesel	• Mature design • Proven durability • High efficiency, particularly at part power	• High NOx and particulate emissions • Power to weight, volume ratios
Four-Stroke Spark Ignition	• Mature design • Good power to weight, volume ratios • Well-developed emissions control systems • Low cost per kilowatt	• Current designs have less durability • Poor part throttle efficiency
Two-Stroke Spark Ignition	• High power to weight, volume ratios • Potential for low cost per kilowatt	• Less developed emissions controls • Current designs have less durability • Poor part power efficiency
Recuperated Gas Turbine	• High power to weight, volume ratios • Minimum maintenance, esp. with air bearings • Potential for good durability • Potentially low emissions, except for NOx • Low noise	• Historically high cost • Efficiency poor without heat recuperator or regenerator • Poor efficiency at low power • Reduced efficiency and durability in on/off cycling
Stirling	• Highest potential efficiency • Potentially low emissions	• Poor power to size, weight ratios • High cost • Unproved durability and reliability

1. Diesel engines. These engines have become the predominant power source in heavy-duty commercial vehicles due primarily to their high efficiency. Diesel designs are mature and reliable, with heavy-duty engine overhaul intervals exceeding 500,000 miles. Current diesel designs for automotive applications reach maximum efficiency at 40 to 50 percent of rated power, and efficiency remains high with increasing power. Engines for industrial applications can reach peak efficiencies at 50 to 75 percent of rated power but are usually heavier than automobile engines. The excellent, below-rated-power efficiency makes the engine particularly attractive for APU applications where

wide variations in power are required. While the injection system and more rugged design make this engine class more expensive than spark-ignition engines of similar displacement, the high production volume keeps cost low.

The two-cycle diesel engine has undergone refinement to the point that it is a serious competitor to the four-cycle engine in weight, power, and fuel consumption. An example of this engine is the Detroit Diesel Corporation's 71 and 92 series. This competition with the four-cycle engine is paid for by complexity and weight.(3) For the large diesel engines, the inlet pumping is accomplished by a positive-displacement blower. Exhaust is accomplished by either valves placed in the cylinder or by the less common exhaust port, as in the gasoline engines. There are some examples of the crankcase-pumped diesel engine; however, these engines are not currently produced.

Diesel engines tend to be larger and heavier than spark-ignition engines of the same power level (Fig. 4). This is partially because of the need to design for extended durability. However, the increase in size is also due to the inherent lower-air utilization of the diesel heterogeneous combustion process.

Diesel emission control has been difficult, particularly control of NOx and particulates. While NOx would continue to be a problem in APU applications, the flexibility of engine control possible can allow the avoidance of rapid speed changes and other operations that contribute to particulate formation.

2. Spark-ignition engines. These engines are the predominant engine in light-duty applications and some medium-duty commercial vehicles. Spark-ignition engines mix fuel and air in closely controlled proportions, then meter the mixture into the combustion chamber. Power is controlled by throttling the intake to reduce the air (and fuel) combusted during each cycle. The lower engine compression ratio, dictated by fuel properties, results in lower peak efficiency than the diesel engine. Throttling for power control further reduces part power efficiency by increasing work lost to intake air pumping.

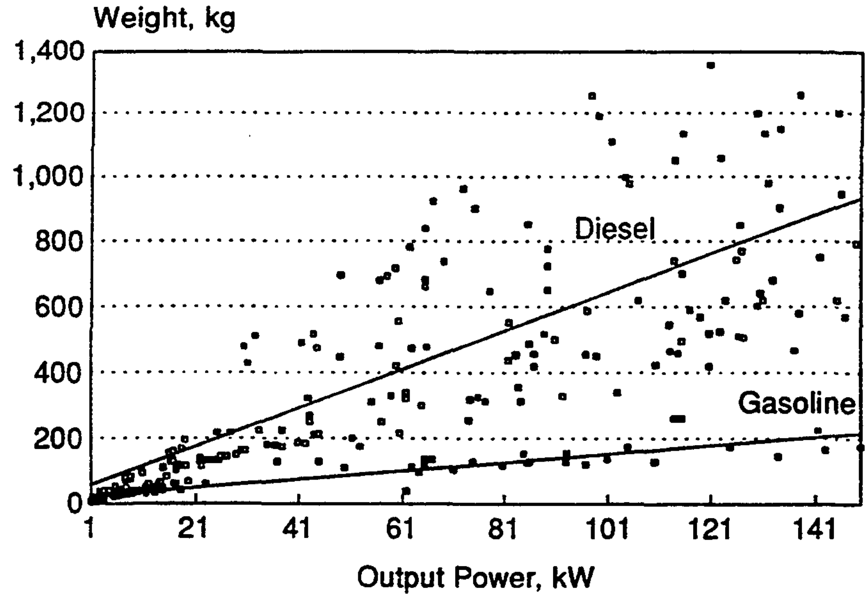

Figure 4. Engine weights (bare engine with accessories)

While genset engines operate at a fixed speed and varying load, APU engines either operate at a single speed, or if power is varied, can vary throughout their operating range. Particularly for the charge maintenance mode of operation, this can have a large impact on spark-ignition engine efficiency. The increased flexibility of a spark-ignition, engine-powered APU can overcome some of the efficiency penalty compared to diesel engines. This is illustrated in Fig. 5, where being able to operate at point C rather than point B improves fuel consumption by 6% while producing the same power. It can also have emission benefits, since partial power control points can be chosen to minimize exhaust emissions.

Currently, there are three configurations of spark-ignition engines in volume production: two-cycle, rotary, and four-cycle. The four-cycle engine has better thermal efficiency and lower inherent exhaust emissions than the other configurations. As a result, it is the predominant configuration and has a more developed emissions control system. The wankel rotary engine has better ratios of power to weight and volume than the four-cycle and is generally believed to have marginally lower production costs at equal production volumes. The rotary has lower inherent NOx but higher

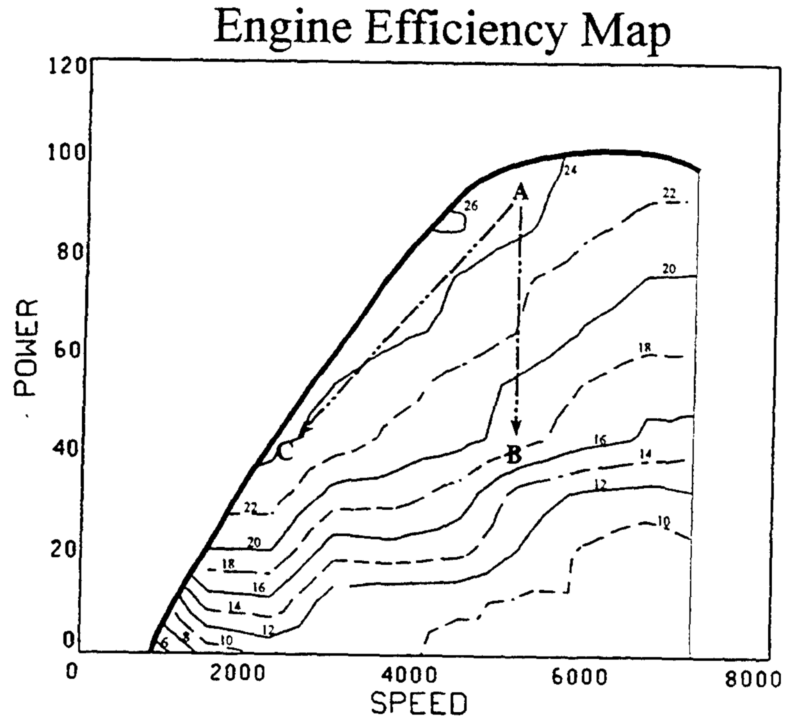

Figure 5. Typical engine efficiency map

unburned hydrocarbon emissions, plus lower thermal efficiency than four-cycle engines (Figs. 6 and 7) due to the combustion chamber geometry. In emission-controlled form, emissions levels are equal to those of four-cycle engines.

The rotary engine is a developed production powerplant that has gained acceptance in specialty markets. Many variants have been proposed; however, only two basic types have gained acceptance in the market. These engines are basically the same except for the cooling of the rotor. One has an oil-cooled rotor, and the other employs a charge-cooled rotor. Generally, the longer life and higher specific power engine is the oil-cooled rotor-type. The charge-cooled engine has the advantage of lighter weight per unit power.

The two-cycle engine has been used primarily in applications where its high ratio of power to weight and volume are advantages. It has been around longer than any of the engines investigated in this section. In its infancy in the industry, the two-cycle engine was competing directly with the double-acting steam engine with two power strokes per cycle. For low-power, small, carbureted two-strokes, the carry over of fresh charge into the exhaust gas port produces considerable unburned hydrocarbons in the exhaust and is one of the causes of high fuel consumption.

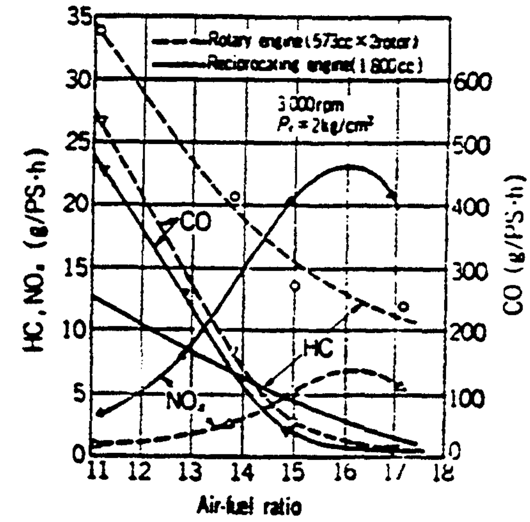

Figure 6. <u>Emissions of the rotary and reciprocating engines at similar power levels</u> (<u>4</u>)

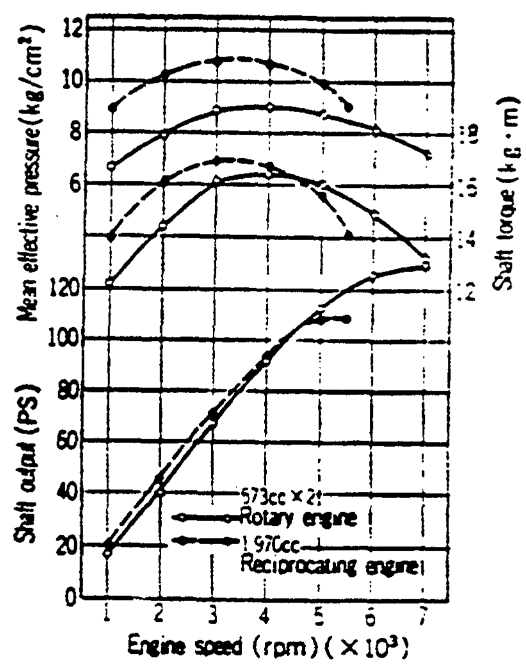

Figure 7. <u>Power levels for the rotary and reciprocating engines</u> (<u>4</u>)

The two-cycle engine with a crankcase inlet charge pump has to be lubricated by oil carried by the fuel or injected by a metering pump. This is also a source of exhaust hydrocarbons.(5)

Current design of the two-cycle engine has concentrated on the shortcomings of the engine. The two-cycle engine has low cylinder pressure for a specific power output. Cylinder pressure has a direct relation to the emissions of nitric oxides. If methods can be found to lower or eliminate the unburned hydrocarbons from the engine, it will be a serious contender for the low-emission category. Current designs have concentrated on injecting the fuel after the exhaust ports have closed. The most notable is a device that uses compressed air to deliver the fuel after exhaust port closure, developed by Orbital Engine Company. The oil consumption (usually burned in a "once-through" system) is lowered to the point where it is not a problem. While Orbital and others have been developing emission-controlled, two-cycle engine designs, none have been introduced into the market, so it is difficult to assess the efficiency and performance of an emission-controlled design.

The two-cycle engine has dominated the market in sizes primarily in the low-price category. This market thrives on simplicity. High fuel consumption is a trait for the two-cycle gasoline engine. This trait is tolerated for lower power output engines or recreational vehicles for the advantages of light weight and high power per unit weight. Potential exists for the two-cycle engine to be a strong competitor in the APU market. However, in a broad announcement soliciting APU options, no two-cycle powered systems were offered.

3. Recuperated or regenerated turbine-powered units. Turbine-powered units with shaft speed generators appear to offer excellent power-to-size and weight ratios. If the unit is properly controlled, and the generator is designed upstream of the turbine to reduce accessory cooling air flow requirements and to assist the pre-heating of turbine inlet gas to more favorable temperatures, these units appear to offer very good efficiency over at least the upper 50 percent of the power range. However, these units may not operate well below approximately 50 percent power without substantial efficiency degradation or compressor stall. Thus, the turbine may be inappropriate for charge maintenance applications where periodic low-power operation may be anticipated, although stopping the engine may be a way to handle this situation. However, the impact of frequent start/stop cycles on recuperator and heat-section durability and emissions are questionable. These

engines should be relatively quiet since they produce little low-frequency noise, and the recuperators and regenerators tend to be effective mufflers for both the intake and exhaust.

Cost has been a problem with gas turbine engines. This is a result of the materials required for the hot section and the low-production volume. Cost projections shown in Fig. 8 indicate that these engines could be reasonably competitive with other engines at sufficient production volume. However, these cost estimates do not include costs of the generator and power conditioning. Capstone Energy, Allied Signal, and others have been developing turbine generators, using low-pressure ratio turbines to minimize turbine inlet temperatures and thus material costs, and maintaining engine efficiency through recuperation or regeneration. Heat recovery efficiency is a major factor in engine efficiency as shown in Fig. 9. Developing an efficient, durable, and low-cost recuperator or regenerator has been the limiting technology of this type of engine.

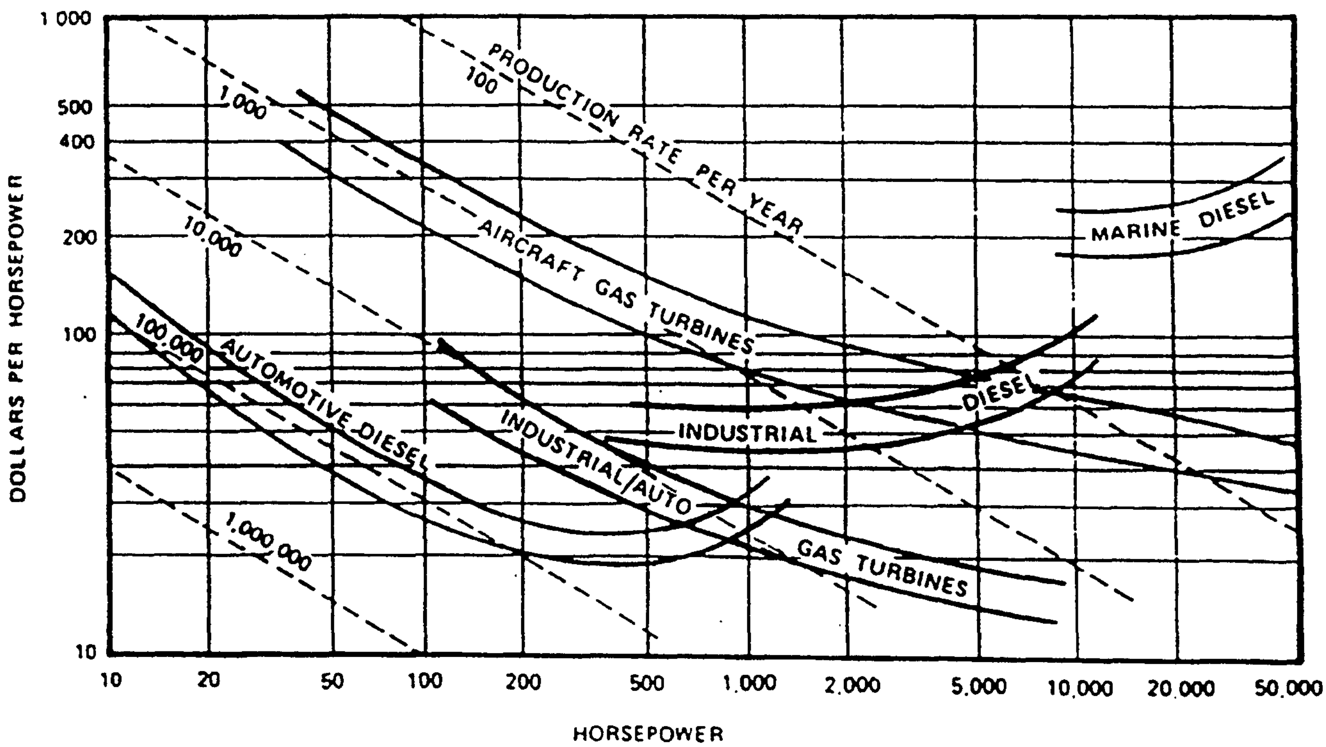

Figure 8. Cost projections (6)

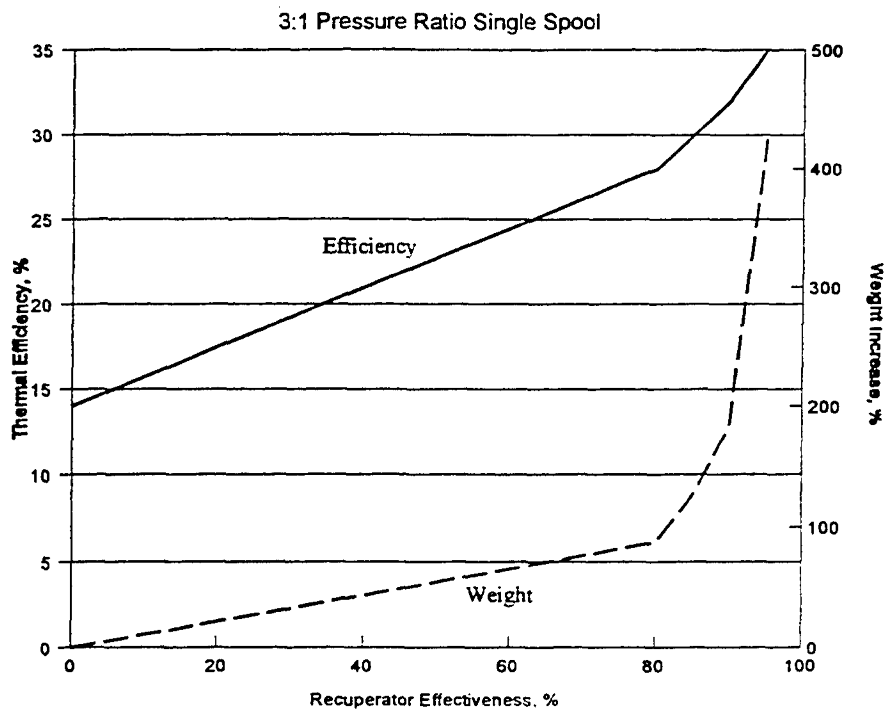

Figure 9. Turbine efficiency and weight impact (7)

4. Stirling Engines. Stirling engines have the potential for higher thermal efficiency than diesel designs. Recent studies with helium working gas demonstrated efficiencies as high as 40 percent, as shown in Fig. 10. The Stirling is fundamentally different from the other engines because its cycle consists of alternately heating and cooling a closed working fluid (usually hydrogen or helium) and using the volume change to drive power-extraction pistons. Power is controlled by varying the volume of the working fluid. The working fluid is heated by external combustion, which offers low emissions and multifuel capability. The working fluid is cooled through heat exchange with the surroundings. In addition to these two heat exchange processes, a regenerator is required to raise the thermal efficiency.

The external combustion feature of Stirling engines is a major advantage in alternative fuel applications because the very nature of the combustion process permits the flexibility for multifuel operation with low emissions. Preliminary measurements of these emissions, conducted on the STM4-120 engine (Stirling Thermal Motors, Inc. and Detroit Diesel Corporation) using natural gas fuel, indicate that the existing hardware already meets the proposed standards for both Heavy-Duty and Ultralow Emissions Vehicles (ULEV), as shown in TABLES 2 and 3.

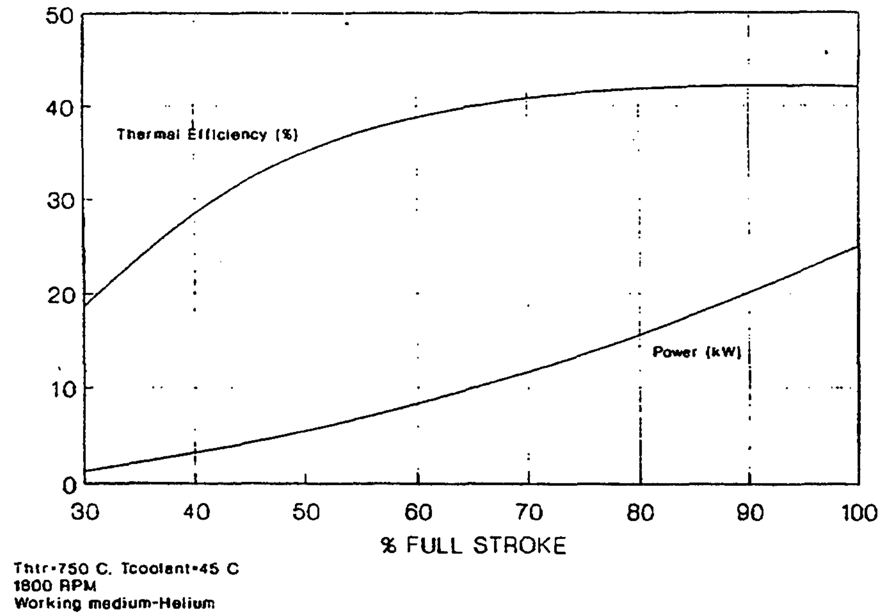

Figure 10. Efficiency of Stirling engines (8)

TABLE 2. Comparison of Typical Emissions for the STM4-120 Stirling Engine With Urban Bus Standards (9)

			STM4-120 Stirling Engine		
			Natural Gas*		Diesel**
Emissions†	California Urban Bus Standard (1996)	Federal Urban Bus Standard (1998)	0% EGR $\lambda = 1.5$	60% EGR $\lambda = 1.3$	0% EGR $\lambda = 1.5$
Hydrocarbons	1.74 (1.3)	1.74 (1.3)	0.29 (0.21)	0.037 (0.027)	0.073 (0.054)
NOx	2.69 (2.0)	5.37 (4.0)	0.57 (0.42)	0.20 (0.15)	0.43 (0.32)
CO	20.8 (15.5)	20.8 (15.5)	1.29 (0.95)	2.86 (2.12)	0.50 (0.37)
Particulate	0.068 (0.05)	0.068 (0.05)	0	0	0

* Emissions measurements conducted by TNO (National Technical Laboratories of The Netherlands) using Dutch natural gas fuel during July-September 1991. TNO conducts vehicle emissions certifications for the Dutch government.

** Diesel emissions data converted from Webasto Model DW 80 burner measurements, assuming 40 percent engine thermal efficiency.

† All emissions data in g/kW$_s$-hr (g/bhp-hr).

TABLE 3. Comparison of Typical Emissions for the STM4-120 Stirling Engine With Ultralow Emission Vehicle Standards (9)

		STM4-120 Stirling Engine		
		Natural Gas*		Diesel**
Emissions†	ULEV Standards	0% EGR $\lambda = 1.5$	60% EGR $\lambda = 1.3$	0% EGR $\lambda = 1.5$
Hydrocarbons	0.04	0.011	0.014	0.027
NOx	0.2	0.21	0.07	0.16
CO	1.7	0.48	1.07	0.19

* Emissions measurements conducted by TNO (National Technical Laboratories of The Netherlands), using Dutch natural gas fuel during July-September 1991. TNO conducts vehicle emissions certifications for the Dutch government.

** Diesel emissions data converted from Webasto model DW 80 burner measurements assuming 40 percent engine thermal efficiency.

† Emissions data in g/mi. Emission unit conversions are based on proprietary vehicle specific data.

Due to problems with heat exchanger size and effectiveness, material costs, complex engine controls, and sealing of the working fluid, these engines have generally been too costly to compete with other engine types. For APU applications, they are further hampered by their operating speed characteristics. Because of heat-transfer limitations, Stirling engines generally operate at low speeds, and efficiency falls as engine speed increases. This results in additional gearing or low generator rotating speed, either of which increases the APU package size. Stirling engines equipped with linear generators have been built, but the operating speed limitation impacts these configurations as well.

TABLE 4. Heat Engine Design Characteristics

Heat Engines	Power Range hp	Max. Efficiency % of Rated Power	Specific Weight lb/hp	Specific Volume ft^3/hp	Min. Fuel Consumption lb/hp-hr
Diesel					
Automotive, general	40 - 100	40 - 50	6 - 8	0.2 - 0.3	0.45 - 0.5
Automotive, specific	50	--	5.3	--	0.45
	70	--	4.0	--	0.44
Industrial, air-cooled	20 - 40	50 - 75	10 - 15	0.16 - 0.30	0.40-0.45
Industrial, water-cooled	40 - 100	50 - 75	7 - 10	0.13 - 0.24	0.38 -0.45
Reciprocating Spark Ignition					
Automotive	40 - 120	40 - 50	4 - 7	0.13 - 0.2	0.45 - 0.6
Industrial	25 - 60	45 - 55	5 - 15	--	0.56 - 0.58
Aircraft	60, 100, 115	50 - 65	2	--	
Gas Turbine					
APU (simple cycle)	20 - 60	--	2 - 3	0.1	1.1
Automotive (regen)	100 - 200	25 - 50	2.5 - 3	0.08 - 0. 0.1	0.5
Stirling	10 - 150	--	7 - 15	--	0.38 - 0.52
Rotary					
Two Rotor	100 - 170	56	1.3 - 2.2	0.05 - 0.07	0.44-0.56
One Rotor	50 - 85		2.3 - 2.5	0.06 - 0.08	0.56-0.60
	20 - 60		2.2 - 3.0	0.11 - 0.17	0.60-0.69

* Source: Collie, M.J.,"Electric and Hybrid Vehicles," Noyes Data Corporation, New Jersey, 1979

TABLE 4 summarizes relevant design and performance characteristics for each heat engine discussed above. The comparison includes each engine's power range, where maximum efficiency occurs, specific weight, specific volume, and peak efficiency. Figure 11 illustrates the variation of efficiency with power for several of the engine types.

The selection of an appropriate heat engine for hybrid vehicle applications is controversial, at best. Lack of more comprehensive data on Stirling, turbine, and rotary engines that have competitive fuel economy characteristics has forced many manufacturers to incorporate spark ignition and diesel

engines into their hybrid vehicle designs. However, a study conducted in the late 1970s, the Near-Term Hybrid Vehicle Program, indicated that spark ignition engines are favored over diesel engines due to uncertainties associated with the diesel engine's likelihood of meeting proposed NOx and particulate standards. On the other hand, one of the program contractors found it advantageous to incorporate a turbocharged diesel engine based on a 38-percent fuel savings (annually) over a comparable, naturally aspirated, spark ignition engine operating under their specialized control strategy.

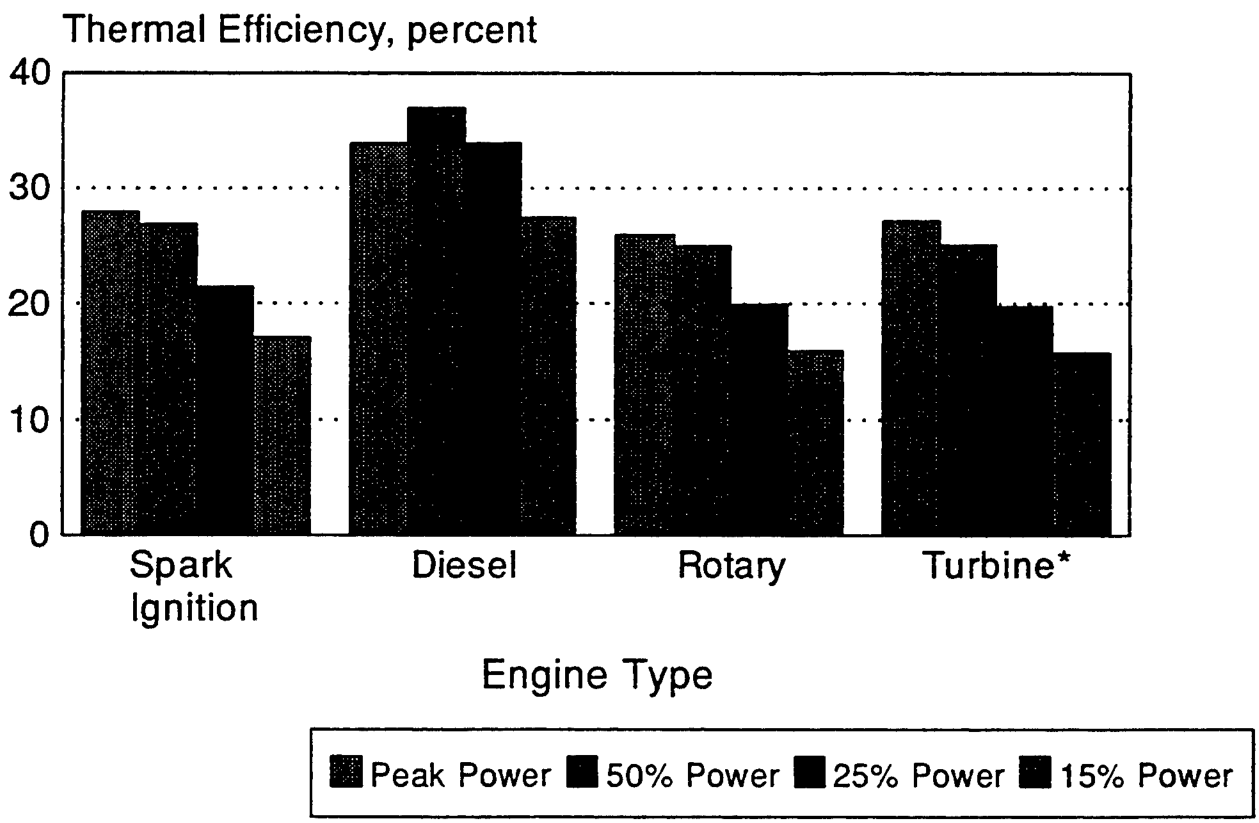

Figure 11. <u>Engine efficiency</u>

As previously mentioned, the initial phase of this APU development program included the selection and assignment of APU manufacturers to build natural gas-fueled prototype units of different technologies and power levels. Evaluation of available technologies led to the selection of three

APU systems: a four-cycle reciprocating piston engine, a four-cycle rotary engine, and a turbine engine. Availability, minimization of risk, technical potential, and manufacturers' experience with gaseous combustion power plants were the primary factors for the selection of the APU manufacturers.

B. Electrical Generators

The electrical generator used in the APU has a large impact on overall weight and package size. However, the efficiency variation between generators is considerably less than the variation resulting from different engine designs and control strategies. As a result, while the total system must be considered in designing an APU, generator efficiency is less of a factor than size and weight. While DC generators can be used, AC generators are superior in efficiency, weight, cost, and durability. Consequently, only AC generators will be discussed.

1. Options for Field Excitation

Two different methods are commonly used to produce the magnetic field in AC generators:

1) field coils requiring field excitation current to produce the excitation magnetic field, designated as wound-field AC generators; and
2) permanent-magnet assemblies that do not require excitation current to produce the excitation magnetic field, designated as PM AC generators.

Wound-field AC generators provide the capability to control the output voltage by controlling the field current. This field current control allows the output voltage of the generator to be controlled independently of the rotational speed. However, the need for field control is being obviated by the development of solid-state devices that can operate on the prevailing generator output voltage and efficiently control the power delivered to the load. Compared to the PM AC generator, the wound-field AC generators are larger and heavier.

As an example of the two different designs, comparative information about wound-field and PM AC generators made by the Onan Corporation are listed in TABLE 5.

TABLE 5. Comparison Between Wound-Field and PM AC Generators

Characteristics	Wound Field	Permanent Magnet
Power output, kW @ 6000 rpm	15	15
Volume, m^3	0.025	0.011
Weight, kg	29.4	12.2
Efficiency at 40 to 100 percent of rated load	82 to 87%	85 to 90%
Cooling method	Forced air	Forced air
Cost of production units (2,000 to 5,000 per year)	\$559	\$325

One of the major reasons for the size and weight reduction in the PM AC generator is the elimination of the size, weight, and power dissipation of the field coils. Because there is no need to allow space for the coils, the magnetic circuit components can also be smaller and lighter. However, magnetic field strength in PM machines is limited to about 0.5 Tesla, while current induced fields can reach the saturation limit for the materials (usually iron) of about 2.0 Tesla.

2. AC Generator Configurations

AC generators using PM materials are commonly available in two configurations, based on the direction of the magnetic field and the placement of the stator (AC output) coils. The common configurations are as follows:

1) The radial magnetic field has magnets mounted on the rotor shaft. The stator coils are mounted on an outer stator structure, and the direction of the magnetic field is perpendicular to the rotor shaft.

2) The axial magnetic field has magnets mounted on disks around the armature shaft. The stator coils are mounted between the magnets, and the direction of the magnetic field in the air gap is parallel to the rotor shaft.

Currently, AC generators using the radial configuration have the advantages of greater availability and lower cost compared to the axial design. Other configurations are in developmental stages and could be of greater interest in the next two to five years.

3. Basic Mechanical Construction of AC Generators

A basic mechanical drawing of a radial-type PM AC generator is shown in Fig. 12. For conceptual purposes, a two-pole machine with a single bar magnet as the rotor is illustrated. A wound field generator is conceptually the same, except a separate field coil is used to generate the magnetic field.

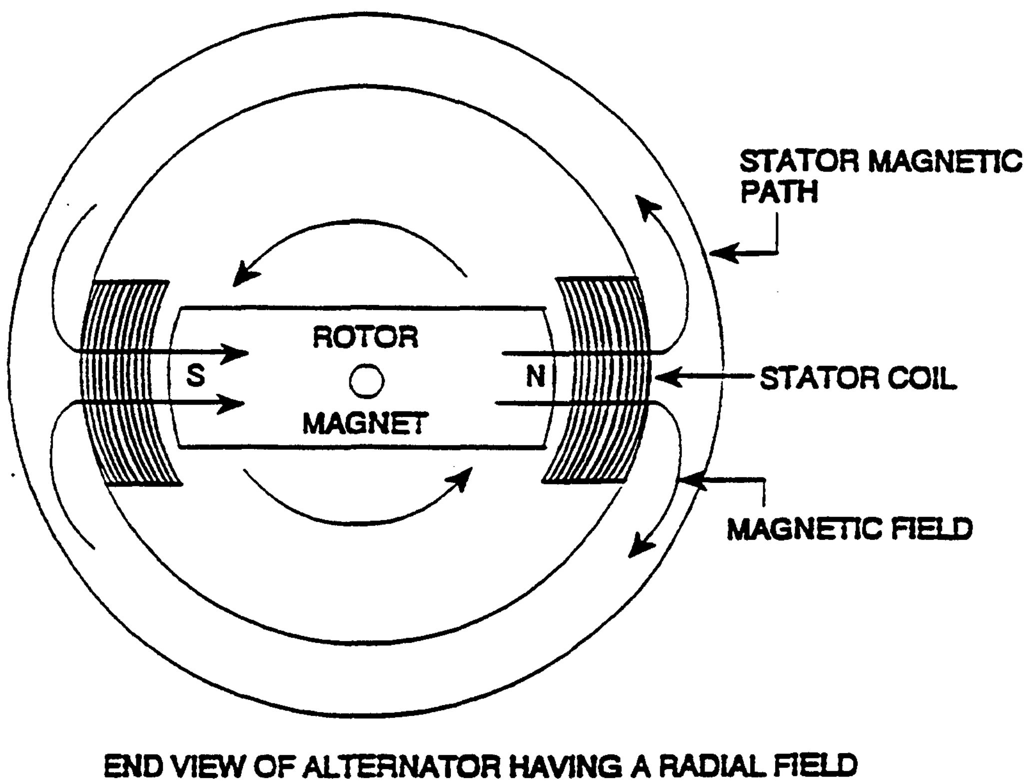

Figure 12. Fundamental operation of an alternator having a PM field

As the rotor turns, the magnetic field through the coils is maximum in the rotor position shown, and is minimum when the rotor has turned 90 degrees. When the rotor has turned 180 degrees, the

magnetic field through the coils is again maximum but has the opposite direction. Thus, the voltage induced in the coils alternates in polarity as the rotor turns; the two-pole configuration will produce one complete voltage cycle for each revolution of the rotor.

Practical and highly efficient AC generators have advanced magnetic circuit designs and coil designs that maximize the output power in a desired rpm range. The number of poles can be varied to produce the desired output frequency vs. rotating speed relationship. As the design speed increases, the size of the generator can be reduced as shown in Fig. 13. In most cases the size reduction with speed is not sufficient to justify gearboxes for speed increase. This generator characteristic tends to favor high speed engines. Higher speeds should also reduce generator cost.

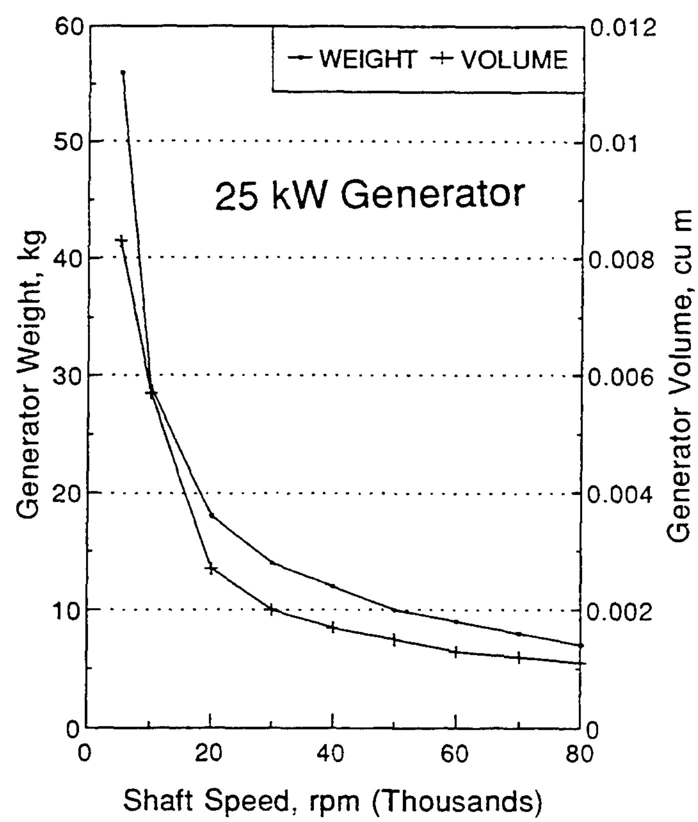

Figure 13. **AC generator speed versus size**

4. Electrical Equivalent Circuit of AC Generators

Figure 14 is an electrical equivalent circuit of a PM AC generator. In the equivalent circuit, the major elements are the windings where the voltage is generated, the inductance and resistance of the winding, and the losses in the magnetic circuit that can be simulated by an added series resistor. The induced voltage is proportional to a) the magnetic field strength, b) the rate of change of the magnetic field through the coil as determined by the rotor rpm, and c) the number of turns in the stator windings.

Losses in the AC generator occur in the electrical elements as described here:

1) The winding inductance causes a reduction in output voltage that is equal to the (output current) × (inductive reactance). Because the inductive reactance increases with frequency, the winding must be designed to have very low inductive reactance in the desired rpm range.

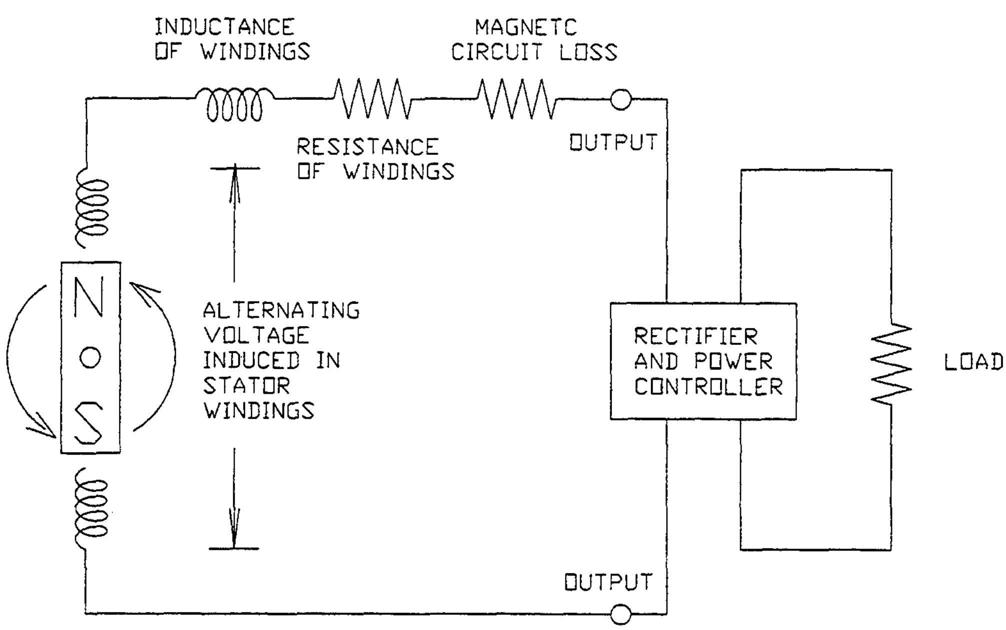

Figure 14. Equivalent circuit of an AC generator

2) Voltage loss in the winding resistance is equal to the (output current) × (winding resistance). The winding design must provide an acceptable resistive loss at the output current rating of the generator.

3) Magnetic circuit losses include "eddy current" losses that are a function of the rotor rpm. These losses cause heating of the magnets and the steel parts of the magnetic circuit. Acceptable magnetic circuit designs must minimize these losses.

A few AC generators having power outputs of 15 kW and 50 kW are provided in TABLE 6. This list is a result of a survey of many manufacturers. Those units listed use modern design practices and are also available as prototype or near-prototype models.

TABLE 6. Permanent Magnet AC Generators and Manufacturers

Rate Power, kW	Configuration of PM Field	AC Generator Volume, m^3	AC Generator Weight, kg	Manufacturer
15	Radial	0.11	12.2	ONAN Corporation
15	Radial	0.006	13.8	Fisher Electric Motor Technology, Inc.
15	Radial	0.0054	27	Neodyne Corporation
15	Axial	0.016	40.8	EML Research, Inc.
50	Radial	0.014	22.7	ONAN Corporation
50	Radial	0.009	15.9	Fisher Electric Motor Technology, Inc.
50	Axial	0.021	63.4	EML Research, Inc.

While PM AC generators would appear to be the preferred generator for APU applications, current PM generators usually require an additional power conditioning unit to convert from the output frequency and voltage to the DC voltage required for electric vehicle battery packs. Unlike wound

field generators where output voltage can be controlled independent of rotational speed, PM generator voltage varies linearly with speed. In order to match the output voltage to that required by the load, a step-up transformer or up-chopper or other rectification and voltage boost device is required if the generator is to be operated at a range of speeds. Otherwise, the driving engine must operate at a constant speed and vary the load by throttling or fuel regulation only.

In applications such as an EV, where DC power is used to charge the batteries and supply power to the propulsion subsystem, a rectifier and power control unit are required. This unit performs the following functions:

1) conversion of AC power to DC power, and

2) control of the voltage and current applied to the load as a function of battery charging and propulsion power requirements.

A typical output voltage versus rotor speed characteristic for an AC generator is shown in Fig. 15. At lower speeds, a constant maximum current is available, limited by the generator wire size and internal resistance. Exceeding this current would result in overheating. Note that the output voltage increases in proportion to the rotor speed until the winding inductance loss and magnetic circuit loss, which increase with rotor speed, cause a reduction in the output voltage. This fall-off point is set by the specific design.

Currently, these power conversion devices for PM generators can more than offset any cost advantage of the PM generator, and may increase the total package volume and weight above that of a wound-field generator. A number of manufacturers are working to reduce the cost and size of these voltage step-up units. In addition, several organizations are working on approaches to varying

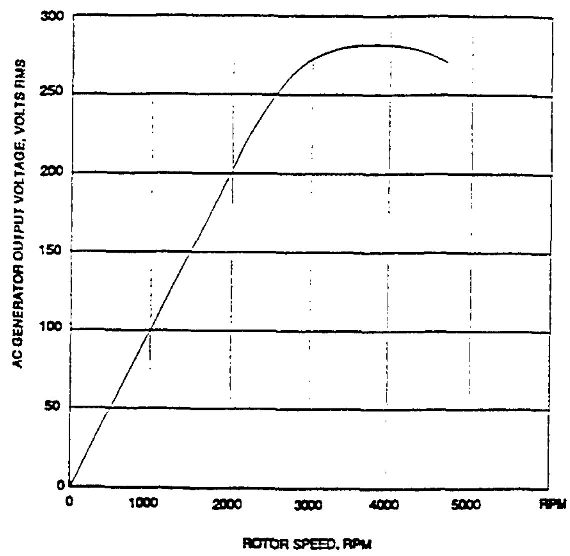

Figure 15. Typical AC generator output voltage

the field strength of PM generators during operation. Approaches being investigated include both electrical and mechanical (alignment control) field weakening. Mixed-mode generators have also been built that include a wound-field coil assembly to allow boosting the permanent magnet-produced field. Advances in PM-generator field control or in electronic power management are likely to have the greatest impact on APU size, weight, and cost.

VI. INTEGRATION OF APU WITH PURE ELECTRIC VEHICLES

A. APU Design Impacts in Commercial Vehicle Design

Conversion of an EV into an HEV, by introducing an on-board power generating unit (APU), requires that the existing EV components be considered with respect to the HEV's ultimate functionality. If the goal is to extend the range using electric power, the EV can be retrofitted in a series configuration. On the other hand, if the ultimate goal is to augment driving power and/or allow for multiple power source (engine only, battery only) operation of an HEV, then configuration changes would be extensive. Consequently, strategies for incorporating an APU into an EV will depend on the configuration selected.

An APU integration into a series configuration HEV would seem to be a simpler effort since the APU produces electrical power that an existing EV is accustomed to accepting and providing with its batteries. The additional complexity introduced would only be the modification of the batteries'

charging circuit and the additional control logic to operate the engine and the generator. This means that there is no fixed mechanical connection between the engine and the drivetrain. Consequently, the design strategy (as mentioned in the preceeding section) is to operate the engine at those points in the engine-speed/torque map with highest efficiency and lowest emissions.

Design integration of an APU into an EV also requires that more efficiency arrangements be considered. An example of such strategy is to evaluate the possibility of bypassing the inefficiencies of battery charging by powering the traction motors directly from the generator output (instead of storing energy in the battery and then extracting that energy to drive the motors). This arrangement does not prohibit the charging of the batteries, but it may create significant control software and hardware difficulties.

B. Auxiliary Loads Issues in APU Designs

Auxiliary loads are typically classified into two categories: vehicle (such as accessories, lights, ignition, etc.) and instrumentation (computer and controllers). It is important that power to the computer and control units be uninterrupted and of a relatively high quality to avoid premature shutdowns and/or undesirable control problems. Several vehicle loads, such as starters and electric power steering, require high current and can easily cause serious voltage-regulation malfunctions if not designed properly. Control computer electrical loads are comparatively less demanding. A proposed GM hybrid electric minivan indicated that a dual, 12-volt auxiliary electrical system, each with its own separate battery and isolated grounds, would be sufficient to satisfy its requirements. GM maintained that a 600-watt, 300-volt to 15-volt DC-DC converter would supply power from the propulsion battery to each system. Additional circuitry was incorporated to limit the converter input voltage to 400 volts, which can occur during regenerative braking.

One significant advantage of a hybrid electric vehicle, which has a heat engine over a purely electric vehicle, is that the HEV engine provides waste heat for heating the interior of the vehicle. An EV would have to utilize electrical power from the batteries to accomplish the same task, decreasing the energy available for propulsion. Therefore, integration of an APU into an EV has a positive impact toward reducing electrical demand on the batteries. Air conditioning and ventilation requirements

imposed on the vehicle's electrical power source, however, are not alleviated with the introduction of an APU. To place these requirements in perspective, it is sufficient at this point to mention that the ASHRAE Code recommends 15 cfm of ventilation air per person for transportation vehicles. According to some literature, 50 percent of the steady-state cooling loads in conventional air-conditioning systems corresponds to ventilation loads alone. TABLE 7 lists estimated steady-state cooling load requirements for a G-Van in BTU/hr.

TABLE 7. G-Van Estimated Steady-State Cooling Loads (BTU/hr) (10)

				Ventilation Load		Metabolic Load Occupants		
Operating Condition	Van Type	Solar Load 83% Trans.	Conduction Load	30 cfm	45 cfm	2	6	Total
Stationary	Panel	3,450	12,180	2,490		1,000		19,120
	Panel w/partition	3,450	4,390	2,490		1,000		11,330
	Window	3,450	5,060		3,730		3,000	15,240
35 mph	Panel	3,450	10,620	2,490		1,000		17,560
	Panel w/partition	3,450	3,550	2,490		1,000		10,490
	Window	3,450	3,880		3,730		3,000	14,060

The important issue when integrating an APU with an electric vehicle, as far as auxiliary loads are concerned, is to consider incorporating (or possibly integrating) cooling or heating components directly into the APU system. Past and current research has placed limited focus on the issue. As a result, the impact of this concept on overall efficiency, performance, and range of HEV is not fully understood. However, direct drive of mechanical accessory loads by the engine may be more efficient than adding an additional electrical motor and suffering the required conversion efficiency losses.

C. APU Noise Considerations

Vehicles radiate interior and exterior acoustic noise, which depends on the operating conditions: stationary/idle, acceleration, and constant speed modes. Although audible sounds can range from

the threshold of hearing (0 dB) to the threshold of pain (over 130 dB), most vehicle-generated noise levels are typically below 80 dB.

Typical noise that reaches the driver's ears originates at the tires, transmission, engine, etc. The most predominant concern of APU integration with an EV is the APU engine-generated noise. TABLE 8 illustrates comparative noise levels between an all-electric vehicle and a conventional ICE vehicle.

TABLE 8. Sound Level Comparison (in dB) for an Electric Vehicle and an ICE Vehicle (11)

Vehicle and Ballast Condition	Stationary/Idle		Acceleration		Constant Speed Tests: 56 km/h		Constant Speed Tests: 72 km/h		Constant Speed Tests: 88 km/h	
	Interior	Exterior	Interior	Exterior	Interior	Exterior	Interior	Exterior	Interior	Exterior
Evcort Electric @ 1,700 kg	37.0	55.4	65.8	59.0	66.3	60.9	67.5	65.3	68.8	67.1
Escort ICE @ 1,700 kg	--	--	--	--	66.6	61.9	67.9	65.9	69.3	67.8
Escort ICE @ 1,200 kg	51.8	65.0	71.9	68.2	65.6	--	66.9	--	68.9	67.6

An interesting result observed from the tests is that for this vehicle at constant speeds, the pure electric and ICE vehicles both exhibited essentially equivalent interior and exterior noise levels. Control of noise from the APU may need to be a factor in the development of the vehicle power management strategy. Noise-control measures may include stopping or idling the engine at low-vehicle speeds, or increasing delayed engine power during accelerations.

D. Life Cycle Cost Impact

One of the unresolved issues of integrating an APU into an EV is its impact on life-cycle costs (LCC) of the vehicle. A preliminary comparison reported by personnel in the Argonne National Laboratory and Regional Transportation Authority indicated that LCC are slightly higher (8 percent compared to a parallel configuration) due to the added weight and cost of the battery, especially for a non-optimum series hybrid system. This implies, however, that a greater emphasis should be

placed on reducing the weight and cost of the batteries to improve LCC. TABLE 9 shows LCC results for a pure internal combustion engine vehicle and two electric vehicle configurations.

TABLE 9. Life Cycle Cost Analysis Results (US cents/km) (12)

	Gasoline ICEV	Low-Performance EV	High-Performance EV
Purchased electricity (accounts for regenerative braking and battery thermal losses)		2.52	1.60
Vehicle, excluding battery	13.27	10.57	9.01
Battery plus tray and auxiliaries		11.09	6.51
Fuel, excluding retail taxes (except fuel used for heating and including taxes)	3.41	0.00	0.00
Home recharging station	0.00	0.06	0.06
Insurance (calculated as a function of vehicle *miles* traveled and vehicle value)	2.22	3.15	3.07
Maintenance and repair	2.89	2.31	2.31
Oil	0.07	0.00	0.00
Replacement tires (calculated as a function of vehicle *miles* traveled and vehicle weight)	0.25	0.40	0.21
Parking and tolls	0.67	0.67	0.67
Registration fee (calculated as a function of vehicle weight)	0.14	0.18	0.13
Inspection and maintenance fee	0.22	0.11	0.11
Fuel taxes	0.90	0.90	0.90
Accessories	0.11	0.11	0.11
Total consumer life-cycle cost, cents/km for light-duty vehicles	24.16	32.07	24.69
The break-even retail price of gasoline*	N/A	4.22	1.67

* The price of gasoline, including retail taxes of US $0.31/gal, that equates the full life-cycle cost per km of the EV with the full life-cycle cost per km of the GV.

It can be inferred from TABLE 9 that introducing an APU into an EV may not significantly increase the life-cycle cost of a "high-performance" vehicle. For example, an ICEV not operating at optimum conditions (as an APU heat engine would) incurs 3.41 cents/km, 0.07 cents/km in oil usage, and 2.89 cents/km in repairs. If we assume an improved configuration (20 percent better), the total life-cycle cost would be approximately 27.33 cents/km.

Other studies seem to substantiate these encouraging operating cost findings. Unique Mobility, for example, developed an electric van with extended range using a HONDA-powered APU. Comparison of operating costs using extensive manufacturer's and test data indicated that their van would incur less operating expenses than a pure ICE van (see TABLE 10).

TABLE 10. Vehicle Operating Costs (US cents/mile) (12)

	Unique Mobility Van	ICE Van
Energy Cost		
Gasoline	1.68	6.94
Electricity	1.10	--
Total	**2.78**	**6.94**
Tuneups	0.74	1.13
Oil, lubricants	0.24	0.35
Tires	0.73	0.58
Batteries (propulsion)	2.04	--
General maintenance	1.83	2.15
Total cents/mile	**8.36**	**11.15**

Both vehicles were modeled to operate 80 miles/day, 250 days/year, with their retirement at 100,000 miles. Cost of gasoline was assumed to be $1.25/gal, and vehicle fuel usage was estimated to be 18 mpg. Battery charger efficiency was assumed to be 85 percent with a cost of $0.05/kWh. The analysis also assumed that the required battery pack be replaced at 50,000 miles. Unique Mobility also investigated the impact of battery life, energy costs and conventional fuel economy on operating cost of their van compared to a conventional minivan. Figure 16 illustrates the results of this comparison.

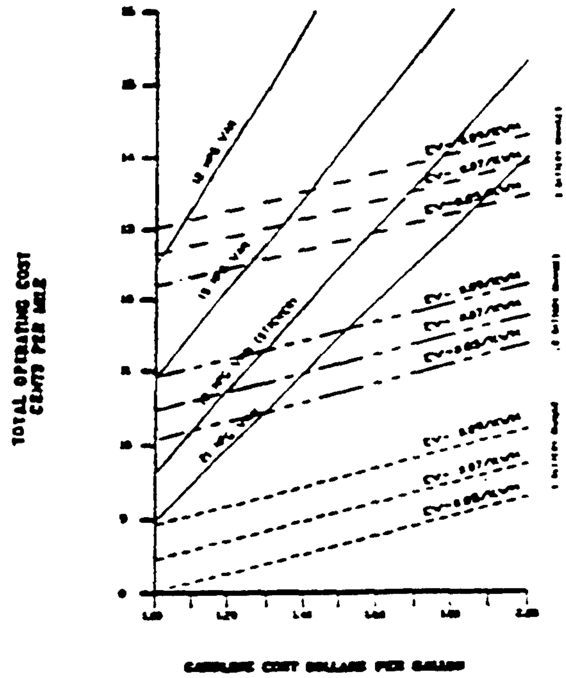

Figure 16. Operating cost comparison (12)

VII. ENHANCEMENT NEEDS IN APU SYSTEM AND COMPONENT DESIGN

Heat engine technological advancement requirements for APU application include optimizing engine performance and durability for high power level operating modes. Designing for durability, however, tends to negatively impact engine size and weight. This indicates a need to investigate more exotic, light-weight materials for all APU system components (and possibly the engine itself) to assist in satisfying overall vehicle weight requirements. Alternative fuels that may become more available or inexpensive in the future, and that could power modified or newly designed engines, is also an identified area of research intended to reduce overall energy costs and air pollution. Ideally, an engine capable of operating with different types of fuel and blends would significantly improve APU flexibility. Other potential improvement requirements in engine design include a more efficient overhead valve design instead of side valve designs. In addition, it is imperative that reduction of formaldehyde and oxides of nitrogen be achieved within compliance levels. Finally, fuel cell development must continue as an alternate power source for futuristic APUs.

One of the main drawbacks in a series hybrid vehicle is the driveline inefficiencies. More specifically, the driveline components (engine, generator and motor) in a series hybrid system are configured in series (thus, the term "series"). As a result, mechanical energy of the engine is converted to electrical energy using the generator, and this electrical energy is then converted back to mechanical energy. Each conversion process subjects the system to additive energy losses resulting from these components' inefficiencies. Ideally, it would be desirable to attain combined generator and electric motor efficiency comparable to a conventional gearbox efficiency (typically, over 90 percent). It would certainly be beneficial to drive research toward achieving levels as high as possible in this respect. In fact, some companies are currently investigating this possibility by developing a generator-motor set using high-speed, synchronous generators and motors with new permanent magnets possessing a very high magnetic energy density. Integrating generator and drive motor functions implies that APU design will be affected as it deviates from conventional stand-alone philosophy to a more flexible combination of a series/parallel configuration approach.

As mentioned earlier, passenger cooling requirements affect vehicle range and performance. It is imperative that the transition be made from commercial air-conditioning systems to EV-specific cooling systems. This implies improving condenser performance levels over standard fin-tube condensers, using an efficient, continuously variable speed, motor/compressor system, etc. This is relevant in APU development since integrated APU/air conditioning systems may be beneficial for achieving superior, overall system efficiency.

Other technological advancement requirements are related directly to generators and inverters. Although manufacturers are proposing to replace AC generators in APUs with more efficient, brushless, motor/inverter combinations, details and specifications of these and other APU components (including advanced, integrated, vehicle/APU, control-unit algorithms) can still undergo several revisions and changes as new ideas are examined.

VIII. LIST OF REFERENCES

1. Teachman, M.E., Scott, D.S., and Rogner, H.H., "Solid Polymer Fuel Cell Versus Spark Ignition Engine Technology for Utility Vehicles," SAE Paper No. 932951, 1993.

2. Burke, A.F., "Hybrid Vehicle Design, Simulation, and Test," presentation, Idaho National Engineering Laboratory.

3. Smith, P.H., "The High Speed Two-Stroke Petrol Engine," copyright 1965, Phillip H. Smith, G.T. Foulis and Sons Co. Ltd., London.

4. Yamamoto, K.,"Rotary Engine," Sankaido Corp., Tokyo, 1981

5. Schweitzer, P.H., "Scavenging of Two-Stroke Cycle Diesel Engines," MacMillan Co., New York.

6. Woodhouse, G.D., "A New Approach to Vehicular-Gas-Turbine Power-Unit Design," Paper 81-GT-152, ASME, New York, 1981.

7. Mackay, R., "Hybrid Vehicle Gas Turbines," 1993.

8. Stirling Thermal Motors, Inc. Brochure

9. Stirling Thermal Motors, Inc. Brochure

10. Dieckmann, J. and Mallory, D., "Climate Control for Electric Vehicles," SAE Paper No. 910250, 1991.

11. MacDowall, R.D., "Comparative Evaluation of Acoustical Noise Levels of Soleq Evcort EV and ICE Counterpart," SAE Paper No. 900138, 1990.

12. Marr, W.W.; Walsh, W.J. of Argonne, "Life-Cycle Cost Evaluations of Electric/Hybrid Vehicles," printed 1992

REFERENCES INCLUDED IN ORIGINAL REPORT BUT NOT CITED IN TEXT

Josefowitz, W. and S. Kohle, "Volkswagen Golf Hybrid - Vehicle Design and Test Results," 1992.

Kalberlah, A., "Electric Hybrid Drive Systems for Passenger Cars and Taxis," SAE Paper No. 910247, 1991.

Marr, W.W. and R.R. Sekar, "Analysis of a Diesel-Electric Hybrid Urban Bus System," Draft Copy.

Keller, A.S. and G.D. Whitehead, "Performance Testing of the Extended-Range (Hybrid) Electric G Van," SAE Paper No. 920439, 1992.

Dorgham, M.A., "Technological Advances in Vehicle Design - Ford Energy Report," Ford Publication SP1, 1982.

Dorgham, M.A., "Technological Advances in Vehicle Design - Electric and Hybrid Vehicles," Ford Publication SP2, 1982.

Proceeding of the First International Electric Vehicle Symposium, November 1969.

Green, A.P., C. McGrath, and J. Murray, "Global Opportunities and Risks for Electric and Hybrid Low Emission Vehicles," SAE Paper No. 931011, 1993.

Collie, M.J., Electric and Hybrid Vehicles, Noyes Data Corporation, New Jersey, 1979.

Society of Automotive Engineers, "Electric Vehicle Design and Development," SAE Publication #SP 862, February 1991.

Society of Automotive Engineers, "Electric Vehicle Technology," SAE Publication #SP 817, February 1990.

DISTRIBUTION LIST

Department of Defense

DEFENSE TECH INFO CTR CAMERON STATION ALEXANDRIA VA 22314	12
ODUSD ATTN: (L) MRM PETROLEUM STAFF ANALYST PENTAGON WASHINGTON DC 20301-8000	1
ODUSD ATTN: (ES) CI 400 ARMY NAVY DR STE 206 ARLINGTON VA 22202	1
DIR ADV RSCH PROJ AGENCY ATTN: ARPA/ASTO 3701 N FAIRFAX DR ARLINGTON VA 22203-1714	3

Department of the Army

HQDA ATTN: DALO TSE DALO SM PENTAGON WASHINGTON DC 20310-0103	 1 1
SARDA ATTN: SARD TL PENTAGON WASHINGTON DC 20310-0103	 1
CDR AMC ATTN: AMCRD S AMCRD IT 5001 EISENHOWER AVE ALEXANDRIA VA 22333-0001	 1 1
CDR ARMY TACOM ATTN: AMSTA TR NAC AMSTA TR R/202 USMC LNO AMCPM LAV AMCPM M113/M60 AMCPM CCE/SMHE WARREN MI 48397-5000	 1 1 1 1 1 1
DEPARTMENT OF THE ARMY MOBILITY TECH CTR BELVOIR ATTN: AMSTA RBF (M E LEPERA) AMSTA RBXA (R E TOBEY) 10115 GRIDLEY RD STE 128 FT BELVOIR VA 22060-5843	 10 1
PROG EXEC OFFICER ARMORED SYS MODERNIZATION ATTN: SFAE ASM S SFAE ASM BV SFAE ASM CV CDR TACOM WARREN MI 48397-5000	 1 1 1
PROG EXEC OFFICER ARMORED SYS MODERNIZATION ATTN: SFAE ASM FR SFAE ASM AF PICATINNY ARSENAL NJ 07806-5000	 1 1
PROG MGR UNMANNED GROUND VEH ATTN: AMCPM UG REDSTONE ARSENAL AL 35898-8060	 1
DIR ARMY RSCH LAB ATTN: AMSRL CP PW 2800 POWDER MILL RD ADELPHIA MD 20783-1145	 1
VEHICLE PROPULSION DIR ATTN: AMSRL VP (MS 77 12) NASA LEWIS RSCH CTR 21000 BROOKPARK RD CLEVELAND OH 44135	 1
CDR AMSAA ATTN: AMXSY CM AMXSY L APG MD 21005-5071	 1 1

CDR ARO
ATTN: AMXRO EN (D MANN) 1
RSCH TRIANGLE PK
NC 27709-2211

CDR ARMY NRDEC
ATTN: SATNC US (J SIEGEL) 1
SATNC UE 1
NATICK MA 01760-5018

CDR ARMY LEA
ATTN: LOEA PL 1
NEW CUMBERLAND PA 17070-5007

CDR ARMY TECOM
ATTN: AMSTE TA R 1
AMSTE TC D 1
AMSTE EQ 1
APG MD 21005-5006

PROG MGR PETROL WATER LOG
ATTN: AMCPM PWL 1
4300 GOODFELLOW BLVD
ST LOUIS MO 63120-1798

PROG MGM MOBILE ELEC PWR
ATTN: AMCPM MEP 3
7798 CISSNA RD STE 200
SPRINGFIELD VA 22150-3199

CDR FORSCOM
ATTN: AFLG TRS 1
FT MCPHERSON GA 30330-6000

CDR TRADOC
ATTN: ATCD SL 5 1
INGALLS RD BLDG 163
FT MONROE VA 23651-5194

CDR ARMY ARMOR CTR
ATTN: ATSB CD ML 1
ATSB TSM T 1
FT KNOX KY 40121-5000

CDR ARMY FIELD ARTY SCH
ATTN: ATSF CD 1
FT SILL OK 73503

CDR ARMY TRANS SCHOOL
ATTN: ATSP CD MS 1
FT EUSTIS VA 23604-5000

CDR ARMY INF SCHOOL
ATTN: ATSH CD 1
ATSH AT 1
FT BENNING GA 31905-5000

CDR ARMY ENGR SCHOOL
ATTN: ATSE CD 1
FT LEONARD WOOD
MO 65473-5000

CDR ARMY CSTA
ATTN: STECS EN 1
STECS LI 1
STECS AE 1
STECS AA 1
APG MD 21005-5059

CDR ARMY YPG
ATTN: STEYP MT TL M 1
YUMA AZ 85365-9130

CDR ARMY CERL
ATTN: CECER EN 1
P O BOX 9005
CHAMPAIGN IL 61826-9005

DIR 1
AMC FAST PROGRAM
10101 GRIDLEY RD STE 104
FT BELVOIR VA 22060-5818

PS MAGAZINE DIV
ATTN: AMXLS PS 1
DIR LOGSA
REDSTONE ARSENAL AL 35898-7466

Department of the Navy

DIR LOGISTICS PLANS & POLICY/
STRATEGIC SEALIFT PROG DIV (N42)
ATTN: N420 1
2000 NAVY PENTAGON
WASHINGTON DC 20350-2000

CDR
NAVAL SEA SYSTEMS CMD
ATTN: SEA 03M3 1
2531 JEFFERSON DAVIS HWY
ARLINGTON VA 22242-5160

CDR
NAVAL SURFACE WARFARE CTR
ATTN: CODE 63 1
CODE 632 1
CODE 859 1
3A LEGGETT CIRCLE
ANNAPOLIS MD 21402-5067

Department of the Navy/U.S. Marine Corps

HQ USMC ATTN: LPP WASHINGTON DC 20380-0001	1	CDR MARINE CORPS SYS CMD ATTN: SSE 2033 BARNETT AVE STE 315 QUANTICO VA 22134-5010	1
PROG MGR COMBAT SER SPT MARINE CORPS SYS CMD 2033 BARNETT AVE STE 315 QUANTICO VA 22134-5080	1	CDR BLOUNT ISLAND CMD ATTN: CODE 922/1 5880 CHANNEL VIEW BLVD JACKSONVILLE FL 32226-3404	1
PROG MGR GROUND WEAPONS MARINE CORPS SYS CMD 2033 BARNETT AVE QUANTICO VA 22134-5080	1	CDR MARINE CORPS LOGISTICS BA ATTN: CODE 837 814 RADFORD BLVD ALBANY GA 31704-1128	1
PROG MGR ENGR SYS MARINE CORPS SYS CMD 2033 BARNETT AVE QUANTICO VA 22134-5080	1		

Department of the Air Force

HQ USAF/LGTV ATTN: VEH EQUIP/FACILITY 1030 AIR FORCE PENTAGON WASHINGTON DC 20330-1030	1	AIR FORCE MEEP MGMT OFC 615 SMSQ/LGTV MEEP 201 BISCAYNE DR STE 2 ENGLIN AFB FL 32542-5303	1
AIR FORCE WRIGHT LAB ATTN: WL/POS 1790 LOOP RD N WRIGHT PATTERSON AFB OH 45433-7103	1	SA ALC/SFT 1014 BILLY MITCHELL BLVD STE 1 KELLY AFB TX 78241-5603	1
		WR ALC/LVRS 225 OCMULGEE CT ROBINS AFB GA 31098-1647	1

Other Federal Agencies

NASA LEWIS RESEARCH CENTER CLEVELAND OH 44135	1	EPA AIR POLLUTION CONTROL 2565 PLYMOUTH RD ANN ARBOR MI 48105	1
DOE CE 151 (MR RUSSELL) 1000 INDEPENDENCE AVE SW WASHINGTON DC 20585	1		

FINAL REPORT

ELECTRIC DRIVE M113 VEHICLE REFURBISHMENT PROJECT

SACRAMENTO ELECTRIC TRANSPORTATION CONSORTIUM RA 93-23 PROGRAM

FEBRUARY 1997

DOCUMENT 3

Electric Drive M113 Vehicle Refurbishment Project Sacramento Electric Transportation Consortium RA 93-23 Program

AD-A322403

February 1997

FMC Corp
Santa Clara, CA

FINAL REPORT

ELECTRIC DRIVE M113 VEHICLE REFURBISHMENT PROJECT

ABSTRACT

The Electric Drive M113 Refurbishment Project involved upgrading an existing M113 personnel carrier with updated electronics to meet current safety and performance standards. Several specific areas were refurbished, including design and installation of an improved power converter and motor controller assembly.

The original design obtained propulsion power from only the engine driven gen-set. The vehicle was modified for "engine-off" operation using battery power only. The vehicle was tested and demonstrated at a number of DARPA conferences and other locations under the purview of Tank Automotive Command (TACOM).

The cover report by the Sacramento Electric Transportation Consortium management essentially refers to the attached Appendix A Final Report by United Defense/FMC for all specific information on the activities and findings of the Project.

INTRODUCTION AND OBJECTIVES

The M1 13 Refurbishment Project was initiated by DARPA to demonstrate the capabilities of current electric drive technologies in a military vehicle. This was an extremely economical initial step in advancing battery and hybrid drives for military use.

As the entire Project was carried out by FMC/United Defense and TACOM, this Final Report will serve only as a cover report for the Final Report prepared by FMC/United Defense, included as Attachment A. The Project was very successful in demonstrating the advantages of electric drive systems in medium duty vehicles.

SUMMARY AND CONCLUSIONS

As this Project essentially involved a first phase of work for the M113 platform, conclusions on the performance of the technologies involved are limited, primarily resulting in recommendations on the next activities to consider for development of system and design improvements. See the attached Appendix A Report for detailed information on these and other conclusions of the Project.

ADMINISTRATIVE ACTIVITIES AND PROJECT EXPENDITURES

The Project spanned two years time, with the vehicle in the possession of TACOM primarily. The term of the SETC RA 93-23 Grant was extended at the time this Project was added to the Grant to provide two full years of use by the Project, under the purview of TACOM.

Expenditures for the Project were generally as planned and approved. A significant increase in matching costs was incurred by United Defense/FMC due to DARPA requested vehicle preparation and logistical support.

Overall Project expenditures totaled over $525,000, with $220,000 being DARPA funds. Each quarterly/triennial/biennial DARPA conference over the term of the Project was attended by SMUD and by a representative of United Defense/FMC.

Sacramento Municipal Utility District
Electric Drive M113 Vehicle Refurbishment Project

Final Report

Prepared for:

Sacramento Municipal Utility District
Mr. Steve Rutter, Principal Engineer
Electric Transportation Department
PO Box 15830 - MS 30A
Sacramento, CA 95817-1899

SMUD Contract Number F-379
FMC Project Number D901

Prepared by: Gordon Shafer	FMC ELECTRIC DRIVE SYSTEMS
Approved by: Michael Rowan	FMC Corporation Energy & Transportation Equipment Group 1205 Coleman Avenue Santa Clara, CA 95052

Table of Contents

—

Section 1. EXECUTIVE SUMMARY

This final technical report, prepared by FMC Corporation Corporate Technology Center for the Sacramento Municipal Utility District under Contract F-379, describes the execution of the Electric Drive M113 Vehicle Refurbishment Project.

The M113 Vehicle Refurbishment Project is part of the Advanced Research Projects Agency (ARPA) Electric and Electric Hybrid Vehicle Technology program. Established in 1993, this program pursues development and demonstrations of technologies for electric and hybrid vehicles that address military missions and cost mitigation. The Sacramento Municipal Utility District (SMUD) is one of six regional consortia selected to participate in the program.

The overall goal of the M113 Vehicle Refurbishment Project was to bring the existing FMC-owned M113 mechanical drive vehicle up to current standards for safety and performance. Several specific areas were targeted for refurbishment which included the design and installation of an improved power converter and motor controller assembly. The original scope of work was amended after the start of the project to include tasks to install two (2) battery packs to allow "engine-off" operation.

The project was completed on schedule and the refurbished vehicle was demonstrated at several ARPA and TACOM sponsored events during the remainder of the contract period. Although no rigorous performance testing of the vehicle was performed, the refurbished M113 demonstrated automotive performance equal to and/or greater than the original mechanical drive M113 vehicle.

Several recommendations resulted from the effort, including recommendations to 1) further upgrade the vehicle to include advanced battery technologies; 2) repackage the batteries to optimize available space; and 3) perform controlled automotive and dynamometer testing to quantify system performance.

Section 2. PROJECT OBJECTIVES

2.1 Background

The Electric Hybrid Vehicle Technology Program

The ARPA Electric and Hybrid Vehicle Technology Program pursues research, development, and demonstrations of technologies for electric and hybrid vehicles that address military missions, modernization, and cost mitigation.

Established by Congress in 1993, the program has accelerated technology development in multiple efforts to respond to increasing electrical power demands of military vehicles and sub-systems, enhance national energy security, and comply with Federal clean air legislation.

Hybrid electric propulsion is identified as a key technology having the following:

- Potential to increase component placement flexibility within vehicles
- Increase fuel economy by continuously operating smaller engines under optimum conditions
- Reduce armor protected volume
- Increase overall power density by combining power generation for weapons, sensors, survivability subsystems, and propulsion systems
- Increase acceleration and maneuverability due to immediate torque to the tracks
- Reduce vehicle thermal and acoustic signatures when operating from on-board energy storage
- Reduce system costs and logistics requirements through component commonalty, industrial stability, and production volume leveraging with commercial suppliers

ARPA Program Approach

The Department of Defense Advanced Research Projects Agency (ARPA) has a decentralized management approach and works directly with seven regional consortia. These diverse consortia provide a minimum of 50% of the funding and work cooperatively to address the challenges of developing electric and hybrid vehicle technologies. Participants include military laboratories, military bases, state and local governments, defense contractors, well-established and startup manufacturers of vehicles and components, electric and gas utilities, public interest groups, and universities.

The technology development is focused on high, specific power engine/generator sets (including turbines and fuel cells), power control devices (including high-performance power semiconductors, cooling systems, control algorithms, and circuit integration and packaging), energy storage devices (including advanced batteries, rapid battery recharging, flywheels, and capacitors), electromechanical conversion (including alternating current, direct current, and linear motors), and lightweight high-strength materials (including space-frames and composites).

Sacramento Electric Transportation Consortium

The Sacramento Municipal Utility District (SMUD) has taken a clear leadership role in electric transportation research and development. This venture seeks to provide for a stronger national defense through economic and energy security and to develop advanced, efficient electric vehicle components and charging infrastructure to minimize utility system impacts of military and civilian electric vehicle charging.

2.2 M113 Project Overview

The objective of this project is to upgrade the FMC Electric Drive M113 so that it can be included as one of the showcase combat vehicles in the ARPA-funded electric drive vehicle program which has the following approach:

- Assemble numerous prototype electric drive military vehicles, at Tank Automotive Command (TACOM) in Warren Michigan, to highlight the advantages of electric drive for the military (and to refute some common misconceptions) by conducting demonstrations for congressional, military, and government lab personnel
- To have a series of military vehicle platforms available for TACOM and industry to install and test alternative or emerging electric drive components
- Rigorously test the vehicles at TACOM's dynamometer facility to validate performance claims of the competing technologies.

The FMC Electric Drive M113 Testbed has been a valuable research and development platform for emerging electric vehicle propulsion technologies and control techniques. Since 1966, when the very first electric propulsion system was installed, the FMC Electric Drive M113 Testbed has been modified and upgraded numerous times. The power control electronics have evolved from a thyristor-based system in the original vehicle to a Bipolar Junction Transistor (BJT)-based system. The on-board electric power source has been batteries, and various engine-drive alternator systems using diesel, rotary, turbine, and gasoline engine type.

However, for lack of funding and other resources, the FMC Electric Drive M113 Testbed has sat idle for the two years prior to this contract. With the continued improvements in power semiconductor devices, FMC has continued to improve power conversion and control electronics to the point where the latest generation bore little resemblance to the system installed in the

M113 prior to this contract. The latest power converter designs use Insulated Gate Bipolar Transistors (IGBTs) and have many other improvements in both the physical bus structure and driver circuitry to accommodate the faster switching devices and provide more reliable operation

A similar advancement in the motor control method and electronics has occurred. The pre-contract M113 system used a six-step, DC link current regulated, slip controller. The latest generation uses field-oriented (vector) control, and motor phase current regulation. The benefits include: higher torque / amp, higher motor efficiency, and faster torque response.

The primary goal of the M113 Vehicle Refurbishment Project was to incorporate these latest advancements in electric drive technology to realize improved system performance. Other changes were made to the vehicle improve its safety and maintainability. The total contract duration, which included demonstration and testing of the vehicle was 24 months.

2.3 Statement of Work

This section provides a detailed description of the specific tasks that comprised the M113 Refurbishment Project. These tasks included specific items identified in the contract *and* subsequent modifications to the contract verbally requested by ARPA to redirect and add scope to the project.

The following statement of work is text taken directly from the SMUD contract F-379. It is followed by a listing of subsequent verbal modifications made by ARPA.

2.3.1 Original Task List from Contract F-379

Project Description:

This project entails refurbishment of the M113 Electric Drive Testbed vehicle, (developed in 1970) and refitting it with an improved power inverter and motor controller sub-components. ARPA desires to bring this vehicle up to current standards of safety and performance for use in electric and hybrid electric military vehicle development.

Specific FMC activities and deliverables:

This project includes, but is not necessarily limited to, the following activities and required deliverables:

1. Design integration and installation of an IGBT-based inverter. Inverter will be a scaled version of the inverter used in the Marine Corps Advanced Propulsion System (APS) vehicle. FMC shall accomplish all necessary assembly and testing of the refitted vehicle.
Deliverables: Installed inverter as described, in fully functional vehicle.

2. Design integration and installation of a field-oriented motor control board. Design will include protective housing for the motor control board and alternator and engine control electronics. FMC shall accomplish all necessary assembly and testing of the refitted vehicle.
Deliverables: Installed motor control board and protective housing as described, in fully functional vehicle.

3. Develop and implement Component Test Plan. FMC shall develop a component test and evaluation plan. FMC shall provide test report at appropriate times to document testing status.
Deliverable Documents: Component Test Plan, Initial Component Test Report, Quarterly Project Status Reports, and Final Reports.

4. Test Data and other technical information. FMC agrees to assure test and other data acquired is consistent with project goals. FMC agrees to provide technical information to ARPA or ARPA's designee as requested to facilitate proper use of, and maintenance and modification to the vehicle.

2.3.2 Verbal Changes to Statement of Work

The following tasks were verbally requested by Major Rick Cope, the Program Director for the ARPA Electric and Hybrid Vehicle Technology Program.

1. Battery Pack Installation (original)

"Design and install a battery pack and power distribution system to allow for "engine-off" operation. Use the GNB lead-acid batteries bought by ARPA with separate funding. Complete installation prior to shipment of vehicle to running vehicle demonstration in Atlanta, in May 1994."

2. Demonstration Support and Field Repair

"Support the M113 at various ARPA-sponsored demonstrations. This support shall include driver training, field repair of components, preparation of safety-related documents, preparation of operation and maintenance manuals, and supply of power supply for battery charging from the utility grid"

3. Battery Pack Modifications

"Modify the existing battery pack to add additional batteries to increase system voltage and high-speed performance. Complete the modifications prior to shipment of vehicle to running vehicle demonstration in Smuggler's Notch, Vermont, in September 1994."

2.4 Project Schedule

Figure 1 shows the overall project schedule for the FMC Electric Drive M113 Refurbishment project.

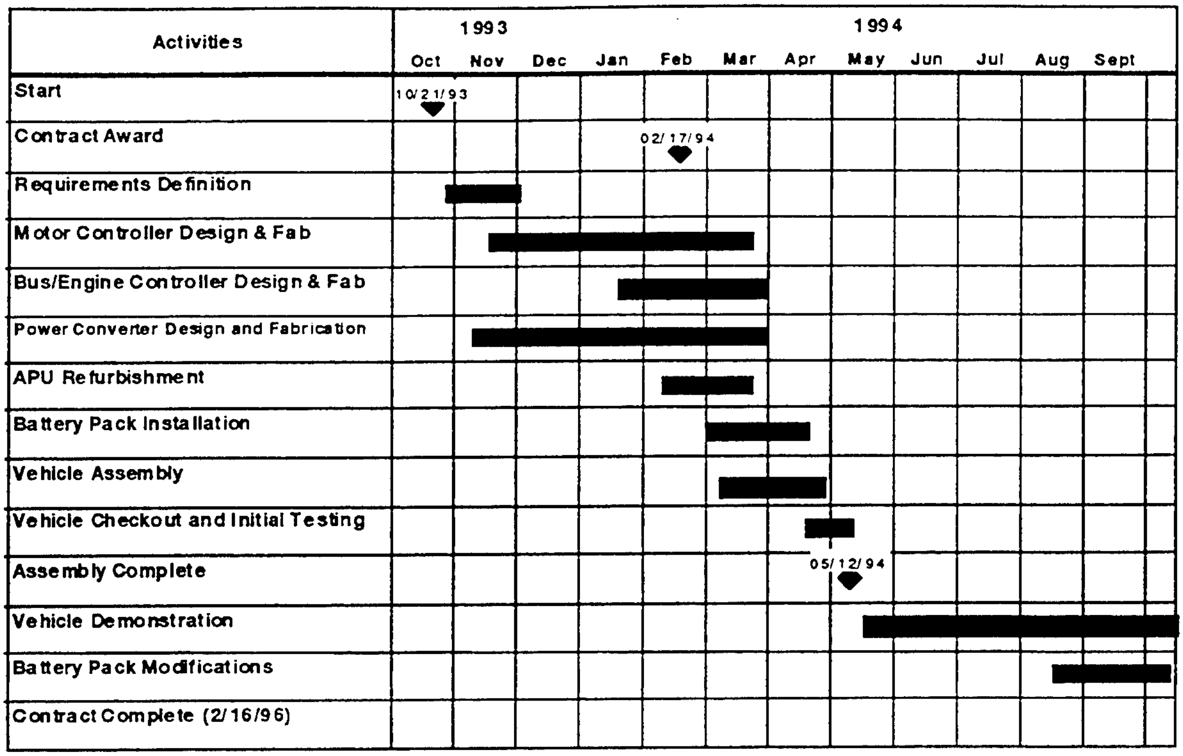

Figure 1: Schedule For The Electric Drive M113 Refurbishment Project.

2.5 Project Organization

Figure 2 shows the project team structure for the FMC Electric Drive M113 Refurbishment effort. The project was managed by Lou McTamaney of CTC; technical leadership was provided by Gordon Shafer of United Defense - Ground Systems Division.

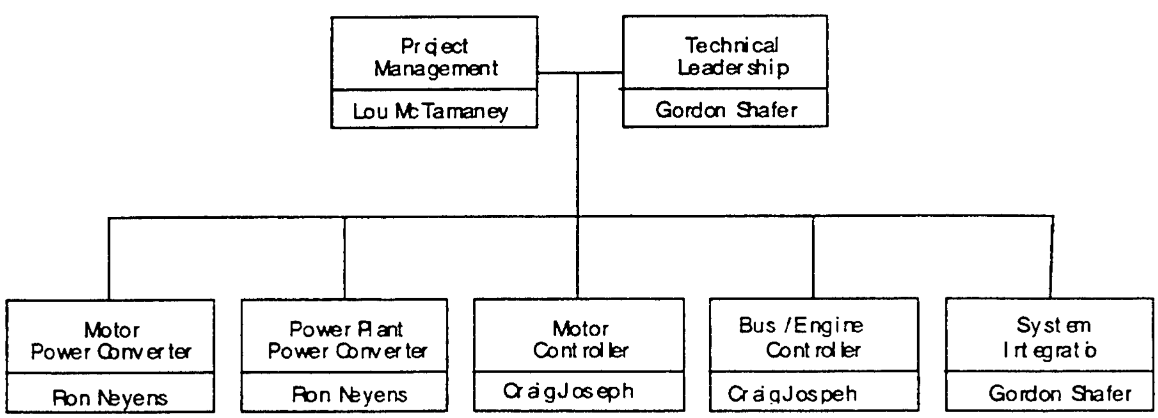

Figure 2: The Project Team Structure For The FMC Electric Drive M113 Refurbishment Effort.

Section 3. SYSTEM DESCRIPTION

3.1 M113 Personnel Carrier

The M113 is one of the most widely used combat vehicles in the world today. It is a tracked personnel carrier with an aluminum hull which is used to provide battlefield protection for 7-9 troops. Figure 3 shows a standard M113-A3 vehicle.

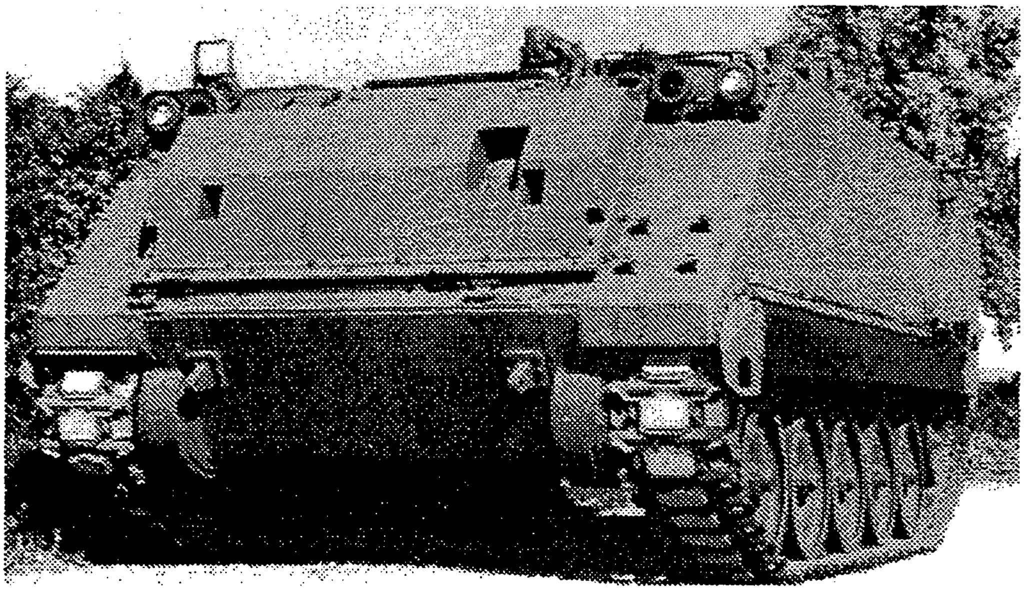

Figure 3: M113A3 Armored Personnel Carrier

3.2 Electric Propulsion System

The M113 Electric Drive Vehicle consists of an M113 vehicle with a modified propulsion system comprised of a dual-motor sprocket drive assembly, a power converter assembly, a auxiliary power unit (APU), battery packs, an energy dissipater, vehicle cooling system, power distribution and cabling, and an energy management and vehicle controller. Figure 4 shows the propulsion system power distribution architecture.

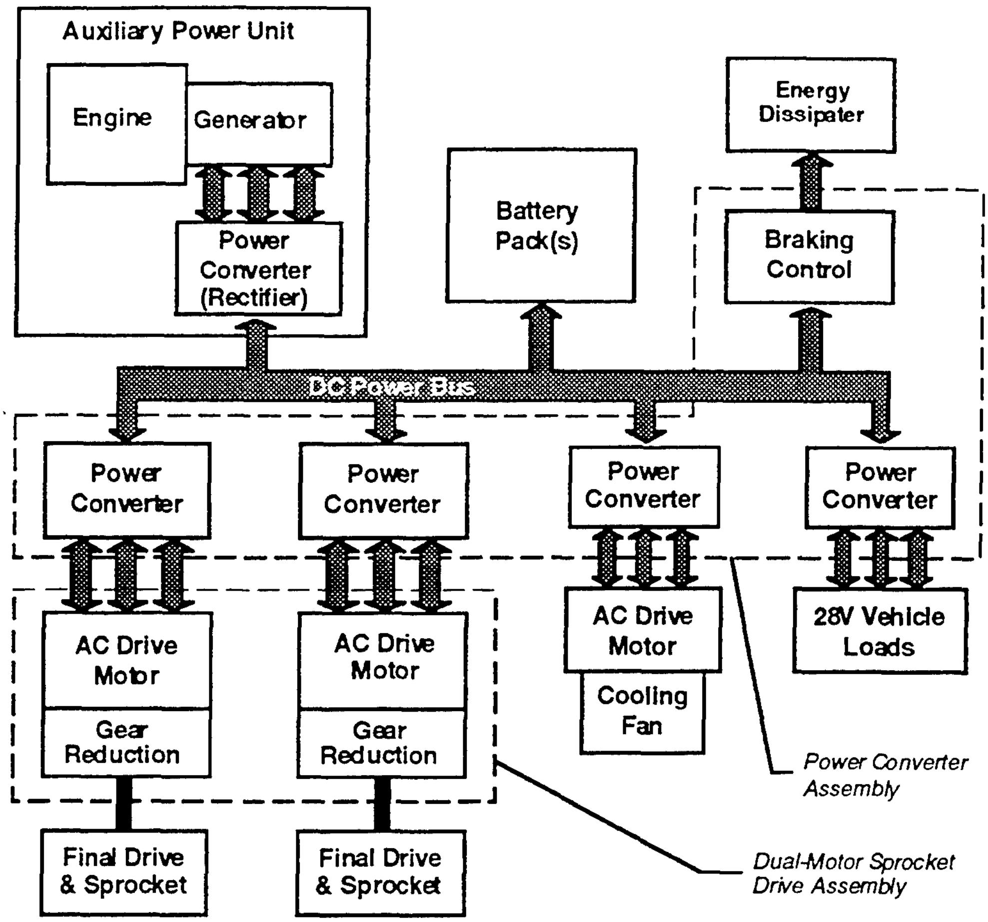

Figure 4: M113 Propulsion System Power Distribution Architecture

3.3 Drive Motor Package

Individual drive motors are used to independently provide torque to drive the left and right sprockets. Each drive motor is a high-speed AC induction machine comprised of a stator assembly within a housing and a rotor assembly on a shaft. The two stator housings mate to a common center housing on the non-drive ends, and to planetary gearboxes at the drive-end. The rotor shaft is supported by bearings that are part of the center housing and gearbox, respectively.

The output from the gearboxes connect to the vehicle's final drives (a second gear reduction set) and powers the sprockets, thus providing the speed and torque necessary to steer, brake and accelerate the vehicle.

Figure 4 is a block diagram showing the major interfaces to the drive motor package.

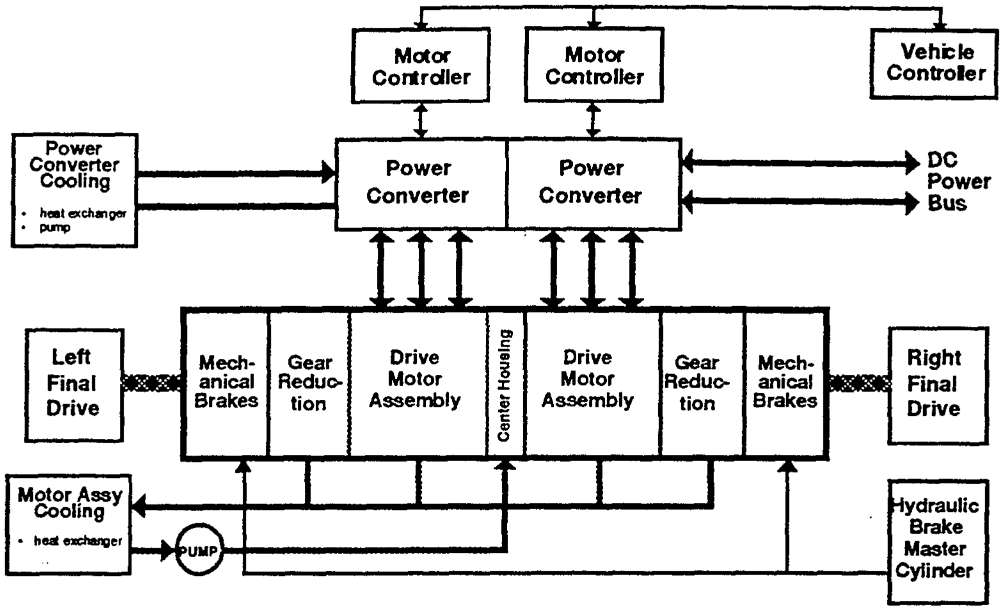

Figure 4 Interfaces to the Drive Motor Package

The drive motors were built for FMC by Allied-Signal AirResearch in 1966 and have proven to be reliable, high-performance machines. Other than the addition of a protective cover, no modifications were made to the drive motor package for this effort.

The motors have a three-phase, four-pole stator winding with 72 slots. Both ends of each phase are terminated at the motor housing, allowing either delta or wye connections. For the present application, the motors are connected delta.

The squirrel cage rotors are cast construction in which the 54 rotor bars and end rings are formed from aluminum cast through a stack of steel rotor laminations. This sub-assembly is shrunk-fit on a hollow shaft to form the complete rotor assembly.

The motors are cooled and lubricated with a low viscosity turbine oil. The stator is cooled by spiral passages in a stator jacket and oil exiting this jacket at both ends of the motor is sprayed on the windings end turns. The rotor is cooled by longitudinal passages between the laminations and the shaft. Rotor cooling oil is delivered to these passages from the inside diameter of the shaft.

Each motor is connected to an integral 5.28:1 planetary gearbox. Mechanical disk brakes are provided for parking and emergency backup braking. The brake calipers are mounted on each end of the motor drive package and a disk is mounted to the output drive yoke. A center housing which joins the two motor assemblies also provides oil passages to the rotors.

The following table (Figure 5) lists key performance characteristics of the drive motor package.

Rated Speed	14,600	RPM
Maximum Over-speed	17,000	RPM
Maximum Torque (at motor output)	322	ft-lb.
Maximum Torque (at gearbox output)	1,700	ft-lb.
Continuous Rated Current	250	amps
Rated Voltage	400	Vrms / phase
Volts per Hz	1.87	V

Figure 5: M113 Drive Motor Characteristics

3.4 Auxiliary Power Generation Unit

The electric power for the M113 vehicle is generated by a 500 hp Auxiliary Power Unit (APU) consisting of a engine-driven wound-field generator. The APU generates controlled three phase AC power which is rectified in the power converter to provide a DC power source for the traction inverters and fan inverter.

Figures 6-7 Show the major components of the APU.

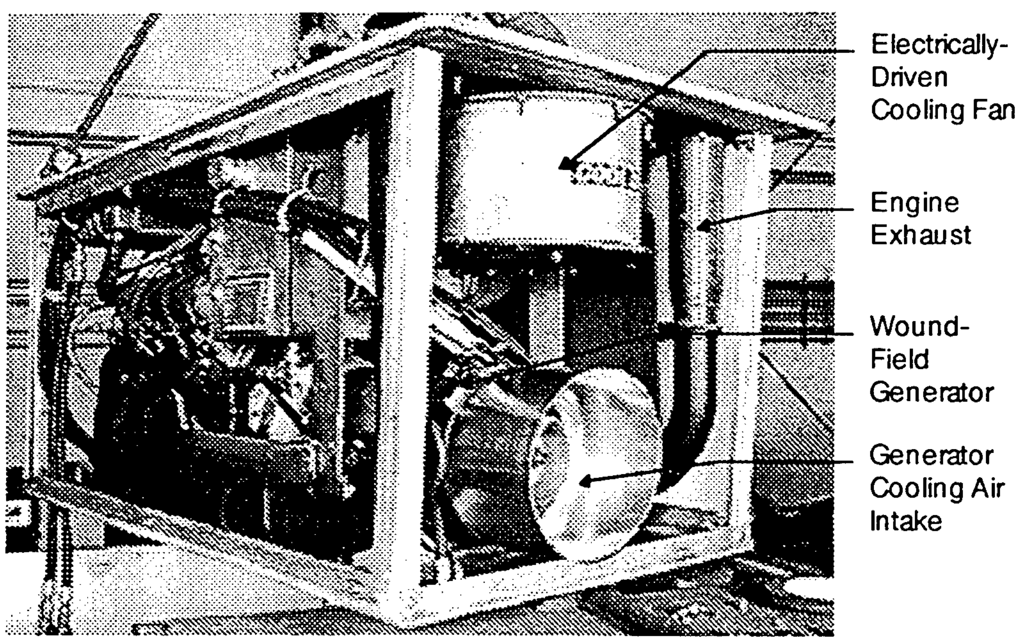

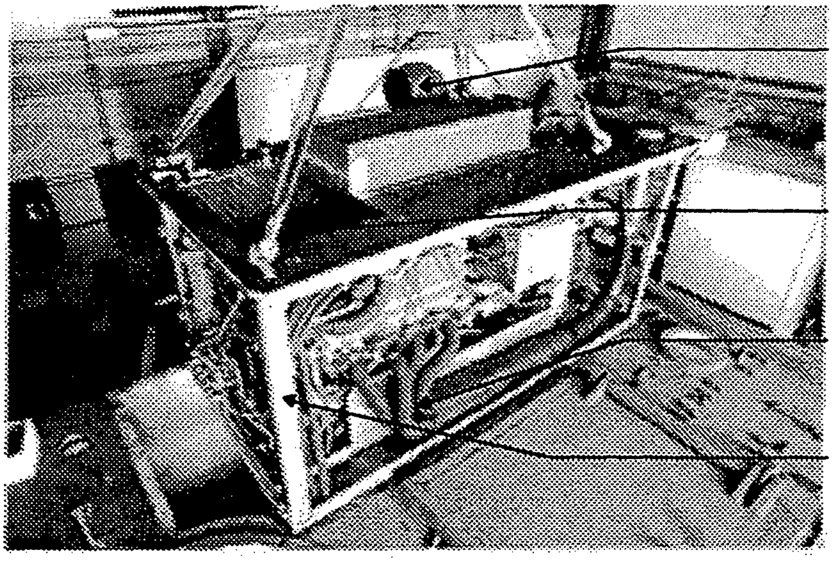

Figures 6-7: APU Is Easily Removed From The Vehicle For Servicing (side covers removed for clarity)

The engine is a gasoline-fuel, 560 cubic, V8 with port fuel injection and a dry sump lubrication system for slope operation. The actual output power has been limited to 375 HP by electronically limiting the maximum engine speed to 4000 RPM. This has been done to increase engine reliability and life.

The generator, which is built by Westinghouse, is a three-phase, six-pole, air-cooled machine rated at 312 kVA and is connected to the engine flywheel with a quill shaft. Originally, the generator was designed operate as a 400 Hz generator to be self excited and operated over a narrow speed range. To obtain operation over a broader speed range, FMC has modified the generator to provide external excitation. This was accomplished with the addition of slip rings and drive circuitry. The generator generates 100 volts DC per 1000 rpm at full excitation. The rated output current is 375 amps per phase.

The auxiliary power unit is cooled with an electric cooling fan. The fan draws air through the radiator to cool engine coolant, electric motor oil and power electronics coolant. The fan is driven by a three phase induction motor and its speed is modulated to control both coolant temperature and engine compartment temperature. An oil-to-water heat exchanger is used to cool engine oil. Airflow through the heat exchangers creates a negative engine compartment pressure with respect to ambient pressure. This pressure differential is used to draw air through the generator in order to provide cooling. An manifold connect one end of the generator to the crew compartment. The other end is open to the lower pressure engine compartment volume.

Engine speed is controlled by a small servo motor which opens and closes four large throttle butterflies at the intake manifold. The servo motor is driven by the vehicle control card.

3.5 Power Converter Assembly

3.5.1 Power Converter Arrangement and Topology

The power converter assembly contains the power and control electronics for the electric propulsion system. The power converter contains the rectifier section that converts the 3-phase AC power from the generator to DC for distribution. DC power distribution is the simplest and most effective configuration because it provides an easy-to-manage single connection for all power sources and users. DC power is converted to AC at the optimal frequency and voltage to drive the motors, resulting in high efficiencies throughout the speed range.

The power converter assembly includes the Insulated Gate Bipolar Transistor (IGBT) power modules, capacitors, bus structure, current sensors, coldplate, control electronics, gate drive and fault detection circuitry for each switch, and internal wiring for the traction drive motors, generator, energy dissipater, and electrically-driven cooling fan. All the high power electronics are mounted to a common coldplate, which functions as a temperature controlled mounting surface. Each inverter section is a three phase, variable frequency, current-regulated, pulse-width-modulated unit (CRPWM). The control and gate drive electronics are located on circuit cards within the power converter assembly.

A schematic diagram for the assembly *(pictured in Figure 8)* shows the connections within the assembly and the interfaces to the vehicle propulsion components.

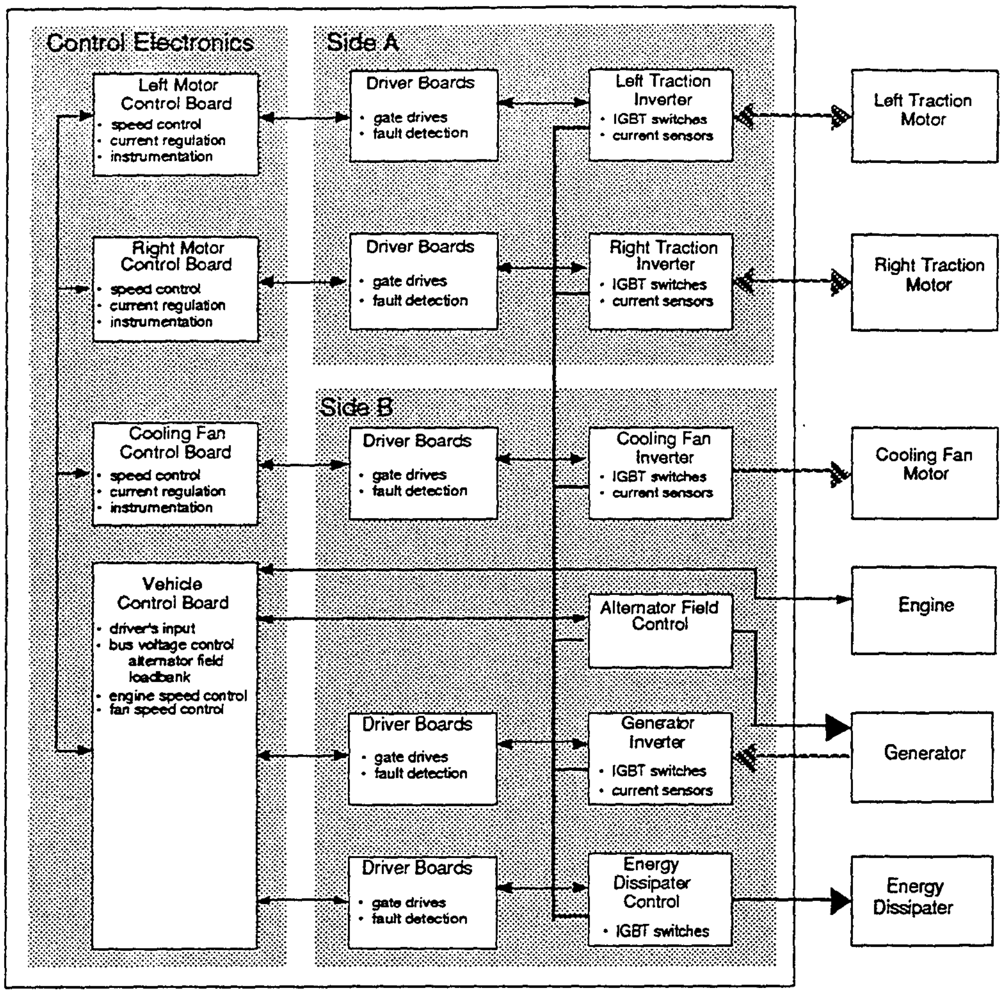

Figure 8: M113 Power Converter Architecture and Interfaces

There are two three-phase traction bridge circuits that provide up to 900 amps rms. line current per each motor. Two paralleled IGBT's per leg of the bridge are used to supply the current. The two traction drive IGBT's are arranged on one side (side A) of the cold plate and are connected to form two three phase inverters.

The gate drive circuitry is an important element of the inverter circuit. It is used to interface the logic level output of the motor controller to the gates of the power devices. A properly design gate drive circuit should include:

- High dV/dt capability (5V/nsec) and low transport delays (<1.5 usec) to support fast switching times.
- Floating supplies unaffected by high dV/dt
- Appropriate gate resistors and filter capacitors for high frequency noise immunity.
- Immunity from capacitively and magnetically coupled noise (input and output wiring isolated, twisted pair outputs to IGBT)

- Over-current protection.

The FMC gate drive circuit uses de-saturation detection to prevent short circuit currents from destroying the IGBTs and is opto-coupled to the motor controller circuitry for capacitively and magnetically coupled noise immunity.

For each leg of the inverter, a single dual driver card which mounts directly to four IGBT's is used. One-half of this card drives a pair of upper switches while the other half of the card drives a pair of lower switches.

The IGBT gates are driven from a common hybrid Integrated Circuit (IC) driver through separate gate drive resistors. To turn the IGBT's on and off, their gates are switched to +15 volts, and to -10 volts, respectively. Each driver circuit has an isolated power supply that provides the required +15 and -10 volts for the hybrid IC driver.

The IC driver is switched on by passing current through an internal optical coupler. This control current is supplied by the motor control card (discussed below) through a differential line driver.

Short circuit protection is provided by a de-saturation circuit., that detects a high collector-to-emitter voltage when the IGBT is on and turns it off at a controlled rate to prevent damage to the switch. If a de-saturation fault is detected, a fault signal is sent to the motor control card from an opto-coupler. The controller then disables the output drive to prevent damage to the system.

The topology of the traction inverter and gate drive circuit is shown in figure 9.

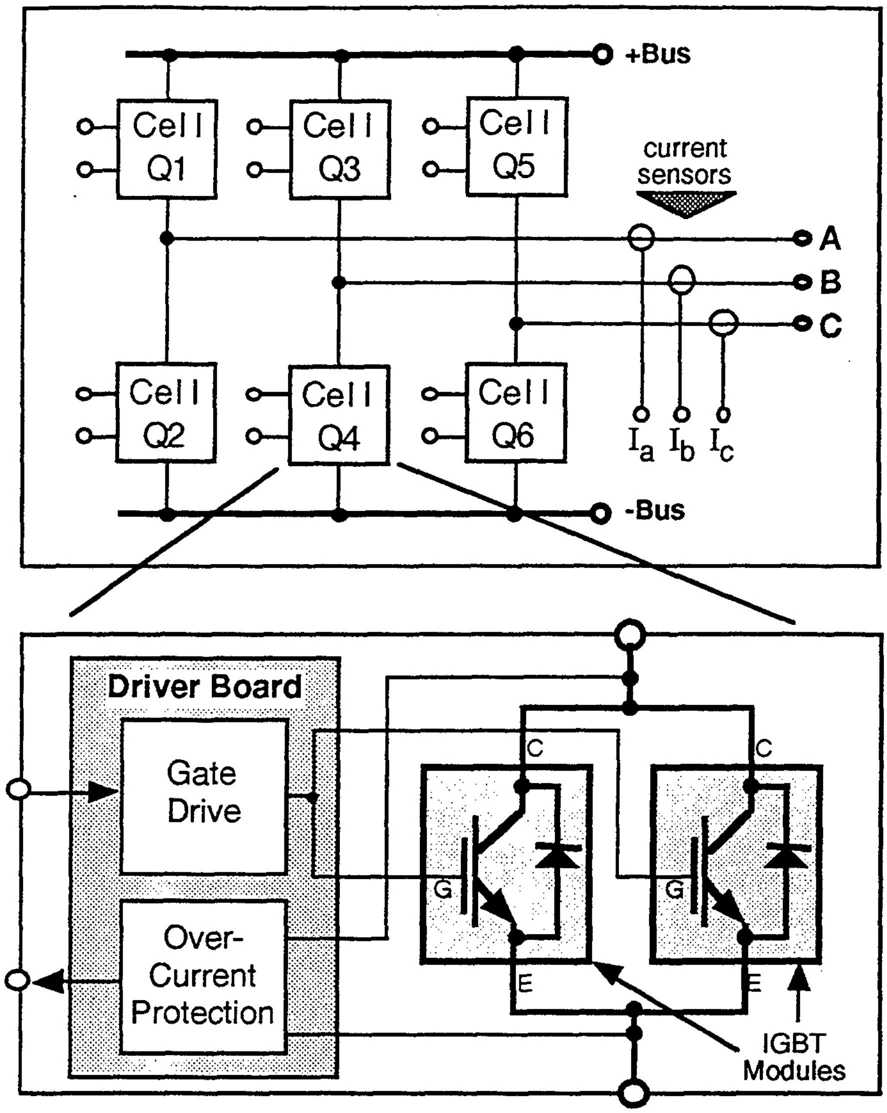

Figure 9: Topology Of Traction Motor Inverter and Drive Circuitry

The generator inverter, braking circuit, and fan inverter are located on the opposite side of the cold plate (side B). The generator inverter is used to convert the AC output of the wound field generator into DC power for distribution. To achieve this, an inverter identical to the traction motor inverter is used. The alternator output is rectified by the integral flyback diodes in the IGBT modules and each IGBT gate is biased at -10 volts to hold it off. As such, only the diodes are used to rectify the AC output of the generator. For future applications, the bridge can be used with an induction motor to generate power for the DC bus. It can also be used to drive the engine for compression braking and engine starting.

The energy dissipater is used to convert excess energy from the power bus to heat and then reject it to ambient. The energy recovered from downhill operation and / or from reducing the velocity of the vehicle must be absorbed or dissipated. During panic stops, or during extended downhill operation, or

in the event of a failure of the energy storage system, the regenerated energy will exceed that which can be consumed by the other bus power demands.

The dissipater uses resistive elements connected electrically between the plus and minus potentials of the power bus and is physically mounted in a coolant tank in the forward right corner of the vehicle. Under regulation of the vehicle controller (discussed below), the dissipater serves as a bus voltage circuit protector to prevent the occurrence of a bus over-voltage condition. In the absence of the dissipater, the bus voltage would rise to unacceptable levels and/or the amount of regeneration (hence retardation of the vehicle) would have to be reduced or eliminated.

The M113 braking energy dissipater circuit uses six IGBT modules. Four IGBT's are used as upper switches and two as flyback diodes. The braking circuit connects the DC bus to a 0.3 ohm braking resistor when the bus voltage rises above the DC bus voltage setpoint plus an adjustable deadband voltage.

The cooling fan inverter uses six single IGBT modules and a hex driver card. The hex driver card contains six gate drive circuits and mounts directly to the six IGBT's. The fan circuit can provide up to 450 line amps rms., which is greatly in excess of the current requirements of the cooling fan motor. This over-capacity, is a result of the fact that the cooling fan inverter uses the identical IGBT modules as the traction motor, generator and energy dissipater circuits, which provided a high degree of commonality and simplified the bus structure design.

With the fast switching (high di/dt) of the IGBT, it is important to minimize stray inductance. Voltage spikes created during turn-off are a potential source of device failure. The FMC power converter used developed for the M113 uses a laminated bus structure that minimizes inductance through flux canceling. The bus structure and key power converter components are shown in figures 10 and 11 below.

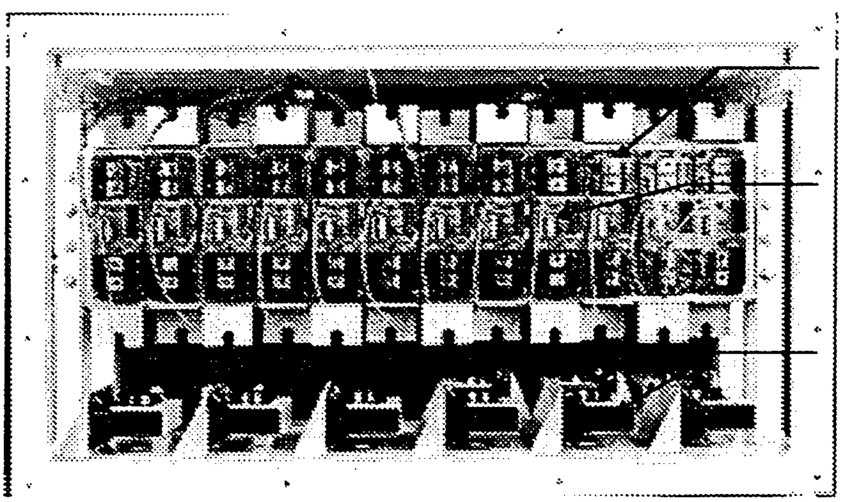

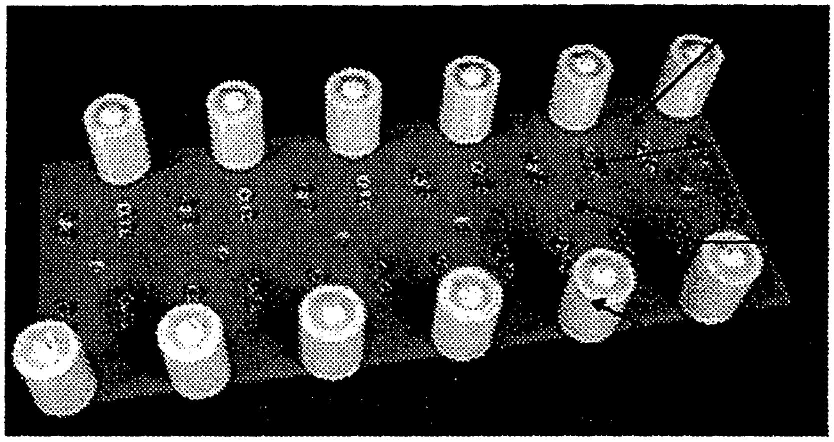

Figures 10-11: Physical Layout of Bus Structure and Inverter Components

3.5.3 Induction Motor Control Boards

The induction motor control board along with the power converters provide regulation of the frequency, amplitude, and harmonic content of the current waveforms in the motors (and generator) by active control of the IGBT's in the inverter.

A block diagram of the motor control and inverter topology in shown in Figure 12.

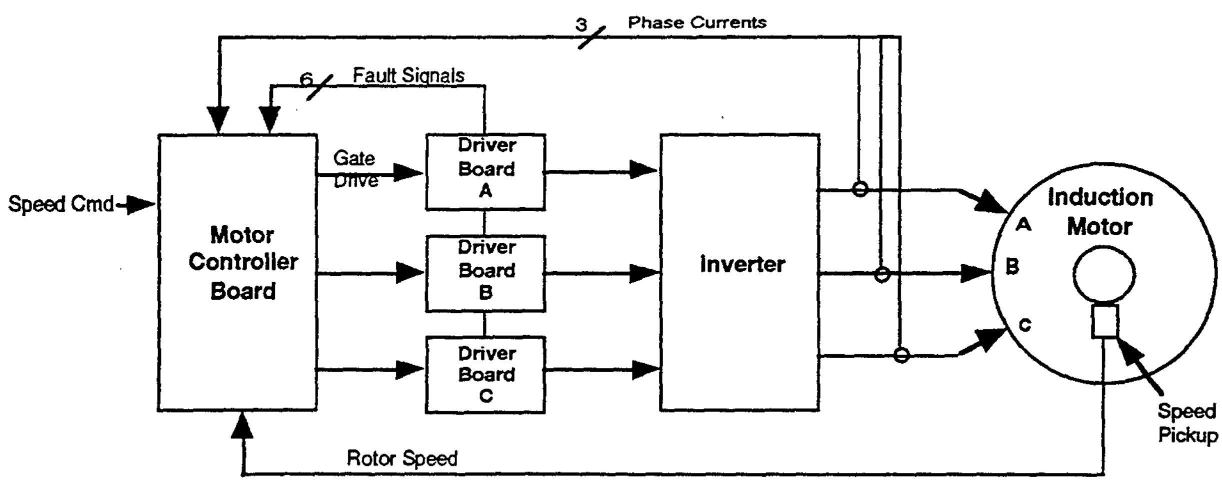

Figure 12 Induction Motor Control Topology

The induction motor card implements a field oriented control (vector control) method. The benefits include:

- High starting torque, limited only by inverter current rating

- High motor efficiency because the magnetization current can be controlled as a function of motor speed. This reduces losses at medium to high motor speeds.
- Smooth control of motoring torque for both motoring, regeneration, and zero speed.
- An increase in the speed/torque envelope due to field weakening schemes.
- Excellent velocity control under varying load conditions.

Three variables contribute to the torque output of induction motors: stator current, slip frequency, and flux. Field oriented control of induction motors provides independent control of two of these components, namely, current and slip. The FMC induction motor controller uses a dedicated vector processor that calculates the optimal slip and the torque and flux producing stator current components. The vector processor performs the synchronous-to-stator transformation and produces the three phase sinusoidal stator reference currents.

There are three motor control cards in the power converter assembly. Two are used to control the left and right traction motors, respectively, and one is used to control the cooling fan motor. Space for a fourth motor control card - used to control an induction generator - was designed into the assembly.

A block diagram of the motor control card is shown in Figure 13.

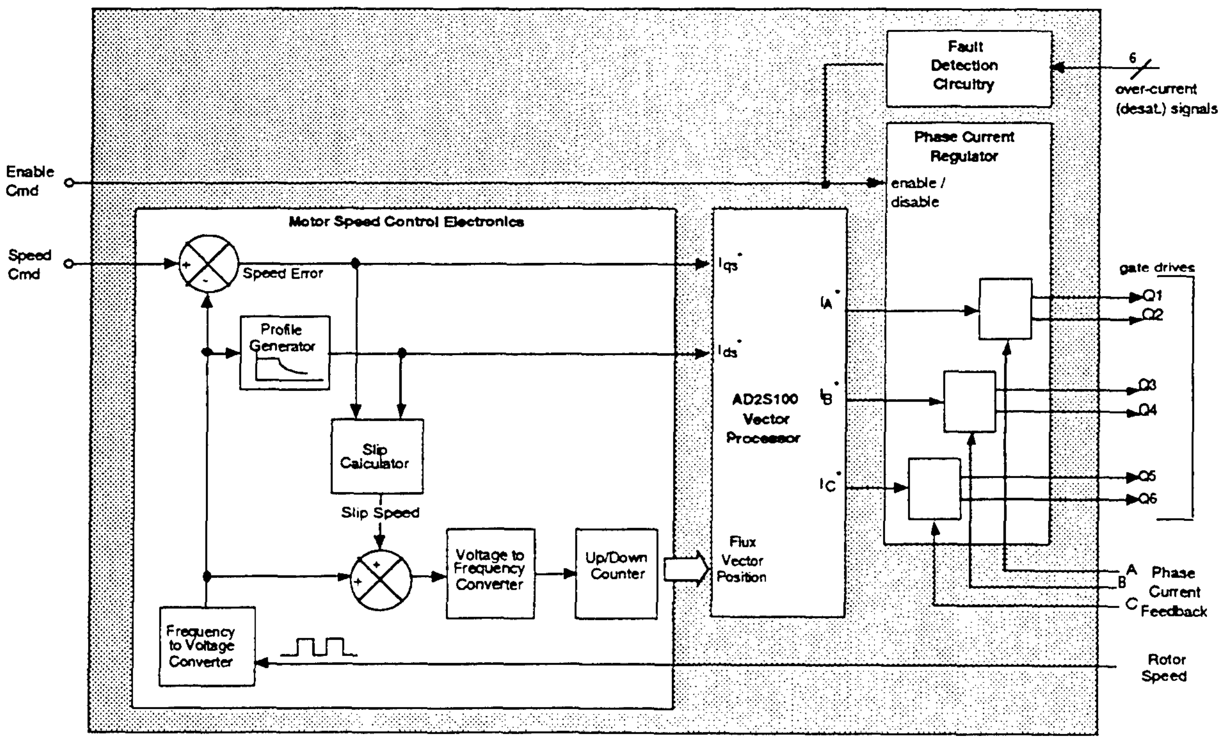

Figure 13 The FMC induction motor card implements a field oriented control (vector control) method.

Each card receives a velocity command from the vehicle control card and controls the motor speed to match the commanded speed. The current and slip is controlled at each motor to produce the torque required to close the velocity loop.

Each motor has a Hall-Effect-type velocity pickup that senses motor speed and direction. The velocity signal is conditioned on the motor control board and compared to a commanded motor speed to produce a signal proportional to the speed error.

The field-orientation (vector) control method provides independent control of both the magnetizing flux-producing (Iqs), and torque-producing (Iqs) components of stator current. Ids controls the air gap flux and the motor volts per Hz. It is held constant up to a certain speed then it is reduced as a function of 1/speed to provide field weakening. Iqs is varied linearly as a function of speed error. The current components are added as two 90 degree vectors by the Vector Processor. The Vector Processor generates three phase reference currents, with each current's amplitude proportional to the amplitude of the vector sum. These are Ia, Ib, and Ic. The current regulator compares the actual current to the commanded current and will switch the upper switch "on" if the current is too low or switch the lower switch "on" if the current is too high. The closed loop current control produces smooth sinusoidal output currents for the motors.

In an induction motor. motor torque is regulated by modulating the frequency of the motor current waveform above and below the synchronous speed of the motor. The difference between the speed of the motor current waveforms and the motor speed is called slip. Positive slip (applied frequency greater than motor speed) produces motoring torque. Negative slip (applied frequency less than motor speed) produces regenerative (braking) torque. To maximize motor efficiency and increase the speed range of the motor, slip is increased linearly as a function of speed error up to the speed where field weakening begins; it is then increased as a function of speed error times 1/Ids.

The motor control cards contains circuitry to shut-off the output drive when a fault occurs. The motor control cards receive de-saturation fault signals from the driver cards. They shut off the drive for their respective inverter. The fault signal is sent to the vehicle control card and all the bridges are then disabled to prevent erratic steering.

3.5.4 Vehicle Control Board

The vehicle control card provides the system-level control of the electric propulsion system. It is a single circuit board located within the power converter assembly (see figure 14) that provides the following functions:

- Driver's Control Input and Interpretation
- Bus Voltage Regulation
- Engine Speed Control
- Cooling Fan Speed Control
- Power Converter Fault Management

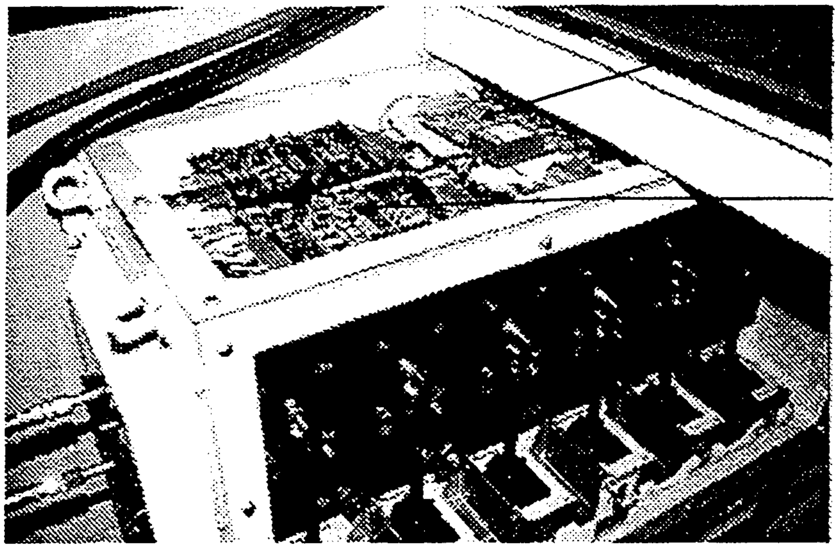

Figure 14 ***The vehicle control card is located within the power converter assembly***

Driver's Controls Input and Interpretation:

The vehicle control card receives commands from the driver's station controls (accelerator, steer, brake) and the vehicle speed feedback from the motor control cards. Based on the difference between the command and actual speeds for each motor (speed error), it then generates left and right track torque commands. The torque commands are sent to the left and right track motor control cards. Precise control of the vehicle is maintained with closed loop control of each track motor.

The speed error commands are also used to determine the engine speed setpoint.

Bus Voltage Regulation:

The vehicle can be operated in the battery-only mode or engine-only mode. When the vehicle is operated in the engine-only mode, bus voltage is controlled as a function of engine speed. The bus voltage is varied from 150 to 350 VDC as the engine speed is varied from 2000 to 4500 rpm. This is required because the generator's ability to output voltage is dependent on its rotational speed. At low generator speeds the output voltage command is reduced to avoid overdriving the field control circuit.

Bus voltage is controlled by modulating the voltage pulse width applied to the alternator field. The control card compares the reference voltage with the feedback voltage and increases the pulse width to the alternator field if the feedback voltage is low.

When the battery mode is selected, the alternator isn't used and the bus voltage is the battery pack voltage.

At present, the APU and battery pack cannot be providing power simultaneously (hybrid operation) to the vehicle propulsion system.

The energy dissipater circuit is energized when the bus voltage exceeds 400 volts DC. The voltage pulse width applied to the braking resistor is increased linearly from 0 to 100% as the bus voltage rises from 400 to 420 volts DC. This may happen during rapid braking if the batteries are unable to absorb the braking energy. If the battery pack circuit breaker or series contactor open while the vehicle is traveling, the braking circuit controls the DC bus voltage. If the bus voltage rises above 450 volts DC, all the motor control cards are disabled and only the braking circuit is enabled.

Engine Speed Control

Engine speed is varied from 2000 to 4500 rpm depending on the difference between desired vehicle speed and actual vehicle speed. When there's a large positive speed error, engine speed is increased to 4500 rpm. When the error is small or negative during braking, engine speed is reduced to 2000 rpm. These limits are adjustable with potentiometers on the control card.

Cooling Fan Speed Control

The vehicle control card modulates cooling fan speed to regulate engine coolant temperature. A thermocouple is used to sense coolant temperature. This low-level signal is fed to a thermocouple amplifier on the card which conditions the signal. A second amplifier outputs the desired fan speed for the fan motor card.

Power Converter Fault Management

Faults from the motor control cards and de-saturation signals from the gate drive cards are fed to the vehicle control card and displayed. The fault signal are latched, i.e. if a fault occurred they will display the fault status until manually reset, even if the fault condition is no longer present. If any fault occurs, a fault signal is also displayed on the drivers control panel.

The control enable switch on the panel enables the motor control cards, the alternator field, and the engine servo circuits. The control enable switch is also used to reset the faults.

3.5.5 Power Converter Cooling System

To maintain reliable operation, the junction temperature IGBT's within the power converters must be kept below safe operating limits. For highest power density, the power converter assembly must be liquid cooled to maintain the required maximum IGBT module baseplate temperature. The M113 power converter assembly uses a internally finned coldplate to transfer heat from the device mounting surface to the cooling fluid.

The coldplate consists of a pair of machined aluminum plates with interlocking cooling fins forming channels in which coolant flows. A single coldplate is shown in Figure 15.

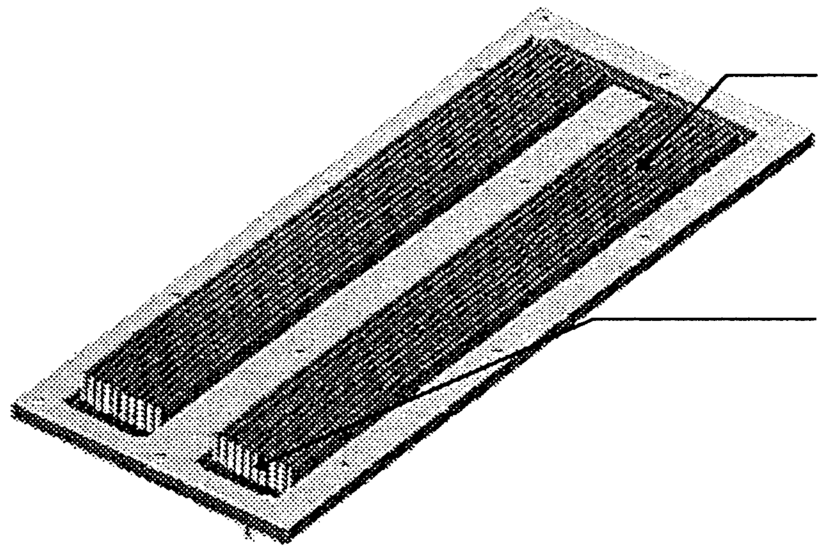

Figure 15: M113 Power Converter Coldplate

The coolant (water-ethylene-glycol) is pumped through the coldplate at a rate of five gallons per minute. The temperature of the coolant entering the coldplate is 160 °F. A heat exchanger in the APU compartment is used to reduce the coolant temperature.

To removed heat generated in the bus structure four cooling fans are installed on the power converter enclosure. These fan are four inch diameter, 12 volt, and produces 85 CFM of airflow. The air flow is directed across the IGBT's and the bus structures and then exits the opposite side through ventilation holes.

Figure 16 shows the power converter installed in the M113 vehicle and identifies the location of the four cooling fans.

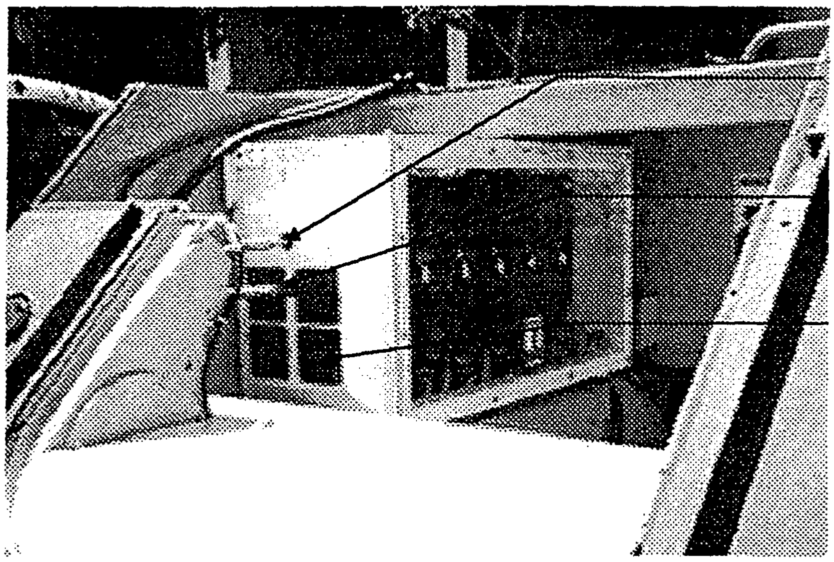

Figure 16: Cooling Fan location and Coldplate Coolant Connections

3.5.6 Power Converter Enclosure and Mounting Structure

The power converter enclosure *(see Figure 17)* is fabricated from aluminum sheet and extruded shapes. The enclosure was mounted to the M113 hull with shock mounts to reduce the vibration level seen by the components within the enclosure. All of the panels on the enclosure are removable for servicing. When installed in the M113, the aluminum front and top closure panels were replaced by clear plastic panels for viewing.

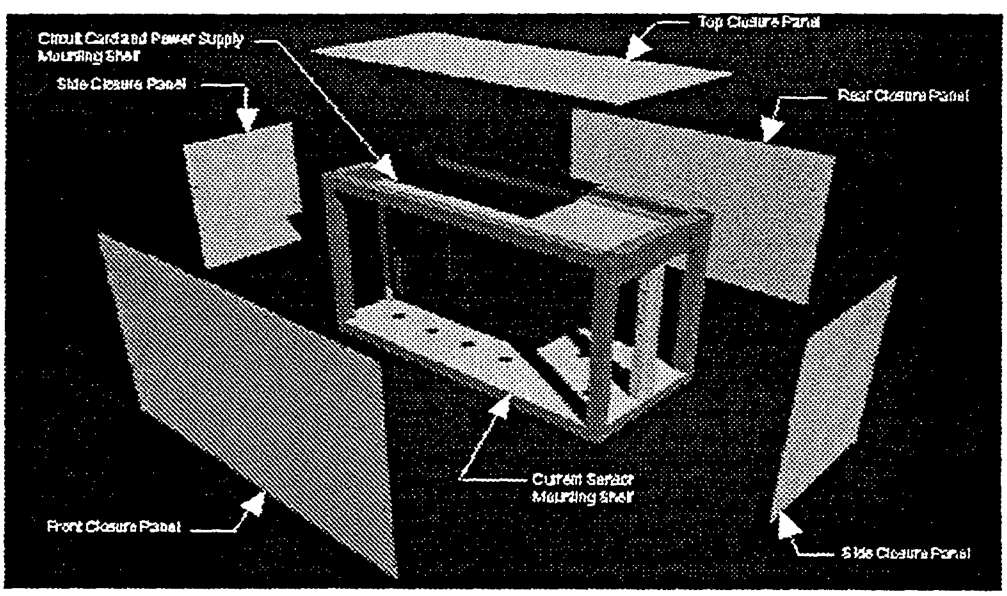

Figure 17: M113 Power Converter Enclosure

3.6 Battery Installation

To allow stealth operation of the M113 and to investigate the utility of battery-only operation, an energy storage system consisting of 90 lead-acid batteries was installed into the M113. The batteries supply power to the vehicle for acceleration, slope operation, and steering.

The installation of the batteries was completed in two separate tasks. The first task installed created a 240 VDC battery pack consisting of 60 batteries, a monitoring system, and a charging system. The second task created a 360 VDC battery pack with an addition of more 30 batteries in the vehicle and integrated them into the vehicle power distribution system.

All the batteries for both groups are of the high density sealed lead-acid type.

3.6.1 240 VDC Battery Pack

The first installation divided the 60 batteries groups of four and configured as five vertical columns and three levels. The batteries were placed on the left sponson of the vehicle and mounted on slides for easy access and maintenance (see Figure 18). The batteries are enclosed within an aluminum compartment with internal ventilation.

The 60 total batteries were divided into two parallel strings of thirty batteries in series. This type of arrangement provided 240 volts and 207 amp/hour continuous power to the power converter.

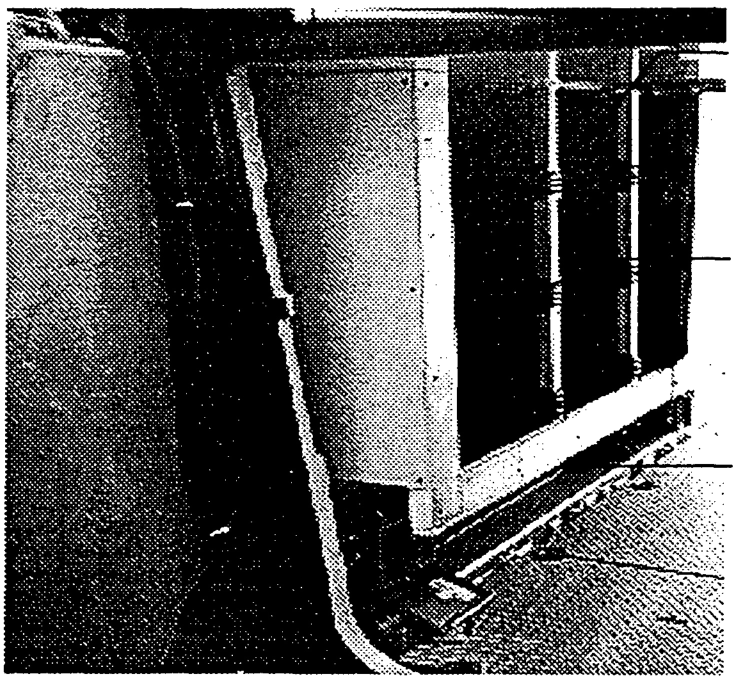

Figure 18: Battery Compartment for 60 Lead-Acid Batteries

3.6.2 360 VDC Battery Pack

The second installation placed 30 batteries on the floor of the vehicle (see Figure 19) between the first battery pack and the APU. The floor mounted batteries were mounted in similar groups of four but without the sliding mechanism. This group of batteries is accessed by removing an insulated aluminum cover.

The 90 total batteries were divided into three parallel strings of thirty batteries in series. This type of arrangement provided 360 volts and 207 amp/hour continuous power to the power converter.

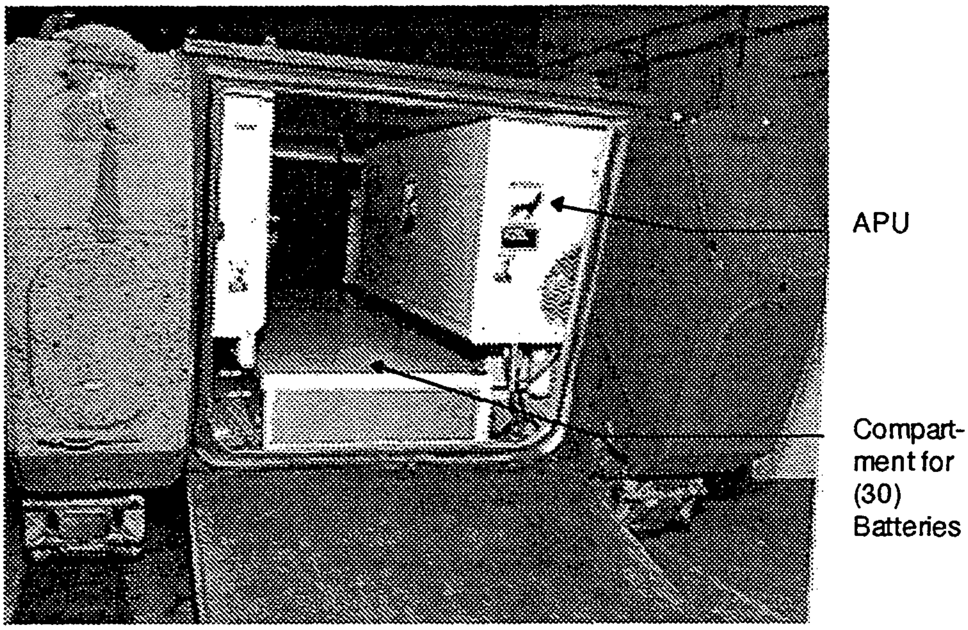

Figure 19: Battery Compartment for 30 Additional Lead-Acid Batteries

3.7 Vehicle Power Distribution

The power distribution diagram is shown in Figure 20. During startup, the capacitors in the power electronic assembly are charged through a 50 ohm resistor. Once changed, the DC contactor then connects the battery pack to the power electronics assembly. This prevents in-rush current from damaging the contactor and circuit breaker contacts. It also prevents the breaker from tripping on closure. On shutdown, the contactor is opened and the DC bus discharged by stepping on the brake and the accelerator. The stored energy in the capacitors is discharged through the motor windings.

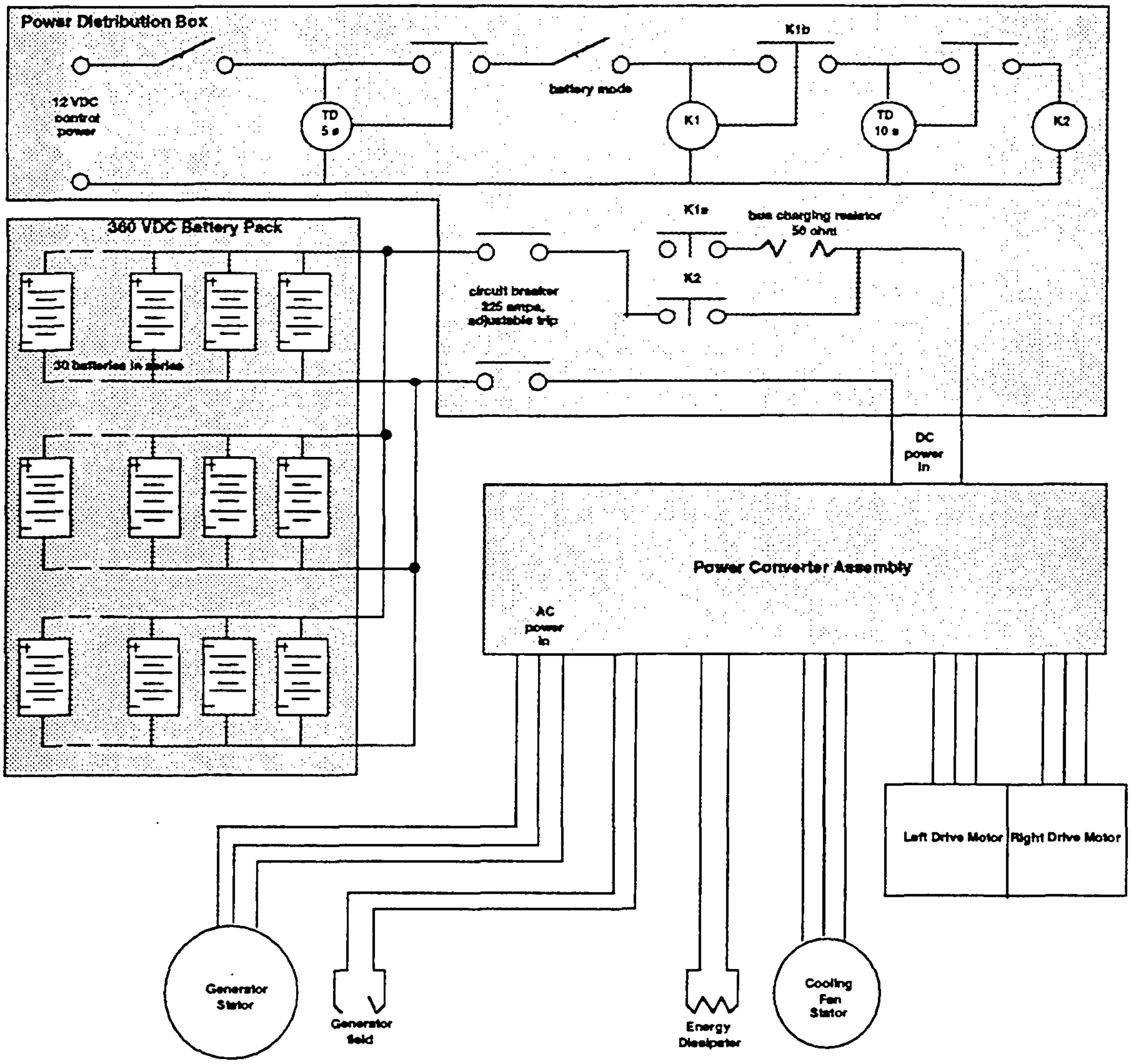

Figure 20: Electric Drive M113 Electrical Power Distribution Diagram

The alternator three phase stator outputs are connected directly to the power electronics assembly without contactors or breakers. The alternator field is excited by the power electronics from the DC bus. During startup, the field is excited by a DC to DC converter powered by the 12 volt accessory batteries.

The drive motors are connected directly to the power electronics assembly with short cables that are routed in a protective manner to prevent exposure to the crew and to prevent damage by pinching or crushing.

Vehicle control cabling from the driver's area is routed in an overhead channel away from the motor wiring to minimize noise on signal circuits.

3.8 Driver's Station

The driver's controls in the electric drive M113 provide the steering, acceleration, and braking input to propulsion system. The driver's controls are shown in Figure 21.

The gunner's control handle installed in the refurbished M113 Electric Drive Vehicle is used to provide steering input. This unit is identical to the gunner's control handle used in the standard Bradley Fighting Vehicle (BFV).

An accelerator pedal is used to control forward vehicle speed and acceleration.

Most of the braking is controlled by backing off on the accelerator pedal. Additional braking effort is provided by a brake pedal which rotates a potentiometer. Mechanical braking is provided by the same pedal. At half pedal travel, the linkage engages a two stage master cylinder and calipers on the motor drive package engage the disk brakes. The mechanical brakes are not required for normal operation. Typically, they are required only if an electrical fault occurs while driving.

A brake lock lever is provided to hold the vehicle still on slopes and during vehicle transit. The brake lock is engaged by stepping on the brake pedal firmly and pulling backwards on the brake lock lever. The brake lock is disengaged by pushing forward on the brake lock lever.

The driver's instrument panel contains the switches and gages needed to operate and monitor the engine and the electric propulsion system.

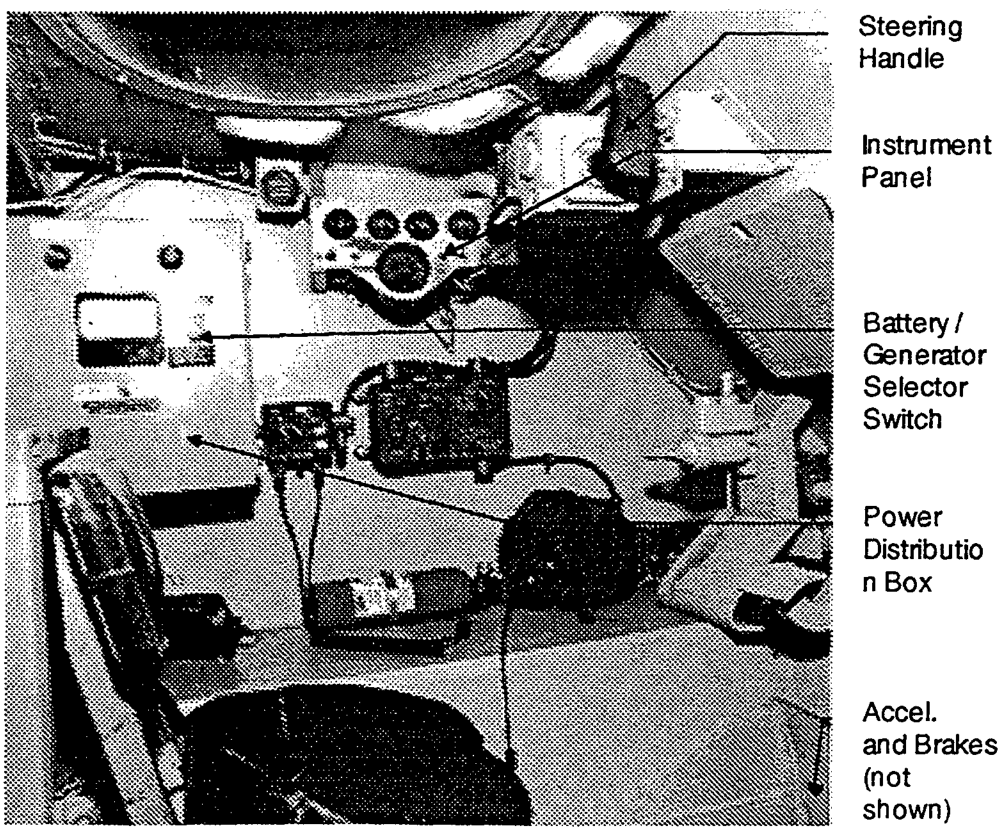

Figure 21: Driver's Station Layout

The push button start switch energizes the engine starter. The run switch turns on the electric fuel pumps, the fuel injection system, and the ignition system. To start the engine, the run switch is turned on then the starter button is depressed until the engine starts. Each time the run switch is turned on the fuel injection system squirts each cylinder with fuel. When the engine is cold the switch should be toggled several times before starting. Once the engine is started, the main power must be turned on to activate the power electronics coolant pump and the traction motor's lubrication and coolant pump. These pumps are powered by the 12 volt accessory batteries.

The forward reverse switch selects the vehicle direction.

The track enable switch enables the track motor control cards and the cooling fan. When this switch is on and there is voltage on the DC bus, the vehicle will respond to the drivers controls. The field switch turns on the DC bus and the voltage level is indicated on the bus voltage gage. Bus current is sensed in the battery mode only by sensing current in the negative battery pack lead. It is difficult to sense the alternator rectified output because it is distributed in the laminated bus structure. However the alternator line currents can be measured and the DC bus current could be calculated. Current sensors are already installed.

3.9 Vehicle Cooling System

The vehicle cooling system consists of an electrically-driven fan and three separate heat exchangers configured in parallel to each other. One circuit is for the low temperature coolant which is used to cool the power converter assembly. A second circuit is for the "high" temperature coolant used to cool the auxiliary power unit. A third circuit is for the oil used to cool the drive motors. The alternator, which is directly driven from the engine, is air-cooled. The overall cooling system of the vehicle is shown in Figure 22.

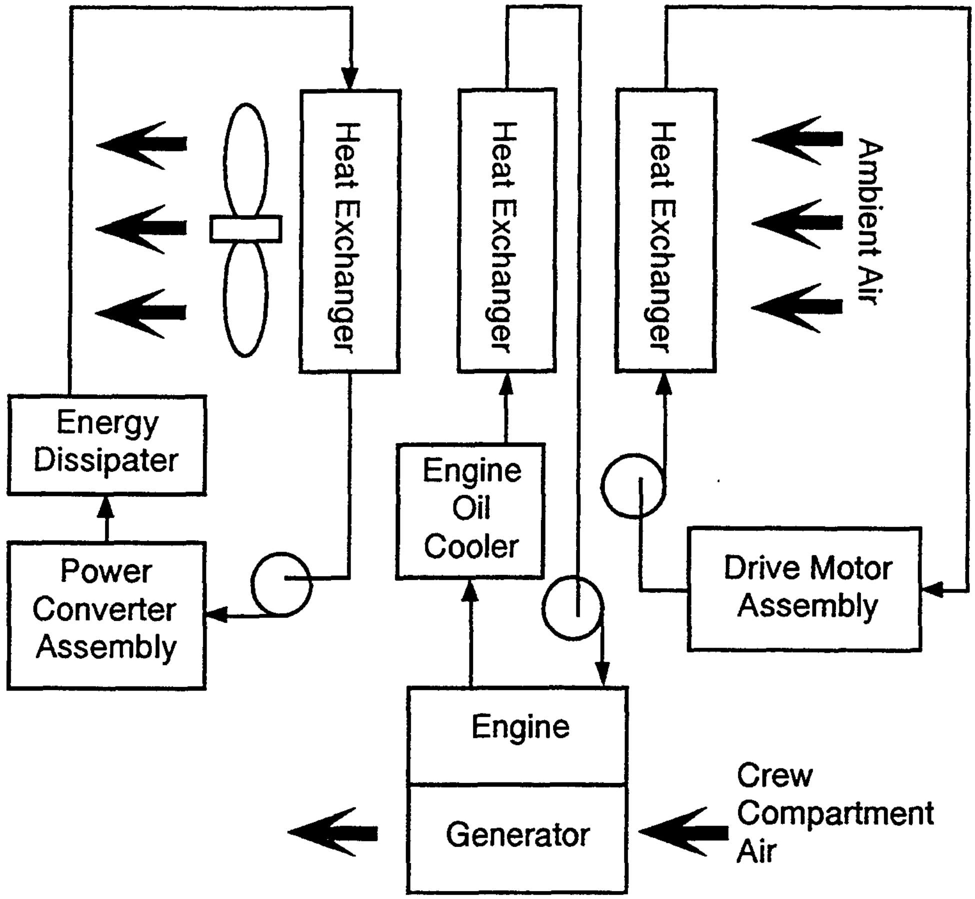

Figure 22: Electric Drive M113 Vehicle Cooling Schematic

The cooling fan, manufactured by Dynamic Air, is a 16 inch diameter, 10 hp AC induction motor unit pulls air through both the heat exchanger and the alternator. This air passes across the engine and then exits through the top of the APU.

Two electrically-driven pumps, located under the front floor plates, provide the circulation through the drive motors and the power converter assemblies. An engine driven water pump provides the circulation through the engine and oil cooler. This cooling system proved to be reliable and sufficient throughout the M113 Electric Drive Vehicle testing and the demonstration periods of this project..

3.10 M113 Suspension and Track

The running gear of the M113 consists of a sprocket driven 15 inch steel, single pin track that is supported by five, 24 inch diameter road wheels per side and a rear idler.

The track is the predominant source of noise on a tracked. In a hybrid-electric vehicle, reducing noise is critical to the effectiveness of the vehicle in combat

situations. To study the reduction of noise in the M113 Electric Drive Vehicle, an effort was undertaken by ARPA/TACOM to incorporate AAI Band Track on the vehicle in an attempt to lower vehicle weight and propulsion losses while minimizing vibration and acoustic signature.

AAI Band Track is a flexible segmented track that reduces interior noise and vibration and eliminates chordal action effects. It has a 5.81 inch pitch and weighs approximately 35 lbs/ft, which is slightly less in pitch and weight than other tracks such as the T130E1 Band Track which weighs 42 lb./ft. Although M113 vehicles normally utilize a 15 inch segmented track, the 17 inch wide AAI Band Track was able to be used on the M113 by spacing the suspension system one inch away from the hull.

Section 4. VEHICLE PERFORMANCE

4.1 Electric Propulsion System Specifications

System voltage: In the battery mode, the system varies between 340 and 400 volts DC depending on the battery state of charge and the current draw.

In the engine mode, bus voltage is varied with vehicle and engine speed from 150 to 350 volts.

Engine Power: The engine produces 500 hp at 5000 rpm. However, to increase engine life, the engine speed is electronically limited to 4000 RPM (approximately 375 HP).

Generator Power: The generator rated output power is 312 kW at 9000 rpm with 120°F inlet air. The output is reduced linearly as the speed is decreased. The generator rated output at 4500 rpm is 156 kW.

Motor Torque: The motor continuous rated torque is 321 ft-lb. with 140°F inlet oil. Peak torques are limited by the inverter line current available. The inverter line current is set at 750 amps which can produce 522 ft-lb.

Motor maximum speed: 14,600 rpm.

Motor Gearbox Ratio: 5.28 to 1.

Final Drive Ratio: 3.93 to 1.

4.2 Predicted Vehicle Performance

4.2.1 Speed-On-Grade

Figure 23 presents predicted grade performance data for the 360 VDC battery pack and existing APU used both singularly and in combination.

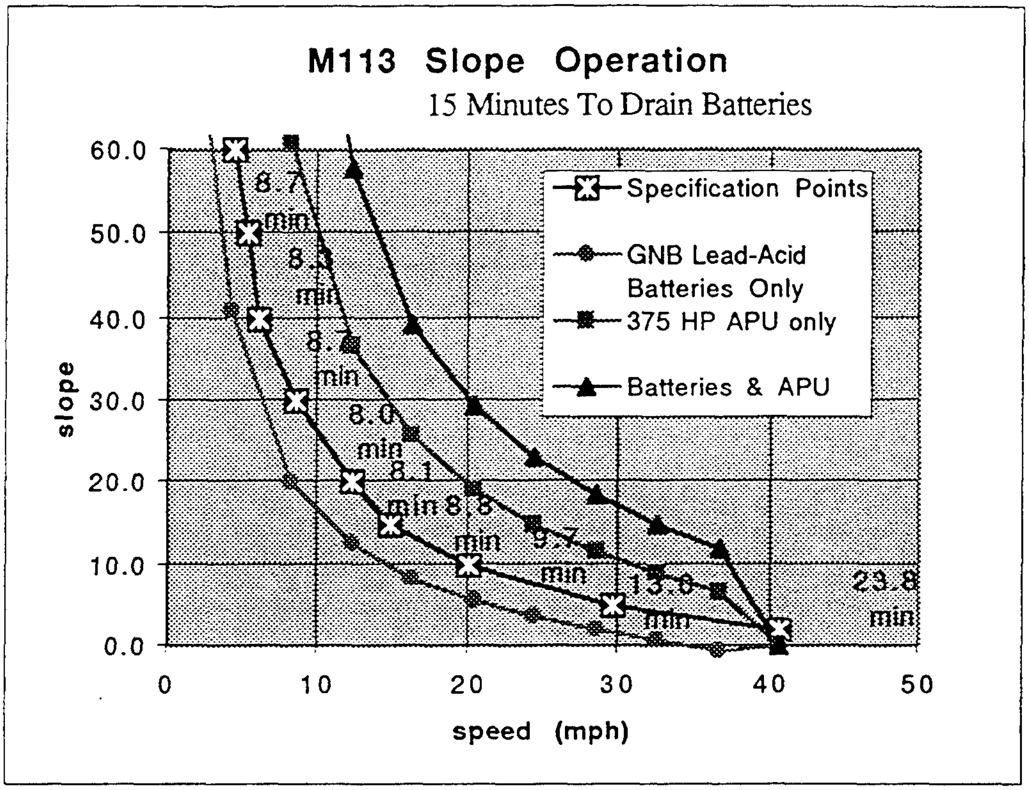

Figure 23: Speed-On-Grade Performance of the Electric Drive M113

It can be seen that the vehicle performance predictions exceeds the requirement at all of the data points. If in service, a grade is encountered that requires the vehicle to operate for a longer duration than the energy stored in the batteries can supply, the vehicle does not just come to a stop. The vehicle will continue to climb the grade with the APU being only source of power.

A benefit that can be seen is the remarkable improvement in grade climbing speed that is realized for duration's of 1 to 15 minutes. Increases 25% to 200% in speed on grade capability would result in significant reduction in time to traverse rolling terrain where the batteries would be able to supply energy going up hills and recover energy normally rejected as heat going down hills.

4.2.2 Acceleration

Figure 24 presents vehicle speed plotted against time for the hybrid vehicle and the standard M113 A3.

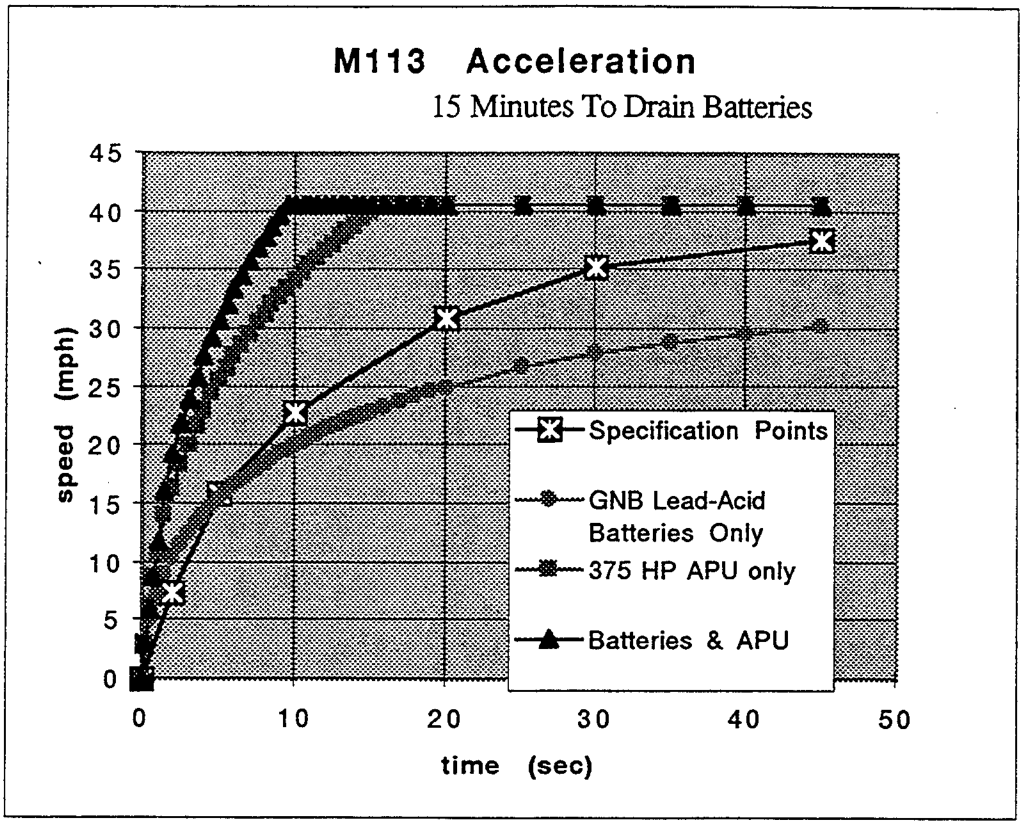

Figure 24: Acceleration Performance of the Electric Drive M113

Section 5. TESTING AND DEMONSTRATION

5.1 Vehicle Testing

No formal vehicle testing was performed.

5.2 Vehicle Demonstrations

After completing the vehicle in May 1994, the M113 has been demonstrated at numerous ARPA and TACOM-sponsored events. These demonstrations have included both static and running displays and are summarized in following table (figure 25).

Date	Where	Purpose and Customer	Activities
May, 1994	Sacramento, CA	ARPA Tri-annual meeting	Static display
May, 1994	Atlanta, GA	EV / Clear Air Show	Running demonstration
Jun, 1994	New York, NY	EV Show	Static Display
July, 1994	Ft Belvoir, VA	TACOM and ARPA Personnel	Running demonstration
Aug, 1994	San Jose	Return to FMC for additional work	Installed second battery pack, safety upgrades, additional seating
Oct, 1994	Chattanooga, TN	TACOM and ARPA Personnel	Running demonstration
Nov, 994	Smuggler's Notch, VE	ARPA Tri-annual meeting	Running demonstration. Hill climbs, races
Dec, 1994	Warren, MI	TACOM and ARPA Personnel	Running demonstration
Jan, 1995	Atlanta, GA	ARPA Tri-annual meeting	Running demonstration, car crushing
Feb, 1995	Warren, MI	Return to TACOM for additional work	Installed AAI track.
May, 1995	Washington, DC	ARPA Tri-annual meeting	Running demonstration
July, 1995 - Present	Warren, MI	TACOM and ARPA Personnel	Static and Running demonstration

Figure 25: Electric Drive M113 Demonstration Schedule

Section 6. CONCLUSIONS AND RECOMMENDATIONS

Several recommendations resulted from the effort, including recommendations to:

1. Replaced the conventional sealed lead-acid batteries with horizon advanced lead-acid batteries
2. Repackage the batteries to optimize available space
3. Modify the vehicle control system to allow true hybrid operation
4. Perform controlled automotive and dynamometer testing to quantify system performance.
5. Replace the AAI track with Quimpax band track to further reduce vehicle noise and increase system reliability

6.1 Horizon Lead-Acid Batteries

The existing 360 VDC battery pack(s) provide good vehicle performance, but do so at the expense of otherwise useable volume and cargo weight within the M113 vehicle. To better demonstrate that hybrid-electric propulsion can be achieved without a significant reduction in useable space and weight, an energy storage system based on a battery with higher specific energy and power is needed. Additional gains can be realized by repackaging the batteries (see section 6.3, below).

Using separate funding, a study was done to identify a more optimum battery This study also included determining configuration details such as, how many to put in the vehicle, and how they should be arranged. Three different battery types were considered. These are the Horizon Advanced Lead-Acid Battery produced by Electrosource, the STH nickel-cadmium batteries by SAFT and GNB MSB Series High Density Lead-Acid (currently used on the M113 ED vehicle). The first two represent recent advances in battery technology that are commercially available while the third is more representative of current automotive battery designs and is included for a comparison base. Both the Horizon and GNB lead-acid batteries are packaged as 12 volts batteries consisting of six 2 volt cells whereas the SAFT Ni-Cad is packaged as individual 1.2 volt cells. Selection criteria for the M113-Hybrid batteries include:

- Power density at varying rates of discharge - W/kg
- Volume density and packaging constraints - W/L
- Recharge rate

The first two requirements are combined in Figure 26 which shows specific power available for various time duration's and demonstrates the Horizon

battery's ability to deliver more power than the other two batteries. This is true for all duration's and discharge rates. The GNB lead-acid batteries have a greater capacity for short duration's and the Ni-Cd showing superior performance for time periods of 10 minutes or greater. Volume density varied between 76 Watt/liter to 39.5 watt/liter with the Horizon having the highest power densities. Despite their long lengths (770 mm), the Horizon batteries produced the most compact packaging arrangement. Because of the individual cell design of the SAFT Ni-Cd additional space is lost to provide the additional terminal connections required between each cell.

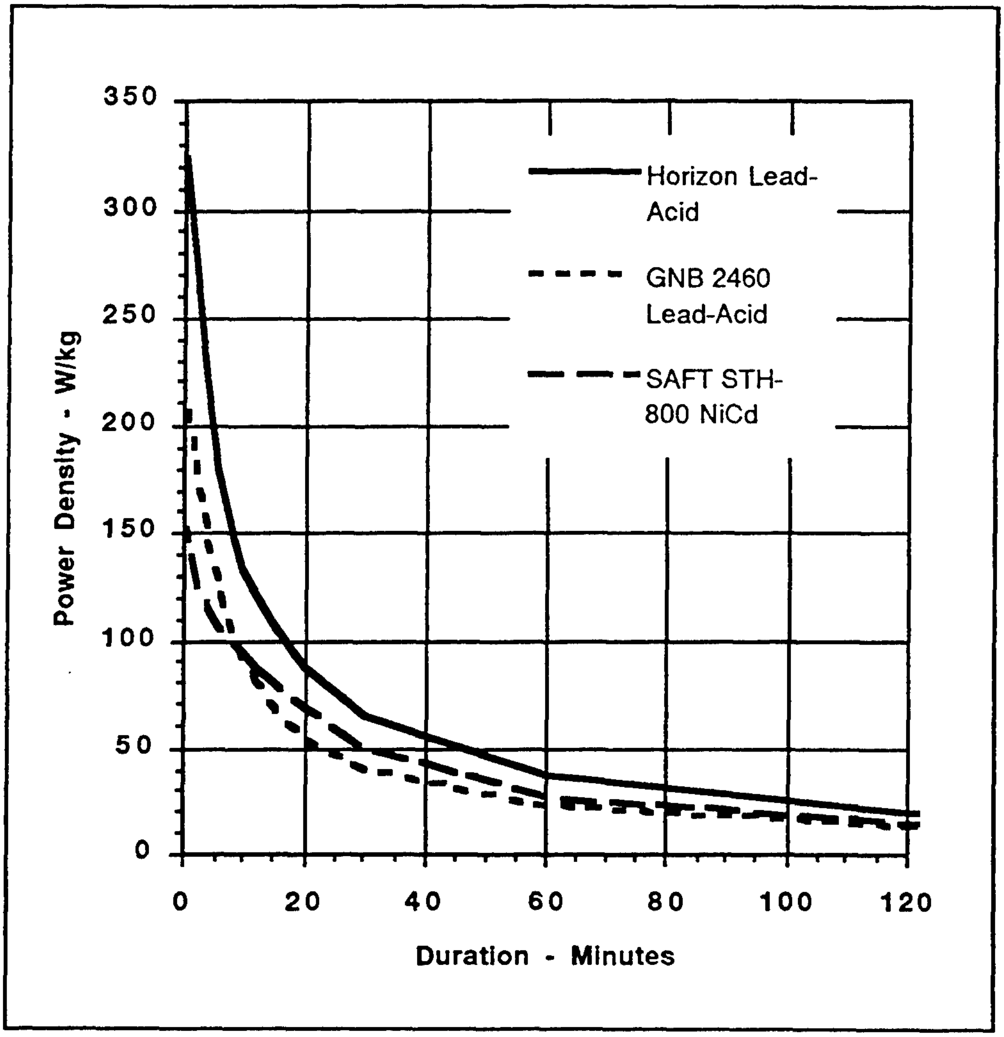

Figure 26: Comparison of power density at varying discharge duration.

Battery recharge rate is an important requirement for an all electric vehicle since this determine the down time between missions. This is of lesser importance with hybrid vehicles since the batteries are constantly being charged through-out the mission except during periods of high power demands. Both the Horizon and Ni-Cd have similar recharge capability with both capable of exceeding a 95% charge within 30 minutes. The standard

lead-acid is far below this requiring up to 8 hours to recharge from a 20% depth of discharge.

It is recommended that 2 parallel strands of 27 Horizon batteries be used (54 total). This will give the vehicle great acceleration and slope climbing ability, along with approximately 30 minutes of operation without the APU on. It is also recommended that a battery management system be used to prevent damage to the system during recharge. The power density and shape of the batteries made these the best choice

In addition, the Horizon batteries needed for the M113 have been purchased by SMUD using separate ARPA funding. SAFT batteries would need to be purchased using project funds.

6.2 Propulsion System Repackaging

Using separate funding, several vehicle concepts were developed to help determine an optimum configuration for the M113 hybrid-electric drive system. This study looked at optional locations for the APU and batteries. The objective was to locate the major components such that:

- Maximum "usable" volume was realized. The back of vehicle should be kept as clear as possible and the driver's space should not be limited.
- The center of gravity of vehicle should be kept close to where it is on standard M113.
- No major changes to hull structure.
- Small number of large groups of batteries is preferable over large number of small groups.

The preferred vehicle configuration is shown in Figure 27.

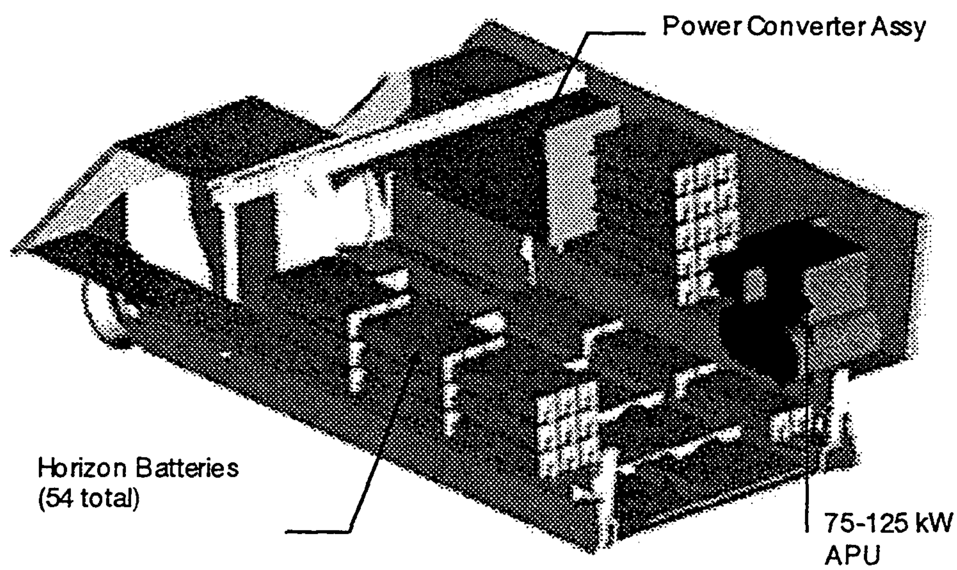

Figure 27: Recommended M113 Propulsion System Layout

The recommended approach has the APU located on the right sponson to replace the existing APU on the M113 electric drive vehicle at the rear of the vehicle. Using this existing location will minimize the amount of rework that would be needed on the hull to relocate the APU to a new location. The power converter assembly is located on the right sponson toward the front of the vehicle. The battery pack consists of (54) advanced lead acid Horizon low profile batteries. The unique size allows 6 batteries to be mounted under the crew seats on each side, resulting in minimal impact to the interior volume. The remaining 42 batteries are located in two packs on the left and right sponsons, respectively.

6.3 Hybrid Operation

At present the electric drive M113 can be powered from either the on-board APU *or* the battery pack(s), but not from both (i.e. hybrid operation). Hardware and software changes are required to convert the existing vehicle to a hybrid.

It is recommended that the vehicle control board (described in section 3.5.4, above) be replaced with the latest generation of the FMC power management controller. This controller is a network-based communication and control system that provides control functions at the "propulsion system-level".

In hybrid operation, the APU will provide the "average" electric power needed to power the sprocket drive motors and auxiliary loads. The batteries will be used as a supplemental source for transient power needs (such as acceleration, steering and grades) and to store regenerated braking energy. The APU will be used to maintain a nearly constant state-of-charge of the battery pack over a typical vehicle mission profile. By using batteries to supply the transient peak power demands, a smaller engine can be installed than would be required for a mechanical drive vehicle. Preliminary studies indicate that an APU engine with a rating of approximately 160-175 HP can be used, rather than the 275 HP engine which is presently installed in the mechanical drive M113-A3 vehicle. Other advantages includes; ability to operate engine along peak efficiency curve and smaller sized auxiliary support systems (radiator, fans, muffler, etc.).

The power management controller will also be capable of controlling the M113 in an "all-electric" mode of operation (i.e. APU off). This mode will be used to demonstrate reduced noise and thermal signatures (stealth operation). The vehicle will also have the capability of recharging the energy storage system from an external power source.

6.4 Quimpax Band Track

As discussed above, in an effort to study the reduction of track-borne noise, TACOM installed the AAI Band Track on the M113 vehicle. While some improvement has been noted, the particular track that has been installed has experienced approximately 700 performance validation / durability miles since its manufacture in 1984. Included in that period has been 2 years of salt water

exposure and there is evidence of degradation of the elastomeric and metallic components.

It is recommended that the AAI track be replaced with Quimpax band track to achieve even greater levels of noise reduction and increase the durability of the system. Quimpax was awarded a TARDEC contract to design and build band track for testing on an M113. This endless belt, segmented, positively driven track is due for roll-out in late October 1994. TARDEC conducted an on site critical design review in mid June 94 where they observed operation of a British APC fitted with Quimpax band track. This vehicle reportedly operated well, leaving TARDEC personnel with the impression that Quimpax will provide a prudent design with high probability of success. Quimpax has also been awarded a contract to provide a medium weight band track for demonstration on a BFV; no activity has taken place on this contract as of this writing.

This track has drive features that enable operation using the standard M113 sprocket and idler. The track is 15 -inches wide and projected to be 26 lb/ft and will retain the same 6-inch pitch and 10-tooth sprocket as the production M113.

6.5 Test and Evaluation

The completed vehicle should be dynamometer tested to evaluate automotive performance. Additionally, testing should be done to quantify signature (thermal and acoustic) reduction levels

It is recommended that the following tests will be performed:

Steering Tractive Effort and Differential Torque: — Steady-state steer performance will be evaluated during these tests using absorption dynamometers. Differential torque will be tested in pivot steer mode, and maximum differential tractive effort will be measured.

Gradeability: — Continuous operation at high power and low/moderate vehicle speeds will constitute this test. The contributions of energy storage to gradeability performance will be quantified during this test.

Heat Rejection: — Cooling tests will be performed at 0.7 TE/GVW continuous.

Vehicle Safety Testing: — Acceptance tests will document that the vehicle meets safety requirements by running typical demonstration scenarios.

DOCUMENT 4

A Survey of Technology for Hybrid Vehicle Auxiliary Power Units

AD-A300457

October 1995

Southwest Research Institute
San Antonio, TX

AD A300457

A SURVEY OF TECHNOLOGY FOR HYBRID VEHICLE AUXILIARY POWER UNITS

INTERIM REPORT
TFLRF No. 311

By

S.K. Widener
Southwest Research Institute
San Antonio, Texas

Prepared for

Advanced Research Projects Agency
3701 N. Fairfax Drive
Arlington, Virginia 22203-1714

Under Contract to

U.S. Army TARDEC
Mobility Technology Center–Belvoir
Fort Belvoir, Virginia

Contract No. DAAK70-92-C-0059

Approved for public release; distribution unlimited

October 1995

Disclaimers

The findings in this report are not to be construed as an official Department of the Army position unless so designated by other authorized documents.

Trade names cited in this report do not constitute an official endorsement or approval of the use of such commercial hardware or software.

DTIC Availability Notice

Qualified requestors may obtain copies of this report from the Defense Technical Information Center, Cameron Station, Alexandria, Virginia 22314.

Disposition Instructions

Destroy this report when no longer needed. Do not return it to the originator.

REPORT DOCUMENTATION PAGE

Form Approved
OMB No. 0704-0188

1. AGENCY USE ONLY (Leave blank)

2. REPORT DATE

October 1995

3. REPORT TYPE AND DATES COVERED

Interim
April 1994 to June 1995

4. TITLE AND SUBTITLE

A Survey of Technology for Hybrid Vehicle Auxiliary Power Units

5. FUNDING NUMBERS

DAAK70-92-C-0059; WD 20 & 36

6. AUTHOR(S)

Widener, Stanley K.

7. PERFORMING ORGANIZATION NAME(S) AND ADDRESS(ES)

Southwest Research Institute
P.O. Drawer 28510
San Antonio, Texas 78228-0510

8. PERFORMING ORGANIZATION REPORT NUMBER

TFLRF No. 311

9. SPONSORING/MONITORING AGENCY NAME(S) AND ADDRESS(ES)

Department of the Army
Mobility Technology Center-Belvoir
10115 Gridley Road, Suite 128
Ft. Belvoir, Virginia 22060-5843

Advanced Research Projects Agency
3701 N. Fairfax Drive
Arlington, Virginia 22203-1714

10. SPONSORING/MONITORING AGENCY REPORT NUMBER

11. SUPPLEMENTARY NOTES

12a. DISTRIBUTION/AVAILABILITY STATEMENT

Approved for public release; distribution unlimited

12b. DISTRIBUTION CODE

13. ABSTRACT (Maximum 200 words)

The state-of-the-art of heat engines for use as auxiliary power units in hybrid vehicles is surveyed. The study considers reciprocating or rotary heat engines, excluding gas turbines and fuel cells. The relative merits of various engine-generator concepts are compared. The concepts are ranked according to criteria tailored for a series-type hybrid drive.

The two top APU concepts were the free-piston engine/linear generator (FPELG) and the Wankel rotary engine. The FPELG is highly ranked primarily because of thermal efficiency, cost, producibility, reliability, and transient response advantages; it is a high risk concept because of unproven technology. The Wankel engine is proven, with high power density, low cost and low noise. Four additional competitive concepts include two-stroke spark-ignition engine, two-stroke gas generator with turboalternator, free-piston engine gas generator with turboalternator, and homogeneous charge compression ignition engine. This study recommends additional work, including cycle simulation development and preliminary design to better quantify thermal efficiency and power density.

Auxiliary concepts were also considered, including two which warrant further study: electrically actuated valves, and lean turndown of a normally stoichiometric engine. These concepts should be evaluated by retrofitting to existing engines.

14. SUBJECT TERMS

Heat Engine	Diesel	Turboalternator
Rotary Engine	Spark-Ignition	Linear Generator
Hybrid Vehicle	Two-Stroke	Gas Generator
Auxiliary Power Unit	Four-Stroke	HCCI
Free-Piston Engine		

15. NUMBER OF PAGES

89

16. PRICE CODE

17. SECURITY CLASSIFICATION OF REPORT	18. SECURITY CLASSIFICATION OF THIS PAGE	19. SECURITY CLASSIFICATION OF ABSTRACT	20. LIMITATION OF ABSTRACT
Unclassified	Unclassified	Unclassified	

EXECUTIVE SUMMARY

Problems: This study was undertaken to survey the state-of-the-art of heat engines for use as power plants in hybrid vehicles. It assumes that the heat engine drives an electric generator providing auxiliary power for charging batteries and/or powering the electric traction motor, which is the primary drive of the vehicle. The study is confined to reciprocating or rotary heat engines, excluding gas turbines and fuel cells.

Objective: The objective of this project was to survey the state-of-the-art of heat engines for use as powerplants in hybrid vehicles.

Importance of Project: While this study is useful, it is necessarily subjective due to the lack of consistently defined quantitative information on engines in the power class needed for a hybrid APU and on advanced concepts. The ranking study is intended to narrow the focus of research by eliminating concepts that are not likely to succeed in the hybrid APU application, and by focusing attention on those parameters that need to be further quantified. The recommended next step is in-depth analysis of those concepts that offer the most promise based on this study.

Technical Approach: A literature survey was performed to determine the relative merits of various engine-generator concepts. The concepts were ranked according to criteria tailored for a series-type hybrid drive. The ranking procedure assigned weights to each criterion according to its relative importance in hybrid APU applications. By this method, it is hoped that those concepts unlikely to be competitive are systematically eliminated, and those concepts most deserving of further study and development are highlighted.

Accomplishments: The two most promising APU concepts were the free-piston engine/linear generator (FPELG) and the Wankel rotary engine. The FPELG is highly ranked primarily because of perceived advantages in thermal efficiency, cost, producibility, reliability, and transient response; however, it is a high risk concept because of unproven technology for the generator. The Wankel engine is a proven concept with high power density and benefits of relatively low cost and noise. Four additional concepts ranked somewhat lower but within the range of competitiveness for this subjective analysis. These include two-stroke spark-ignition engine, two-stroke gas generator with turboalternator, free-piston engine gas generator with turboalternator, and homogeneous charge compression ignition engine. This study recommends additional evaluation of these concepts, including cycle simulation work and preliminary design to better quantify thermal efficiency and power density.

Auxiliary concepts were also considered, which include those ideas that are not specific to a given engine design but may be applied to a number of different engine types. Of these, two stood out as warranting further study: electrically actuated valves, and lean turndown of a normally stoichiometric engine. It is recommended that these concepts be evaluated by retrofitting to existing engines.

Military Impact: Identification of alternative power plants for hybrid electric vehicle application provides options for military selection. The most optimum engine for military use would be determined from cost benefit and trade-off studies, commercial availability, and requirements for technology demonstration. Of major significance is whether the hybrid electric vehicle drive would be used for administrative-tactical wheeled vehicle or combat-tracked vehicle applications.

FOREWORD/ACKNOWLEDGEMENTS

This work was performed by Southwest Research Institute (SwRI), San Antonio, TX, during the period April 1994 to June 1995 under Contract No. DAAK70-92-C-0059. The work was funded by the Advanced Research Projects Agency (ARPA), Arlington, VA, and administered by the U.S. Army TARDEC, Mobility Technology Center-Belvoir (MTCB), Ft. Belvoir, VA. Major Richard Cope and Dr. John Gully served as the ARPA project technical monitors. Mr. T.C. Bowen (AMSTA-RBFF) served as the MTCB contracting officer's representative, and Mr. M.E. LePera (AMSTA-RBF) served as the MTCB project technical monitor.

The author would like to acknowledge the assistance provided by Mses. N.A. Wilkes and M.M. Clark in report preparation and editing.

TABLE OF CONTENTS

TABLE OF CONTENTS, CONT'D

LIST OF ILLUSTRATIONS

LIST OF TABLES

I. INTRODUCTION

The Advanced Research Projects Agency (ARPA) has taken an initiative in developing hybrid vehicle technology, focusing on the unconventional technologies needed to make hybrid vehicles successful as energy-saving and pollution-reducing alternatives to current automotive technology. The model hybrid electric drivetrain consists of an auxiliary power unit (APU) comprising a combustion engine driving an electric generator, an electric power storage device (battery), electric traction motors, and a control system. The APU must provide electric power under conditions very different from the conventional automotive driving cycle and must meet a different set of objectives. It is natural, then, that the power plant itself may be unconventional. This study explores the alternative combustion engine power plants that may be used for hybrid electric vehicles. The intent is to discriminate between both conventional and unconventional alternatives to find those concepts that are most worthy of further study in the form of simulation, analysis, and ultimately, prototype demonstration.

The study was initiated as a brainstorming exercise among a number of engineers at Southwest Research Institute (SwRI) involved in engine design and development, and in hybrid vehicle development. The author then proceeded to review the literature available on conventional and unconventional engines and develop a list of concepts, which were then assessed and ranked according to their perceived ability to meet the objectives of a hybrid APU. The concepts, criteria, and ranking are discussed in this report, and recommendations for further study are provided.

II. OBJECTIVE

The objective of this study is to discern which concepts for combustion engines are the best choices for detailed study as alternative power plants to the conventional reciprocating engine in application to hybrid electric vehicle APUs. The study is limited to internal combustion engines or reciprocating external combustion (Stirling) engines suitable for coupling to electric generators; turbine engines, fuel cells, and other concepts are also viable alternatives but are not considered

here. The criteria are tailored for series-type hybrid drivetrains in which the combustion engine drives electric generation as a supplemental charging source for battery storage. Other types of hybrid drives are possible, such as a parallel arrangement whereby the combustion engine directly drives the traction wheels through a transmission in combination with electric motors (the criteria for these systems will be markedly different).

III. CRITERIA

Hybrid powertrains are considered alternatives to conventional combustion engines for two primary reasons: fuel economy and emissions. The fuel economy benefit arises from two fundamental factors: power leveling by energy storage in the batteries, and the ability to operate the APU power plant at constant, peak efficiency conditions. Emissions are improved because the overall fuel consumption is low, allowing the engine to operate at a near steady state cycle. Thus, the criteria for selection of an engine for a hybrid vehicle are very different from those for a conventional automotive power plant. The criteria that are important to hybrid APUs are listed below, roughly in their order of precedence.

A. Power Density

The volume available for the power plant is limited, as space must be allotted for energy storage, traction motors, generator, and controls, as well as the engine itself. The weight is important, since vehicle weight directly impacts fuel economy. High power density, in terms of both power-to-volume ratio and power-to-weight ratio, is desirable. Power density in consideration of both engine and generator tends to favor high-speed engines, as the generator volume and weight for a given power rating decreases with increasing speed.

B. Emissions

If an engine has good power density but substantially worse emissions characteristics than its conventional competitor, it ultimately will not fulfill the objectives of hybrid vehicles. Thus,

concepts that improve power density at the expense of emissions will not be completely satisfactory. However, brake-specific emissions that are higher than the conventional technology may be tolerable as the duty factor for the APU is much lower than the conventional drivetrain.

C. Thermal Efficiency

Thermal efficiency--a measure of fuel economy--must be high to achieve overall vehicle fuel economy benefits over conventional drivetrains. While the hybrid drivetrain has key advantages, it must also overcome losses associated with energy storage and retrieval, and generator and motor inefficiencies, as well as the simple problem that the package generally tends to be heavier than a conventional drivetrain.

D. Cost

To be competitive as a commercial product, a hybrid vehicle must have comparable cost to conventional vehicles. This equation will have to factor in total life cycle costs, which include reduced fuel cost as well as the expense of battery replacement and system maintenance. It is clear that the drivetrain will be significantly more expensive due primarily to the energy storage system. Thus, the engine itself will have to be as inexpensive as possible.

E. Transient Response

Transient response characteristics of a hybrid APU are a lower priority, as the system is designed to operate at near steady state conditions. However, a rapid transient response is desirable for rapid engine catalyst warm-up, assuming a catalyst is used. The response of most interest is the start-up from cold to full power.

F. Producibility

Closely linked to the cost issue is the producibility of the engine. Will it be manufactured by conventional methods, or will new or expensive, unconventional processes be required?

G. Reliability

Also ultimately a life cycle cost issue, the reliability of combustion engines is a factor to consider. Many small power plants for utility applications are designed for much shorter life than their automotive counterparts. However, engine replacement or major overhaul should not be any more frequent for hybrid powertrains than for conventional engines. The design of APU engines for reliability must take into account the high power factor. The APU will be operated primarily at its design point, instead of primarily at low load conditions like a conventional automotive engine.

H. Cranking Torque

During start-up, most engines absorb a considerable amount of power from the starter motor to overcome friction and inertia. This start-up energy can be characterized as the cranking torque and is highly dependent upon engine design. It is a direct penalty to overall thermal efficiency and must be taken into consideration for drivetrains where the APU is cycled frequently between running and nonrunning conditions.

I. Noise, Vibration, and Harshness

Noise, vibration, and harshness (NVH) are measures of the comfort level of passengers in vehicles or of bystanders. These factors are increasingly important for customer satisfaction and acceptance. In this regard, the hybrid drivetrain should not be appreciably worse, and preferably should be better than its conventional counterpart.

J. Technical Risk

The technical risk of a new concept is not a measure of how well it will perform its intended function, but of how much is unknown about its viability, and how much research effort may need to be expended to make it viable.

K. Multifuel Capability

Some engine concepts are limited to certain types of fuel. Alternative fuels such as natural gas and methanol are of increasing interest primarily due to environmental concerns. The ability to be tolerant of different fuels would be an advantage.

IV. RANKING PROCEDURE

As a systematic means of distinguishing between APU concepts, a ranking procedure was applied. In this procedure, each concept was assigned a score relative to each of the previously described criteria. The criteria were also weighted according to their importance in the APU application. Where possible, the assigned scores were based on actual quantifiable data. Thermal efficiency is defined as the ratio of electric power out to fuel energy in. The power density for an engine type is scored as an actual (reciprocal) specific weight in kW/kg, or specific volume in kW/L (the reciprocal is used to conform to the overall strategy of "higher is better"). For parameters which have no quantifiable level, a relative score was assigned with a baseline level of 1.0. Weighting factors were assigned as the product of a normalizing factor established as the reciprocal of the difference between maximum and minimum values of the parameter, and a significance weight in the range of 0 through 5.

V. STATE-OF-THE-ART

As part of this study, an extensive literature review was conducted to assess the current state-of-the-art for automotive combustion engines and particularly for hybrid APUs in relation to the above criteria, and to examine the potential for advanced concepts to improve the state-of-the-art. It is important to understand the best attainable performance of a conventional engine-generator combination in order to assess the value of unconventional technologies in improving this performance. During this study, a total of 58 references were reviewed. Supplementary

information was obtained from the SwRI engine database, which is a comprehensive listing of published data on reciprocating engines from all over the world.

One key reference is a similar study that was conducted eleven years ago by JPL for the U.S. Department of Energy (1)*, written by Mr. H.W. Schneider. The objectives of that study were somewhat different in that the primary focus was for parallel drivetrains; however, the document fairly summarizes the state-of-the-art for that time, and also makes recommendations for series drivetrains. The author considers in his discussion the following alternatives:

- Four-stroke piston engines
- Four-stroke rotary engines (Wankel)
- Two-stroke piston engines
- Indirect injection diesel engines
- Direct injection diesel engines
- Brayton cycle engines (gas turbine)
- Stirling engines
- Rankine cycle engines (steam engine)
- Free-piston engines.

After consideration of the relative merits for series drivetrains, the author recommended research to be prioritized as follows: direct-injected spark-ignited two-stroke engines, fuel-injected rotary engines, and free-piston engines.

This study was revised and updated in 1992 by A.F. Burke, with special consideration of the driving cycle requirements for a series hybrid drivetrain.(2) The developments in the years between 1984 and 1992 had made the series option more feasible, primarily because of advancements in electric drivetrain component sizes and efficiencies. For a series drivetrain application to a passenger car, gradability and minimum sustained highway speed requirements dictate an APU of about 25 to 30 kW output, suggesting that an appropriate target power rating

* Underscored numbers in parentheses refer to the list of references at the end of this report.

for the engine is 30 kW. Mr. Burke places a lower priority on fuel economy for the combustion engines in a series drivetrain because the vehicle is assumed to be operating in a purely electric mode for 80 to 90 percent of the driving miles, based on results of a Monte Carlo analysis of typical driving patterns.(3) For the series hybrid, start-stop operation is also less of a consideration than for the parallel configuration because the periods of continuous operation and continuous non-operation are longer. According to Mr. Burke's analysis, the series drivetrain may go for days at a time without using the heat engine due to short urban trips with battery charging from the wall plug between trips. In a similar study, Mr. Burke focussed on the effects of start-stop operation indicating that for range extender type operation, where the vehicle would be operated for extended periods in highway driving with fairly low, continuous power demand, the overall fuel economy could be greatly improved if the APU were operated intermittently at its peak efficiency rather than continuously at low load.(4) These updates redefined the APU engine development priorities as 1) rotary, 2) direct injection two-stroke, and 3) gas turbine engines, omitting discussion of Stirling, Rankine, or free-piston engines.

The survey of literature done by Mr. Schneider and updated by Mr. Burke distills the state-of-the-art into estimates of performance and power density attainable by the various current technology engine types. These summaries are included in the Appendix, which also incorporates data from other sources as described below. Figure 1 shows the projections of specific weight for the conventional technology engines, as presented by these two references.

In the legend, "2-S SI" refers to two-stroke spark-ignition engines, "Rotary" to Wankel-type rotary engines, "4-S SI" to four-stroke spark-ignition engines, "4-S DI CI" to four-stroke direct injection compression ignition (Diesel) engines, and "4-S IDI CI" to four-stroke indirect injection compression ignition (Diesel) engines. The later reference applies a bit more pessimism to the two-stroke gasoline engines but still ranks them at the lowest specific weight. Schneider presented both DI and IDI diesel engines but discounted them as contenders for the APU due to high specific volume and weight; Burke did not consider these engines. Burke was more optimistic for rotary and four-stroke spark-ignition engines. Figure 2 shows the comparison for specific volumes, which follows similar trends to specific weight. However, Burke was more

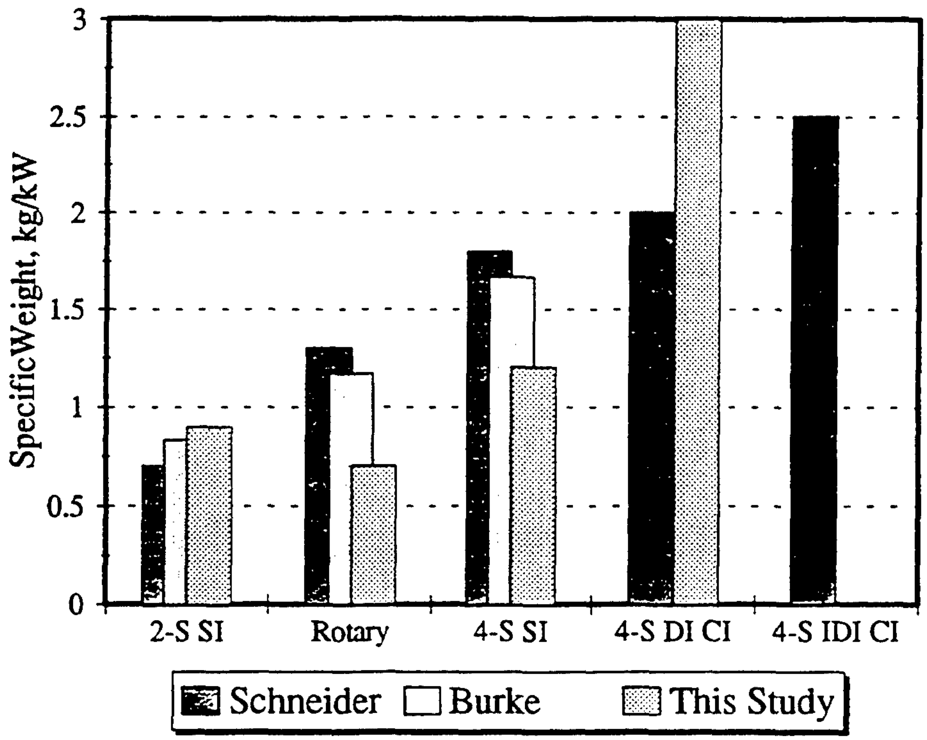

Figure 1. Specific weight comparisons from References 1 and 2

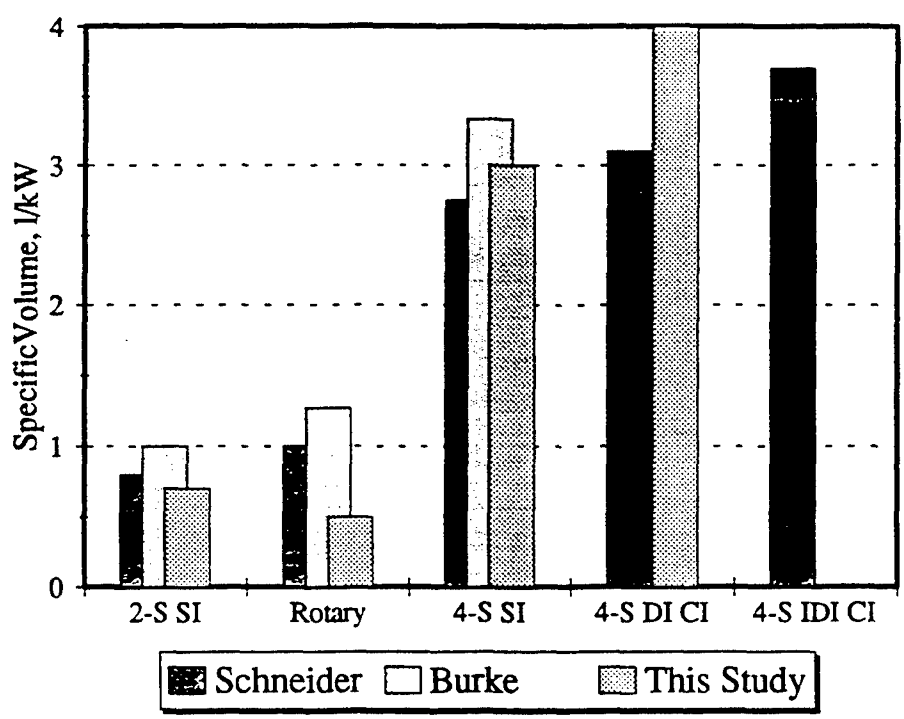

Figure 2. Specific volume comparisons from References 1 and 2

pessimistic than Schneider in his predictions. In terms of fuel consumption (see Fig. 3), the two-stroke spark-ignition engine was a strong contender, with fuel economy approaching or exceeding that of the IDI diesel. Fuel economy (along with simplicity) was a key reason for Schneider's recommending the two-stroke SI engine. Burke's update has added some pessimism to this prediction, but this engine still appears to be a strong contender in his analysis. Of course, the DI diesel scores best in fuel consumption, but it is still discounted by these researchers because of its perceived weight and volume penalties.

Reference 5 analyzes key driving conditions of acceleration, gradability, and steady state fuel economy and compares alternative engines in application to a range-extender vehicle (REV) based on an existing Ford Taurus platform (two other platforms were analyzed but not explicitly discussed in the reference). This study determined that the power rating for the APU engine should be in the range of 25 to 50 kW for this type of application. Several alternative engines were considered as substitutes for a small (6.5-kW) genset that was considered in a previous

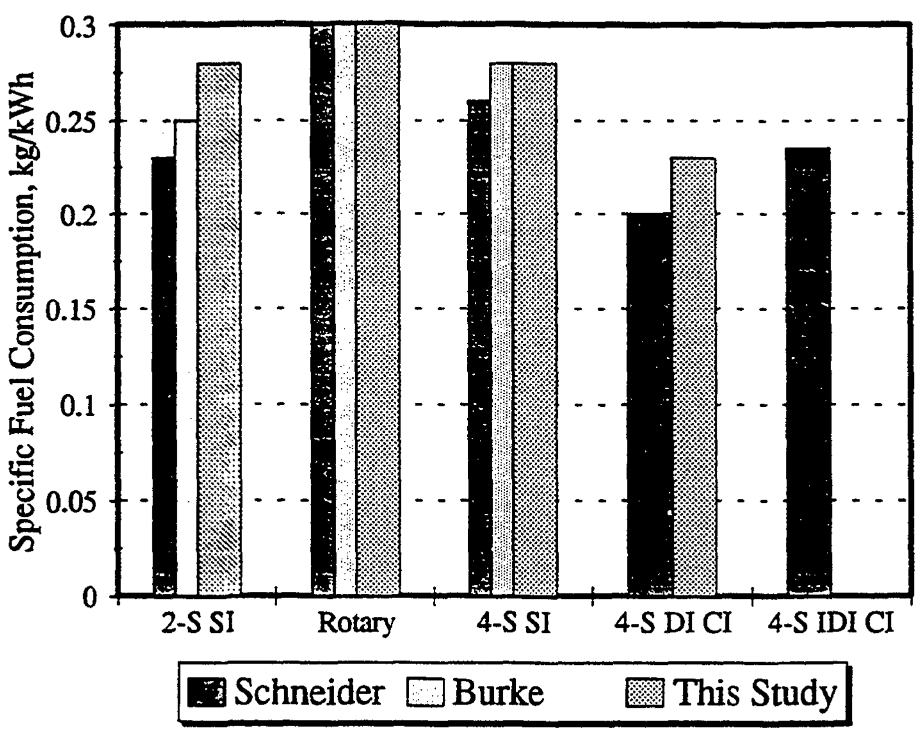

Figure 3. Fuel consumption comparisons from References 1 and 2

phase of that analysis. The alternatives included the Orbital OCP "X" engine rated at 37.6 kW, the GM Quad 4 four-stroke SI engine rated at 62.7 kW, the Nomac gas turbine genset at 24.0 kW, the NASA Series 70 rotary engine at 28.1 kW, and an MTI Mod II Stirling engine at 32.2 kW. The comparison criteria based on vehicle performance with these options are not very useful in distinguishing between alternative engine categories because the power ratings of the different engines vary widely. Obviously, acceleration and gradability criteria favored the larger power plants, whereas fuel economy favored the Stirling engine. This reference does provide a useful comparison of performance data for several state-of-the-art engine categories, which is included in the Appendix.

The current state-of-the-art for conventional technologies is discussed in the sections that follow. In this context, conventional technologies are those currently in production for automotive engines, or in imminent production status. Such technologies as free-piston engines or Stirling engines are still very much in the research stage and will therefore be considered as advanced concepts.

A. Generator Technology

Since the objective is electric power out, the generator characteristics must be considered as well as the engine characteristics. The power density of conventional rotating generators is significantly enhanced by increasing the shaft speed. The efficiency is less affected, as proper design can achieve high efficiency at virtually any design speed. At higher speeds, windage losses tend to degrade the efficiency somewhat; however, for this study, it is assumed that efficiency is constant with speed. For those concepts that work with a conventional rotating generator, it is assumed that the generator efficiency is 92 percent. The overall design requirements of a hybrid APU favor those engines that have higher shaft speed for compactness of both engine and generator. Figure 4 shows the characteristic tradeoff of generator size and weight with shaft speed for a 25-kW generator.(6) For a baseline unit operating at 6,000 rpm and generating 30 kW, specific volume and weight are assumed to be 0.3 L/kW and 1.5 kg/kW, respectively. These values are additive to engine specific volume and weight to obtain system

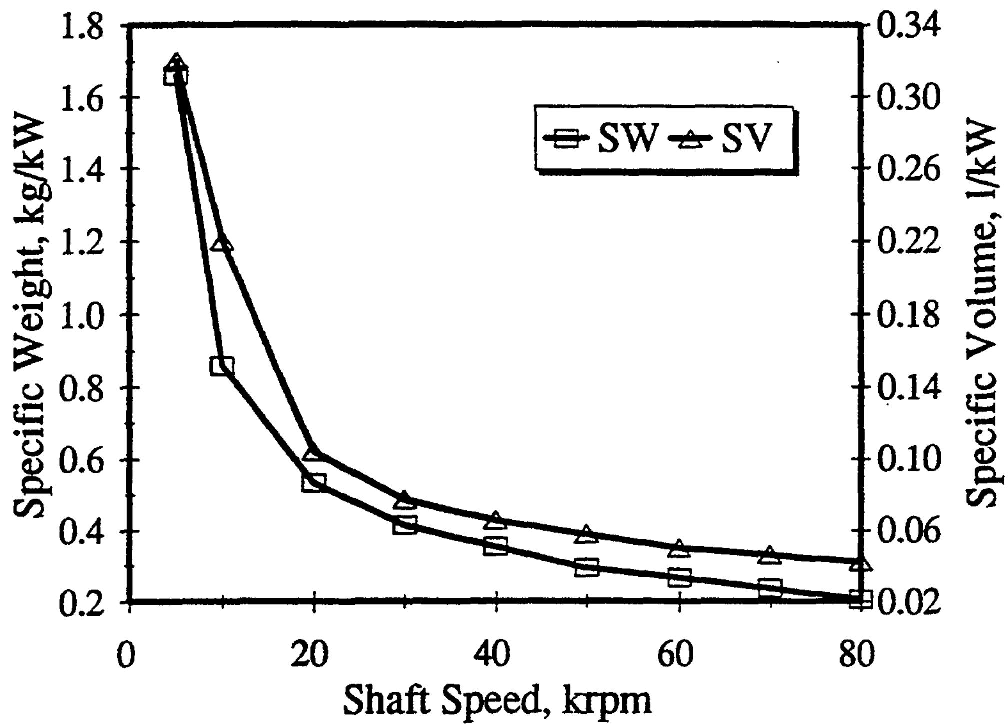

Figure 4. Generator size and weight as a function of shaft speed

characteristics. For systems which afford higher shaft speeds, these values are reduced according to the relationships shown in Fig. 4.

B. Four-Stroke Spark-Ignited Engines

The most highly developed and sophisticated reciprocating engines currently in wide use are the automotive four-stroke spark-ignited engines. Most domestic automobiles employ some version of this class of engine, burning gasoline. The characteristics of the current four-stroke SI are as follows:

- Overhead cams, frequently separate intake and exhaust cams
- Four valves per cylinder
- Electronic fuel injection at the intake port
- Electronic spark control
- Sophisticated digital feedback control systems
- Tuned induction systems
- Variable valve timing (in advanced engines)

- Variable intake geometry (in advanced engines)
- Lightweight materials (aluminum, plastics, composites).

Most of these technologies have not yet been incorporated in engines of the size class appropriate to hybrid APUs. Turbocharging was a common feature of automotive engines in the mid-1980s but has gradually disappeared due primarily to durability issues and cost, the advantages in power density being largely displaced by the improvements due to other technologies. The durability problems with turbocharging the SI engine are attributed to high turbine inlet temperatures, since these engines run with stoichiometric fuel-air ratios. Figure 5 (reproduced from Reference 7) illustrates the trends in power density based on ninety 1988 passenger car engines. Those engines incorporating multivalve technology approach the turbocharged engines in power density. It seems unlikely that turbocharging will be a feasible option to obtain high power density on an SI engine of the power class needed for a hybrid vehicle APU. The remaining technologies previously listed are all feasible for consideration in the development of the hybrid APU.

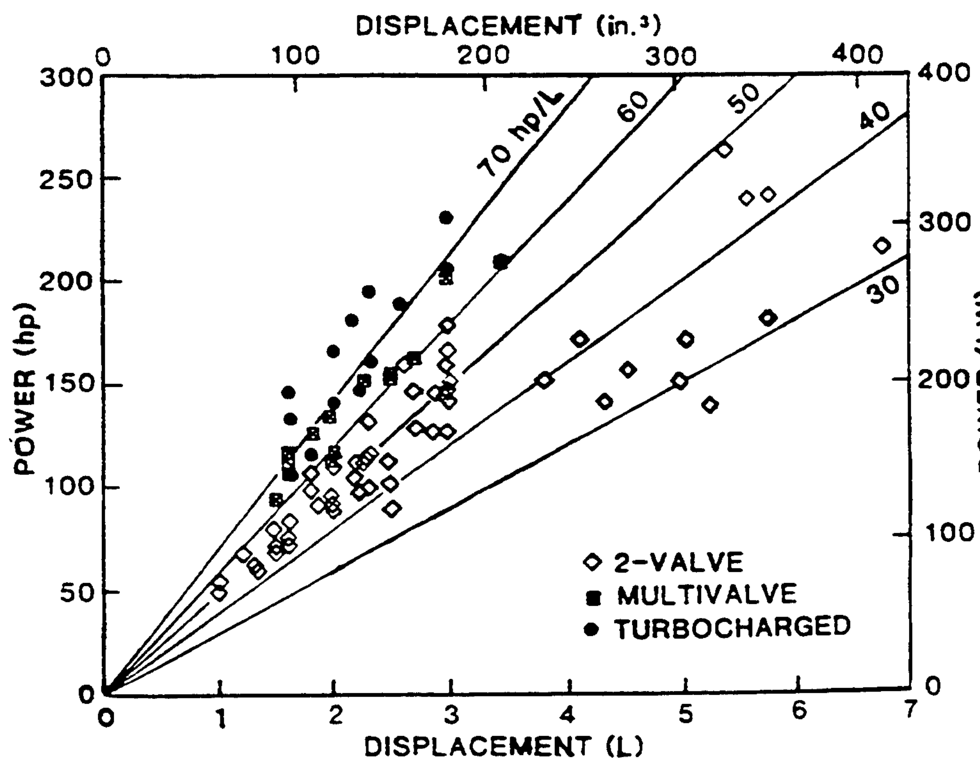

Figure 5. Power density trends from Reference 7

TABLE A-1 in the Appendix summarizes the state-of-the-art of automotive SI gasoline engines, based on the current literature. Production engines are shown along with racing engines to illustrate the range of performance attainable by applying higher technologies.

Figure 6 shows the state-of-the-art for specific weight for four-stroke spark-ignition engines. There is a noticeable increase in specific weight as the power drops below 50 kW into the size class appropriate to APUs. The best obtained specific weight for a 30-kW engine is about 1.9 kg/kW, slightly higher than values suggested by Schneider and Burke. However, the significant sensitivity to power rating in this range (and the lack of engines at 30- to 40-kW rating) suggests that this level may be challenged by focused effort on this application using existing technologies. The higher specific weight of engines below 30-kW output is likely attributable to the lack of penetration of the latest automotive technologies listed above. It is not unreasonable to presume that a small (30-kW) engine incorporating the latest technologies could achieve specific weight of 1.2 kg/kW.

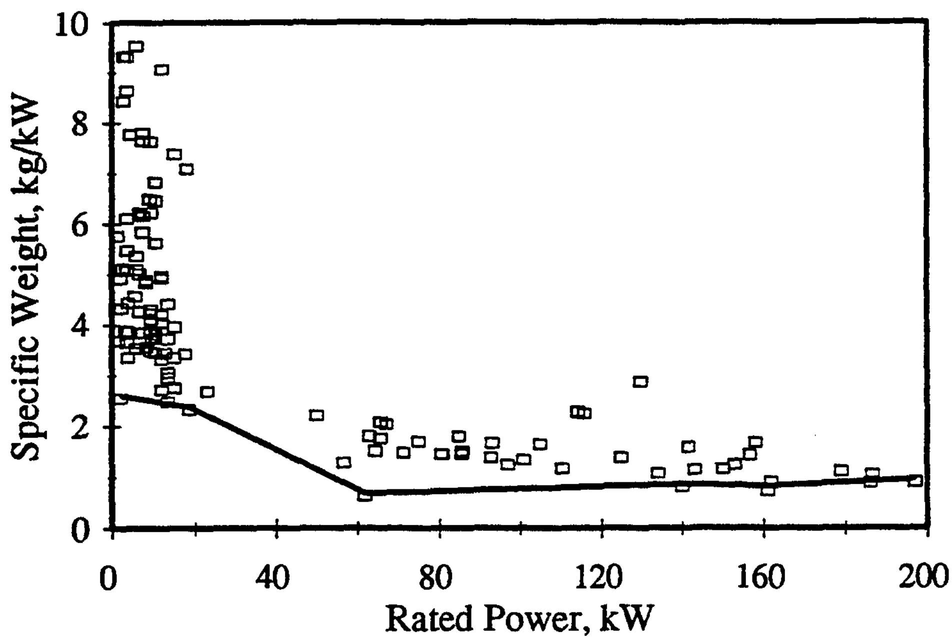

Figure 6. Specific weight of four-stroke spark-ignited engines

Specific volume for four-stroke spark-ignition engines is shown in Fig. 7. Again, there is a substantial increase in the state-of-the-art specific volume as the rated power drops below 50 kW. The best obtained specific volume for an engine 30 kW or less is about 3.6 L/kW, higher than the data of Schneider and Burke. Challenging this level will be more difficult than the specific weight objective, as some of the advanced technologies for weight reduction and power increase have no impact or adverse impact on package volume. A specific volume of 3.0 L/kW is probably achievable by a four-stroke SI engine developed specifically for the APU application.

Fuel consumption of four-stroke SI engines is rarely reported in the literature in the form used for comparison by Schneider and Burke (i.e., BSFC), as these engines are generally more concerned with fuel economy (i.e., miles per gallon) on vehicle driving cycles. Nevertheless, the limited data available from the literature are shown in Fig. 8. Best BSFC from this chart is about 0.26 kg/kW·h, consistent with the data of Burke. It may be surmised that for lower output engines, BSFC will be somewhat higher still, as friction and heat transfer losses proportionally increase with decreasing engine displacement. Best BSFC for a 30-kW engine is probably about 0.28 kg/kW·h.

Emissions from four-stroke SI engines are rarely reported in the literature. Even if they were, the comparisons would probably not be useful for the APU application because emissions are generally measured on a vehicle driving cycle that would be entirely different from the operating cycle of the APU. The state-of-the-art for emissions control is well developed and is well represented by the current legislated emissions limits, as engine manufacturers generally calibrate their engines to just meet these limits with adequate margin for variability. Four-stroke spark-ignition engines for vehicle applications almost universally use a three-way catalyst for control of emissions of oxides of nitrogen (NO_x), hydrocarbons (HC), and carbon monoxide (CO) in combination with a feedback control system to manage the engine air-fuel ratio within very tight limits around the stoichiometric condition. The feedback control uses an oxygen sensor in the exhaust to detect the presence of oxygen (O_2), which indicates a lean condition. A few engines are applying lean-burn technology with stratified charge to improve fuel consumption; in this case, wide-range O_2 sensors are used to apply feedback control over a wider stoichiometry range,

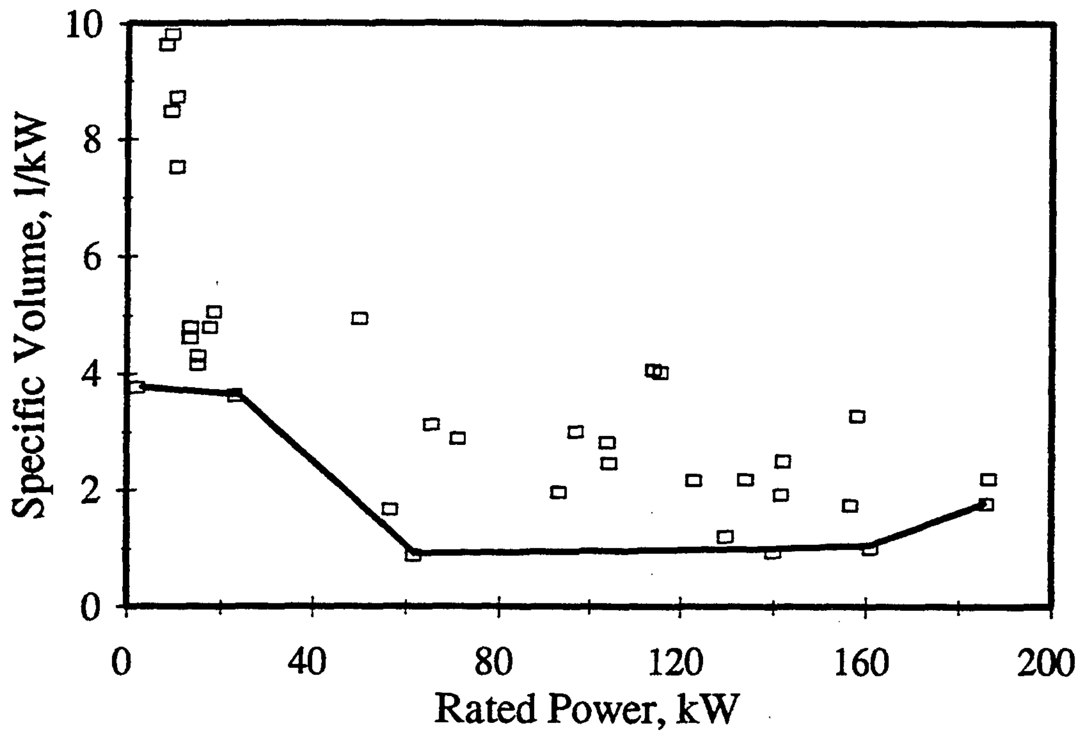

Figure 7. <u>Specific volume of four-stroke spark-ignited engines</u>

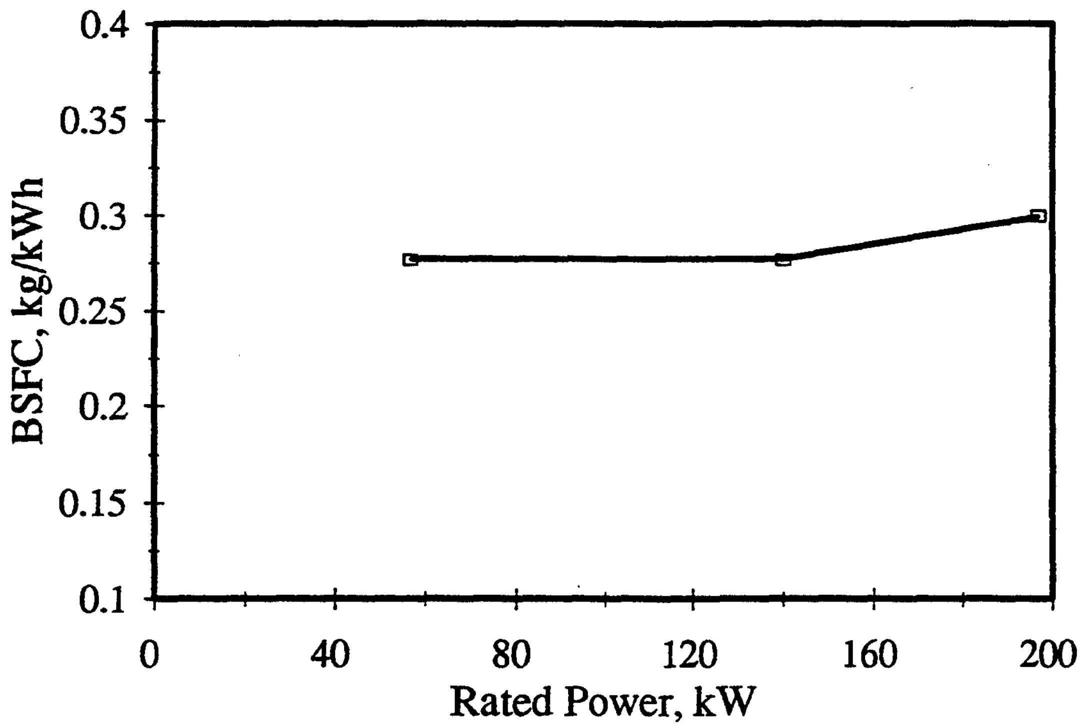

Figure 8. <u>Fuel consumption of four-stroke spark-ignited engines</u>

and NO_x is controlled by a combination of three-way catalyst and lean burn for lower in-cylinder temperatures. However, this technology is going the wrong direction for hybrid APUs, as it reduces power density.

A key consideration in emissions of gasoline engines for hybrid APUs, as it is for conventional vehicle applications, is the catalyst warm-up period. At start-up, the catalyst is cold and ineffective, and warm-up takes several minutes until the catalyst is fully effective. During this period, HC and CO emissions are high, both because of catalyst ineffectiveness and high engine-out emissions due to flame quenching on the cold cylinder internal surfaces and start-up enrichment of the fuel-air mixture. In conventional drivetrains, this happens only once per drive cycle. In hybrid applications, particularly for serial drivetrains, it may happen many times over the driving cycle. The problem will be highly sensitive to the control of the APU, in terms of the number of start-stop cycles encountered and the time between operating cycles during which the catalyst and engine cool down. An electrically heated catalyst can be used to overcome the problem of catalyst warm-up, at some added cost and penalty in power consumption. The APU engine application, then, will favor engines that have a short warm-up cycle and good combustion characteristics during cold start such that cold-start enrichment can be minimized. This will favor gaseous fuels over gasoline, and application of advanced techniques such as high in-cylinder turbulence, variable valve timing, and variable intake geometry.(8-10).

For the purpose of ranking, the four-stroke SI engines are assigned scores according to the above arguments for power density and fuel economy; on other criteria, the four-stroke SI engines are considered to be the baseline and are assigned a score of 1.0.

C. Four-Stroke Compression Ignition Engines

Diesel engines were largely discounted by Schneider and Burke because of a perception of low power density. This is a result of high cylinder pressures requiring heavier cylinder, piston and head structure, and lean-burn operation, which necessitates a higher air consumption than the comparative stoichiometric spark-ignition engines to achieve a target power level. With regard to technological development, these engines are highly developed for medium-duty and heavy-

duty highway vehicles, and also highly developed for stationary utility applications where weight is not a major issue. However, they are not highly developed in high power-density applications.

In terms of power density, the state-of-the-art is represented in Figs. 9 and 10. The state-of-the-art for specific weight (Fig. 9) is largely independent of power class and is, in fact, somewhat higher than that reported by Schneider (Fig. 1), based on data available to SwRI. A specific weight of 3 kg/kW would represent the best current technology for a 30-kW engine developed specifically for power density. Specific volume follows a similar trend (Fig. 10), with slight increase as rated power decreases, as would be expected. The state-of-the-art for a 30-kW engine is about 4 L/kW, higher than the values reported by Schneider of 3.1 for DI diesel engines and 3.7 for IDI engines. Since the rated speeds are limited to lower values by the combustion system, the generators would be expected to be proportionally heavier and bulkier.

The state-of-the-art for fuel consumption is shown in Fig. 11. This follows a gradually rising trend as power rating decreases. A level of about 0.23 kg/kW·h could be expected for a 30-kW engine; Burke reported levels of 0.2 for DI engines and 0.23 for IDI engines.

A word regarding direct injection versus indirect injection is appropriate. Direct injection is widely applied in larger displacement engines, and works in those applications primarily due to the ability to induce in-cylinder air motion by port design, and the ability to use heavy-duty fuel injection equipment with high injection pressures to achieve the required fuel-air mixing for good combustion. IDI systems are employed widely in smaller, higher speed engines where the rate of combustion must be enhanced by vigorous charge motion induced by the flow of air into a prechamber through a small orifice. This air motion enables the use of lower injection pressures and lighter injection equipment. IDI engines typically require higher overall compression ratios to overcome the fluid flow restriction across the prechamber orifice, but experience lower cylinder pressures due to the same restriction of flow as the combustion process proceeds. Fuel economy is degraded by the pumping losses into and out of the prechamber. IDI engines have been almost universally used in light-duty applications up until recent years. Advances in fuel injection and general engine technology, however, have now made DI systems more attractive

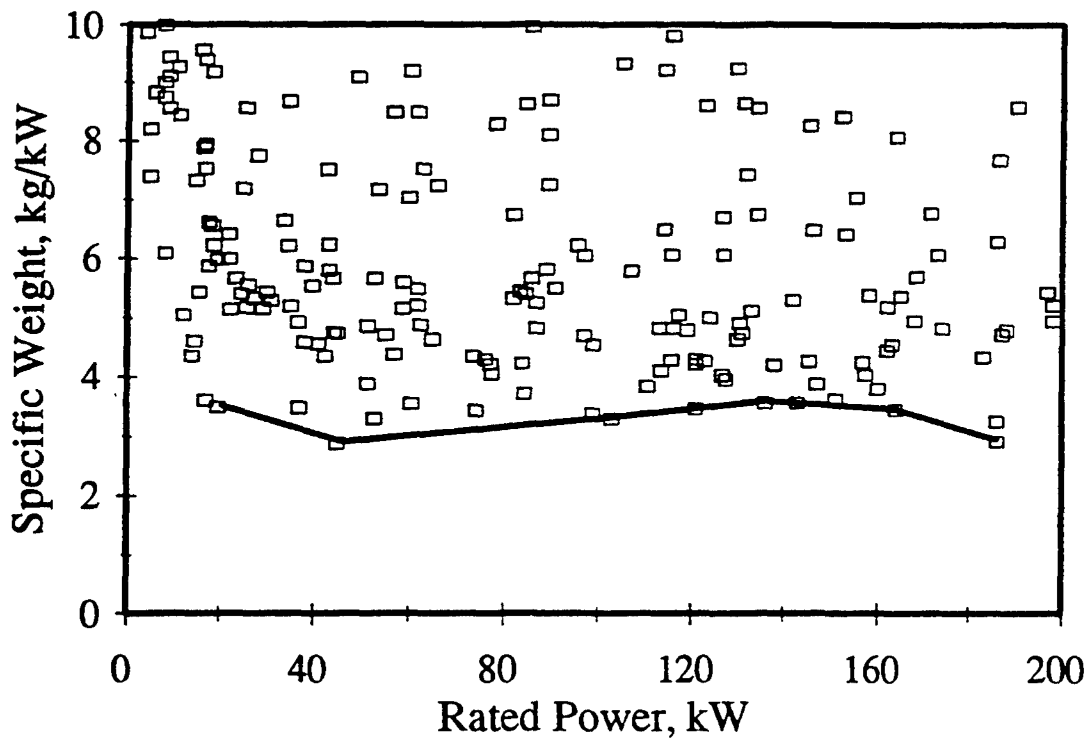

Figure 9. Specific weight of four-stroke diesel engines

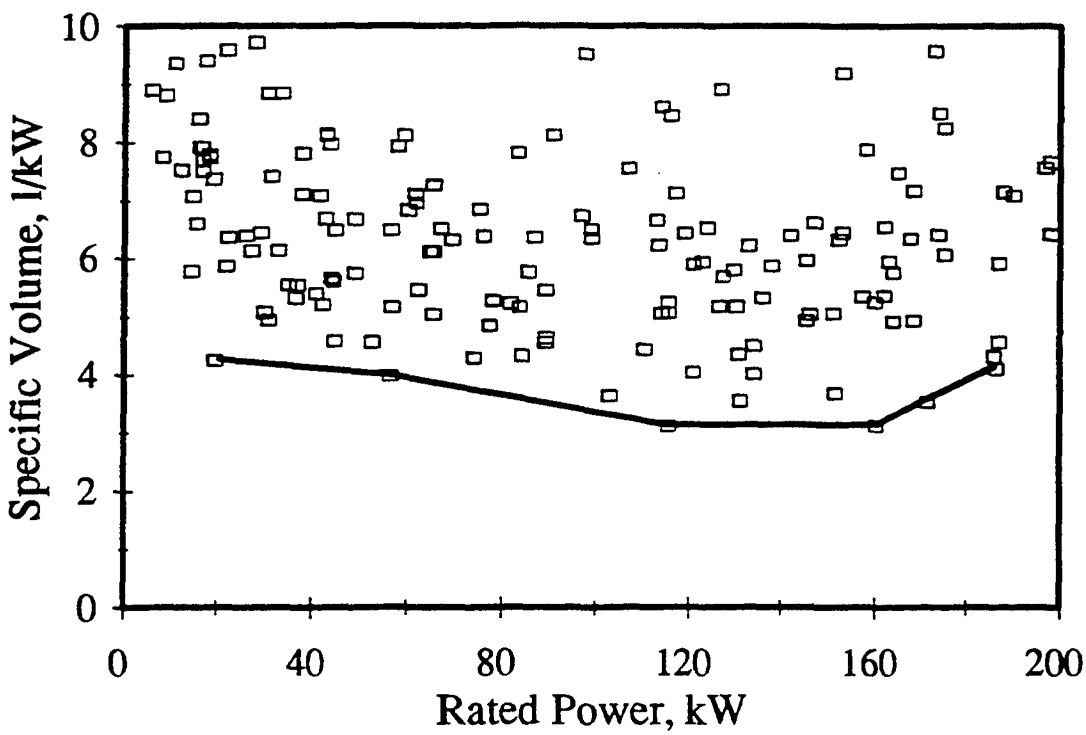

Figure 10. Specific volume of four-stroke diesel engines

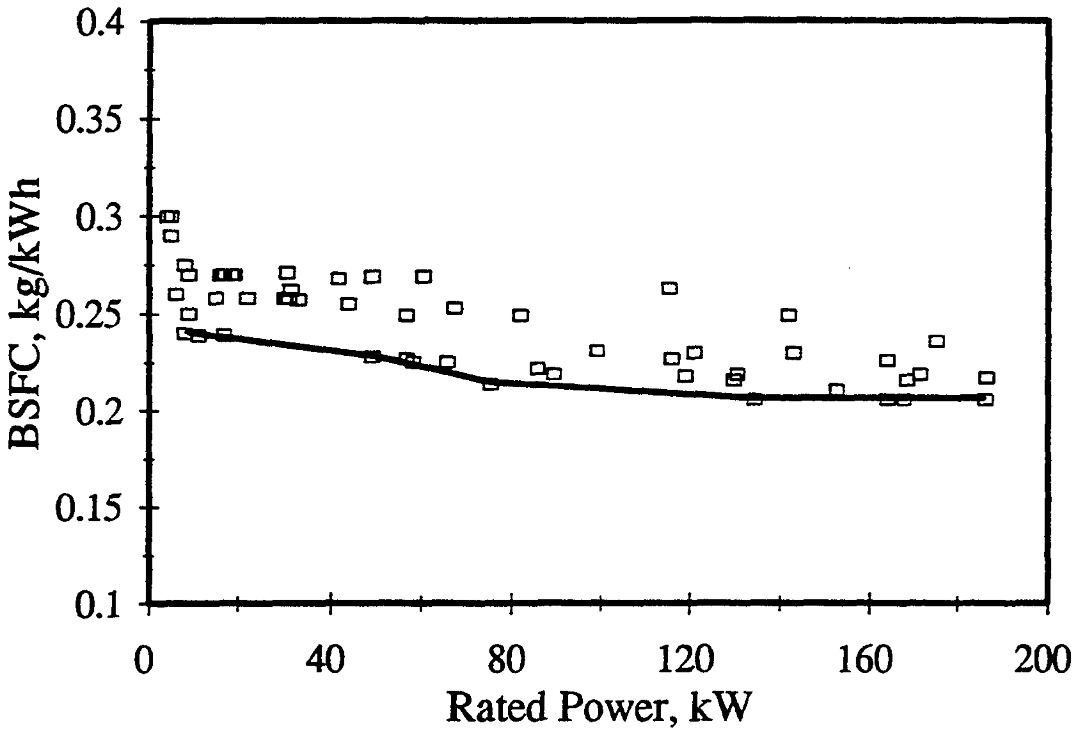

Figure 11. <u>Fuel consumption of four-stroke diesel engines</u>

to the automotive community. Particularly in Europe, the automotive DI diesel engine is making significant inroads. Audi produces perhaps the best engine in this class.(11) There is no fundamental reason why this technology cannot be applied to smaller output engines.

Emissions from diesel engines behave quite differently from those of spark ignition engines. The key emissions are particulates and NO_x. Substantial amounts of hydrocarbons can also be emitted, particularly during cold start. Aftertreatment for oxidation control of particulates and hydrocarbons is being introduced for many 1994 engines, but it is not as effective as aftertreatment for SI engines. Aftertreatment for NO_x is not yet feasible. Particulates are primarily produced when the engine undergoes hard transient load application or operates at high torque and low speed. NO_x primarily results from high load operation where the in-cylinder temperatures are highest. These engines offer the potential to be very low emitters when properly warmed up and when operated at constant speed and load outside the regions of high NO_x emissions; however, their power density at these conditions is not very good. The baseline emissions score assigned to diesel engines is 0.9.

The cost of current diesel engines is somewhat higher than that for SI engines as a result of more sophisticated fuel injection equipment and generally robust construction. However, higher technology SI engines are comparable in cost and may be more expensive and heavier if designed to equivalent reliability, which is excellent for diesel engines. Producibility is comparable to four-stroke SI engines. Transient response is slightly worse than that for SI engines because of larger reciprocating and rotating mass.

Cranking torque is an issue with diesel engines because of the high compression needed to attain the temperatures to sustain combustion. Smaller engines are more of a problem in this area because of torque fluctuations with fewer cylinders. Cold startability of smaller engines is also a concern because of higher relative heat transfer from the combustion chamber. This may become an issue with APUs in frequent start-stop operation. However, with appropriately designed power electronics and controls, the generator can also be used as a starter motor, providing high cranking torque to overcome these issues.

NVH problems are significant for diesel engines, primarily due to the high rate of pressure rise in the initial stages of combustion. Automotive diesel engines are typically associated with a "clatter" noise, the sound of diesel combustion. This noise can be regulated by injection rate control and by turbocharging, at significant increase in cost. Turbocharging may not be an option for a 30-kW engine.

Multifuel capability is less with diesel engines than with SI engines when considering light hydrocarbons. Diesel combustion will only work with fuels that contain significant quantities of long-chain hydrocarbons, which will initiate the combustion process by thermal decomposition to shorter molecules and free radicals. Organic fuels such as vegetable oils are potential alternatives, but natural gas, propane, hydrogen, or other alternatives cannot be used without significant changes to the combustion system.

D. Two-Stroke Spark-Ignited Engines

The top ranking in the analyses by Schneider and Burke for two-stroke SI engines was based on the status of research at that time, indicating great promise for automotive two-strokes with direct fuel injection. Eleven years later, these engines have not yet lived up to their predictions of rapid inroads into automotive application. The primary reasons for this slower-than-expected development are difficulties with durability and emissions. The durability issues are associated with lubrication of the piston-ring-cylinder wall interface, particularly where the rings are used to control ports in the cylinder walls for admission of air and exhaust of products. Durability of crankshaft parts is also an issue in those engines that utilize crankcase pumping as a means of supplying scavenging air and cannot use conventional pressure lubrication and plain bearings. Catalyst durability is a problem because of the presence of lubricating oil in the exhaust. The emissions issues are related to the fact that two-stroke engines inherently contain excess oxygen in the exhaust, which makes the application of three-way catalysts impossible. Unburned hydrocarbons and CO can be effectively treated with oxidation catalysts, but research has yet to perfect a lean catalyst for NO_x emissions. Nevertheless, research continues into automotive two-stroke engines, and reports from key developers such as Orbital Engine Company and Chrysler suggest that these problems are not insurmountable.

The key advantages of the two-stroke engine are small, lightweight construction (high power density, both volumetric and weight) and low cost associated with smaller parts count. The elimination of the overhead valvetrain is largely responsible for both of these advantages; yet some researchers are still applying overhead valves in their two-stroke engines to overcome the durability and exhaust oil contamination issues.(12-15)

The availability of specific engine data for automotive class two-stroke engines is poor because of the highly competitive environment; current developers are not anxious to release their data. Thermal efficiency gains attributed to lower friction are generally offset by losses associated with scavenging and pumping; thus, thermal efficiency of the two-stroke engines is comparable to that of four-stroke engines. Information obtained in an industry survey by SwRI in 1991 indicates that automotive class engines can achieve a specific weight of 0.9 kg/kW (16); this level is also

probably reasonable for APUs. Despite higher "weight overhead" associated with smaller size, these engines would also benefit from power density associated with higher speed. No data was obtained on specific volume, but a level of 0.7 times that for four-stroke SI engines is reasonable, accounting for the reduction in engine height associated with elimination of the overhead valves, and for the reduced size and weight of a generator running at higher speed.

Cost of piston-ported two-stroke engines is significantly lower than the poppet-valved engines because of the greater simplicity and lower parts count. The same argument holds for gains in producibility and reliability. Emissions are harder to control. The technical risk is higher because of the immaturity of this technology. NVH is probably about the same as with four-stroke engines. Mechanical noise may be lower without the valvetrain, but exhaust noise and bearing noise are increased for two-strokes with rolling-element bearings. Transient response should be better than for a four-stroke engine because of reduced overall inertia. Cranking torque fluctuations for a multicylinder engine should be lower because there is a compression stroke on each revolution.

E. Two-Stroke Compression Ignition Engines

Two-stroke diesel engines are in widespread use for high horsepower applications such as locomotives and ships. The scaling of two-stroke compression ignition technology to small, lightweight engines has been largely ignored due to lack of application. However, the military interest in small power plants for unmanned aerial vehicles (UAVs) that burn diesel or jet fuels has renewed the interest in small two-stroke diesels. SwRI has developed a design for a UAV engine that is of appropriate size and possesses the characteristics for the hybrid APU.(17) This design was demonstrated in limited testing, and further development is needed to take it to production-ready status. Key features of the engine are piston compressors driving scavenging air, allowing for cooling of the backside of the power pistons by oil jets; reed valve controlled transfer ports; and an IDI combustion system using low pressure injectors, unit injector pumps, and air cooling. The design targets are 30-hp (22-kW) output at 4,500 rpm, with BSFC of 0.25 kg/kW·h. Production weight was estimated at 35 lb (16 kg). Operating speed is somewhat lower than for SI combustion systems, resulting in greater generator size and weight. This engine

will be the benchmark for comparison. For greater reliability, some weight would be expected to be added to this engine design, such that estimated engine weight for a hybrid APU would be around 22 kg. Because of the high compression ratio requirements and the heat losses working against compression ignition, cranking torque and cold startability will be somewhat worse than with spark-ignited engines.

F. Wankel Rotary Engine

The Wankel rotary engine, invented by Felix Wankel in the mid-1960s, is certainly the most well-developed of rotary engine concepts, having been in production in automotive and aerospace applications since the early 1970s. The development status of this concept is such that the technical risks associated with its application are well known and have been dealt with in great detail. Its key advantage over state-of-the-art reciprocating engines is power density on both weight and volume basis; with direct injection, its fuel consumption can also be competitive.

The basic principle of operation of the Wankel engine is shown in Fig. 12 (reproduced from Reference 18). A three-cornered rotor is constrained to rotate about its center of gravity, which in turn orbits around the crankshaft centerline. The rotor turns at one-third the crankshaft speed, driven by a gear on the crankshaft meshing with a ring gear on the rotor. The three corners divide the trochoid-shaped rotor housing into three working chambers, each of which executes a full four-stroke cycle on each rotation of the rotor. Thus, the engine achieves one power stroke per revolution of the crankshaft. By counterbalancing the crankshaft, the system is completely dynamically balanced.

The limitations of the system arise from several sources. There is a large amount of surface area compared with the chamber volume; therefore, heat transfer rates are high, causing relatively higher heat rejection and associated inefficiency and component loads. Also, combustion quenching is high, resulting in more difficulty in controlling hydrocarbon and CO emissions from their source in a homogeneous charge. These problems have led most advanced engines to use stratified-charge combustion systems, confining the fuel-laden charge to a portion of the useful

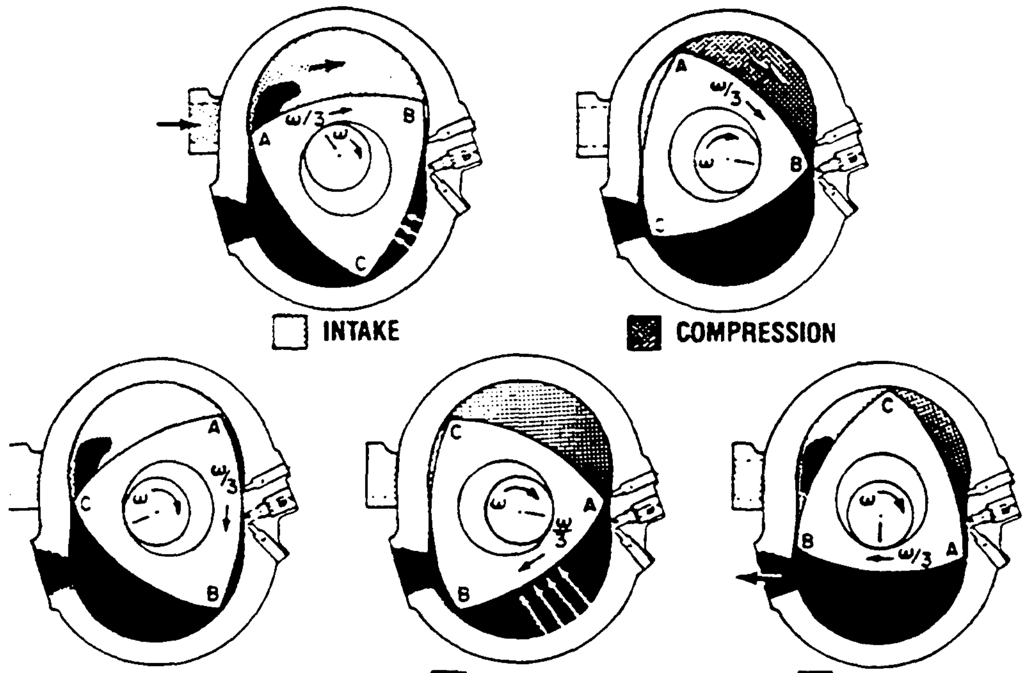

Figure 12. Basic operation of the Wankel rotary engine

volume, which reduces the power density. The high heat transfer rates cause cooling problems in the rotor, since a large portion of its surface is exposed to hot gases. Internal cooling by oil is the most common method of rotor cooling; air-cooled engines have great difficulty in this area. Sealing of the rotor apex and sides has been the focus of much development, and problems in these areas are generally solved; however, the large amount of rubbing contact, along with fairly high operating speeds, leads to higher friction in comparison with piston engines.

Despite these issues, the Wankel rotary engine has experienced some degree of success in research applications where high power density is a priority, and still retains interest among developers of lightweight aircraft, particularly unmanned aerial vehicles. Significant development activities continue for commercial and military applications at Mazda Motor Corporation (19, 20), John Deere Technologies International, Inc. (now Rotary Power International) (18, 21, 22), and AAI Corporation (23). Also, a single-rotor air-cooled engine of 38-hp output is manufactured for UAV and target drone applications by Alvis UAV Engines Ltd.(24) The available data regarding Wankel engine power density and fuel economy are shown in Figs. 13 through 15. From the limited data available, it is clear that these engines significantly challenge the power

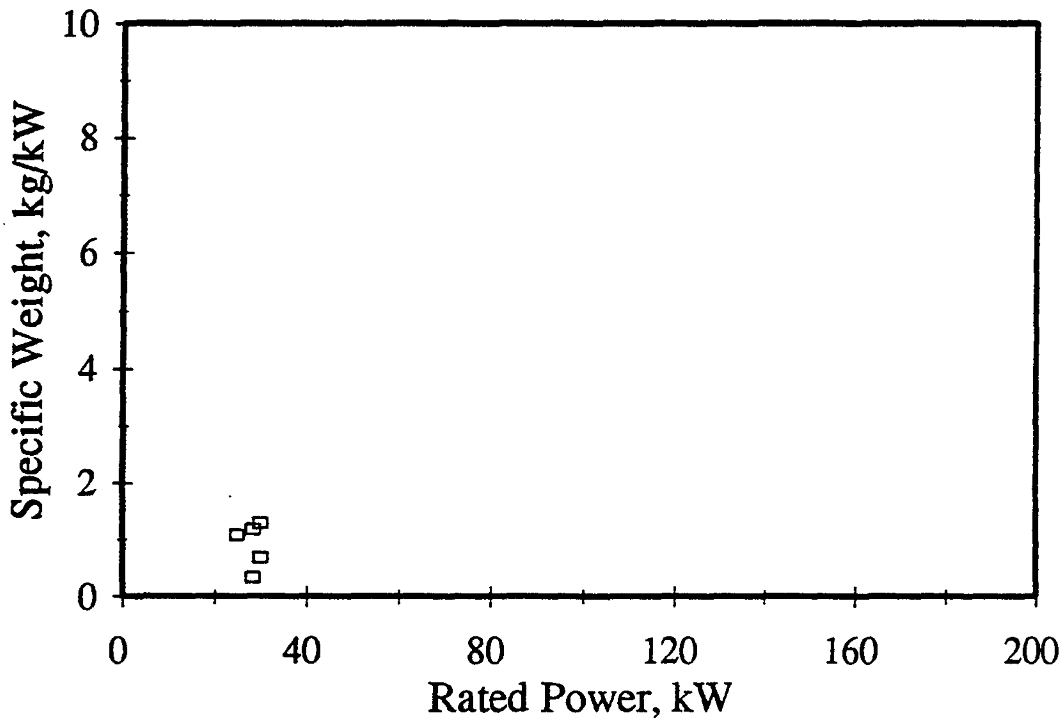

Figure 13. Specific weight of Wankel rotary engines

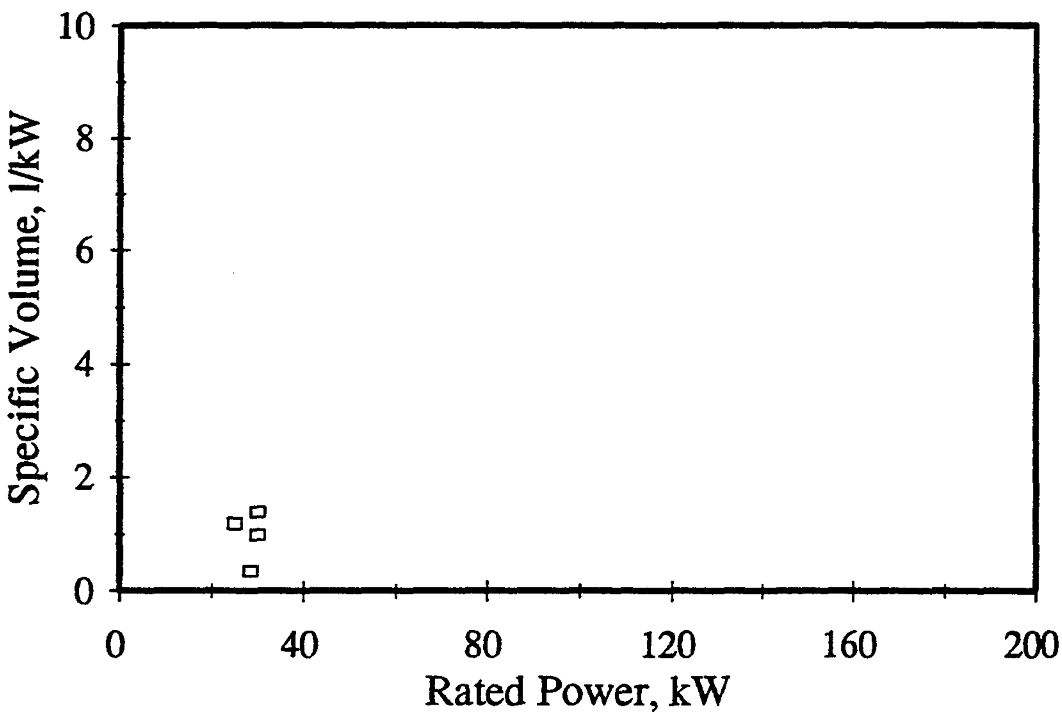

Figure 14. Specific volume of Wankel rotary engines

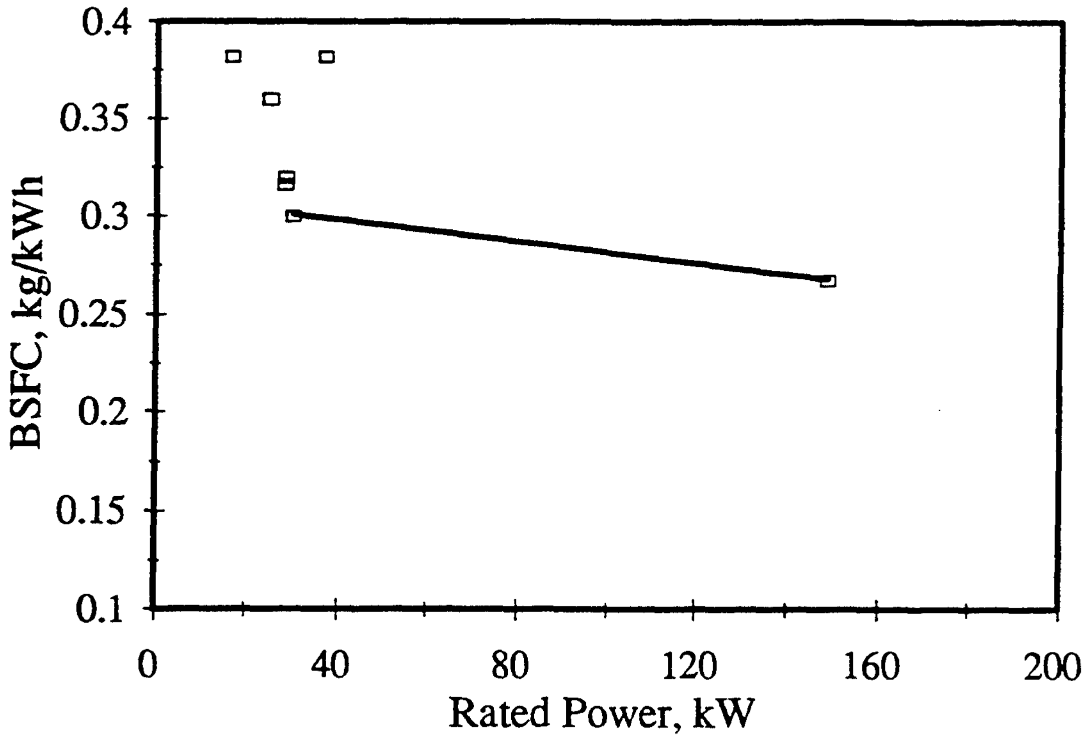

Figure 15. Fuel consumption of Wankel rotary engines

density of conventional reciprocating engines in the under 40-kW power class and can nearly compete with conventional technology in fuel consumption.

For an engine developed for the APU system, thermal efficiency could be expected to be 27 percent; coupled with the generator, overall efficiency would be 25 percent. Engine specific weight and volume of about 0.7 kg/kW and 0.6 L/kW, respectively, appear feasible. Operating speed could be at about 8,000 rpm, resulting in generator specific weight and volume of 1.18 kg/kW and 0.26 L/kW, respectively.

Cost of the Wankel engine should be close to that of conventional two-stroke engines due to the simplicity of the mechanism. Emissions may be more difficult to control. Producibility and reliability should be good. Since there is no reciprocating motion, the sliding surfaces never reverse their sliding motion, which is a prime cause of wear in reciprocating engines. Also, Wankel engines use total consumption lubrication, which means that fresh oil is continually supplied to the rubbing surfaces and cannot become degraded or diluted by mixing with fuel. The technical risks are well established but somewhat higher than for conventional four-stroke engines. Noise and vibration are well controlled by the balanced system. Multifuel capability

is questionable; however, rotary engines have run successfully on gasoline, heavy fuels, and gaseous fuels. Transient response should be equivalent to two-stroke engines. Cold startability should be good, with smooth and low cranking torque.

VI. ADVANCED CONCEPTS

The advanced concepts considered in this study are explored in the sections that follow. The concepts are classified either as "APU System Concepts," which involve a radical departure from conventional engine technology, and "Technology Concepts," which include ideas that can be integrated with otherwise conventional engine systems. The system concepts are scored and ranked along with the conventional technologies; technology concepts are scored and ranked separately.

A. APU System Concepts

1. Free-Piston Engine

The free-piston engine (FPE) is an idea that has been considered by many researchers since the early 1900s. The basis of the concept is a piston reciprocating in a cylinder without any kinematic constraint or mechanical connection, as illustrated in Fig. 16. Power is produced by a more or less conventional combustion system operating on a two-stroke cycle, firing once per engine cycle. The combustion system can be diesel, spark-ignited, or can consider some of the advanced concepts discussed later. The thermal energy is converted into kinetic energy in the piston and is then absorbed by one of several means and turned into useful work. As the kinetic energy is absorbed, the piston slows and reverses direction, returning to the combustion chamber for the next stroke. The reversal is aided by pressure building up in a chamber at the opposite end of the device from the combustion chamber, typically referred to as the "bounce" chamber. The precise means of controlling the piston motion without hitting either end of the cylinder is the subject of much research and has been successfully demonstrated in several cases.

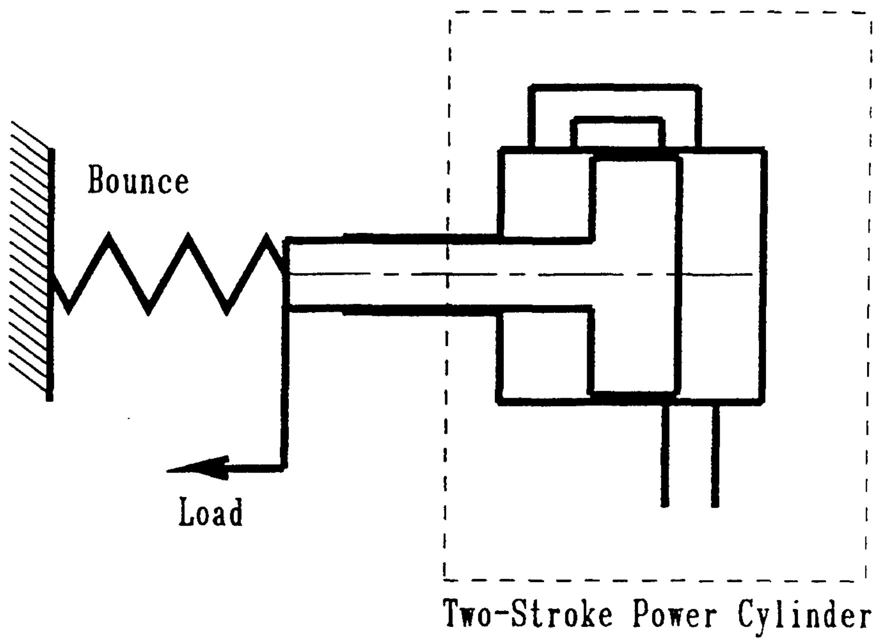

Figure 16. **Basic concept of free-piston engine**

The FPE has several peculiar characteristics that set it apart from conventional engines. It operates at theoretically higher mechanical efficiency due to the reduced friction from the fewer number of moving joints and mechanical parts. It operates over a very narrow reciprocating speed band because it is controlled by the natural frequency of the spring mass system, the mass being the piston and the spring being the effective gas spring of the compression and expansion events at either end of the piston. The speed can be controlled to a certain extent by modifying the compression ratio and the gas pressures. The compression ratio and piston stroke are variable and can be varied stroke-by-stroke. However, the stroke range is limited by the natural dynamics and cannot be controlled independently of operating conditions. Its transient response is very good, as it reaches its operating speed essentially instantaneously. One drawback is that because of the narrow speed band and the need to maintain appropriate compression ratios for the targeted combustion system, the ability to turn down from the rated condition is limited. The engine is ideally suited to fixed operating point cycles, as in the APU application.

The primary perceived advantages of the FPE over conventional technology are as follows:

- Thermal efficiency – Eliminating crankshaft friction should result in a thermal efficiency improvement of 3 to 5 percent;

- Cost and reliability – Fewer moving parts means less cost and more reliability;

- Mechanical integrity – Combustion pressures are not limited by structural considerations in the crank system;

- Transient response – Transient response is very good;

- Power density – The power density advantages, if any, are not as clear, as the engine cannot be run at high speed independently of the natural dynamics. High power density can be achieved by running at high boost levels, with higher natural frequency owing to the increased gas spring constant.

The earliest recorded work with the FPE concept was by the Marquis R. De Pescara, an Argentinean researcher working in France who patented the concept in the U.S. in 1928.(25) His patent covered a gas generator application, whereby the power from a diesel cylinder was absorbed by an air compressor which drove the scavenging air through the power cylinder into a gas turbine. All shaft power output was provided by the gas turbine. This concept was developed commercially by the Als-Thom Company into a 770-hp unit, and later by the SIGMA organization in France, resulting in the GS-34 engine rated at 1,200 hp. The GS-34 unit was installed on several ships and in stationary power plants and saw considerable service in the 1930s.

After WWII, sporadic development of free-piston gas generators was pursued by researchers in France and England.(26) General Motors (GM) Corporation and Ford Motor Corporation both pursued free-piston engines as a vehicle power source in the 1950s.(27-29) Both companies focused on the gasifier-turbine configuration, wherein the FPE produces no output work other than the high-pressure exhaust gas, which is routed to a turbine to produce shaft power. GM took the work as far as a vehicle demonstration. Their device was a siamesed pair of inward-

compressing diesel cylinders with stepped bores such that the compressor cylinders were of larger diameter than the engine cylinders. This is shown conceptually in Fig. 17.

Each pair of power pistons was synchronized by a mechanical linkage, but there was no linkage between the two siamesed units to maintain their phase relationship. Instead, pneumatic means were used to maintain their 180° out-of-phase operation, thereby permitting optimum utilization of the compression pulses from one unit to scavenge the other unit. This demonstrates that phase control of FPEs is feasible by other than mechanical means. The engine in fact started in parallel operation but achieved its proper phase relationship within a few strokes. Starting was by pneumatic means with an accumulator supply pressure of 206 kPa (30 psi).

For tractive power, the GM 4-4 Hyprex engine used a five-stage axial turbine, with a 7:1 gear reduction into a four-speed transmission. The peak turbine efficiency was approximately 70 percent. Fuel efficiency of the FPE was stated in terms of "gas hp-hr," being based on the exhaust stream pressure and temperature rather than shaft power output from the turbine. Demonstrated fuel consumption was 0.45 lb/gas hp-hr (0.274 kg/kW·h), which translates to a gas thermal efficiency of approximately 30 percent. This is much lower than might be hoped for from this device. With the turbine efficiency, the brake thermal efficiency to shaft output would be about 21 percent. The researchers predicted a developed fuel economy of 0.36 lb/gas hp-hr (0.219 kg/kW·h), which with a well-developed turbine of 80 percent efficiency would result in thermal efficiency of 30 percent, still much lower than current crankshaft engine technology. One reason for this less than stellar performance was pointed out by Mr. Samolewicz: the free-piston gasifier must move substantially more air than it utilizes in the combustion process.(26) Irreversible energy losses are associated with this air handling and pumping. The large volume of air consumption must also be accommodated by larger filters and ducting than would be required for a conventional engine of comparable power output, which is a space claim disadvantage.

Specific weight demonstrated in these experiments of the 1950s was near 3 lb/hp (1.8 kg/kW). Specific weight could be reduced by lighter materials and by increasing the cyclic speed, which

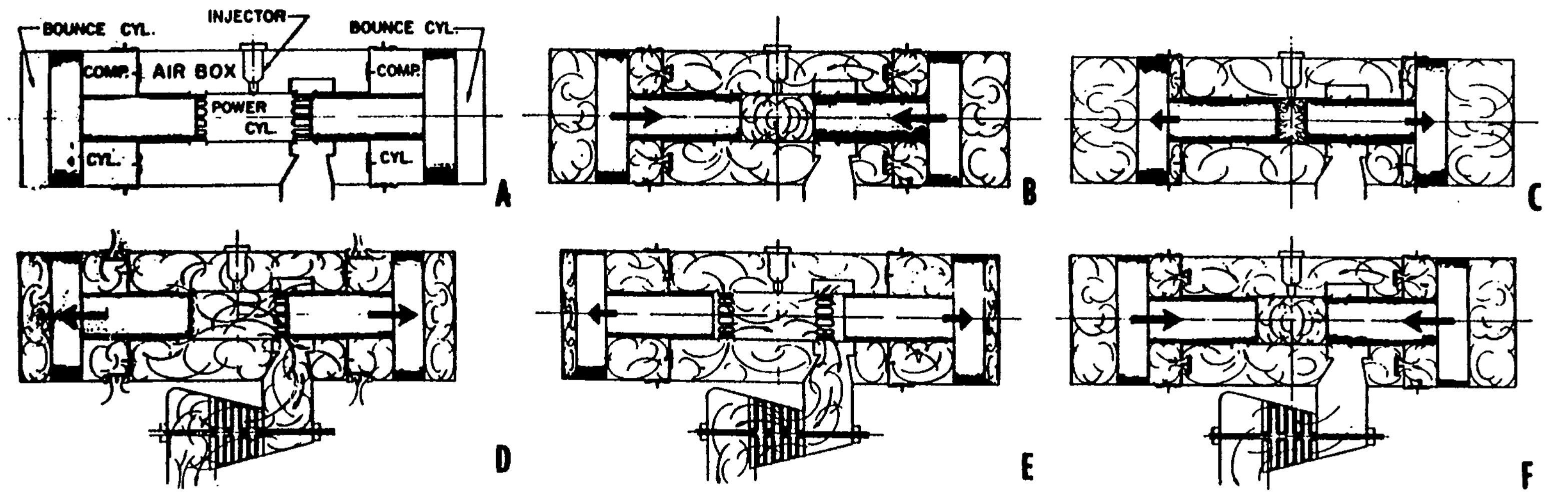

Figure 17. Operating principle of GMR 4-4 Hyprex free-piston gas generator

can be accomplished by greater boost, higher bounce pressures, and reduced reciprocating mass. All of these are development challenges.

In the mid-1960s, free-piston gasifier research was carried on in Canada by the Free-Piston Development Company and at the National Research Council of Canada.(26, 30) The unit developed was considerably smaller than those of previous research, at about 65 gas hp (48 kW), approaching appropriate size for hybrid APUs. Its weight and volume were 410 lb (186 kg) and 4.69 cu. ft. (133 L), respectively, without accessories. Without provision for a power turbine and alternator, but assuming a gas-to-electric conversion efficiency of 75 percent, the specific weight and volume work out to 5.1 kg/kW and 2.7 L/kW, respectively. Minimum specific fuel consumption was approximately 0.45 lb/gas hp-hr, consistent with that developed by the GM researchers. These numbers are not encouraging. The reciprocating speed was 2,015 cpm. Further development of the system for higher speed and lighter weight could presumably improve these numbers somewhat. Predictions by Wallace, et. al. (30) were that at high boost pressures and turbine pressure ratio of 5 to 1, the FPE gas generator-turbine combination could achieve overall brake thermal efficiency of 39.2 percent, still short of current diesel engines but competitive with spark-ignition engines. At the higher cycle pressures and temperatures, NO_x emissions may become an issue.

More recent development of FPEs has focused on their use as dedicated gas compressors and hydraulic pumps. As a hydraulic pump, the FPE could be used in hybrid vehicles in one of two ways: hydraulic motors could be used for traction or for driving an electric generator. Since this study focuses on the hybrid electric vehicle, the traction motor configuration will not be pursued here but is well worth considering in the overall view of high efficiency vehicles. Under certain conditions, hydraulic motors can have efficiencies on the order of 95 percent or better, well in excess of that of state-of-the-art turbine expanders; therefore, the FPE-hydraulic pump/motor/generator combination is an attractive alternative to the FPE gas generator.

Research in Japan by Dr. A. Hibi of Toyohashi University has demonstrated several aspects of the FPE hydraulic pump.(31, 32) Their solution to the problem of poor turndown is to intermittently cycle the engine, with a dead period between cycles. In demonstration testing, the

reported overall thermal efficiency of their device is poor at 14.3 percent; however, they demonstrated good conversion of indicated gas power to hydraulic power at an efficiency of 84 percent, including losses to drive a scavenging pump. The poor thermal efficiency can be attributed to the use of a motorcycle-type carbureted two-stroke cycle, with inherent losses of unburned fuel-air mixture during scavenging. In a later publication, Dr. Hibi suggested an attainable overall thermal efficiency of 41 percent; however, his assumption of 50 percent indicated thermal efficiency for the combustion process is optimistic.(33)

The FPE hydraulic pump, with a spark-ignited combustion system, was studied analytically by P.C. Baruah.(34) A fairly comprehensive first-principles thermodynamic simulation was used, including the effects of flame speed on combustion rates. However, the analysis omitted the gas exchange effects, which may be significant. In comparison with a conventional crank engine, this study pointed out one reason why the thermal efficiency of the FPE may not reach its full perceived potential. The reversal of the piston at top dead center is controlled entirely by the dynamics of the spring mass system. Upon commencement of combustion, the piston undergoes rapid acceleration toward the load end of the engine and achieves substantially higher velocities during the expansion stroke. The timing of combustion is less flexible than with conventional engines and must take into consideration the need to appropriately control compression ratio. As a consequence, the combustion process tends to occur over a greater proportion of the expansion stroke, in terms of volume, not time. Thus, the thermal energy of combustion is used less effectively. To overcome this problem, FPEs would have to achieve higher rates of combustion. One advantage of later combustion, as pointed out by Mr. Baruah, is lower NO_x emissions.

In gas compressor applications, FPE research has been carried out recently by AiResearch Los Angeles Division of Allied Signal Aerospace Company (35) and by Tectonics, Inc. (36). The AiResearch work focused on a compressed air supply for Army tanks and developed an FPE design similar in concept to those developed by GM and Ford. Since clean, compressed air was the desired output, an outward-compressing arrangement was used, with two opposed pistons and a diesel combustion system, as shown in Fig. 18. This arrangement allowed the use of the larger

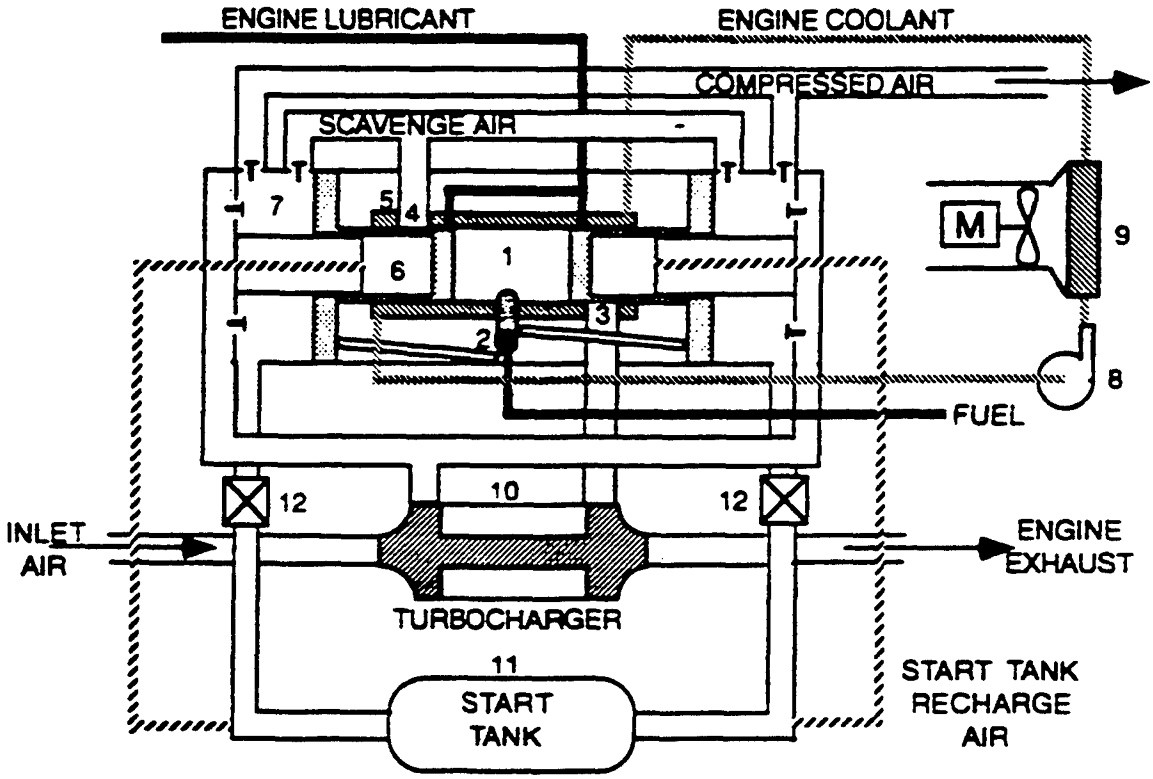

1. Diesel cylinder
2. Fuel injector and synchronizing mechanism
3. Diesel cylinder exhaust port
4. Diesel cylinder scavenge port
5. Diesel cylinder cooling jacket
6. Bounce cylinder
7. Compressor cylinder with reed valves
8. Coolant pump
9. Coolant radiator and cooling air fan
10. Turbocharger
11. Start tank
12. Start valves

Figure 18. Conceptual design of AiResearch Mark II free-piston compressor

bore to supply air both for scavenging and for the output. The best obtained indicated specific fuel consumption of this unit was 0.388 lb/hp-hr (0.236 kg/kW·h), based on the power cylinder indicator diagram. However, based on the compressed air output, specific fuel consumption was 0.621 lb/hp-hr (0.378 kg/kW·h), representing thermal efficiency of approximately 22 percent. About half the difference between "indicated" and "brake" output can be attributed to mechanical friction and half to the portion of the compressed airstream diverted to scavenge the engine. Some of this pumping loss could presumably be averted by rearranging the valving and porting such that the scavenging air is diverted at the desired pressure, not first pumped to the compressor output pressure. Thermal efficiency of 25 to 28 percent might be attainable by using this arrangement.

Tectonics, Inc. was engaged in the development of FPEs for dedicated air and gas compressors before the company dissolved in 1993. SwRI was contracted with Tectonics for the design and development of their FPE compressors. The units designed by Tectonics were targeted for stationary applications and were not designed for compactness or weight. A single, conventionally scavenged two-stroke SI natural gas engine cylinder was used for the power unit, driving a conventional single- or multistage compressor cylinder with a rack-and-pinion-driven counterweight for balance. In tests at SwRI laboratories, these units achieved about 23 to 24 percent gas thermal efficiency. Inefficiencies were attributed to incomplete combustion, scavenging losses, heat transfer, and friction primarily in the ringpacks, which were not optimally designed.

The key to achieving high power density in FPEs is high cyclic speed. It has been reported that Mr. Frank Stelzer of Germany has designed a free-piston engine capable of cyclic speeds on the order of 30,000 cpm.(37, 38) This is achieved by employing two opposed combustion chambers driving both sides of the piston, such that the bounce pressure is the combustion pressure. The claim of 30,000 cpm seems doubtful, but it is likely that cyclic speeds could be boosted substantially by this approach. The limit to reciprocating speed will most likely be ring wear.

There are several possibilities for applying FPE technology to a hybrid APU. These are discussed as separate engine concepts.

a. Free-Piston Engine With Linear Generator (FPELG)

An approach to power production is to provide a linear electric generator at the "bounce" end of the cylinder. The concept is shown schematically in Fig. 19. This generator will convert the kinetic energy of the piston directly to electric current, slowing the piston motion in the process. SwRI, in partnership with The University of Texas Center for Electromechanics (UTCEM) and sponsored by ARPA, has investigated the possible design configurations for a linear alternator and developed a design concept that integrates nicely with the FPE and has high predicted efficiencies.(39) The elements of the generator include an iron core with an air gap, an excitation coil, a generator coil, and the lower edge of the piston skirt. Magnetic flux is induced in the iron core by the excitation coil. As the piston skirt passes through the air gap, it alters the shape of the magnetic field, inducing current in the generator coil. This concept is mechanically simple in that the only moving part is the piston itself, and there is no requirement for electrical contact to the piston. For this reason, mechanical losses should be extremely low. The nature of the device is such that current is only generated during the expansion stroke of the cycle, and the power generation during expansion also exerts a restoring force on the piston, helping to slow its travel toward the bottom end. Gas bounce is necessary to achieve the next compression stroke. A test is currently underway at SwRI to demonstrate the highest risk element of this concept, the generator.

Preliminary design of the SwRI-UTCEM FPELG focused on a demonstrator unit of approximately 6-in. bore and stroke, based on the Tectonics engine unit. Design calculations indicated that this concept could achieve a peak thermal efficiency of approximately 30 percent, including generator losses. The demonstrator unit was not packaged for minimum weight; however, power-to-weight ratios of about 2.5 kg/kW are probably achievable. The demonstrator represents a specific volume of about 2.8 L/kW, and with development, the level of 1.8 L/kW is probably achievable, including power electronics.

Cost, reliability, and producibility should be much better than with conventional engine-generator configurations because of the tight integration of the system and the single moving part.

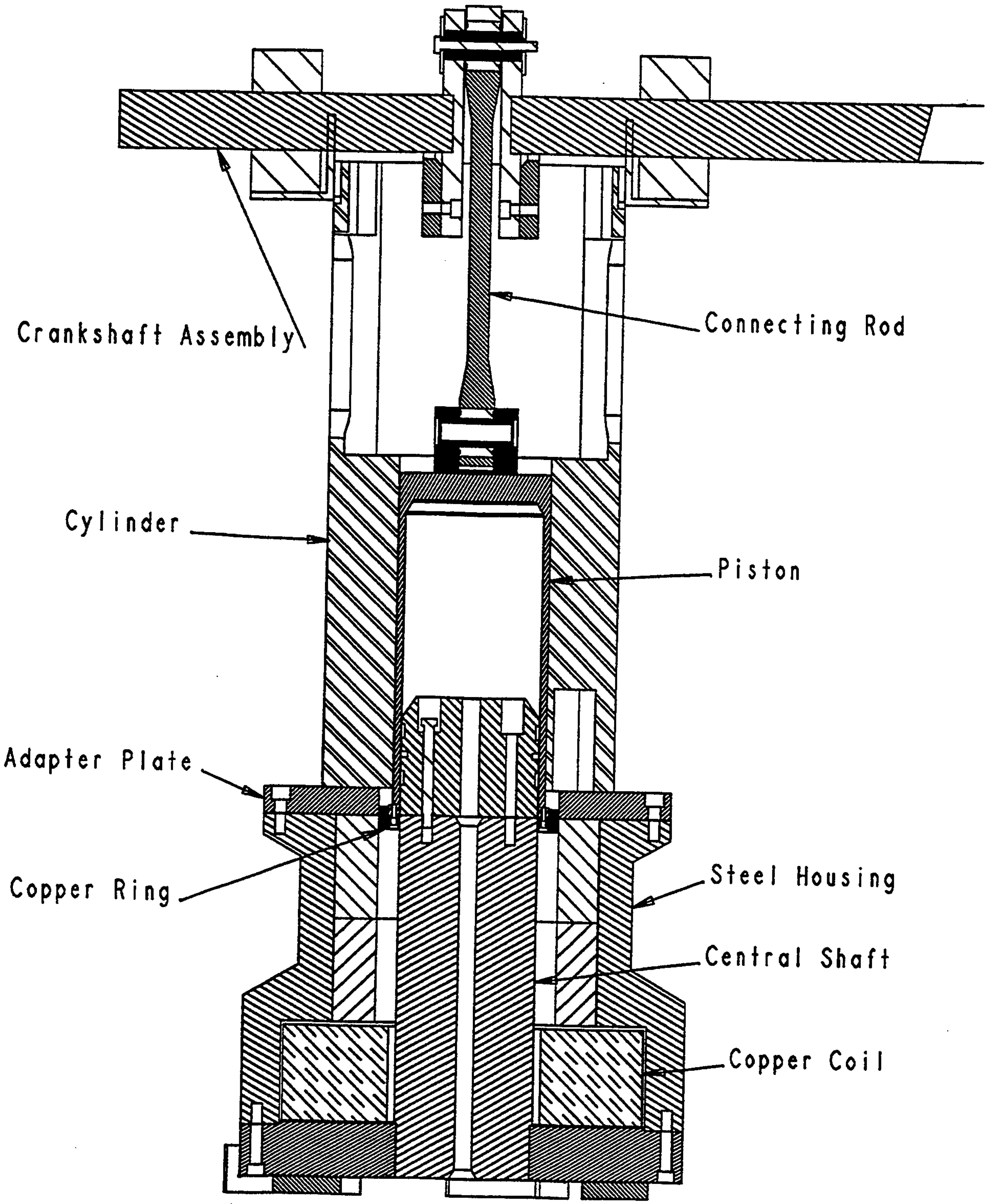

Figure 19. <u>**Linear generator for free-piston engine in rig testing configuration**</u>

Emissions issues are the same as with conventional two-stroke engines. There is great technical risk associated with this technology, as the generator concept is unproven and the integration of the engine with the generator presents challenges. Using two opposed units, there are no unbalanced reactions, so NVH should be better than with conventional engines; however, exhaust and intake pulsations will have to be dealt with. Multifuel capability is a bonus for the FPE, since its compression ratio can be adjusted to suit the fuel used. Transient response is excellent, as the engine reaches its operating speed instantaneously. This is also reflected in startability; for a properly designed system, starting is accomplished with a single impulse from either the electromagnetic system of the generator or a compressed air bottle attached to the bounce chamber.

b. Free-Piston Gas Generator With Turboalternator

Another option for using the FPE technology is to update the technology of the 1950s and 1960s by routing the exhaust gas to a turboalternator. The FPE technology for gas generators is fairly well developed, if somewhat obsolete. Updates of this technology could be expected to achieve overall specific fuel consumption of 0.48 kg/kW·h, including 0.35 kg/gas kW·h for the gas generator, turbine efficiency of 80 percent, and generator efficiency of 92 percent. This translates to a thermal efficiency of roughly 17 percent. Gains would be made in specific power and weight owing to the high speed generator. Gas generator specific volume could be around 2.0 L/kW and specific weight about 1.5 kg/kW, if developed specifically for these criteria.

Cost of the turboalternator may be somewhat higher than the cost of the linear generator plus power electronics required in the previous concept; in addition, the FPE is somewhat larger and more expensive because a stepped bore and valving are needed for the compressor cylinder. Emissions again are equivalent to the two-stroke engine. Producibility is probably equivalent to the conventional four-stroke engine, gains of the FPE compensated by complexity of the turboalternator. Reliability should be somewhat better than conventional engines, as there are fewer moving parts, and the turbine does not see high exhaust temperatures. The technical risk is relatively low, as each component has been fairly well developed. With a balanced FPE, the noise and vibration characteristics should be even better than the FPELG because the turbine will

serve to muffle exhaust noise. Multifuel capability is the equivalent of the FPELG. Transient response is not as good as with the FPELG, or even with conventional engines, because of the lag of the turboalternator. However, startability is as good, relying upon a compressed air supply. The compressed air can come from a bottle and can be stored during system operation.

2. Rotating Combustion Chamber Engine

In 1993, SwRI contracted with Mr. Ross Riney to evaluate his concept of a rotary engine.(40) The essence of the concept includes separate compression and expansion rotors on a common crankshaft, with a combustion chamber attached to a third rotor on a shaft rotating at one-half crank speed at right angles to the crankshaft. This is illustrated in Fig. 20. Floating vanes riding on the rotors divide the compression and expansion housings into two chambers, allowing for intake and compression processes to occur simultaneously in the compression rotor, and expansion and exhaust processes to occur simultaneously in the expansion rotor. The air charge

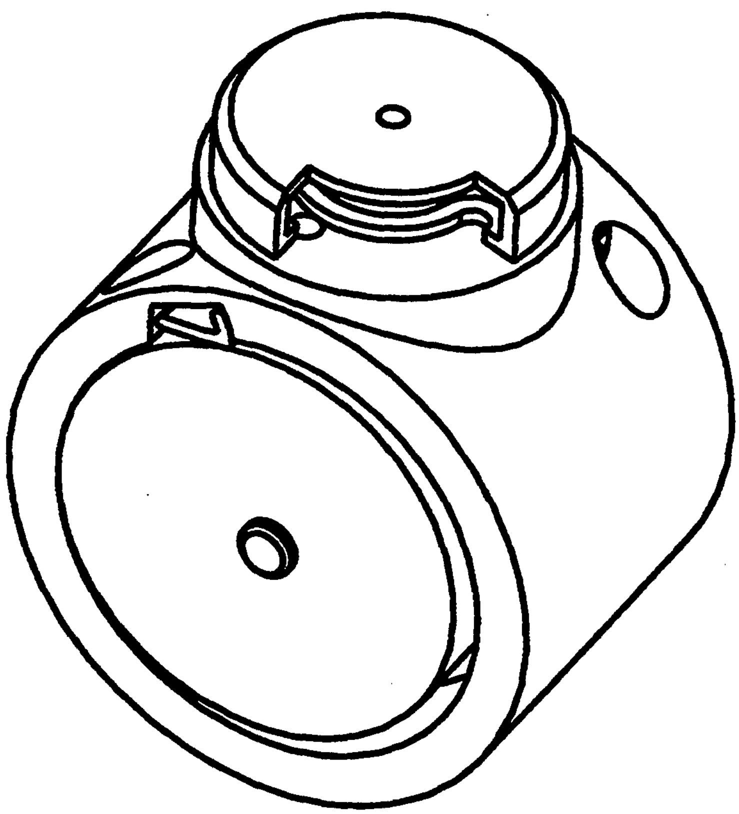

Figure 20. Rotating combustion chamber engine

is transferred from the compression stroke to the combustion chamber and subsequently to the expansion chamber through ports that are timed by the rotating combustion chamber, which also serves as a rotary valve.

The study done by SwRI utilized thermodynamic cycle simulation to examine the invention and determine its potential as an alternative power plant. The study found that its significant advantages were as follows:

- Separate compression and expansion rotors allow the expansion ratio to be substantially higher than the compression ratio, permitting more complete utilization of the heat energy.

- Port timings can be arbitrarily established to optimize the gas exchange processes.

- Constant or near-constant volume combustion can be achieved by port timing.

- The duration at constant volume can be tailored to the combustion process.

- Perfect balance assures that the engine can operate at high speed.

- The engine achieves a power stroke on every revolution while retaining the benefits of a four-stroke cycle.

While these benefits are important, there are also some significant technical risks:

- The sealing challenge is more significant than for the Wankel engine because of a large number of sealing surfaces.

- The seal between the rotor and housing depends upon close tolerances and cannot permit a floating seal member because of the need to pass under a floating vane.

- The separate expansion rotor will be highly thermally loaded.
- The dynamics of the floating vanes may limit speed.
- The gas exchange process also limits the speed at which good efficiency can be maintained.

The SwRI study only investigated the thermodynamic cycle and did not address sealing, lubrication, or cooling issues, which are the significant technical challenges. While the study predicted power density to be substantially higher than for conventional automotive engines, the thermal efficiency was predicted to be lower, owing primarily to large amounts of heat transfer due to large surface area. This concept is attractive because of its potential for high power density at high shaft speed; however, it is also extremely high risk at its current conceptual stage. Working prototypes have not been built.

Based on the estimates of SwRI's study, the engine would have specific volume of about 1.5 L/kW and specific weight of about 1.2 kg/kW. At a rated speed of 10,000 rpm, the corresponding generator would have specific volume at roughly 0.22 L/kW and weight of about 0.8 kg/kW. Thermal efficiency of around 19 percent was predicted for the engine, for an overall system efficiency of 17.5 percent. Cost of the engine may be fairly high because of high-temperature materials requirements. Emissions should be equivalent to the four-stroke engines. Producibility and reliability would be questionable due to expensive materials and hot environment of the combustion chamber and expansion rotor. This concept has very high technical risk. NVH should be well controlled due to good balance. Multifuel capability is equivalent to SI engines, and transient response should be fairly good due to low inertia. Starting may be difficult because of the high leakages around the large sealing surfaces and resulting poor compression at low speed.

3. HCCI Engine With Pressure Relief

Homogeneous Charge Compression Ignition (HCCI) is an unconventional combustion process wherein a premixed charge of fuel and air is ignited by compressing it to the point of autoignition. It is similar in many respects to detonation or knock, the uncontrolled combustion that can damage or destroy SI engines. However, it differs in that an engine designed for HCCI does not necessarily initiate combustion by a spark and does not experience the travel of a flame through the mixture, compressing the unburned charge to the point of detonation. Nor is HCCI generally initiated at hot surfaces of the combustion chamber, as is knock. Rather, the ignition is initiated at a multitude of points within the combustion chamber volume by the presence of active radicals, or combustion precursors. Combustion progresses rapidly and consumes the entire mixture within a short period of time. The intense combustion process has discouraged most researchers from pursuing HCCI as a feasible commercial process; however, if a means of dealing with the extreme rates of pressure rise can be devised, there are many benefits to be gained from HCCI.

Evan Guy Enterprises, Inc., of San Antonio, Texas, has demonstrated a small two-cylinder engine with several unique features devised to take advantage of HCCI for the combustion of heavy distillate fuel. The engine is targeted at the UAV application and operates on a two-stroke cycle. The key feature of the engine is a proprietary cylinder head device designed to soften the combustion process by limiting the peak pressure. Energy is stored mechanically during the combustion process and returned to the cylinder during the expansion stroke for useful work. The engine has been successfully demonstrated burning several fuels, including diesel, JP-8, and gasoline. Its efficiency is relatively high as a result of high effective compression ratio and an effective combustion process, which works well with lean mixtures. Durability problems encountered in early designs have largely been solved.

Based on the limited test data obtained to date, the developed engine has predicted fuel consumption of 0.3 kg/kW·h, for a brake thermal efficiency of 0.275. Its operating speed is relatively high at 6,000 rpm, which will lead to compact generator configuration. The expected specific weight and volume of a developed engine are 1.1 kg/kW and 2.1 L/kW, respectively.

The cost should be advantaged relative to conventional four-stroke engines. In its current configuration, the engine admits a premixed fuel-air charge, so it is subject to emissions problems due to scavenging losses. However, direct injection is an ultimate goal, so emissions should be better than for direct-injected SI two-strokes owing to the clean combustion process. A particular emissions benefit results if the HCCI process can be used to take advantage of the low NO_x possible with extremely lean mixtures, a strong possibility with this engine. Producibility should be good, but obtaining automotive class reliability will require significant development. Noise characteristics should be comparable to competing two-stroke engines. The multifuel capability is very good with volatile fuels but dependent upon preheating of the fuel when running with diesel or other heavy fuels. Transient response is good; however, because of the required fuel preheating, startability is not as good. This should be considered a high risk option since the technology is in early development stages.

4. High-Speed Detonation Engine

It has been observed in the racing industry that engines running at very high crankshaft speed (13,000 to 15,000 rpm) are relatively insensitive to fuel octane rating. Despite high compression ratios, they do not suffer from knock problems, and they are not adversely affected by fuels of octane ratings that would be intolerable in engines of similar compression ratio at conventional speeds. The explanation is that at these high speeds, the expansion process is so fast that the gas is expanded before significant pressure excursions can occur. The combustion process is largely a detonation process, similar to HCCI, but no component damage is encountered because of the rapid expansion. Since high speed is also desired for the generator of an APU, this approach to the engine and combustion system may be of interest for the APU system.

The chief advantage of the high-speed detonation engine (HSDE) over conventional technology is high power density owing to high crankshaft speed. The disadvantages are several, including durability, thermal efficiency due to high friction, noise, and risk. Scores for the high-speed detonation engine are based on a three-cylinder engine of 60-mm bore and 50-mm stroke, for a total displacement of 0.43 L, running at 13,000 rpm. Cycle simulation predictions with this engine indicate that it could produce 30 kW·h assuming a generator efficiency of 92 percent.

Predicted thermal efficiency of the engine was 24.6 percent, lower than conventional four-stroke engines primarily because of friction and pumping losses at high speed. With generator, a thermal efficiency of 22.6 percent is predicted. The engine could be packaged with a specific volume of about 1.75 L/kW and specific weight of 0.7 kg/kW, assuming weight scales with volume from conventional engines.

Cost of the HSDE should be comparable or slightly higher than a conventional four-stroke engine. Emissions should also be comparable or slightly worse, as alteration of valve events to achieve good volumetric efficiency at high speed may cause increased hydrocarbon emissions. Producibility will be similar, but reliability will be markedly worse. This is a high risk option, since the technologies are currently only used in racing engines that do not have to meet cost and durability constraints. Noise would be worse than with conventional technology. The multifuel capability would be slightly better than with conventional SI engines, since the octane requirements would be reduced. Transient response should be fairly good, although it may take the engine longer to reach the high speeds at which it is designed to operate. Startability will be limited by high compression ratios, requiring relatively high cranking torque.

5. Model Airplane Engine

Another type of engine which utilizes a homogeneous compression-ignition type combustion system are the small engines used for model airplanes. These engines typically run at very high rpm enabled by small displacement, short stroke, and low reciprocating mass, and use either alcohol fuel or diesel fuel heavily doped with additives to control knock and assure stable combustion. They are attractive from the standpoint of high power-to-weight ratio and high shaft speed, but currently only exist in small power ratings, generally of 10 kW and below. Two possibilities exist to use this technology for hybrid APUs: 1) develop a multicylinder engine with enough cylinders to make 30 kW (roughly 12 to 15 cylinders would be needed), or 2) develop a smaller APU and equip the vehicle with several model airplane engines to achieve the desired power rating. The second option is intriguing because the individual package volume would be small and several units could conceivably be distributed to various locations in the vehicle that would otherwise be unutilized. It is also of interest because of a general need for small,

lightweight motor-generator units for applications other than hybrid vehicles, particularly for military use. Hence, the scoring of this concept for the hybrid vehicle will be based on the second option.

The key to success of these engines for hybrid APUs will be the development of a combustion system that burns conventional fuels and that is nonpolluting. The model airplane engine is typically a carbureted two-stroke, and thus unacceptable for vehicle emissions. Direct fuel injection is difficult to accomplish in the scale required for the small cylinders; therefore, the most likely option is a four-stroke engine. There are many model airplane four-stroke engines currently in production, so the technology already exists, but the power density will suffer somewhat in comparison with the two-strokes. To achieve conventional fuel compatibility, a spark-ignited combustion system is the likely candidate, with gasoline or natural gas fuel. HCCI might also be contemplated, at significant added risk.

Estimates for scoring are developed primarily from advertising information of model airplane engine manufacturers. An engine power-to-weight ratio of 0.6 is probably achievable, along with specific volume of 1 L/kW. Fuel consumption is likely to be significantly worse than for automotive technology engines, as these engines typically use a rich fuel-air mixture; however, an engine designed for the hybrid APU application could improve greatly upon the current fuel consumption of this class of engine. BSFC is estimated at 0.35 kg/kW·h, resulting in thermal efficiency of 24 percent. Assuming the engine turns at 10,000 rpm, the generator specific volume and weight are estimated to be 0.22 L/kW and 0.86 kg/kW, respectively. Cost should be low in mass production. Emissions are questionable and would require significant development work. Producibility is good, but reliability would also require significant development, as model aircraft engines are not currently designed for long life. This is a high risk option due to the immaturity of the technology for this application. Noise is a significant issue for high rpm engines but can be dealt with primarily by mufflers. Multifuel capability would be equivalent to conventional SI engines. Transient response would be better because of low inertia, and cranking torque should be low.

6. Two-Stroke Gas Generator With Turboalternator

As an option to the FPE gas generator driving a turboalternator, a fairly conventional two-stroke engine could also serve as the gas generator. In this system configuration, the two-stroke engine would provide shaft power to a compressor, which may be a rotating or reciprocating machine. The compressor would boost the scavenging air for the two-stroke cycle to an elevated pressure, where it would then pass through the engine. The exhaust of the engine would be routed to the turboalternator. This concept is shown schematically in Fig. 21.

A cursory analysis of this concept was done using a cycle simulation program for externally scavenged two-stroke engines, backpressuring the engine with an orifice restriction to represent the turbine. Turbine power was calculated based on the developed pressure and temperature in the exhaust manifold, assuming 80 percent efficiency. The engine was driving a compressor at 77 percent efficiency. This analysis determined that the appropriate flowrates for a 30-kW

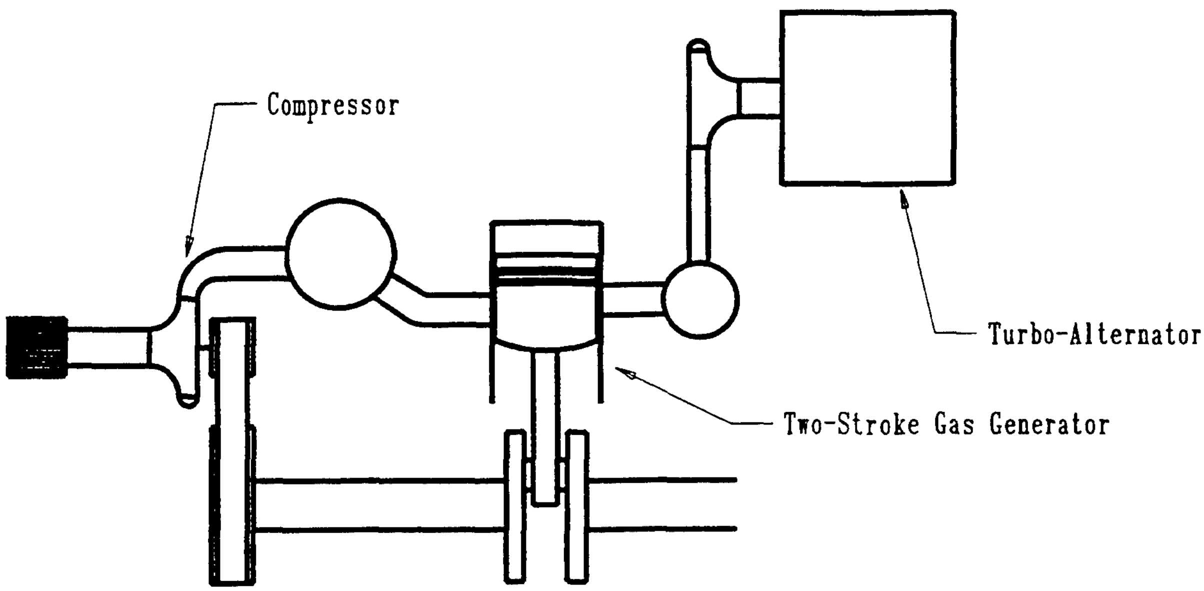

Figure 21. Conceptual design of two-stroke gas generator/turboalternator

generator could be achieved with a three-cylinder engine of about 0.8-L total displacement. Thermal efficiency of the complete cycle was predicted to be 22 percent. This engine would have a specific weight of around 1.2 kg/kW and specific volume of about 2.6 L/kW. Its scores for specific weight and volume are not as good as for the conventional SI two-stroke engine because to achieve the proper balance of airflow and pressure rise for the turboalternator, a lean-burn engine condition was assumed. Also, the engine deals with a proportionally larger volumetric flow of air than an equivalent sized conventional engine, so there is a penalty for the air handling ducts and filters. It would benefit from the generator size and weight advantages of high speed.

Cost for this system would be about the equivalent of a conventional four-stroke engine/generator; cost advantages of the simple two-stroke engine would be offset by the added cost of high speed turbomachinery. Emissions should be good, as a lean-burn combustion system will lead to low NO_x emissions. Producibility should be comparable with conventional two-stroke engines, and reliability should be good, as the turbine inlet temperature is very low. There is some technical risk associated with the development of an engine tailored to this application, but the technologies are all fairly well developed. Noise should be better than with conventional engines because of the noise suppression effects of the turbine. Multifuel capability is equivalent to conventional engines. Transient response is somewhat worse than conventional engines because of the turbine inertia. In starting, the ease of cranking the two-stroke engine may be offset by the reliance upon the compressor for scavenging air.

7. Regenerative Internal Combustion Engine

SwRI maintains an interest in more advanced engine concepts, and has performed studies on a number of concepts related to Stirling cycle engines. The promise of these ideas is increased thermal efficiency and reduced emissions; however, they have always been associated with high weight, volume, and cost penalties, as well as technical risk, and have not yet become viable commercial products. One such concept was investigated in an internal research project in 1987 and has since been refined.(42) It has now been named the Regenerative Internal Combustion Engine (RICE). A thermodynamic analysis of the engine cycle predicted an indicated thermal

efficiency of 44 percent. Indicated power of 84 kW was predicted from a single-working cylinder engine of 0.8-L displacement. The analysis was based on no-loss flow conditions and idealized timing of valve events; more realistic estimates would reduce the efficiency and power output somewhat.

The RICE concept is illustrated in Fig. 22. Two cylinders are employed, one serving as the compressor and one as the expander. A transfer valve controls flow out of the compressor and into a regenerator volume, into which a matrix of heat absorbing material is placed. The purpose of the regenerator is to recover thermal energy from the burned products after the expansion event, transferring this energy to the compressed gas from the compressor prior to combustion. Thus, a portion of the heat energy supplied to the gas before expansion comes from the previous burned charge, reducing the amount of thermal input needed from combustion. Upon completion of the expansion event, the burned charge is pumped back through the regenerator and out the exhaust valve.

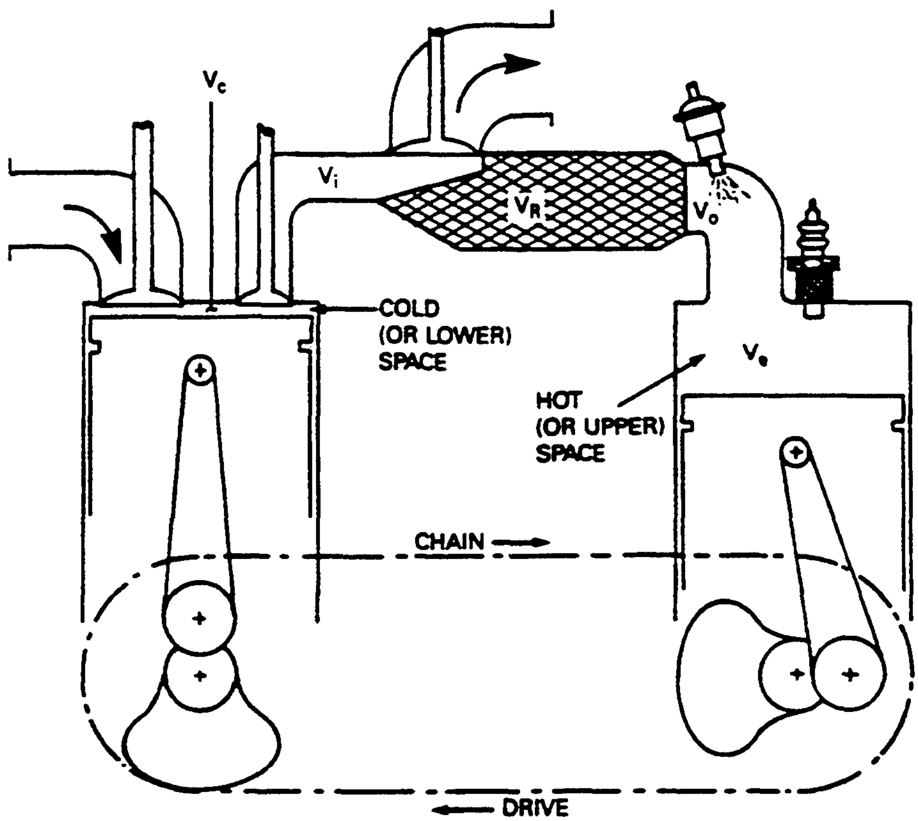

Figure 22. <u>Conceptual design of regenerative internal combustion engine</u>

Accounting for realism in fluid flow losses, valve events, and dead volumes, as well as mechanical friction, the brake thermal efficiency of this device may be as high as 33 percent. An APU utilizing this concept would then have brake thermal efficiency of 30.4 percent. It is difficult to predict weight and volume from a conceptual design, but it could be expected to be heavier and bulkier than conventional engines for a given working displacement. The first analysis, however, predicted a very high power density based on displacement. Accounting for the realistic inefficiencies, the displacement of the working cylinder needed for a 30-kW power plant is about 0.41 L, and the engine could be well represented by a two-cylinder engine of 0.82 L total displacement. This engine may be expected to have a weight of 50 kg and volume of 82 L, giving specific weight and volume of 1.7 kg/kW and 2.7 L/kW, respectively. The generator weight and volume would be the equivalent of conventional systems.

Cost will be relatively high, owing primarily to the regenerator, which will require high temperature materials. Some development of the fuel injection and combustion system will be needed to assure low emissions, and NO_x emissions may be a problem due to preheating of the air or air/fuel mixture. Producibility and reliability may be slightly worse than for conventional engines, owing again to the regenerator. This is a relatively high technical risk approach. NVH is probably better than for conventional engines, as the regenerator will serve to reduce exhaust pulsation. Multifuel capability is unclear, as the combustion system is as yet unspecified, but is probably better than conventional spark-ignited engines since the charge is preheated. The transient response characteristics will be worse than for conventional engines, and starting will be slow with the need to warm up the regenerator.

B. Subsystem Concepts

For the purpose of ranking the subsystem concepts, they are considered as applied to the baseline engine, the four-stroke spark-ignited engine. Thus, they can be compared on an equivalent basis. The scores are expressed as increments to the baseline. Most of the ideas are applicable to several of the system concepts.

1. Electric Valves

A limitation to the speed and performance of conventional poppet-valved four-stroke engines is the valvetrain, both in terms of valve dynamics limiting engine speed and fluid dynamics producing pumping losses for flow into and out of the cylinders. Aura Systems, Inc. has patented an electromagnetic valve actuation system which helps to overcome some of these limitations.(41) Its claimed advantages are

- elimination of the conventional valvetrain for reduced engine friction;
- low electric power consumption (53 W per valve on a 16-valve engine at 7,500 rpm);
- rapid valve actuation, achieving near square-wave valve motion; and
- variable, programmable valve timing.

With further development, the system could likely increase the speed capability of conventional engines. Aura Systems predicts increased power by 10 to 20 percent, increased fuel economy by 10 to 20 percent, and emissions improvement in comparison with conventional SI engines. These predictions seem plausible if the system does mechanically what they claim. Even more increase in power density could be achieved if the engine rated speed is increased. The developed system cost in production is probably equivalent to a conventional valvetrain; the added electromagnetic components and power electronics replace the conventional camshaft and valvetrain components. NVH may be reduced by the elimination of valvetrain mechanical noise. Transient response may also be improved by programmable valve timing. An automatic compression release function could be programmed into the valves to aid in starting. There are technical risks associated with this technology.

2. Stepwise Mixture Control and Turndown

Conventional emissions control in a SI engine depends upon a three-way catalyst and tight control of fuel-air ratio around the stoichiometric condition. If the fuel-air ratio deviates far from stoichiometric on either side, HC and CO or NO_x emissions are adversely affected by poor catalyst performance. However, if the engine is operated far enough to the lean side, NO_x emissions are again reduced by virtue of lower combustion temperatures. One approach to emissions control is to operate the engine at stoichiometric fuel-air ratio for rated condition and reduce power by a combination of throttling and lean mixture. If stepwise power transients are desired, as is likely the case with a hybrid APU, this control mode is feasible; however, it is probably not useful for a direct-drive vehicle. The advantages of this concept are improved part-load fuel economy and emissions, which may or may not be a strong driver for the hybrid APU. There are no other perceived advantages.

3. Step-Up Gearbox

To take advantage of the reduced weight and size associated with generators running at high shaft speed, one approach is simply to employ a step-up gearbox. The tradeoffs of this approach are increased size, weight, cost, and reduced efficiency associated with the gearbox, with reduced size and weight of the generator. This idea is applicable to any crankshaft engine. Estimates for the relative effects of incorporating this idea are based on the assumption of a 4:1 step-up gear ratio to achieve 24,000 rpm with the engine speed at 6,000 rpm. The gearbox for this application would likely be a two-step geartrain with 2 to 1 ratios on both gear sets. Its weight and volume would be about 20 kg and 12 L, respectively. The torque losses would be about 3 percent, resulting in an effective generator efficiency of 89 percent. Slight penalties would be incurred in system cost, noise, startability, and transient response.

4. Step-Up Gearbox Integrated With Crank

To limit the penalties associated with a step-up gearbox, an engine could be designed to incorporate the features of the gearbox into the crankshaft system, thus reducing somewhat the weight, volume, and cost penalties. Other effects on system characteristics would be unchanged.

5. Blowdown Capture Turbocharging

Proponents of turbocharging have long recognized the importance of exhaust system pressure pulsations in the performance of the turbine. Pulse effects are often credited for improvements in turbine efficiency on the order of 10 to 30 percent, and "effective" efficiency values based on mean exhaust manifold conditions are often greater than one. Recognizing that a typical reciprocating engine wastes a significant proportion of the exhaust gas energy in the process of blowing down the cylinder from its final expansion pressure to the manifold pressure, SwRI engineers have theorized a means of capturing this otherwise wasted energy. The concept is to utilize separate exhaust valves for the blowdown process and for the exhaust stroke, capturing the higher pressure exhaust products in a separate manifold and achieving higher availability of exhaust energy for work in the turbine. An additional feature of the concept is the use of acoustic elements in the blowdown manifold to further enhance the recovery of blowdown energy. While this concept primarily benefits large, highly turbocharged engines, it also has potential applications to the APU.

One possibility for application to hybrid APUs is to simply highly turbocharge a conventional engine. This could result in improvements in power densities on the order of 30 to 50 percent over the naturally aspirated engine; however, turbocharging is difficult for smaller engines. Fuel economy would also be improved. The improvement attributable to blowdown capture is unclear without further study but could be on the order of 10 percent in power density and 5 percent in fuel economy. Another option would be to take an otherwise naturally aspirated engine and capture the blowdown pulses in a separate manifold, routing them to a turboalternator. This would be of special interest in parallel drivetrains where the shaft power of the engine would be used for direct drive and the turbine power for charging the batteries. Further investigation is

perhaps merited for this option but outside the scope of consideration in this study. Risks associated with the idea are primarily to the durability of the turbine, which will be exposed to higher temperature air.

For the purposes of ranking in this study, the application to the conventional turbocharged engine is assumed, with the benefits noted above. The applicability of the concept depends upon whether a turbocharged engine is indicated, which is highly dependent upon the required power rating. For smaller vehicles, turbocharging is probably not a reasonable option because of the unavailability of commercial turbochargers in an appropriate size. However, for power ratings of 50 kW or above, turbocharging is a possibility.

6. Combined Cycle Heat Recovery

The primary source of wasted energy in an internal combustion engine is thermal energy in the exhaust system. For SI engines, this energy is of relatively high quality (high temperature) and could be utilized in a combined cycle, similar to cogeneration. This option, referred to as a "bottoming cycle," has been studied by several researchers.(43-46) The technologies to do this include Rankine cycle machines, Brayton cycle machines and Stirling engines, as well as other possibilities. The technologies are not well developed for automotive prime movers and are likely to have significant cost, weight, and volume penalties. Estimates made by one study indicated a potential improvement of about 15 percent in fuel economy at rated conditions for a baseline diesel engine.(43) Volume and weight penalties were not given, but it is assumed for this study that the additional equipment would require about 50 percent of the baseline engine volume, weight, and cost.

VII. DISCUSSION OF CONCEPT RANKING

The comparison analysis of APU system concepts is summarized in TABLE 1. This table presents the raw scores on each of eleven criteria, the calculation of scoring statistics to establish

TABLE 1. Ranking of Hybrid APU System Concepts

RAW SCORES BY CRITERION*:	1	2	3	4	5	6	7	8	9	10	11	12	Composite Score
Free-Piston with Linear Generator	0.30	0.56	0.40	1.40	0.80	1.20	1.40	2.00	0.50	1.20	1.20	2.00	
Wankel Rotary Engine	0.25	1.32	0.53	1.30	0.90	1.00	1.10	1.50	0.90	1.10	1.10	1.10	
Two-Stroke SI Engine	0.27	0.42	0.48	1.30	0.80	1.20	1.20	1.20	0.90	1.00	1.00	1.10	
Two-Stroke Gas Generator/Turboalternator	0.22	0.38	0.70	1.00	1.10	1.00	1.20	1.00	0.80	1.10	1.00	0.80	
Free-Piston with Turboalternator	0.17	0.49	0.50	1.20	0.80	1.00	1.10	2.00	0.90	1.30	1.20	0.90	
HCCI Two-Stroke with Pressure Relief	0.25	0.42	0.38	1.20	1.20	1.00	0.70	0.80	0.50	1.00	1.10	1.10	
Two-Stroke CI Engine	0.30	0.41	0.36	1.20	0.70	1.10	1.10	0.70	0.80	0.90	0.80	1.10	
Multicylinder Model Airplane Engine	0.22	0.82	0.68	1.00	0.70	0.60	0.60	1.05	0.60	0.80	1.00	1.20	
Four-Stroke SI Engine	0.27	0.30	0.37	1.00	1.00	1.00	1.00	1.00	1.00	1.00	1.00	1.00	
High Speed Detonation Engine (HSDE)	0.23	0.52	0.68	0.95	0.95	0.50	0.50	0.80	0.50	0.50	1.10	0.95	
Four-Stroke CI Engine	0.33	0.23	0.21	1.00	0.90	1.10	1.10	0.50	1.00	0.80	0.80	0.80	
Regenerative Internal Combustion Engine	030	0.33	0.31	0.85	0.90	0.95	0.95	0.50	0.60	1.10	1.10	0.90	
Rotating Combustion Chamber Engine	0.18	0.58	0.50	0.90	1.00	0.50	0.50	0.70	0.30	1.10	1.00	1.10	
SCORING STATISTICS													
Mean	0.25	0.52	0.47	1.10	0.90	1.02	0.96	1.06	0.72	0.99	1.03	1.08	
Max	0.33	1.32	0.70	1.40	1.20	1.20	1.40	2.00	1.00	1.30	1.20	2.00	
Min	0.17	0.23	0.21	0.85	0.70	0.80	0.50	0.50	0.30	0.50	0.80	0.80	
Significance	4	5	5	4	4	3	3	2	1	2	1	2	
Normalizing Factor	6.20	0.92	2.02	1.82	2.00	2.50	1.11	0.67	1.43	1.25	2.50	0.83	
Weight	24.81	4.60	10.08	7.27	8.00	7.50	3.33	1.33	1.43	2.50	2.50	1.67	
WEIGHTED SCORES BY CRITERION:													
Free-Piston with Linear Generator	7.44	2.56	4.03	10.18	6.40	9.00	4.67	2.67	0.71	3.00	3.00	3.33	57.00
Wankel Rotary Engine	6.20	6.06	5.36	9.45	7.20	7.50	3.67	2.00	1.29	2.75	2.75	1.83	56.06
Two-Stroke SI Engine	6.62	1.95	4.85	9.45	6.40	9.00	4.00	1.60	1.29	2.50	2.50	1.83	51.99
Two-Stroke Gas Generator/Turboalternator	5.46	1.74	7.10	7.27	8.80	7.50	4.00	1.33	1.14	2.75	2.50	1.33	50.93
Free-Piston with Turboalternator	4.22	2.25	5.04	8.73	6.40	7.50	3.67	2.67	1.29	3.25	3.00	1.50	49.51
HCCI Two-Stroke with Pressure Relief	6.28	1.92	3.88	8.73	9.60	7.50	2.33	1.07	0.71	2.50	2.75	1.83	49.10
Two-Stroke CI Engine	7.53	1.87	3.60	8.73	5.60	8.25	3.67	0.93	1.14	2.25	2.00	1.83	47.41
Multicylinder Model Airplane Engine	5.48	3.77	6.91	7.27	5.60	7.50	2.00	1.40	0.86	2.00	2.50	2.00	47.29
Four-Stroke SI Engine	6.62	1.39	3.73	7.27	8.00	7.50	3.33	1.33	1.43	2.50	2.50	1.67	47.28
High Speed Detonation Engine (HSDE)	5.61	2.38	6.91	6.91	7.60	7.50	1.67	1.07	0.71	1.25	2.75	1.58	45.93
Four-Stroke CI Engine	8.22	1.06	2.10	7.27	7.20	7.50	3.67	0.67	1.43	2.00	2.00	1.33	44.44
Regenerative Internal Combustion Engine	7.54	1.53	3.15	6.18	7.20	7.13	3.17	0.67	0.86	2.75	2.75	1.50	44.43
Rotating Combustion Chamber Engine	4.34	2.68	5.04	6.55	8.00	6.00	1.67	0.93	0.43	2.75	2.50	1.83	42.72
MEAN WEIGHTED SCORE:	6.27	2.40	4.75	8.00	7.23	7.64	3.19	1.41	1.02	2.48	2.58	1.80	48.7

*CRITERIA:

1.	Thermal Efficiency	2.	Volume (Power density)	3.	Weight (Power density)
4.	Cost (as product)	5.	Emissions	6.	Producibility
7.	Reliability	8.	Cranking Torque and Startability	9.	Technical Risk
10.	Noise, Vibration, Harshness	11.	Multifuel Capability	12.	Transient Response

final weighting, and the weighted scores. Composite scores at the right of the table are the sum of weighted scores for all criteria. The concepts are ranked in order of their score, from highest to lowest. The mean weighted score is provided as a means of evaluating the general merit of a concept.

The highest scoring concept was the free-piston engine linear generator (FPELG). The primary contributors to this ranking were perceived advantages in thermal efficiency, cost, producibility, reliability, NVH, fuel tolerance, and transient response. It is less attractive from the standpoints of power density and risk; however, it still ranks ahead of the baseline four-stroke SI engine in the power density categories. It should be noted that the power density of the FPELG is still unknown and could be grossly overestimated, hence the technical risk. This concept certainly merits detailed investigation.

The next highest ranked concept is the Wankel rotary engine. By contrast with the FPELG, its advantages are primarily in the area of power density and risk, with lesser (but still substantial) benefits in terms of cost and NVH. The Wankel engine is well-established and offers a low risk alternative for advanced high power-density APUs.

These top two concepts were very closely ranked. Considering the subjectiveness of this analysis, their order of ranking should be considered interchangeable. By contrast, the next highest ranked concept, the two-stroke SI engine, scored significantly lower. It scored well in the categories of thermal efficiency, cost, producibility, reliability, and risk. Interestingly, it did not score as well in power density. Although the two-stroke engine has been touted as a high power-density alternative, its advantages are weakened by the need to consider the weight of a generator in the system. The two-stroke engine has some advantages in the respect that it can run at higher rpm than a conventional engine; however, the Wankel engine is even better at achieving high power in a small package.

The combination of a two-stroke gas generator with a turboalternator scored fairly well, primarily owing to a high power-to-weight ratio and a fairly well developed state of technology for the

system components. It is disadvantaged with respect to thermal efficiency, cost, and volumetric power density, the latter attributable to the large air handling requirement.

The free-piston engine/turboalternator combination scored about 1.4 points below the conventional two-stroke engine gas generator with turboalternator. This lower score is attributed to lower thermal efficiency, weight power density, and emissions. The emissions difference is debatable and is based on the presumption of a lean-burn cycle for the conventional crank-driven two-stroke. The lean-burn conditions could also be applied to the free-piston engine, making its score equivalent to the crank engine. Both options should be investigated further to better quantify the differences, particularly in power density.

The HCCI two-stroke engine with pressure relief scored ahead of the mean overall but is seen as a high risk approach. It has the potential of low cost, good thermal efficiency, and inherently low NO_x emissions. Its score is very close to that of the FPE-turboalternator, suggesting that further investigation is also warranted.

The composite scores of remaining concepts were below the average. Many of these ideas are good in one or two respects but suffer in one or several key areas needed to achieve the overall goals of a hybrid APU. The primary discriminators are thermal efficiency and power density.

The scoring summary for the auxiliary concepts is shown in TABLE 2. For these ideas, the composite score represents the overall ability to improve over the state-of-the-art for the hybrid application. Only two of the six concepts scored positive: electric valves and stepwise mixture control. The potential benefits of electric valves are strong; their main drawback is technical risk. The stepwise mixture control approach can be implemented by a control system strategy, without additional cost. Therefore, it offers a low risk technique for improved emissions and thermal efficiency.

TABLE 2. Ranking of Hybrid APU Auxiliary Concepts

RAW SCORES BY CRITERION*:	1	2	3	4	5	6	7	8	9	10	11	12	
Electric Valves	0.04	0.05	0.03	0.00	0.10	0.00	0.00	0.20	-0.20	0.10	0.00	0.05	
Stoich. NG 4-Stroke w/Lean Turndown	0.02	0.00	0.00	0.00	0.10	0.00	0.00	0.00	0.00	0.00	0.00	0.00	
Step-up Gearbox Integrated w/Crank	-0.01	-0.01	0.08	-0.03	0.00	0.00	0.00	-0.05	0.00	-0.05	0.00	-0.05	
Step-Up Gearbox	-0.01	-0.02	0.06	-0.05	0.00	0.00	0.00	-0.05	0.00	-0.05	0.00	-0.05	
Blowdown Capture Turbocharging	0.01	0.03	0.02	-0.10	0.00	-0.10	-0.10	0.00	-0.10	0.10	0.00	-0.10	
Combined-Cycle Heat Recovery	0.04	-0.09	-0.07	-0.20	0.00	-0.10	-0.20	0.00	-0.30	0.10	0.00	-0.10	
SCORING STATISTICS													
Mean	0.02	-0.01	0.02	-0.06	0.03	-0.03	-0.05	0.02	-0.10	0.03	0.00	-0.04	
Max	0.04	0.05	0.08	0.00	0.10	0.00	0.00	0.20	0.00	0.10	0.00	0.05	
Min	-0.01	-0.09	-0.07	-0.20	0.00	-0.10	-0.20	-0.05	-0.30	-0.05	0.00	-0.10	
Significance	4	5	5	4	4	3	3	2	1	2	1	2	
Normalizing Factor	19.99	7.02	6.79	5.00	10.00	10.00	5.00	4.00	3.33	6.67	n/a	6.67	
Weight	79.97	35.08	33.94	20.00	40.00	30.00	15.00	8.00	3.33	13.33	n/a	13.33	
WEIGHTED SCORES BY CRITERION:													Composite Score
Electric Valves	3.20	1.68	0.90	0.00	4.00	0.00	0.00	1.60	-0.67	1.33	0.00	0.67	12.71
Stoich. NG 4-Stroke w/Lean Turndown	1.60	0.00	0.00	0.00	4.00	0.00	0.00	0.00	0.00	0.00	0.00	0.00	5.60
Step-up Gearbox Integrated w/Crank	-0.80	-0.35	2.71	-0.60	0.00	0.00	0.00	-0.40	0.00	-0.67	0.00	-0.67	-0.77
Step-Up Gearbox	-0.64	-0.58	1.87	-1.00	0.00	0.00	0.00	-0.40	0.00	-0.67	0.00	-0.67	-2.08
Blowdown Capture Turbocharging	1.07	1.06	0.58	-2.00	0.00	-3.00	-1.50	0.00	-0.33	1.33	0.00	-1.33	-4.12
Combined-Cycle Heat Recovery	2.94	-3.32	-2.29	-4.00	0.00	-3.00	-3.00	0.00	-1.00	1.33	0.00	-1.33	-13.66
MEAN WEIGHTED SCORE:	1.23	-0.25	0.63	-1.27	1.33	-1.00	-0.75	0.13	-0.33	0.44	0.00	-0.56	-0.39

*CRITERIA:

1.	Thermal Efficiency	2.	Volume (Power density)	3.	Weight (Power density)
4.	Cost (as product)	5.	Emissions	6.	Producibility
7.	Reliability	8.	Cranking Torque and Startability	9.	Technical Risk
10.	Noise, Vibration, Harshness	11.	Multifuel Capability	12.	Transient Response

VIII. RECOMMENDATIONS

All of these concept scorings and rankings are subject to substantial error. Many of the concepts have only been subjected to cursory evaluation and limited analysis, whereas others represent near production-ready technology. This is reflected in the risk scores. It should be borne in mind that the evaluation is highly subjective in nature and could have a different outcome if a different person was doing the analysis. Nonetheless, it is believed that these results present as fair and unbiased an analysis as can be conducted in a study of this scope.

Bearing in mind the potential for error, it is recommended that these rankings be considered as a screening test. SwRI recommends further study for the top six concepts. Although it appears from this analysis that there are two concepts that clearly rank above the rest, these rankings may change as more detailed information develops. The objective of this study will be to further quantify and confirm their ranking relative to each other. This should be done in two steps as follows:

1. Perform an in-depth cycle simulation study of each concept. The thermodynamic cycle simulation can provide system-level comparisons of performance, fuel economy, and emissions. This will directly refine the scoring in the categories of thermal efficiency and emissions and will provide essential information on key component dimensions to further quantify the power density. Thus, most of the higher significance scoring factors will be refined. At the conclusion of this study, the concepts should be reranked and the rankings studied to adjust downward those concepts which are less competitive. This analysis can be done largely in parallel for all six concepts but may concentrate on the top ranked concepts at first.

2. Perform a preliminary design analysis of each remaining concept to gain further refinement of the volume and weight power density. This design analysis will consist of layouts of all key engine and generator components using a CAD system that will provide component mass properties for weight rollups. It will also include systems analysis to assure that accounting is done for weight and size of necessary accessory

systems. At this point, the scoring estimates for volume and weight can be more accurately determined.

At the conclusion of these analyses, it is likely that one or two concepts will emerge as meriting full-scale development into prototype demonstration systems.

For the subsystem concepts, demonstration tests are the most useful means of further quantifying their benefits. It is recommended that the top two concepts be considered for implementation in demonstration test APU systems. Electric valves can be implemented in a conventional engine to quantify their performance and emissions benefits. The lean turndown approach to achieving fuel economy improvements in a four-stroke NG engine can be implemented by simply modifying a control strategy. It can even be investigated by compiling existing data on engines that can run at both stoichiometric and lean conditions and using these data in an appropriate hybrid vehicle simulation.

This analysis has been very useful in establishing a framework for decision making regarding choices of APU systems for hybrid vehicles. It is necessarily subjective but can be greatly improved by the accumulation of more precise data on the comparison parameters. It is hoped that ARPA finds this approach useful as well.

IX. LIST OF REFERENCES

1. Schneider, H.W., "Evaluation of Heat Engines for Hybrid Vehicle Application," JPL Publication 84-14, DOE/CS/54209-15, 31 August 1984.

2. Burke, A.F., "Hybrid/Electric Vehicle Design Options and Evaluations," SAE Paper No. 920447, February 1992.

3. Burke, A.F., and Smith, G.E., "Impact of Use-Pattern on the Design of Electric and Hybrid Vehicles," SAE Paper No. 810265, February 1981.

4. Burke, A.F., "On-Off Engine Operation for Hybrid Vehicles," SAE Paper No. 930042, 1993.

5. Gelman, D.J., and Perrot, T.L., "Advanced Heat Engines for Range Extender Hybrid Vehicles," SAE Paper No. 930041, March 1993.

6. BVFLR Report

7. Amann, C.A., "The Automotive Engine – A Future Perspective," SAE Paper No. 891666, 1989.

8. Fraidl, G.K., Quissek, F., and Winklhofer, E., "Improvement of LEV/ULEV Potential of Fuel-Efficient High Performance Engines," SAE Paper No. 920416, 1992.

9. Kreuter, P., Heuser, P., and Schebitz, M., "Strategies to Improve SI-Engine Performance by Means of Variable Intake Lift, Timing and Duration," SAE Paper No. 920449, 1992.

10. Endres, H., Neuber, H.J., and Wurms, R., "Influence of Swirl and Tumble on Economy and Emissions of Multi Valve SI Engines," SAE Paper No. 920516.

11. Stock, D., and Bauder, R., "The New Audi 5-Cylinder Turbo Diesel Engine: The First Passenger Car Diesel Engine with Second Generation Direct Injection," SAE Paper No. 900648, February 1990.

12. Hundleby, G.E., "Development of a Poppet-Valved Two-Stroke Engine – The Flagship Concept," SAE Paper No. 900802, 1990.

13. Stokes, J., Hundleby, G.E., Lake, T.H., and Christie, M.J., "Development Experience of a Poppet-Valved Two-Stroke Flagship Engine," SAE Paper No. 920778, 1992.

14. Sato, K., Ukawa, H., and Nakano, M., "A Two-Stroke Cycle Gasoline Engine with Poppet Valves in the Cylinder Head – Part II," SAE Paper No. 920780, 1992.

15. Ukawa, H., Nakano, M., and Sato, K., "A Two-Stroke Cycle Engine with Poppet Valves in the Cylinder Head – Part III: An Application of Gaseous Fuel Direct Injection System," SAE Paper No. 930983, 1993.

16. Widener, S.K., and Swenson, K.R., "Two-Stroke Engines for Automotive Applications," Fourth Quarterly Report, SwRI Project No. 03-1464, March 1991.

17. Widener, S.K., Boyer, L., Gale, N.F., and Wood, C.D., "A Heavy-Fueled Engine for Unmanned Aerial Vehicles – Design, Analysis and Prototype Demonstration," SAE Paper No. 950773, 1995.

18. Mount, R.E., and LaBouff, G.A., "Advanced Stratified Charge Rotary Engine Design," SAE Paper No. 890324, 1989.

19. Fujimoto, Y., Tatsutomi, Y., Ozeki, H., and Tadokoro, A., "Present and Prospective Technologies of Rotary Engine," SAE Paper No. 870446, 1987.

20. Tashima, S., Taqdokoro, T., Okimoto, H., and Niwa, Y., "Development of Sequential Twin Turbo System for Rotary Engine," SAE Paper No. 910624, 1991.

21. Mount, R., and Bartel, J., "Advanced Liquid-Cooled, Turbocharged and Intercooled Stratified Charge Rotary Engines for Aircraft," SAE Paper No. 871039, 1987.

22. Jones, C., "Stratified Charge Rotary Engine Developments at JDTI from 1984 to 1991," SAE Paper No. 920310, 1992.

23. Louthan, L., "Development of a Lightweight Heavy Fuel Rotary Engine," SAE Paper No. 930682, 1993.

24. "AR 731 Rotary Engine for Target Drones and UAVs", Technical Specifications from Alvis UAV Engines, Ltd., Lynn Lane, Shenstone, Lichfield WS14 0DT, UK.

25. Pescara, R.P., "Motor Compressor Apparatus," U.S. Patent No. 1,657,641, 31 January 1928.

26. Samolewicz, J.J., "Experimental and Analytical Study of a Small Free-Piston Gasifier," ASME Paper No. 71-DGP-5, 1971.

27. Underwood, A.F., "The GMR 4-4 "Hyprex" Engine, A Concept of the Free-Piston Engine for Automotive Use," *SAE Transactions*, **65**, 1957, pp. 377-391.

28. Flynn, Jr., G., "Observations on 25,000 Hours of Free-Piston Engine Operation," *SAE Transactions*, **65**, 1957, pp. 508-515.

29. Frey, D.N., Klotsch, P., and Egli, A., "The Automotive Free-Piston-Turbine Engine," *SAE Transactions*, **65**, 1957, pp. 628-634.

30. Wallace, F.J., Wright, E.J., and Campbell, J.S., "Future Development of Free-Piston Gasifier Turbine Combinations for Vehicle Traction," SAE Paper No. 660132, 1966.

31. Hibi, A., "Hydraulic Free-Piston Internal Combustion Engine," *Power*, April 1984, pp. 87-91.

32. Hibi, A., and Kumagai, S., "Hydraulic Free-Piston Internal Combustion Engine – Test Result," *Power*, September 1984, pp. 244-249.

33. Hibi., A., and Hu, Y., "A Prime Mover Consists of a Free-Piston Internal Combustion Hydraulic Power Generator and an Hydraulic Motor," SAE Paper No. 930313, 1993.

34. Baruah, P.C., "A Free-Piston Engine Hydraulic Pump for an Automotive Propulsion System," SAE Paper No. 880658, 1988.

35. "Free-Piston Power Unit (FPPU) Integrated System Test Program," Final Report, 90-63865, Rev. A, AiResearch Los Angeles Division of Allied-Signal Aerospace Co., Contract DAAK70-89-C-0082, 22 February 1991.

36. Kubesh, J.T., and Meyer, R.C., "Evaluation of Tectonics Free-Piston Engine," Final Report for SwRI Project 03-4849, November 1992.

37. Stelzer, F., "Two-Stroke Internal Combustion Engine," US Patent No. 4,385,597.

38. Beachley, N.H., and Fronczak, F.J., "Design of a Free-Piston Engine-Pump," SAE Paper No. 921740, 1992.

39. Callahan, T., and Ingram, K., "Free-Piston Engine Linear Geneartor for Hybrid Vehicles Modeling Study," SwRI Draft Report for Project 02-5137.

40. Widener, S.K., "Concept Evaluation of a Rotating Combustion Chamber Engine," Final Report for SwRI Project 03-5221-004, May 1993.

41. "Proposal for Compact, Light Weight Natural Gas Fueled Electric Generator Using the Electromagnetic Valve Actuator/Rotary Actuator Motor Generator (EVA/RAMG)," Proposal by Aura Systems, Inc., to SwRI Belvoir Fuels and Lubricants Research Facility, 02 September 1993.

42. Thring, R.H., "Computer Analysis of the Open-Cycle Stirling Engine," Final Report for SwRI Internal Research Project No. 03-9459, March 1987.

43. Leising, C.J., Purohit, G.P., DeGrey, S.P., and Finegold, J.G., "Waste Heat Recovery in Truck Engines," SAE Paper No. 780686, 1978.

44. Sakono, T., Takizawa, S., Harada, S., Ikeda, T, and Abe, H., "Mazda New Lightweight and Compact V6 Engines," SAE Paper No. 920677, 1992.

45. Hiereth, H., Baehrens, W. E., Müller, W., and Withalm, G., "The Mercedes-Benz Group C Engines for the World Sports Prototype Racing Championships 1989 and 1990," SAE Paper No. 920674, 1992.

46. Ogata, Y., Shinbara, H., and Kimura, S., "Development of a Compact 3-Liter V6 Nissan Engine," SAE Paper No. 920672, 1992.

47. Foss, J.E., Jacques, R.L., Marsh, R.A., and Brooks, P.J., "The Northstar DOHC V-8 Engine for Cadillac," SAE Paper No. 920671, 1992.

48. Close, W.H., Fountain, G.H., and Daniel, M.R.L., "The New Collins Compact Scotch Yoke Engine," SAE Paper No. 920675, 1992.

49. SwRI Engine Database (A compilation of engine data from multiple sources).

50. Tsujita, M., Niino, S., Ishizuka, T., Kakinai, A., and Sato, Akihiko, "Advanced Fuel Economy in Hino New P11C Turbocharged and Charge-Cooled Heavy Duty Diesel Engine," SAE Paper No. 930272, 1993.

51. Stock, D., and Bauder, R., "The New Audi 5-Cylinder Turbo Diesel Engine: The First Passenger Car Diesel Engine with Second Generation Direct Injection," SAE Paper No. 900648, 1990.

52. Lawrence, R.J., and Evans, R.W., "The Ford 1.8L Four Cylinder Turbocharged Diesel Engine for Passenger Car Application," SAE Paper No. 901716, 1990.

53. Osake, N., Tsutsui, Y., Kakoi, Y., Sakino, Y., and Okazaki, K., "New Mitsubishi 2.8L Four-Cylinder Diesel Engine," SAE Paper No. 940587, 1994.

54. Duret, P., and Moreau, J.F., "Reduction of Pollutant Emissions of the IPAPC Two-Stroke Engine with Compressed Air Assisted Fuel Injection," SAE Paper No. 900801, 1990.

55. Blair, G.P., "Further Developments of a 500 cc Single Cylinder 2-Cycle Engine for Motorcycle Racing and Moto-Cross Applications," SAE Paper No. 740745, 1974.

56. Yamaoka, K., and Tado, H., "The Rotary Engines of Yanmar Outboard Motor," SAE Paper No. 710581, 1971.

57. Louthan, L., "Development of a Lightweight Heavy Fuel Rotary Engine," SAE Paper No. 930682, 1993.

58. Jones, C., "Stratified Charge Rotary Engine Developments at JDTI from 1984 to 1991," SAE Paper No. 920310, 1992.

APPENDIX

Database of Current Production and Research Engines

Four-Stroke Spark Ignition Engines

Reference	Mfg	Model	Rated kW	Spec. Vol. l/kW	Spec. Wt. kg/kW	Min BSFC kg/kWh
44	Mazda	KL	123.00	2.178		
44	Mazda	KF	104.00	2.826		
44	Mazda	KB	97.00	3.007		
45	Mercedes-Benz	M119 HL	530.00		0.400	0.235
46	Nissan	3-L V6	142.00	2.502		
47	GM	Northstar	216.00	1.227	0.972	
48	Collins	Scotch Yoke	56.67	1.676	1.288	0.277
48	Collins	Scotch Yoke	140.00	0.941	0.821	0.277
49	JUNKERS FLUGZEUG, A.G.	211B	782.98	4.128	0.874	
49	NISSAN MOTOR CO. LTD.	2.960 L VG30DETT	223.71	1.709		
49	NISSAN MOTOR CO. LTD.	4.5 L VH45DE	207.30	2.303		
49	JAGUAR CARS LTD.	5.343 L	202.83	2.631	0.789	
49	LOTUS CARS PLC	910 SE 2.2 L	197.00		0.914	0.300
49	TOYOTA MOTOR CORP.	4.0 L 1UZ-FE	186.42	2.208	1.046	
49	NISSAN MOTOR CO. LTD.	2.988 L VQ	186.00	1.771	0.892	
49	AUDI AG	3.562 L	178.97		1.118	
49	FUJI HVY INDSTR (SUBARU	1.994 L TURBO	161.81		0.908	
49	COSWORTH	MBA	161.00	1.011	0.745	
49	TOYOTA MOTOR CORP.	4.5 L 1FZ-FE	158.00	3.289	1.677	
49	FORD MOTOR CO.	4.605 L	156.60	1.748	1.437	
49	GENERAL MOTORS CORP.	3.786 L	152.87		1.256	
49	VOLVO AB	2.922 L B6304F	150.00		1.167	
49	FORD MOTOR CO.	2.5 L MOD V6	143.17		1.157	
49	FORD MOTOR CO.	4.605 L	141.68	1.932	1.588	
49	NISSAN MOTOR CO. LTD.	VQ 2.495 L	134.00	2.190	1.082	
49	VOLKSWAGEN AG	VR6	129.75	1.218	2.867	
49	VOLVO AB	2.435 L	125.00		1.384	
49	TOYOTA MOTOR CORP.	3.956 L	115.58	4.028	2.249	
49	TOYOTA MOTOR CORP.	3.956 L	114.09	4.080	2.279	
49	FUJI HVY INDSTR (SUBARU	1.994 L	110.33		1.178	
49	VOLVO AB	1.984 L	105.00		1.648	
49	NISSAN MOTOR CO. LTD.	1.998 L SR20DE	104.40	2.461		
49	TOYOTA MOTOR CORP.	3S-GE 1.998 L	101.00		1.347	
49	FUJI HVY INDSTR (SUBARU	2.212 L	96.94		1.248	
49	PEUGEOT,RENAULT,VOLVC	2.664 L	93.21	1.971	1.674	
49	FORD OF EUROPE	ZETA (1.8LHO)	93.00		1.392	
49	TOYOTA MOTOR CORP.	3S-FE 1.998 L	86.00		1.512	
49	TOYOTA MOTOR CORP.	1.998 L	85.76		1.458	
49	GENERAL MOTORS CORP.	2.8 L	85.00		1.805	
49	FUJI HVY INDSTR (SUBARU	1.820 L	80.91		1.458	
49	FORD OF EUROPE	ZETA (1.8LSO)	75.00		1.713	
49	NISSAN MOTOR CO. LTD.	1.497 L GA15	71.30	2.900	1.487	
49	GENERAL MOTORS CORP.	1.991 L	67.10		2.038	
49	NISSAN MOTOR CO. LTD.	1.974 L	65.60	3.124	1.753	
49	GENERAL MOTORS CORP.	1.841 L	65.60		2.079	
49	CHRYSLER MOTOR CORP.	2.213 L	64.50		1.519	
49	FORD MOTOR CO.	2.307 L	63.00		1.810	
49	ZAVODI CREVNA (YUGO)	1.585 L	61.89	0.894	0.638	
49	VOLKSWAGEN AG	026.2	50.00	4.946	2.220	
49	BRIGGS & STRATTON	DM 950(DAIHATSU E	23.12	3.637	2.682	
49	KOHLER ENGINES	CH25 COMMAND	18.40	5.052	2.337	
49	ONAN	P224	17.90		7.095	

Four-Stroke Spark Ignition Engines

Reference	Mfg	Model	Rated kW	Spec. Vol. l/kW	Spec. Wt. kg/kW	Min BSFC kg/kWh
49	BRIGGS & STRATTON	DM 700(DAIHATSU E	17.52	4.797	3.424	
49	ONAN	P220	14.91		3.346	
49	HONDA	GX620	14.91	4.157	2.743	
49	KOHLER ENGINES	CH20 (COMMAND)	14.90	4.307	2.752	
49	KOHLER ENGINES	MV20 (MAGNUM)	14.90		3.960	
49	ONAN	P220V	14.90		7.383	
49	KOHLER ENGINES	M20 (MAGNUM)	14.90		3.960	
49	BRIGGS & STRATTON	350700	13.42		2.481	
49	BRIGGS & STRATTON	350400	13.42		2.481	
49	BRIGGS & STRATTON	422400	13.42		2.951	
49	HONDA	GX610	13.42	4.619	3.048	
49	KOHLER ENGINES	MV18 (MAGNUM)	13.40		4.403	
49	KOHLER ENGINES	M18 (MAGNUM)	13.40		4.403	
49	ONAN	P218	13.40		3.724	
49	KOHLER ENGINES	CH18 (COMMAND)	13.40	4.789	3.060	
49	KAWASAKI	FC540V	12.68		3.431	
49	BRIGGS & STRATTON	402400	11.93		3.319	
49	BRIGGS & STRATTON	303400	11.93		2.716	
49	BRIGGS & STRATTON	326400	11.93		4.049	
49	ONAN	P216V	11.90		4.193	
49	KOHLER ENGINES	M16 (MAGNUM)	11.90		4.916	
49	ONAN	P216	11.90		9.076	
49	KOHLER ENGINES	MV16 (MAGNUM)	11.90		4.958	
49	KOHLER ENGINES	CV14 (COMMAND)	10.50	8.729	3.762	
49	KOHLER ENGINES	CH14 (COMMAND)	10.50	7.527	3.810	
49	KAWASAKI	FC420V	10.44		3.448	
49	KAWASAKI	KF150D	10.44		6.466	
49	ONAN	140	10.40		6.827	
49	KOHLER ENGINES	M14 (MAGNUM)	10.40		5.625	
49	KAWASAKI	FC400V	9.69		3.714	
49	KOHLER ENGINES	CV12.5 (COMMAND)	9.33	9.823	4.234	
49	KAWASAKI	FB460V	9.32		3.862	
49	TECUMSEH	OVXL/C125	9.32		6.223	
49	BRIGGS & STRATTON	260700	9.32		4.104	
49	BRIGGS & STRATTON	290400	9.32		3.476	
49	ONAN	125	9.30		7.634	
49	KOHLER ENGINES	CH12.5 (COMMAND)	9.30	8.499	4.301	
49	KOHLER ENGINES	M12 (MAGNUM)	9.00		6.500	
49	TECUMSEH	OVXL120	8.95		6.480	
49	HONDA	EL5000	8.95		28.721	
49	KOHLER ENGINES	CH11 (COMMAND)	8.20	9.636	4.877	
49	HONDA	EW171	8.20	30.937	29.503	
49	HONDA	WT40X	8.20		18.287	
49	BRIGGS & STRATTON	254400	8.20		3.554	
49	KOHLER ENGINES	CV11 (COMMAND)	8.20	11.177	4.817	
49	KOHLER ENGINES	M10 (MAGNUM)	7.50		7.800	
49	BRIGGS & STRATTON	221400	7.46		3.846	
49	TECUMSEH	TVXL220	7.46		7.641	
49	BRIGGS & STRATTON	243400	7.46		5.836	
49	KAWASAKI	KF100D	7.46		6.169	
49	KAWASAKI	FE290D	6.71		5.006	
49	KAWASAKI	FC290V	6.71		3.651	

Four-Stroke Spark Ignition Engines

Reference	Mfg	Model	Rated kW	Spec. Vol. l/kW	Spec. Wt. kg/kW	Min BSFC kg/kWh
49	BRIGGS & STRATTON	161400	6.71		4.259	
49	BRIGGS & STRATTON	233400	6.71		6.219	
49	KOHLER ENGINES	M8 (MAGNUM)	6.00		5.367	
49	TECUMSEH	TVXL195	5.97		9.548	
49	BRIGGS & STRATTON	195400	5.97		3.533	
49	KAWASAKI	FE250D	5.89		5.092	
49	KAWASAKI	FG300D	5.59		4.559	
49	TECUMSEH	TVXL170	5.22		10.920	
49	TECUMSEH	TVM140	4.47		7.774	
49	KAWASAKI	FE170D	3.95		4.428	
49	KAWASAKI	FA210V	3.88		3.868	
49	KAWASAKI	FA210D	3.88		3.353	
49	TECUMSEH	TVM125	3.73		9.316	
49	BRIGGS & STRATTON	104700	3.73		5.067	
49	KOHLER ENGINES	CH5 (COMMAND)	3.73		5.469	
49	BRIGGS & STRATTON	132200	3.73		3.646	
49	KAWASAKI	FG200D	3.73		6.115	
49	HONDA	EB2200X	3.73		25.480	
49	WISCONSIN ROBIN	W1-185V	3.70		8.649	
49	KAWASAKI	FC150V	3.36		3.874	
49	WISCONSIN ROBIN	W1-145V	3.00		9.333	
49	WISCONSIN ROBIN	WT1-125V	3.00		8.433	
49	KAWASAKI	FG150D	2.68		5.103	
49	HONDA	WD20X	2.61		21.073	
49	KAWASAKI	FA130D	2.31		4.326	
49	BRIGGS & STRATTON	82200	2.24		4.911	
49	US ENGINES INC.	41cc	2.20	3.763	2.546	
49	SHINDAIWA	S45B	1.72	35.893	12.419	
49	SHINDAIWA	SM45P	1.72		10.029	
49	SHINDAIWA	EC350	1.64		10.058	
49	US ENGINES INC.	35cc	1.49		3.688	
49	KAWASAKI	FA76D	1.27		5.759	
49	SHINDAIWA	S25P	0.97		13.204	
49	SHINDAIWA	S20HT	0.67	94.040	17.732	

Four-Stroke Compression Ignition Engines

Reference	Mfg	Model	Rated kW	Spec. Vol. l/kW	Spec. Wt. kg/kW	Min BSFC kg/kWh
50	Hino	P11C-P-IV	239.0	7.626	3.791	0.185
50	Hino	P11C-P-III	221.0	8.247	4.054	0.184
49	BRIGGS & STRATTON	DM 700(DAIHATSU BUILT)	14.5	5.781	4.608	
49	BRIGGS & STRATTON	DM 950(DAIHATSU BUILT)	19.8	4.254	3.492	
49	CATERPILLAR	3306B DITA	201.3	6.663	4.599	0.208
49	CATERPILLAR	3406	242.4		5.116	
49	CATERPILLAR	3176: 250 hp FAMILY	187.0	5.923	4.717	
49	CATERPILLAR	3176: 325 hp FAMILY	242.0	4.577	3.645	
49	CATERPILLAR	3412	484.7		3.837	
49	CATERPILLAR	3176	242.0	4.577	3.645	
49	CATERPILLAR	3304T0	142.0	6.405	5.289	0.249
49	CATERPILLAR	3406C DITAA	316.9	5.590	4.023	0.202
49	CATERPILLAR	3408 TA	325.0	6.020	4.701	0.220
49	CATERPILLAR	3208 NA	130.5	5.173	10.154	0.219
49	CATERPILLAR	3208 DIT	186.4	4.110	7.671	0.217
49	CATERPILLAR	3408	298.3		4.794	
49	CATERPILLAR	3406B DITA	298.3	5.947	4.375	0.201
49	CATERPILLAR	3412	559.3		3.328	
49	CATERPILLAR	3406	279.6		4.434	
49	CATERPILLAR	3408	354.2		4.037	
49	CATERPILLAR	3176: 275 hp FAMILY	205.0	5.403	4.302	
49	CATERPILLAR	3116	186.0		2.925	
49	CATERPILLAR	3176: 300 hp FAMILY	224.0	4.944	3.938	
49	CUMMINS	NTC400 BCIV	298.3	5.534	8.884	0.201
49	CUMMINS	KTTA19-C	484.7	5.170	7.840	0.206
49	CUMMINS	6B5.9	85.8	5.771	9.970	0.222
49	CUMMINS	6CTA8.3	186.0	4.312	3.258	0.206
49	CUMMINS	N-855-C BCI	175.2	8.254	14.780	0.236
49	CUMMINS	4B3.9	56.7	6.497	11.999	0.227
49	CUMMINS	LTA-10	223.7	5.154	8.627	0.203
49	CUMMINS	N14: ESP1	290.0		4.386	
49	CUMMINS	LT-10-C	167.8	6.350	11.593	0.206
49	CUMMINS	NTC-475	354.0	5.007	7.599	0.207
49	CUMMINS	KTTA38-C	1006.7	5.366	9.189	0.208
49	CUMMINS	VTA28-C	596.6	7.264	9.723	0.215
49	CUMMINS	6CT	160.0	5.250	3.800	
49	CUMMINS	6C8.3	119.0	6.442	4.790	0.218
49	CUMMINS	KTTA-50	1342.2	5.597	8.117	0.214
49	CUMMINS	VT-903-C	279.6	5.357	8.511	0.220
49	CUMMINS	6BTA5.9	134.2	4.020	6.742	0.206
49	CUMMINS	4BTA3.9	89.5	4.633	8.102	0.219
49	DAEWOO HEAVY IND. LTD.	1.8 L(3AB1)	28.0	9.730	7.750	
49	DAEWOO HEAVY IND. LTD.	7.3 L (D0846M)	107.0	7.566	5.794	
49	DAEWOO HEAVY IND. LTD.	2.4 L(C240)	38.0	7.817	5.868	
49	DAEWOO HEAVY IND. LTD.	7.3 L (D0846HM)	124.0	6.528	5.000	
49	DAEWOO HEAVY IND. LTD.	8.1 L (D1146)	133.0	6.226	5.113	
49	DAEWOO HEAVY IND. LTD.	11.1 L (D2366)	165.0	7.485	5.358	
49	DAEWOO HEAVY IND. LTD.	10.4 (D2156HM)	158.0	7.885	5.380	
49	DAEWOO HEAVY IND. LTD.	14.6 L (D2848T)	245.0	5.889	3.633	
49	DAEWOO HEAVY IND. LTD.	19.8 L (MD336)	110.0	32.307	23.091	
49	DAEWOO HEAVY IND. LTD.	21.9 L (D2842T)	364.0	5.202	3.077	
49	DAEWOO HEAVY IND. LTD.	13.2 L (MD334)	74.0	21.658	22.027	

Four-Stroke Compression Ignition Engines

Reference	Mfg	Model	Rated kW	Spec. Vol. l/kW	Spec. Wt. kg/kW	Min BSFC kg/kWh
49	DAEWOO HEAVY IND. LTD.	21.9 L (D2842L)	429.0	4.414	2.937	
49	DAEWOO HEAVY IND. LTD.	4.8 L(D0844M)	66.0	11.135	7.242	
49	DAEWOO HEAVY IND. LTD.	10.4 L (D2156MT)	188.0	7.156	4.787	
49	DAEWOO HEAVY IND. LTD.	3.3 L(4BC2)	65.0	6.122	4.631	
49	DAEWOO HEAVY IND. LTD.	11.1 L (D2366T)	212.0	5.552	4.358	
49	DAEWOO HEAVY IND. LTD.	19.8 L (MD336TI)	147.0	33.913	17.347	
49	DAEWOO HEAVY IND. LTD.	8.1 L (D1146T)	162.0	5.363	4.444	
49	DAEWOO HEAVY IND. LTD.	2.4 L(C223)	45.0	6.500	4.733	
49	DAEWOO HEAVY IND. LTD.	14.6 L (D2848M)	162.0	6.552	5.185	
49	DAEWOO HEAVY IND. LTD.	5.4 L(6BB1)	99.0	6.515	4.545	
49	DAEWOO HEAVY IND. LTD.	18.3 L (D28480T)	324.0	4.751	3.333	
49	DAF	DKZ-1160	270.7	5.333	7.518	
49	DAF	DKA-1160	173.7	6.418	11.292	
49	DAF	DE385	59.7	8.122	12.019	
49	DAF	DHS 825	190.2	7.090	8.577	
49	DAIMLER-BENZ	OM617	60.4	6.839	9.205	0.269
49	DAIMLER-BENZ	OM364	69.3	6.323	10.656	
49	DAIMLER-BENZ	OM366	105.1		9.330	
49	DAIMLER-BENZ	OM617A	82.0	5.227	6.742	0.249
49	DAIMLER-BENZ	OM366LA	155.1		7.034	
49	DAIMLER-BENZ	OM422	211.0	3.965	8.890	
49	DAIMLER-BENZ	OM616	49.2	5.748	9.103	0.269
49	DALIAN DIESEL ENGINE WOR	CA6110	116.0	8.469	4.828	0.227
49	DETROIT DIESEL	SERIES 60: 11.1L	239.0	7.169	5.088	
49	DETROIT DIESEL	6.2 HD	115.6	3.117	6.065	0.263
49	DETROIT DIESEL	V8-8.2T	171.5	3.532	6.775	0.219
49	DETROIT DIESEL	SERIES 60: 12.7L	298.0	5.741	4.111	
49	FARYMANN DIESEL	18W	5.0	12.906	7.400	0.290
49	FARYMANN DIESEL	75W	17.0	7.922	9.412	0.270
49	FARYMANN DIESEL	36E	8.0	15.619	10.000	0.275
49	FARYMANN DIESEL	29C	8.0	11.587	8.750	0.240
49	FARYMANN DIESEL	41A	9.0	14.532	9.111	0.270
49	FARYMANN DIESEL	18D	5.0	11.062	8.200	0.290
49	FARYMANN DIESEL	32A	8.0	11.587	9.000	0.240
49	FARYMANN DIESEL	32W	9.0	8.814	8.556	0.250
49	FARYMANN DIESEL	86W	22.0	5.877	6.409	0.258
49	FARYMANN DIESEL	71W	16.2	8.407	9.568	0.270
49	FARYMANN DIESEL	95A	18.5	7.747	9.189	0.270
49	FARYMANN DIESEL	57	15.0	7.083	7.333	0.258
49	FARYMANN DIESEL	41E	9.0	13.884	9.444	0.270
49	FARYMANN DIESEL	95W	19.2	7.374	10.156	0.270
49	FARYMANN DIESEL	85	22.0	5.877	6.409	0.258
49	FARYMANN DIESEL	15W	5.0	12.906	7.400	0.300
49	FARYMANN DIESEL	15D	4.0	13.827	9.875	0.300
49	FARYMANN DIESEL	66A	17.0	7.509	7.529	0.239
49	FARYMANN DIESEL	44A	11.0	9.360	9.273	0.239
49	FARYMANN DIESEL	115 W	30.0	5.078	5.433	0.258
49	FARYMANN DIESEL	58W	15.0	7.083	7.333	0.258
49	FARYMANN DIESEL	36A	8.0	14.833	10.250	0.275
49	FARYMANN DIESEL	75A	17.0	7.694	7.941	0.270
49	FARYMANN DIESEL	71A	16.5	7.927	7.879	0.270
49	FARYMANN DIESEL	114	30.8	4.946	5.292	0.258

Four-Stroke Compression Ignition Engines

Reference	Mfg	Model	Rated kW	Spec. Vol. l/kW	Spec. Wt. kg/kW	Min BSFC kg/kWh
49	FARYMANN DIESEL	21A	6.0	8.908	8.833	0.260
49	FIAT	8340.04	75.3	6.862	12.003	0.214
49	FIAT	8140.61	56.7	3.988	8.487	0.249
49	GARDNER	6LXCT	169.3		11.177	
49	GARDNER	6LXDT	205.2	6.160	9.220	
49	HINO MOTORS	EM100	114.0	8.621	6.491	
49	HINO MOTORS	EK130-T	173.0	9.581	6.069	
49	HINO MOTORS	EP100-T	127.0	8.913	6.063	
49	HINO MOTORS	WO4C-T	103.0	3.648	3.301	
49	HINO MOTORS	WO4D	84.5	4.327	3.716	
49	HINO MOTORS	EF750T	272.0	6.720	4.441	
49	HINO MOTORS	HO6C-T	151.0	5.060	3.616	
49	HINO MOTORS	P11C	239.0	7.626	3.791	
49	HINO MOTORS	EK100	198.0	7.669	4.949	
49	HINO MOTORS	WO6D	110.5	4.430	3.837	
49	HINO MOTORS	EP100-TI	212.5	5.327	7.999	
49	HINO MOTORS	EH700	91.0	8.127	5.495	
49	HINO MOTORS	WO4C-T	84.0	5.171	4.228	
49	HINO MOTORS	EM10U	174.0	8.505	4.828	
49	HINO MOTORS	EH700	121.0	5.903	4.298	
49	HINO MOTORS	P09C	232.0	7.220	3.953	
49	HINO MOTORS	HO6C-TI	138.0	5.873	4.203	
49	HINO MOTORS	HO6C-T	113.0	6.669	4.823	
49	HINO MOTORS	EF750	243.0	7.474	4.815	
49	HINO MOTORS	WO4C	77.5	4.848	4.052	
49	HINO MOTORS	HO7C	132.0	11.504	7.424	
49	HINO MOTORS	WO6D	87.0	6.374	4.828	
49	HINO MOTORS	EM100	163.0	5.962	4.540	
49	HINO MOTORS	EF750T	243.8	10.277	11.278	0.214
49	HINO MOTORS	EK200	198.0	6.428	5.202	
49	HINO MOTORS	EK100	153.0	9.193	6.405	
49	HINO MOTORS	EF750	186.0	11.876	6.290	
49	HINO MOTORS	WO4D	62.0	6.966	5.484	
49	HINO MOTORS	EP100-TI	214.0	5.940	4.028	
49	HINO MOTORS	HO6C-T	129.8	5.805	9.249	0.216
49	HINO MOTORS	EF750T	214.0	11.690	5.607	
49	HINO MOTORS	WO6E	121.0	4.046	3.471	
49	ISUZU MOTORS LIMITED	6BG1T	127.5	5.696	3.960	
49	ISUZU MOTORS LIMITED	UM6BD1MTC3	157.3	5.343	4.029	
49	ISUZU MOTORS LIMITED	QD-40	30.6	8.855	15.635	0.271
49	ISUZU MOTORS LIMITED	4HF1	99.0		3.384	
49	ISUZU MOTORS LIMITED	6BG1TC	147.0	6.624	3.878	
49	ISUZU MOTORS LIMITED	6BD1	113.3	6.234	4.102	
49	ISUZU MOTORS LIMITED	6BD1T	123.0	5.948	8.599	
49	ISUZU MOTORS LIMITED	2KC1	11.3	12.368	8.437	
49	ISUZU MOTORS LIMITED	QD-60	41.8	7.087	11.758	0.268
49	ISUZU MOTORS LIMITED	6WA1TC	280.0		3.857	
49	ISUZU MOTORS LIMITED	6SA1T	145.4	5.973	4.264	
49	ISUZU MOTORS LIMITED	4BD1T	76.1	6.390	4.299	
49	ISUZU MOTORS LIMITED	6BD1T	115.6	5.253	4.283	
49	ISUZU MOTORS LIMITED	6RB1	168.5	7.179	5.696	
49	ISUZU MOTORS LIMITED	4JB1	43.3	8.152	5.803	

Four-Stroke Compression Ignition Engines

Reference	Mfg	Model	Rated kW	Spec. Vol. l/kW	Spec. Wt. kg/kW	Min BSFC kg/kWh
49	ISUZU MOTORS LIMITED	6RB1T	196.9	7.571	5.435	
49	ISUZU MOTORS LIMITED	4BD1	61.9	7.106	5.203	
49	ISUZU MOTORS LIMITED	3KC1	17.5	9.399	5.878	
49	ISUZU MOTORS LIMITED	3KR1	22.0	9.595	6.001	
49	ISUZU MOTORS LIMITED	6BD1	96.9	6.740	4.694	
49	ISUZU MOTORS LIMITED	QD-90	58.2	7.938	11.932	0.225
49	ISUZU MOTORS LIMITED	C240	43.3	8.130	6.243	
49	ISUZU MOTORS LIMITED	C240	33.6	8.852	6.646	
49	ISUZU MOTORS LIMITED	3AB1	25.4	10.745	8.559	
49	ISUZU MOTORS LIMITED	6RA1T	210.0	9.293	4.929	0.213
49	ISUZU MOTORS LIMITED	6SA1T	164.1	4.917	3.444	0.226
49	ISUZU MOTORS LIMITED	6HE1-N	121.0		4.207	0.230
49	ISUZU MOTORS LIMITED	6HE1-S	143.0		3.559	0.230
49	ISUZU MOTORS LIMITED	6SA1	117.1	7.136	5.040	
49	ISUZU MOTORS LIMITED	6BB1	83.5	7.824	5.448	
49	ISUZU MOTORS LTD.	1.817 L 4FB1	38.0	7.127	4.579	
49	JOHN DEERE	6068D	97.0		6.062	
49	JOHN DEERE	6059D	89.0		5.820	
49	JOHN DEERE	3179D	43.0	6.698	7.512	
49	JOHN DEERE	6076H	183.0		4.339	
49	JOHN DEERE	4039D	60.0		7.033	
49	JOHN DEERE	6059T	123.0		4.268	
49	JOHN DEERE	4045T	86.0		5.663	
49	JOHN DEERE	4239A	87.0		5.253	
49	JOHN DEERE	4039T	82.0		5.329	
49	JOHN DEERE	6619A	225.0		4.929	
49	JOHN DEERE	6076A	168.0		4.946	
49	JOHN DEERE	3179T	59.0		5.593	
49	JOHN DEERE	4045D	63.0		7.524	
49	JOHN DEERE	6359A	131.0	4.350	4.733	
49	JOHN DEERE	6068T	130.0		4.631	
49	JOHN DEERE	6466A	168.5	4.928	10.681	0.216
49	KOMATSU	SA6D110-1	164.1	5.758	8.065	0.206
49	KOMATSU	6D125-1	152.9	6.446	12.187	0.211
49	KOMATSU	SA6D140	368.0	3.885	3.342	
49	KOMATSU	SA12V170	1102.9	4.248	8.755	
49	KOMATSU	S6D140	294.0	4.863	4.082	
49	KOMATSU	SA8V140	459.3	3.656	7.384	
49	KOMATSU	SA6D125-1	275.9	3.884	7.191	0.196
49	KUBOTA	D1105-B	18.6		6.222	
49	KUBOTA	D1005-B	19.4		5.983	
49	KUBOTA	V1205-B	23.5		5.662	
49	KUBOTA	D3200B	49.2	6.683	14.122	0.228
49	KUBOTA	V1505-B	24.6		5.405	
49	KUBOTA	WG750-B	17.2		3.597	
49	KUBOTA	D905-B	17.5		6.620	
49	KUBOTA	V4300B	65.6	6.124	12.816	0.225
49	KUBOTA	V1902B	31.3	7.422	13.666	0.262
49	KUBOTA	V1305-B	25.7		5.170	
49	KUBOTA	WG600-B	14.2		4.355	
49	M.A.N.	D2566MK	237.9	7.595	7.878	
49	M.A.N.	DO226MKF	146.2	5.041	6.486	

Four-Stroke Compression Ignition Engines

Reference	Mfg	Model	Rated kW	Spec. Vol. l/kW	Spec. Wt. kg/kW	Min BSFC kg/kWh
49	MACK	E6-350-4VHCMCAC	261.0		7.989	0.206
49	MITSUBISHI MOTORS CORP.	4D31T	89.5	4.555	7.264	
49	MITSUBISHI MOTORS CORP.	6D14	115.6	5.065	9.820	
49	MITSUBISHI MOTORS CORP.	6D16	136.1	5.323	3.564	
49	MITSUBISHI MOTORS CORP.	6D22T3	246.1	7.593	8.550	
49	MITSUBISHI MOTORS CORP.	6D22	167.8	12.176	11.759	
49	MITSUBISHI MOTORS CORP.	6D14T	145.4	4.928	8.259	
49	MWM	D 226-4	62.6	5.462	12.500	
49	MWM	D 226.6T	114.1	5.063	9.221	
49	NAVISTAR	T 444E: HEUI	160.3	3.121		
49	NAVISTAR	DT-239	67.1	6.521	13.783	0.253
49	NAVISTAR	6.9 L	126.8	5.180	6.705	
49	NISSAN DIESEL	SD1604	25.0		7.197	
49	NISSAN DIESEL	PE6	151.4	3.691	12.089	
49	NISSAN DIESEL	SD33	65.6	7.269	10.073	
49	NISSAN DIESEL	PE6-TA	216.3		10.173	
49	NISSAN DIESEL	SD226J	34.6		8.678	
49	NISSAN DIESEL	TD2704	51.5		4.855	
49	NISSAN DIESEL	BD3004	55.2		4.714	
49	NISSAN DIESEL	TD2304	44.1		5.665	
49	NISSAN DIESEL	ND6	97.7	9.528	12.868	
49	NISSAN DIESEL	FD3504	62.5		4.878	
49	NISSAN DIESEL	NE6	130.5		4.904	
49	NISSAN DIESEL	SD3304	53.0		5.665	
49	NISSAN DIESEL	SD336J	53.7		7.171	
49	NISSAN DIESEL	SD22	44.7	5.612	10.594	
49	NISSAN DIESEL	FD3304	58.8		5.150	
49	NISSAN DIESEL	FD35TA16	95.6		6.223	
49	NISSAN DIESEL	FD614	84.6		5.403	
49	NISSAN DIESEL	SD2204	34.6		6.219	
49	NISSAN DIESEL	FD35T04	77.2		4.208	
49	NISSAN DIESEL	FD33T04	73.6		4.351	
49	NISSAN DIESEL	SD33T6	61.8		8.498	
49	NISSAN DIESEL	SD2504	39.7		5.539	
49	NISSAN DIESEL	ND6T	120.8	15.433	11.225	
49	NISSAN DIESEL	FD606	84.6		8.631	
49	NISSAN DIESEL	NE6T	156.6		4.246	
49	NISSAN DIESEL	FE6	126.8		4.023	
49	NISSAN DIESEL	SD33T	78.3	5.281	8.289	
49	PERKINS	4.2032	44.0	7.980	11.728	0.255
49	PERKINS	4.108	32.8	6.154	15.544	0.257
49	PERKINS	T6.60 CC	134.2	4.498	8.568	
49	PERKINS	TV8.640	187.2	4.564	10.258	
49	PERKINS	T4.40 CC	89.5	5.454	8.694	
49	PEUGEOT SA	2.3 L XD2S	60.7		3.542	
49	PEUGEOT SA	2.3 L XD2	51.5		3.883	
49	POYAUD	060212	131.2	3.553	8.648	
49	POYAUD	062030S	175.2	6.072	10.985	
49	RENAULT	062045 MIDR	220.0	4.965	8.819	
49	RENAULT	063540	231.2	6.301	10.962	
49	RENAULT	720	65.6	5.047	10.408	
49	SCANIA	DSC11.03	254.3		8.585	0.204

Four-Stroke Compression Ignition Engines

Reference	Mfg	Model	Rated kW	Spec. Vol. l/kW	Spec. Wt. kg/kW	Min BSFC kg/kWh
49	SCANIA	DSC9	211.8	5.198	8.330	
49	SCANIA	DS14.01	324.4	5.456	8.086	0.209
49	SSANGYONG HEAVY IND.	WARTSILA 12V32	4920.0	15.618	15.152	
49	SSANGYONG HEAVY IND.	MAN B&W 9L28/32H	1980.0	21.668	12.741	
49	SSANGYONG HEAVY IND.	WARTSILA 12V22	2100.0	9.405	13.074	
49	SSANGYONG HEAVY IND.	WARTSILA 8V22	1400.0	8.691	12.662	
49	SSANGYONG HEAVY IND.	WARTSILA 18V32	7380.0	11.890	6.898	
49	SSANGYONG HEAVY IND.	WARTSILA 16V32	6560.0	14.345	12.611	
49	SSANGYONG HEAVY IND.	WARTSILA 6R22/26	1125.0	12.819	7.515	
49	SSANGYONG HEAVY IND.	WARTSILA 16V32	6560.0	11.315	7.206	
49	SSANGYONG HEAVY IND.	WARTSILA 6R22/26	1065.0	12.475	14.938	
49	SSANGYONG HEAVY IND.	MAN B&W 6L28/32H	1320.0	19.494	14.291	
49	SSANGYONG HEAVY IND.	WARTSILA 16V22	2800.0	10.434	6.591	
49	SSANGYONG HEAVY IND.	MAN B&W 8L28/32H	1760.0	21.968	12.887	
49	SSANGYONG HEAVY IND.	WARTSILA 4R22/26	710.0	15.274	19.462	
49	SSANGYONG HEAVY IND.	WARTSILA 4R32	1640.0	16.340	18.847	
49	SSANGYONG HEAVY IND.	WARTSILA 9R32	3690.0	16.479	17.246	
49	SSANGYONG HEAVY IND.	WARTSILA 8R22/26	1500.0	11.384	6.848	
49	SSANGYONG HEAVY IND.	MAN B&W 5L23/30	800.0	20.591	13.807	
49	SSANGYONG HEAVY IND.	MAN B&W T23LH-4E	550.0	14.274	16.033	
49	SSANGYONG HEAVY IND.	WARTSILA 8R22	1400.0	12.197	7.338	
49	SSANGYONG HEAVY IND.	WARTSILA 8R32	3280.0	17.068	17.461	
49	SSANGYONG HEAVY IND.	MAN B&W 7L28/32H	1540.0	22.099	13.312	
49	SSANGYONG HEAVY IND.	WARTSILA 8R22	1400.0	14.970	13.506	
49	SSANGYONG HEAVY IND.	WARTSILA 8V22	1400.0	12.838	6.558	
49	SSANGYONG HEAVY IND.	WARTSILA 4R22	700.0	16.811	9.870	
49	SSANGYONG HEAVY IND.	WARTSILA 16V22	2800.0	8.948	12.240	
49	SSANGYONG HEAVY IND.	WARTSILA 8R32	3280.0	15.361	9.839	
49	SSANGYONG HEAVY IND.	WARTSILA 9R32	3690.0	16.386	9.855	
49	SSANGYONG HEAVY IND.	MAN B&W 8L23/30	1280.0	20.516	11.222	
49	SSANGYONG HEAVY IND.	WARTSILA 6R32	2460.0	17.454	9.608	
49	SSANGYONG HEAVY IND.	WARTSILA 4R22	700.0	17.403	19.740	
49	SSANGYONG HEAVY IND.	WARTSILA 12V22	2100.0	11.864	6.667	
49	SSANGYONG HEAVY IND.	MAN B&W 7L23/30	1120.0	17.929	11.607	
49	SSANGYONG HEAVY IND.	MAN B&W 6L23/30	960.0	19.038	12.216	
49	SSANGYONG HEAVY IND.	WARTSILA 6R22	1050.0	13.735	8.052	
49	SSANGYONG HEAVY IND.	WARTSILA 4R32	1640.0	20.008	10.255	
49	SSANGYONG HEAVY IND.	WARTSILA 4R22/26	750.0	15.690	9.212	
49	SSANGYONG HEAVY IND.	WARTSILA 18V32	7380.0	14.223	12.318	
49	SSANGYONG HEAVY IND.	SULZER 9S20	1440.0	17.022	8.144	
49	SSANGYONG HEAVY IND.	WARTSILA 6R32	2460.0	14.485	16.630	
49	SSANGYONG HEAVY IND.	SULZER 8S20	1280.0	17.763	8.381	
49	SSANGYONG HEAVY IND.	MAN B&W 18V28/32H	3960.0	15.790	10.813	
49	SSANGYONG HEAVY IND.	SULZER 6S20	960.0	18.384	8.902	
49	SSANGYONG HEAVY IND.	WARTSILA 6R22	1050.0	14.304	15.152	
49	SSANGYONG HEAVY IND.	WARTSILA 8R22/26	1420.0	13.000	13.316	
49	SSANGYONG HEAVY IND.	MAN B&W 12V28/32H	3585.0	9.679	8.381	
49	SSANGYONG HEAVY IND.	MAN B&W 5L28/32H	1100.0	21.004	15.000	
49	SSANGYONG HEAVY IND.	MAN B&W 16V28/32H	4785.0	11.081	8.673	
49	SSANGYONG HEAVY IND.	WARTSILA 12V32	4920.0	13.802	7.945	
49	STEYR	610	99.2	6.358	11.999	0.231
49	STEYR	615.68	230.4	3.575	7.725	

Four-Stroke Compression Ignition Engines

Reference	Mfg	Model	Rated kW	Spec. Vol. l/kW	Spec. Wt. kg/kW	Min BSFC kg/kWh
49	STEYR	815.67	249.1	5.250	9.207	
49	VOLKSWAGEN AG	074.Y	53.0	4.565	3.302	
49	VOLKSWAGEN AG	068.D	37.0	5.548	3.486	
49	VOLKSWAGEN AG	028.B	45.0	4.586	2.889	
49	VOLVO	TD 121F	283.4	5.376	8.470	
49	VOLVO	TD 61 F	152.1	6.322	8.414	
49	VOLVO	TD 101F	220.0	4.881	9.910	
49	WARTSILA	9R20	1170.0	10.999	10.085	
49	WARTSILA	4R20	520.0	14.229	12.308	
49	YANMAR	3TNA72E	15.7	6.610	5.428	
49	YANMAR	4TN82E	35.0	5.555	5.193	
49	YANMAR	3TNC78C	22.4	6.373	5.141	
49	YANMAR	3TN66E	12.3	7.525	5.039	
49	YANMAR	4TN82TE	41.0	5.407	4.560	
49	YANMAR	4TN84E	36.5	5.329	4.926	
49	YANMAR	3TN84E	27.2	6.141	5.327	
49	YANMAR	3TN100E	44.2	5.659	4.749	
49	YANMAR	2TN66E	8.2	7.758	6.096	
49	YANMAR	4TN84TE	42.5	5.217	4.352	
49	YANMAR	3TN82E	26.1	6.404	5.556	
49	YANMAR	3TN75E	18.3	7.803	6.568	
49	YANMAR	3TNC78E	22.4	6.373	5.141	
49	YANMAR	3TN82TE	29.1	6.457	5.158	
49	YANMAR	4TN100E	57.1	5.171	4.377	
49	YANMAR	4TN100TE	74.2	4.294	3.437	
51	Audi	2.5-L	88.0			0.198
52	Ford	1.8-L	55.0			0.255
53	Mitsubishi	4M40	69.0			0.249
53	Mitsubishi	4M40-TI	92.0			0.249

Two-Stroke Spark-Ignition Engines

Reference	Mfg	Model	Rated kW	Spec. Vol. l/kW	Spec. Wt. kg/kW	Min BSFC kg/kWh
54	Peugeot	IAPAC SCRE	28.00			0.288
16	Confidential	Confidential	77.00		0.909	
16	Confidential	Confidential	82.00		0.915	
55	URM	500	29.75		1.143	
55	QUB	500	48.12			0.358

Two-Stroke Compression Ignition Engines

Reference	Mfg	Model	Rated kW	Spec. Vol. l/kW	Spec. Wt. kg/kW	Min BSFC kg/kWh
17	SwRI	UAV	22.37	2.079	0.710	0.247
49	DETROIT DIESEL	2-71	47.72	12.164	20.116	0.285
49	DETROIT DIESEL	3-53N	73.08	7.078	13.205	0.279
49	DETROIT DIESEL	4-53N	101.60	6.252	10.925	0.269
49	DETROIT DIESEL	6-71N	186.60	7.141	11.522	0.254
49	DETROIT DIESEL	12V-92N	397.20	6.630	9.844	0.252
49	DETROIT DIESEL	12V-149N	592.80	9.252	14.322	0.249
49	DETROIT DIESEL	16V-149	797.89	7.320	13.147	0.249
49	DETROIT DIESEL	8V-71N	248.80	6.157	9.285	0.246
49	DETROIT DIESEL	4-71N	124.40	6.739	14.309	0.246
49	DETROIT DIESEL	6V-92N	217.20	5.670	9.024	0.241
49	DETROIT DIESEL	8V-92N	289.60	5.402	8.097	0.240
49	DETROIT DIESEL	4-53T	137.95	5.232	9.134	0.237
49	DETROIT DIESEL	3-53T	104.40	6.022	9.579	0.234
49	DETROIT DIESEL	8V-149TI	596.80	7.648	10.054	0.231
49	DETROIT DIESEL	12V-149TIB	1006.68	6.383	9.000	0.224
49	DETROIT DIESEL	4-71T	157.34	6.357	11.631	0.221
49	DETROIT DIESEL	16V-92TA	715.86	5.015	6.761	0.221
49	DETROIT DIESEL	6V-53T	238.80	4.060	7.098	0.220
49	DETROIT DIESEL	16V-149TIB	1342.24	5.632	8.352	0.218
49	DETROIT DIESEL	8V-92TA	357.93	3.741	6.761	0.217
49	DETROIT DIESEL	12V-92TA	805.92	3.509	5.311	0.215
49	DETROIT DIESEL	8V-71TA	298.28	5.822	8.365	0.214
49	DETROIT DIESEL	6V-92TA	354.60	3.136	5.697	0.212
49	DETROIT DIESEL	6-71TA	324.60	4.690	6.762	0.209
49	DIESEL UNITED, LTD.	7RTA84T	27184.07	37.980		
49	DIESEL UNITED, LTD.	7RTA52	9936.60	23.439		
49	DIESEL UNITED, LTD.	9RTA84T	34950.94	38.181		
49	DIESEL UNITED, LTD.	7RTA76	18946.47	34.462		
49	DIESEL UNITED, LTD.	10RTA84C	38245.98	30.335		
49	DIESEL UNITED, LTD.	5RTA52	7097.57	25.686		
49	DIESEL UNITED, LTD.	6RTA52	8517.09	24.375		
49	DIESEL UNITED, LTD.	12RTA84M	44747.80	35.529		
49	DIESEL UNITED, LTD.	6RTA62	12179.87	27.839		
49	DIESEL UNITED, LTD.	4RTA52	5678.06	27.652		
49	DIESEL UNITED, LTD.	6RTA76	16239.83	35.626		
49	DIESEL UNITED, LTD.	7RTA62	14209.85	26.791		
49	DIESEL UNITED, LTD.	8RTA62	16239.83	26.006		
49	DIESEL UNITED, LTD.	8RTA84M	29831.86	38.705		
49	DIESEL UNITED, LTD.	7RTA84M	26102.88	37.461		
49	DIESEL UNITED, LTD.	5RTA76	13533.19	37.256		
49	DIESEL UNITED, LTD.	8RTA76	21653.11	33.589		
49	DIESEL UNITED, LTD.	10RTA76	27066.39	34.139		
49	DIESEL UNITED, LTD.	5RTA84C	19122.99	33.599		
49	DIESEL UNITED, LTD.	6RTA72	16493.23	31.679		
49	DIESEL UNITED, LTD.	4RTA62	8119.92	31.505		
49	DIESEL UNITED, LTD.	8RTA84C	30596.78	31.903		
49	DIESEL UNITED, LTD.	8RTA52	11429.66	22.590		
49	DIESEL UNITED, LTD.	9RTA84C	34421.38	31.032		
49	DIESEL UNITED, LTD.	5RTA72	13717.07	33.375		
49	DIESEL UNITED, LTD.	4RTA84C	15298.39	35.982		
49	DIESEL UNITED, LTD.	12RTA84C	45895.18	29.290		

Two-Stroke Compression Ignition Engines

Reference	Mfg	Model	Rated kW	Spec. Vol. l/kW	Spec. Wt. kg/kW	Min BSFC kg/kWh
49	DIESEL UNITED, LTD.	8RTA72	21947.31	29.701		
49	DIESEL UNITED, LTD.	7RTA72	19203.90	30.576		
49	DIESEL UNITED, LTD.	7RTA84C	26772.19	30.874		
49	DIESEL UNITED, LTD.	9RTA84M	33538.78	37.671		
49	DIESEL UNITED, LTD.	6RTA84C	22947.59	32.009		
49	DIESEL UNITED, LTD.	12RTA76	32479.66	33.028		
49	DIESEL UNITED, LTD.	5RTA62	10149.89	29.305		
49	DIESEL UNITED, LTD.	10RTA84M	37289.83	36.800		
49	SSANGYONG HEAVY INI	MAN B&W L35MC	3920.00		17.625	
49	FAIRBANKS MORSE EN(	PC2.5	6530.00	14.191	11.593	
49	FAIRBANKS MORSE EN(	38ETDD8-1/8	3165.00	15.272	12.351	
49	FAIRBANKS MORSE EN(	PC2.5	5600.00	14.979	11.786	
49	SSANGYONG HEAVY INI	MAN B&W L35MC	3360.00		17.857	
49	FAIRBANKS MORSE EN(	PC2.5	8400.00	17.085	10.714	
49	FAIRBANKS MORSE EN(	38ETD8-1/8	1580.00	23.142	17.837	
49	FAIRBANKS MORSE EN(	PC2.5	7465.00	15.143	11.119	
49	SSANGYONG HEAVY INI	MAN B&W L35MC	4480.00		17.045	
49	FAIRBANKS MORSE EN(	38ETD8-1/8	2370.00	19.975	14.384	
49	FAIRBANKS MORSE EN(	38ETDS8-1/8	2585.00	18.726	15.122	
49	SSANGYONG HEAVY INI	MAN B&W S26MC	1825.00		14.944	
49	SSANGYONG HEAVY INI	MAN B&W S26MC	2190.00		14.529	
49	SSANGYONG HEAVY INI	MAN B&W S26MC	2920.00		14.010	
49	FAIRBANKS MORSE EN(	38ETDS8-1/8	2150.00	20.816	16.490	
49	SSANGYONG HEAVY INI	MAN B&W S26MC	1460.00		15.567	
49	SSANGYONG HEAVY INI	MAN B&W S26MC	2555.00		14.232	
49	FAIRBANKS MORSE EN(	38ETDS8-1/8	1720.00	19.984	18.499	
49	DIESEL UNITED, LTD.	4RTA76	10826.55	39.700		
49	DIESEL UNITED, LTD.	4RTA84M	14915.93	43.674		
49	DIESEL UNITED, LTD.	4RTA72	10973.65	35.824		
49	DIESEL UNITED, LTD.	8RTA84T	31067.50	39.308		
49	DIESEL UNITED, LTD.	6RTA84M	22373.90	38.842		
49	DIESEL UNITED, LTD.	9RTA76	24359.75	35.089		
49	DIESEL UNITED, LTD.	5RTA84T	19417.19	41.508		
49	DIESEL UNITED, LTD.	5RTA84M	18644.92	40.775		
49	DIESEL UNITED, LTD.	6RTA84T	23300.63	39.450		
49	SSANGYONG HEAVY INI	MAN B&W L35MCE	3600.00		21.212	
49	SSANGYONG HEAVY INI	MAN B&W L35MCE	3150.00		21.934	
49	SSANGYONG HEAVY INI	MAN B&W L35MC	2800.00		18.831	
49	SSANGYONG HEAVY INI	MAN B&W L35MC	2240.00		20.698	
49	SSANGYONG HEAVY INI	MAN B&W L35MCE	2250.00		23.434	
49	SSANGYONG HEAVY INI	MAN B&W L35MCE	1800.00		25.758	
49	SSANGYONG HEAVY INI	MAN B&W L35MCE	2700.00		22.222	
49	FAIRBANKS MORSE EN(	38ETDS8-1/8	1240.00	28.296	22.727	

Rotary Engines

Reference	Mfg	Model	Rated kW	Spec. Vol. l/kW	Spec. Wt. kg/kW	Min BSFC kg/kWh
1	Predicted best attainable		30.00	1.000	1.300	0.300
24	Alvis	AR731	28.30	0.360	0.350	0.316
2	Norton		30.00	1.400	0.700	0.300
2	Rotac		25.00	1.200	1.100	0.360
56	Yanmar	R220	16.55			0.382
56	Yanmar	R450	36.78			0.382
57	Norton, AAI Modifications	NR631	28.50		1.195	0.320
58	JTDI Dem/Val	2116 R	560.00			0.230
58	JTDI	580 Series	846.37			0.224
58	JTDI	580 Series	149.14			0.268
58	JTDI	580 Series	300.00		0.760	0.237

Two-Stroke Compression Ignition Engines

Reference	Mfg	Model	Rated kW	Spec. Vol. l/kW	Spec. Wt. kg/kW	Min BSFC kg/kWh
17	SwRI	UAV	22.37	2.079	0.710	0.247
49	DETROIT DIESEL	2-71	47.72	12.164	20.116	0.285
49	DETROIT DIESEL	3-53N	73.08	7.078	13.205	0.279
49	DETROIT DIESEL	4-53N	101.60	6.252	10.925	0.269
49	DETROIT DIESEL	6-71N	186.60	7.141	11.522	0.254
49	DETROIT DIESEL	12V-92N	397.20	6.630	9.844	0.252
49	DETROIT DIESEL	12V-149N	592.80	9.252	14.322	0.249
49	DETROIT DIESEL	16V-149	797.89	7.320	13.147	0.249
49	DETROIT DIESEL	8V-71N	248.80	6.157	9.285	0.246
49	DETROIT DIESEL	4-71N	124.40	6.739	14.309	0.246
49	DETROIT DIESEL	6V-92N	217.20	5.670	9.024	0.241
49	DETROIT DIESEL	8V-92N	289.60	5.402	8.097	0.240
49	DETROIT DIESEL	4-53T	137.95	5.232	9.134	0.237
49	DETROIT DIESEL	3-53T	104.40	6.022	9.579	0.234
49	DETROIT DIESEL	8V-149TI	596.80	7.648	10.054	0.231
49	DETROIT DIESEL	12V-149TIB	1006.68	6.383	9.000	0.224
49	DETROIT DIESEL	4-71T	157.34	6.357	11.631	0.221
49	DETROIT DIESEL	16V-92TA	715.86	5.015	6.761	0.221
49	DETROIT DIESEL	6V-53T	238.80	4.060	7.098	0.220
49	DETROIT DIESEL	16V-149TIB	1342.24	5.632	8.352	0.218
49	DETROIT DIESEL	8V-92TA	357.93	3.741	6.761	0.217
49	DETROIT DIESEL	12V-92TA	805.92	3.509	5.311	0.215
49	DETROIT DIESEL	8V-71TA	298.28	5.822	8.365	0.214
49	DETROIT DIESEL	6V-92TA	354.60	3.136	5.697	0.212
49	DETROIT DIESEL	6-71TA	324.60	4.690	6.762	0.209
49	DIESEL UNITED, LTD.	7RTA84T	27184.07	37.980		
49	DIESEL UNITED, LTD.	7RTA52	9936.60	23.439		
49	DIESEL UNITED, LTD.	9RTA84T	34950.94	38.181		
49	DIESEL UNITED, LTD.	7RTA76	18946.47	34.462		
49	DIESEL UNITED, LTD.	10RTA84C	38245.98	30.335		
49	DIESEL UNITED, LTD.	5RTA52	7097.57	25.686		
49	DIESEL UNITED, LTD.	6RTA52	8517.09	24.375		
49	DIESEL UNITED, LTD.	12RTA84M	44747.80	35.529		
49	DIESEL UNITED, LTD.	6RTA62	12179.87	27.839		
49	DIESEL UNITED, LTD.	4RTA52	5678.06	27.652		
49	DIESEL UNITED, LTD.	6RTA76	16239.83	35.626		
49	DIESEL UNITED, LTD.	7RTA62	14209.85	26.791		
49	DIESEL UNITED, LTD.	8RTA62	16239.83	26.006		
49	DIESEL UNITED, LTD.	8RTA84M	29831.86	38.705		
49	DIESEL UNITED, LTD.	7RTA84M	26102.88	37.461		
49	DIESEL UNITED, LTD.	5RTA76	13533.19	37.256		
49	DIESEL UNITED, LTD.	8RTA76	21653.11	33.589		
49	DIESEL UNITED, LTD.	10RTA76	27066.39	34.139		
49	DIESEL UNITED, LTD.	5RTA84C	19122.99	33.599		
49	DIESEL UNITED, LTD.	6RTA72	16493.23	31.679		
49	DIESEL UNITED, LTD.	4RTA62	8119.92	31.505		
49	DIESEL UNITED, LTD.	8RTA84C	30596.78	31.903		
49	DIESEL UNITED, LTD.	8RTA52	11429.66	22.590		
49	DIESEL UNITED, LTD.	9RTA84C	34421.38	31.032		
49	DIESEL UNITED, LTD.	5RTA72	13717.07	33.375		
49	DIESEL UNITED, LTD.	4RTA84C	15298.39	35.982		
49	DIESEL UNITED, LTD.	12RTA84C	45895.18	29.290		

Two-Stroke Compression Ignition Engines

Reference	Mfg	Model	Rated kW	Spec. Vol. l/kW	Spec. Wt. kg/kW	Min BSFC kg/kWh
49	DIESEL UNITED, LTD.	8RTA72	21947.31	29.701		
49	DIESEL UNITED, LTD.	7RTA72	19203.90	30.576		
49	DIESEL UNITED, LTD.	7RTA84C	26772.19	30.874		
49	DIESEL UNITED, LTD.	9RTA84M	33538.78	37.671		
49	DIESEL UNITED, LTD.	6RTA84C	22947.59	32.009		
49	DIESEL UNITED, LTD.	12RTA76	32479.66	33.028		
49	DIESEL UNITED, LTD.	5RTA62	10149.89	29.305		
49	DIESEL UNITED, LTD.	10RTA84M	37289.83	36.800		
49	SSANGYONG HEAVY IND.	MAN B&W L35MC	3920.00		17.625	
49	FAIRBANKS MORSE ENGINES	PC2.5	6530.00	14.191	11.593	
49	FAIRBANKS MORSE ENGINES	38ETDD8-1/8	3165.00	15.272	12.351	
49	FAIRBANKS MORSE ENGINES	PC2.5	5600.00	14.979	11.786	
49	SSANGYONG HEAVY IND.	MAN B&W L35MC	3360.00		17.857	
49	FAIRBANKS MORSE ENGINES	PC2.5	8400.00	17.085	10.714	
49	FAIRBANKS MORSE ENGINES	38ETD8-1/8	1580.00	23.142	17.837	
49	FAIRBANKS MORSE ENGINES	PC2.5	7465.00	15.143	11.119	
49	SSANGYONG HEAVY IND.	MAN B&W L35MC	4480.00		17.045	
49	FAIRBANKS MORSE ENGINES	38ETD8-1/8	2370.00	19.975	14.384	
49	FAIRBANKS MORSE ENGINES	38ETDS8-1/8	2585.00	18.726	15.122	
49	SSANGYONG HEAVY IND.	MAN B&W S26MC	1825.00		14.944	
49	SSANGYONG HEAVY IND.	MAN B&W S26MC	2190.00		14.529	
49	SSANGYONG HEAVY IND.	MAN B&W S26MC	2920.00		14.010	
49	FAIRBANKS MORSE ENGINES	38ETDS8-1/8	2150.00	20.816	16.490	
49	SSANGYONG HEAVY IND.	MAN B&W S26MC	1460.00		15.567	
49	SSANGYONG HEAVY IND.	MAN B&W S26MC	2555.00		14.232	
49	FAIRBANKS MORSE ENGINES	38ETDS8-1/8	1720.00	19.984	18.499	
49	DIESEL UNITED, LTD.	4RTA76	10826.55	39.700		
49	DIESEL UNITED, LTD.	4RTA84M	14915.93	43.674		
49	DIESEL UNITED, LTD.	4RTA72	10973.65	35.824		
49	DIESEL UNITED, LTD.	8RTA84T	31067.50	39.308		
49	DIESEL UNITED, LTD.	6RTA84M	22373.90	38.842		
49	DIESEL UNITED, LTD.	9RTA76	24359.75	35.089		
49	DIESEL UNITED, LTD.	5RTA84T	19417.19	41.508		
49	DIESEL UNITED, LTD.	5RTA84M	18644.92	40.775		
49	DIESEL UNITED, LTD.	6RTA84T	23300.63	39.450		
49	SSANGYONG HEAVY IND.	MAN B&W L35MCE	3600.00		21.212	
49	SSANGYONG HEAVY IND.	MAN B&W L35MCE	3150.00		21.934	
49	SSANGYONG HEAVY IND.	MAN B&W L35MC	2800.00		18.831	
49	SSANGYONG HEAVY IND.	MAN B&W L35MC	2240.00		20.698	
49	SSANGYONG HEAVY IND.	MAN B&W L35MCE	2250.00		23.434	
49	SSANGYONG HEAVY IND.	MAN B&W L35MCE	1800.00		25.758	
49	SSANGYONG HEAVY IND.	MAN B&W L35MCE	2700.00		22.222	
49	FAIRBANKS MORSE ENGINES	38ETDS8-1/8	1240.00	28.296	22.727	

DISTRIBUTION LIST

Department of Defense

DEFENSE TECH INFO CTR 12
CAMERON STATION
ALEXANDRIA VA 22314

ODUSD
ATTN: (L) MRM 1
PETROLEUM STAFF ANALYST
PENTAGON
WASHINGTON DC 20301-8000

ODUSD
ATTN: (ES) CI 1
400 ARMY NAVY DR
STE 206
ARLINGTON VA 22202

DIR DLA
ATTN: DLA MMSLP 1
8725 JOHN J KINGMAN RD
STE 2533
FT BELVOIR VA 22060-6221

DIR ADV RSCH PROJ AGENCY
ATTN: ARPA/ASTO 10
3701 N FAIRFAX DR
ARLINGTON VA 22203-1714

Department of the Army

HQDA
ATTN: DALO TSE 1
500 PENTAGON
WASHINGTON DC 20310-0500

SARDA
ATTN: SARD TT 1
PENTAGON
WASHINGTON DC 20310-0103

CDR AMC
ATTN: AMCRD S 1
AMCRD E 1
5001 EISENHOWER AVE
ALEXANDRIA VA 22333-0001

CDR ARMY TACOM
ATTN: AMSTA IM LMM 1
AMSTA IM LMB 1
AMSTA IM LMT 1
AMSTA TR NAC 1
AMSTA TR R 1
AMSTA TR D 1
AMSTA TR M 1
AMSTA TR M (C RAFFA) 1
AMSTA TR M (D HERRERA) 1
AMSTA TR M (R MUNT) 1
AMCPM ATP 1
USMC LNO 1
AMCPM LAV 1
AMCPM M113/M60 1
AMCPM CCE/SMHE 1
WARREN MI 48397-5000

MOBILITY TECH CTR BELVOIR
ATTN: AMSTA RBF (M E LEPERA) 10
AMSTA RBXA (R E TOBEY) 1
10115 GRIDLEY RD STE 128
FT BELVOIR VA 22060-5843

PROG EXEC OFFICER
ARMORED SYS MODERNIZATION
ATTN: SFAE ASM H 1
CDR TACOM
WARREN MI 48397-5000

PROG EXEC OFFICER
TACTICAL WHEELED VEHICLES
ATTN: SFAE TWV TVSP 1
SFAE TWV FMTV 1
SFAE TWV PLS 1
CDR TACOM
WARREN MI 48397-5000

PROG MGR
UNMANNED GROUND VEH
ATTN: AMCPM UG 1
REDSTONE ARSENAL
AL 35898-8060

DIR
ARMY RSCH LAB
ATTN: AMSRL PB P 1
2800 POWDER MILL RD
ADELPHIA MD 20783-1145

VEHICLE PROPULSION DIR
ATTN: AMSRL VP (MS 77 12) 1
NASA LEWIS RSCH CTR
21000 BROOKPARK RD
CLEVELAND OH 44135

CDR ARO
ATTN: AMXRO EN (D MANN) 1
RSCH TRIANGLE PK
NC 27709-2211

CDR ARMY ATCOM
ATTN: AMSAT I WM 1
AMSAT R EP (V EDWARD) 1
4300 GOODFELLOW BLVD
ST LOUIS MO 63120-1798

CDR AVIA APPL TECH DIR
ATTN: AMSAT R TP (H MORROW) 1
FT EUSTIS VA 23604-5577

CDR ARMY SOLDIER SPT CMD
ATTN: SATNC US (J SIEGEL) 1
SATNC UE 1
NATICK MA 01760-5018

US ARMY INDUSTRIAL ENGRG ACTIVITY
ATTN: AMXIBP 1
ROCK ISLAND IL 61299-6000

CDR APC
ATTN: SATPC L 1
NEW CUMBERLAND PA 17070-5005

CDR ARMY TECOM
ATTN: AMSTE TA R 1
AMSTE TC D 1
APG MD 21005-5006

PROJ MGR PETROL WATER LOG
ATTN: AMCPM PWL 1
4300 GOODFELLOW BLVD
ST LOUIS MO 63120-1798

PROJ MGR MOBILE ELEC PWR
ATTN: AMCPM MEP T 1
AMCPM MEP L 1
7798 CISSNA RD STE 200
SPRINGFIELD VA 22150-3199

CDR TRADOC
ATTN: ATCD SL 5 1
INGALLS RD BLDG 163
FT MONROE VA 23651-5194

CDR ARMY ARMOR CTR
ATTN: ATSB CD ML 1
ATSB TSM T 1
FT KNOX KY 40121-5000

CDR ARMY QM SCHOOL
ATTN: ATSM PWD 1
FT LEE VA 23001-5000

CDR ARMY TRANS SCHOOL
ATTN: ATSP CD MS 1
FT EUSTIS VA 23604-5000

CDR ARMY ENGR SCHOOL
ATTN: ATSE CD 1
FT LEONARD WOOD
MO 65473-5000

CDR ARMY ABERDEEN TEST CTR
ATTN: STEAC EN 1
STEAC LI 1
STEAC AE 1
STEAC AA 1
APG MD 21005-5059

CDR ARMY YPG
ATTN: STEYP MT TL M 1
YUMA AZ 85365-9130

CDR ARMY CERL
ATTN: CECER EN 1
P O BOX 9005
CHAMPAIGN IL 61826-9005

Department of the Navy

OFC CHIEF NAVAL OPER
ATTN: DR A ROBERTS (N420) 1
2000 NAVY PENTAGON
WASHINGTON DC 20350-2000

CDR
NAVAL SEA SYSTEMS CMD
ATTN: SEA 03M3 1
2531 JEFFERSON DAVIS HWY
ARLINGTON VA 22242-5160

CDR
NAVAL SURFACE WARFARE CTR
ATTN: CODE 63 1
CODE 632 1
CODE 859 1
3A LEGGETT CIRCLE
ANNAPOLIS MD 21402-5067

Department of the Navy/U.S. Marine Corps

HQ USMC
ATTN: LPP 1
WASHINGTON DC 20380-0001

PROG MGR COMBAT SER SPT 1
MARINE CORPS SYS CMD
2033 BARNETT AVE STE 315
QUANTICO VA 22134-5080

PROG MGR GROUND WEAPONS 1
MARINE CORPS SYS CMD
2033 BARNETT AVE
QUANTICO VA 22134-5080

PROG MGR ENGR SYS 1
MARINE CORPS SYS CMD
2033 BARNETT AVE
QUANTICO VA 22134-5080

CDR 1
2ND MARINE DIV
PSC BOX 20090
CAMP LEJEUNNE
NC 28542-0090

CDR 1
1ST MARINE DIV
CAMP PENDLETON
CA 92055-5702

Department of the Air Force

HQ USAF/LGSF
ATTN: FUELS POLICY 1
1030 AIR FORCE PENTAGON
WASHINGTON DC 20330-1030

HQ USAF/LGTV
ATTN: VEH EQUIP/FACILITY 1
1030 AIR FORCE PENTAGON
WASHINGTON DC 20330-1030

SA ALC/SFT 1
1014 BILLY MITCHELL BLVD STE 1
KELLY AFB TX 78241-5603

SA ALC/LDPG
ATTN: D ELLIOTT 1
580 PERRIN BLDG 329
KELLY AFB TX 78241-6439

WR ALC/LVRS 1
225 OCMULGEE CT
ROBINS AFB
GA 31098-1647

Other Federal Agencies

NASA
LEWIS RESEARCH CENTER 1
CLEVELAND OH 44135

NIPER 1
P O BOX 2128
BARTLESVILLE OK 74005

DOE
CE 151 (MR RUSSELL) 1
1000 INDEPENDENCE AVE SW
WASHINGTON DC 20585

EPA
AIR POLLUTION CONTROL 1
2565 PLYMOUTH RD
ANN ARBOR MI 48105

Electronic References

Internet Locations

Note: The following URLs are current as of the date of publication

DOE Hybrid Propulsion Program sponsored by NREL- ***http://www.hev.doe.gov/***
On-line Resource Center

National Renewable Energy Lab ***-http://pix.nrel.gov:8020/basisbwdocs/public/homepubp.html***
Publications Database searchable by keyword also includes recent publications by subject one is HEV

Bibliography and Reference List related to Hybrid Electric Vehicles arranged by category - ***http://www.hev.doe.gov/general/bibli.html***

INEL Hybrid/Electric Vehicle Test Laboratory ***http://spiderman.inel.gov/dynamometer.html***

Partnership for a New Generation of Vehicles ***http://www.ta.doc.gov/pngv/***
Patent Archive

United States Council for Automotive Research ***http://www.uscar.org/***

US DOE Office of Transportation Technologies ***http://www.ott.doe.gov/***

Argonne National Laboratory - 21st Century Vehicles and Transportation ***http://www.es.anl.gov/htmls/projects.html#transportation***

DARPA HEV Home page ***http://web-ext2.darpa.mil/tto/ele_hyb.html***

ADDITIONAL REFERENCES

Note: refer to the order form following the bibliographies for ordering information.

AD-P006254/JAA

WRIGHT RESEARCH AND DEVELOPMENT CENTER
WRIGHT-PATTERSON AFB, OH

(U) Application of Advanced Technologies to Future Military Transports

DEC 1990 8 PAGES
PERSONAL AUTHORS: Clark, Rodney L.; Lange, Roy H.; Wagner, Richard D.

UNCLASSIFIED REPORT

ABSTRACT: (U) This paper addresses long range military transport technologies with emphasis on defining the potential benefits of the hybrid laminar flow control (HLFC) concept currently being flight tested in a cost shared NASA, USAF, and Boeing program. Results of 1990's global range transport study are presented showing the expected payoff from application of advanced technologies. The paper concludes with a technology forecast for military transports.

DESCRIPTORS: (U) BENEFITS, CONTROL, COSTS, HYBRID SYSTEMS, LAMINAR FLOW, TECHNOLOGY FORECASTING.

IDENTIFIERS: (U) *MILITARY AIRCRAFT, *JET TRANSPORT, AIRCRAFT.

AD-A336935/JAA

SANDIA CORP
ALBUQUERQUE, NM

(U) Recycling Readiness of Advanced Batteries for Electric Vehicles

SEP 1997 14 PAGES
PERSONAL AUTHORS: Jungst, Rudolph G.

UNCLASSIFIED REPORT

ABSTRACT: (U) Maximizing the reclamation/recycle of electric-vehicle (EV) batteries is considered to be essential for the successful commercialization of this technology. Since the early 1990s, the US Department of Energy has sponsored the ad hoc advanced battery readiness working group to review this and other possible barriers to the widespread use of EVs, such as battery shipping and in- vehicle safety. Regulation is currently the main force for growth in EV numbers and projections for the states that have zero- emission vehicle (ZEV) programs indicate about 200,000 of these vehicles would be offered to the public in 2003 to meet those requirements. The ad hoc advanced battery readiness working group has identified a matrix of battery technologies that could see use in EVs and has been tracking the state of readiness of recycling processes for each of them. Lead-acid, nickel/metal hydride, and lithium-ion are the three EV battery technologies proposed by the major automotive manufacturers affected by ZEV requirements. Recycling approaches for the two advanced battery systems on this list are partly defined, but could be modified to recover more value from end-of-life batteries.

DESCRIPTORS: (U) *STORAGE BATTERIES, *ELECTRIC PROPULSION, *ELECTRIC AUTOMOBILES, IONS, HYDRIDES, OPERATIONAL READINESS, TRACKING, LITHIUM BATTERIES, AUTOMOTIVE COMPONENTS, LEAD ACID BATTERIES.

IDENTIFIERS: (U) *ELECTRIC VEHICLES, DOE COLLECTION, RECYCLING READINESS, ZEV(ZERO EMISSION VEHICLE), NICKEL/METAL HYDRIDE BATTERIES

AD-A335961/JAA

MILLEN (ROD) SPECIAL VEHICLES
HUNTINGTON BEACH, CA

(U) Joint Tactical Electric Vehicle Differential Development

DESCRIPTIVE NOTE: Final report
APR 1996 9 PAGES

UNCLASSIFIED REPORT

ABSTRACT: (U) As part of Rod Millen special vehicle's contract number MDA972-95-1-0011 (ARPA RA94-24 program), effective April 1,1996, under the aegis of Calstart's propulsion system development project for advanced hybrid reconnaissance vehicles effort, the joint tactical electric vehicle (JTEV) differentials were to be evaluated with the intent of improving the overall performance level of the vehicle. JTEV's current drive system incorporates a Weismann locker differential system to allow the rotational rate of the wheels to vary from left to right across the vehicle, and allows the wheel with the most traction to receive the full driving torque available. This type of drive was selected for maximum mobility in an off-the- shelf system. This system has the advantage of always providing drive to the ground, but under very poor or rapidly changing traction conditions, it has the potential to overload the driving wheel and break traction, thus shifting all drive to the opposite wheel.

DESCRIPTORS: (U) *MILITARY VEHICLES, *VEHICLE EQUIPMENT, GROUND LEVEL, MOBILITY, OFF THE SHELF EQUIPMENT, RATES, PROPULSION SYSTEMS, SHIFTING, TRACTION, TACTICAL RECONNAISSANCE, WHEELS, DRIVES, HYBRID SYSTEMS, HANDLING, ROTATION, OVERLOAD, TORQUE, ELECTRIC PROPULSION.

IDENTIFIERS: (U) JTEV(JOINT TACTICAL ELECTRIC VEHICLE)

AD-A335278/JAA

AEROVIRONMENT INC
MONROVIA, CA

(U) Development of a Woven-Grid Quasi-Bipolar Battery

DESCRIPTIVE NOTE: Final report 1 JUL-31 DEC 97
15 JAN 1998 50 PAGES
PERSONAL AUTHORS: Tokumaru, P.; Rippel, W.; Zambrano, T.

UNCLASSIFIED REPORT

ABSTRACT: (U) This report describes an analytical and experimental investigation of Aerovironment's quasi-bipolar battery concept. The modeling battery design part of the study demonstrates that there is a trade-off between thermal and specified electrical performance. Even so, quasi-bipolar batteries can be designed, with ten times better thermal uniformity, that meet or exceed current state of the art hybrid electric vehicle battery pack performance, even using the same active materials. The thermal uniformity, power, and energy for these quasi-bipolar battery packs is projected to be very good. The experimental part of the investigation demonstrates the concept of the quasi-bipolar plate applied to a lead foil current collector wrapping around two sides of an inexpensive plastic film core. Approximately 50 quasi-biplate samples were fabricated using a hot laminating press. Hot lamination with texture between the plastic and lead shows some promise as a low cost method for fabricating the plates. Five of these plates were assembled into two cells plus one two cell battery. Data from these test cells were compared with existing data for similar true bipolar batteries. The positive side of the plates exhibited corrosion where not protected by the active material.

DESCRIPTORS: (U) *BIPOLAR SYSTEMS, *LEAD ACID BATTERIES, HEAT TRANSFER, STATE OF THE ART, ELECTROCHEMISTRY, HOT PRESSING, STRESS CORROSION, ENERGY STORAGE, THERMAL INSULATION, HYBRID PROPULSION.

AD-A335020/JAA

JOINT PUBLICATIONS RESEARCH SERVICE
ARLINGTON, VA

(U) JPRS Report, Science & Technology, USSR: Electronics & Electrical Engineering

17 JUL 1990 24 PAGES

UNCLASSIFIED REPORT

ABSTRACT: (U) This report contains information concerning the USSR's science and technology relating to electronics and electrical engineering. Specific topics include: (1) broadcasting, consumer electronics; (2) circuits, systems; (3) industrial electronics, control instrumentation; (4) communications; (5) power engineering; (6) transportation; (7) aerospace, electronic systems; (8) computers; (9) components, hybrids, manufacturing technology; (10) quantum electronics, electrooptics; and (11) solid state circuits. Descriptors: (u) *signal processing, *electrooptics, *radio broadcasting, fiber optics, USSR, foreign technology, electronic equipment, integrated circuits, hybrid systems, quantum electronics, digital communications, radio waves, radio engineering, television equipment, power engineering.

IDENTIFIERS: (U) FBIS COLLECTION

AD-A333298/JAA

TACOM RESEARCH DEVELOPMENT AND ENGINEERING CENTER
WARREN, MI

(U) Development of a Natural Gas-Powered APU for a Hybrid Electric S-10 Pickup Truck.

DESCRIPTIVE NOTE: Interim report MAY 94-APR 95,
DEC 1997 82 PAGES
PERSONAL AUTHORS: Podner, Daniel J.; Capshaw, William K.

UNCLASSIFIED REPORT

ABSTRACT: (U) A natural gas-fueled auxiliary power unit (APU) was developed for use in a hybrid electric vehicle. The project involved conversion and development of the power plant from gasoline to natural gas operation, application of an engine control system, application of a three-way catalyst system, development of an APU controller, and integration and testing of the APU in the laboratory and vehicle environment the project was divided into three phases: (1) engine development, (2) APU control system development, and (3) APU integration/testing. The resultant APU was integrated into a hybrid electric utility truck for use as a range extender in a series hybrid configuration. The project resulted in an APU configuration producing ultra-low emissions levels while achieving high efficiency due to implementation of a unique APU operating strategy.

DESCRIPTORS: (U) *ELECTRIC POWER, *TRUCKS, *NATURAL GAS, *EXTENDABLE STRUCTURES, TEST AND EVALUATION, EMISSION, CONTROL SYSTEMS, EFFICIENCY, INTEGRATION, CONFIGURATIONS, ENGINES, HYBRID SYSTEMS, ELECTRIC PROPULSION, UTILITY VEHICLES.

IDENTIFIERS: (U) *APU(AUXILIARY POWER UNIT), *HYBRID ELECTRIC VEHICLE, NATURAL GAS ENGINES

AD-A332549/JAA

MASSACHUSETTS INST OF TECH
CAMBRIDGE, MA

(U) A Unified Framework for Verification and Complexity Analysis of Real-Time and Distributed Systems

DESCRIPTIVE NOTE: Final technical report AUG 93-FEB 97
13 JUN 1997 57 PAGES
PERSONAL AUTHORS: LYNCH, NANCY

UNCLASSIFIED REPORT

ABSTRACT: (U) We have developed the timed i/o automaton model, a basic compositional formal model for describing and analyzing real- time systems and distributed systems (in particular, distributed systems with precise timing sumptions and requirements). We have developed proof techniques, both manual and computer-assisted, for use with timed i/o automata, and have used the model and methods for analyzing a variety of problems and systems. These examples arise from a diverse set of application areas, including connection management protocols, clock synchronization, fault-tolerant distributed consensus, group communication, and real-time process control systems. We have extended the basic timed i/o automaton model in three directions: to include liveness constraints (live timed i/o automata), hybrid continuous/discrete behavior (hybrid I/O automata), and probabilistic behavior (probabilistic timed i/o automata). In each case, we have developed proof methods and have applied the models and methods to substantial problems. For example, in the hybrid systems area, we have carried out an extended case study of safety aspects of automated transportation systems.

DESCRIPTORS: (U) *DISTRIBUTED DATA PROCESSING, SOFTWARE ENGINEERING, COMPUTER COMMUNICATIONS, REAL TIME, PROGRAMMING LANGUAGES, INPUT OUTPUT PROCESSING, SYNCHRONIZATION(ELECTRONICS), HYBRID SYSTEMS, COMPUTER PROGRAM VERIFICATION, AUTOMATA.

AD-A331791/JAA

MITRE CORP, JASON PROGRAM OFFICE
MCLEAN, VA

(U) Nanoflyer

13 OCT 1997 12 PAGES
PERSONAL AUTHORS: Katz, J.; Garwin, R.; Press, W.

UNCLASSIFIED REPORT

ABSTRACT: (U) A recent proposal to use electrostatic forces to lift and propel a small airborne vehicle is examined. We show here that although this is permitted by the laws of physics, it is very inefficient, and is limited to low areal loads by the requirement to avoid electric breakdown. Electrostatic propulsion offers no special advantages which might justify the price of its inefficiency.

DESCRIPTORS: (U) *ELECTROSTATICS, *ELECTRIC PROPULSION, *AIRWORTHINESS, AERODYNAMIC DRAG, CHARGE DENSITY, AERODYNAMIC LIFT, ELECTROSTATIC FIELDS, ELECTRON MOBILITY, LIFT TO DRAG RATIO.

AD-A331528/JAA

CALSTART
BURBANK, CA

(U) Electric and Hybrid Electric Vehicle Technologies.

DESCRIPTIVE NOTE: Quarterly report 1 JUL-30 SEP 97,
5 NOV 1997 449 PAGES

UNCLASSIFIED REPORT

ABSTRACT: (U) This document contains quarterly reports on various aspects of research and testing being conducted concerning electric and hybrid electric vehicle technologies under cooperative agreement MDA972-95-2-0011.

DESCRIPTORS: (U) *ELECTRIC AUTOMOBILES, MANUFACTURING, PROPULSION SYSTEMS, STORAGE BATTERIES, FUEL INJECTORS, AUTOMOTIVE VEHICLES, ENERGY MANAGEMENT, ELECTRIC BATTERIES, FLYWHEELS.

IDENTIFIERS: (U) *HYBRID ELECTRIC VEHICLES, RECONNAISSANCE VEHICLES

AD-A327958/JAA

EUROPEAN MATERIALS RESEARCH SOCIETY

(U) International Conference on Advanced Materials ICAM '97; European Materials Research Society Spring Meeting E-MRS '97 Held in Strasbourg (France) on June 16-20, 1997.

DESCRIPTIVE NOTE: Spring meeting
JUN 1997 301 PAGES

UNCLASSIFIED REPORT

ABSTRACT: (U) Partial contents: fullerenes and carbon based materials; epitaxial thin film growth and nanostructures joint with EPS-solid state division; recent developments in electron microscopy and x- ray diffraction of thin film structures; computational modeling of issues in materials science; materials aspects for electric vehicles including batteries and fuel cells; second international symposium on advanced materials; biomaterials: perspectives for research & industry at the century change; biodegradable polymers & macromolecules; interrelation of science, economics & policy in materials research & processing; light-weight materials for transportation; coatings and surface modifications for surface protection and tribological applications; iii-v nitrides semiconductors and ceramics from material growth to device applications; materials, physics and devices for molecular electronics and photonics.

DESCRIPTORS: (U) *COMPOSITE MATERIALS, *CERAMIC MATERIALS, MATHEMATICAL MODELS, SYMPOSIA, COMPUTATIONS, MODIFICATION, MATERIALS, POLYMERS, STRUCTURES, THIN FILMS, X RAY DIFFRACTION, EPITAXIAL GROWTH, SEMICONDUCTORS, CARBON, NITRIDES, ELECTRON MICROSCOPY, SURFACES, COATINGS, PHYSICS, FRANCE, PROTECTION, LIGHTWEIGHT, MACROMOLECULES, VEHICLES, FUEL CELLS, ELECTRIC PROPULSION, TRIBOLOGY, MOLECULAR ELECTRONICS, BIODETERIORATION.

IDENTIFIERS: (U) ICAM(INTERNATIONAL CONFERENCE ON ADVANCED MATERIALS), FOREIGN REPORTS, ELECTRIC VEHICLES

AD-A325996/JAA

CALIFORNIA UNIV
BERKELEY, CA

(U) A Next Generation Architecture for Air Traffic Management Systems.

DESCRIPTIVE NOTE: Technical report
21 JAN 1997 30 PAGES
PERSONAL AUTHORS: Tomlin, C.; Pappas, G.; Lygeros, J.; Godbole, D.; Sastry, S. S.

UNCLASSIFIED REPORT

ABSTRACT: (U) The study of hierarchical, hybrid control systems in the framework of air traffic management systems (ATMS) is presented. The need for a new ATMS arises from the overcrowding of large urban airports and the need to more efficiently handle larger numbers of aircraft, without building new runways. Recent technological advances, such as the availability of relatively inexpensive and fast real time computers both on board the aircraft and in the control tower, make a more advanced air traffic control system a reality. The usefulness of these technological advances is limited by today's air traffic control (ATC), a ground-based system which routes aircraft along predefined jet ways in the sky, allowing the aircraft very little autonomy in choosing their own routes. In this paper, we propose an architecture for an automated ATMS, in which much of the current ATC functionality is moved on board each aircraft so that the aircraft may calculate their own deviations from predefined trajectories without consulting ATC. Within the framework of this architecture, we describe our work in on-board conflict resolution strategies between aircraft, and in deriving the flight mode switching logic in the flight vehicle management systems of each aircraft.

DESCRIPTORS: (U) *PERSONNEL MANAGEMENT, *AIR TRAFFIC CONTROL SYSTEMS, QUICK REACTION, STRATEGY, MANAGEMENT, REAL TIME, COMPUTERS, RESOLUTION, TOWERS, FLIGHT, HYBRID SYSTEMS, CONFLICT, SKY, GROUND BASED, AIRPORTS, ONBOARD, URBAN AREAS, SWITCHING LOGIC.

AD-A325918/JAA

SOUTHWEST RESEARCH INST TARDEC FUELS AND LUBRICANTS RESEARCH FACILITY
SAN ANTONIO, TX

(U) Development of Auxiliary Power Units for Electric Hybrid Vehicles.

DESCRIPTIVE NOTE: Interim report JUL 93-FEB 94,
JUN 1997 45 PAGES
PERSONAL AUTHORS: Owens, Edwin C.; Steiber, Joe

UNCLASSIFIED REPORT

ABSTRACT: (U) Electric drive is being considered for a wide variety of urban vehicles. Larger urban commercial vehicles (such as shuttle and transit buses), various delivery and service vehicles (such as panel and step vans), and garbage trucks and school buses are particularly well suited for this type of propulsion system due to their relatively short operating routes, operation and maintenance from central sites. Furthermore, these vehicles contribute a proportionately large amount to metropolitan air pollution by virtue of their continuous operation in those areas. Thus, reductions of emissions from these vehicles can have a large impact on urban air quality. It is, therefore, a necessity to develop auxiliary power units (APUs) that minimize emissions and in addition, increase range of electric vehicles. This report focuses on the first phase study of the development of APUs for large, electric drive commercial vehicles, intended primarily for metropolitan applications.

DESCRIPTORS: (U) *ELECTRIC PROPULSION, *HEAT ENGINES, *ELECTRIC AUTOMOBILES, *HYBRID PROPULSION, LIFE EXPECTANCY(SERVICE LIFE), AIR POLLUTION, LAND TRANSPORTATION, COST ESTIMATES, PROTOTYPES, MILITARY APPLICATIONS, COMMERCIAL EQUIPMENT, HYBRID SYSTEMS, POLLUTION ABATEMENT, ENERGY STORAGE, DRIVES(ELECTRONICS), ALTERNATORS, AUXILIARY POWER PLANTS, STANDBY GENERATORS.

IDENTIFIERS: (U) APU(AUXILIARY POWER UNIT)

AD-A323983/JAA

CALSTART
BURBANK, CA

(U) Joint Tactical Electrical Vehicle, Active Ride Height and Damping Control, Final Report for FY '95: Calstart System Development Project for Advanced Hybrid Reconnaissance Vehicles.

DESCRIPTIVE NOTE: Final report
8 APR 1997 294 PAGES

UNCLASSIFIED REPORT

ABSTRACT: (U) The active suspension system developed for this project is based on an active damper for controlling the medium and high speed dynamics involved with vehicle body and wheel motions, and an active ride height system for controlling the low speed body motions. This type of system makes improvements over a passive system by allowing the optimal damping required for differing terrain and vehicle control requirements to be automatically set by the suspension system while the active ride height system controls the vehicle attitude without sacrificing either passenger isolation or handling. This type of system has been shown to be very competitive with fully active systems over a wide range of running conditions with lower cost, lower energy usage and improved failure modes. The vehicle properties of the joint tactical electric vehicle, which this suspension system will be implemented on, have been determined and are listed in the main body of this report. Parameters for a selection of tires which are used on this and similar vehicles have been determined for a range of tire pressures and other test conditions, some of this data is given in the appendix.

DESCRIPTORS: (U) *DAMPING, *GROUND VEHICLES, *SUSPENSION DEVICES, REQUIREMENTS, TEMPERATURE, OPTIMIZATION, LOW COSTS, DYNAMICS, DEFLECTION, ISOLATION, MOTION, PASSIVE SYSTEMS, TERRAIN, ELECTRICAL PROPERTIES, PRESSURE MEASUREMENT, LOW VELOCITY, LOW ENERGY, WHEELS, HYBRID SYSTEMS, ACOUSTICS, TIRES, RANGE(EXTREMES), FAILURE(MECHANICS), HEIGHT, PASSENGERS, ELECTRIC PROPULSION, RECONNAISSANCE AIRCRAFT, ATTITUDE(INCLINATION).

AD-A322547/JAA

AMERICAN FLYWHEEL SYSTEMS INC
MEDINA, WA

(U) Electromechanical Flywheel Battery EDU Development Project.

DESCRIPTIVE NOTE: Final report
DEC 1996 77 PAGES

UNCLASSIFIED REPORT

ABSTRACT: (U) In January 1993, American flywheel systems inc. (AFS) initiated a program to develop and commercialize its proprietary electro-mechanical flywheel battery (EMFB) for commercial deployment in electric vehicles. The operational prototype was to demonstrate the technical viability and operation of the electro mechanical flywheel battery (EMFB) as a commercially feasible replacement to conventional chemical batteries. As an intermediate technical step in that process, and to provide an opportunity to evaluate a pre-prototype EMFB, an engineering development unit (EDU) was also to be constructed. EMFBs present the prospect of providing an environmentally compatible energy source offering outstanding life and performance for electric vehicles. Contrasted with the chemical species of battery, the EMFB is not an electro-chemical device. Instead it is an electro-mechanical system that efficiently converts (through its motor-generator) the mechanical kinetic energy stored in a high speed rotating flywheel rotor into usable electrical power.

DESCRIPTORS: (U) *ELECTROMECHANICAL DEVICES, *FLYWHEELS, PROTOTYPES, ENERGY TRANSFER, FEASIBILITY STUDIES, KINETIC ENERGY, POWER SUPPLIES, ELECTRIC POWER, ROTORS, MECHANICAL ENERGY, REGENERATION(ENGINEERING), ELECTRIC AUTOMOBILES.

IDENTIFIERS: (U) *MECHANICAL BATTERY, ACCELERATION, REGENERATIVE BRAKING, ENGINEERING DEVELOPMENT UNIT, THERMAL DEGRADATION

AD-A322527/JAA

SACRAMENTO MUNICIPAL UTILITY DISTRICT
CA

(U) Advanced Lead Acid Battery Development Project.

DESCRIPTIVE NOTE: Final report
FEB 1997 219 PAGES

UNCLASSIFIED REPORT

ABSTRACT: (U) This project involved laboratory and road testing of the horizon(registered) advanced lead acid batteries produced by Electrosource, Inc. A variety of electric vehicles in the fleet operated by the Sacramento municipal utility district and McClellan Air Force Base were used for road tests. The project was sponsored by the defense advanced research projects agency under RA 93-23 entitled electric vehicle technology and infrastructure. The horizon(registered) battery is a valve regulated, or sealed, lead acid battery produced in a variety of sizes and performance levels. During the project, several design and process improvements on the horizon(registered) battery resulted in a production battery with a specific energy approaching 45 watt-hours per kilogram (whr/kg) capable of delivering a peak current of 450 amps. The 12 volt, 95 amp-hour (ahr) horizon(registered) battery, model number 12n95, was placed into service in seven (7) test vehicles, including sedans, prototype lightweight electric vehicles, and passenger vans. Over 20,000 miles have been driven to date on vehicles powered by the horizon(registered) battery. Road test results indicate that when the battery pack is used with a compatible charger and charge management system, noticeably improved acceleration characteristics are evident, and the vehicles provide a useful range almost 20% greater than with conventional lead-acid batteries.

DESCRIPTORS: (U) *LEAD ACID BATTERIES, ACCELERATION, ENERGY, ELECTROCHEMISTRY, PROTOTYPES, TEST VEHICLES, LIGHTWEIGHT, ROAD TESTS, AIR FORCE FACILITIES, VALVES, BATTERY COMPONENTS, ELECTRIC PROPULSION.

IDENTIFIERS: (U) *HORIZON(REGISTERED) BATTERY, ELECTRIC VEHICLE TECHNOLOGY AND INFRASTRUCTURE, CHARGER, CHARGE MANAGEMENT SYSTEM

AD-A322403/JAA

FMC CORP ENERGY AND TRANSPORTATION
EQUIPMENT GROUP
SANTA CLARA CA

(U) Electric Drive M113 Vehicle Refurbishment Project: Sacramento Electric Transportation Consortium RA 93-23 Program.

DESCRIPTIVE NOTE: Final report
FEB 1997 45 PAGES

UNCLASSIFIED REPORT

ABSTRACT: (U) The electric drive m-113 refurbishment project involved upgrading an existing m-113 personnel carrier with updated electronics to meet current safety and performance standards. Several specific areas were refurbished, including design and installation of an improved power converter and motor controller assembly. The original design obtained propulsion power from only the engine driven gen-set. The vehicle was modified for 'engine-off' operation using battery power only. The vehicle was tested and demonstrated at a number of DARPA conferences and other locations, under the purview of tank automotive command (TACOM). The cover report by the Sacramento Electric Transportation Consortium Management essentially refers to the attached Appendix A final report by United Defense/FMC for all specific information on the activities and findings of the project.

DESCRIPTORS: (U) *HYBRID SYSTEMS, *ARMORED PERSONNEL CARRIERS, *ELECTRIC MOTORS, PROPULSION SYSTEMS, ELECTRIC POWER, INVERTERS, CONVERTERS, POWER ENGINEERING.

IDENTIFIERS: (U) *TRACTION MOTORS, M-113 VEHICLES, FLYBACK DIODES, ELECTRIC DRIVES, POWER CONVERTERS

AD-A322339/JAA

NAVAL POSTGRADUATE SCHOOL
MONTEREY, CA

(U) Autonomous Control of Underwater Vehicles and Local Area Maneuvering.

DESCRIPTIVE NOTE: Doctoral thesis
SEP 1996 359 PAGES
PERSONAL AUTHORS: Marco, David B.

UNCLASSIFIED REPORT

ABSTRACT: (U) The major thrust of this work is the development and demonstration of new capabilities for the use of small autonomous vehicles in mine countermeasure applications. Key to the new capabilities lies in an open architecture tri-level software structure for hybrid control, of which this work is the first validated implementation. The two upper levels run asynchronously in computing logical operations based on numerical decision making, while the lowest, the execution level, runs synchronously to maintain stability of vehicle motion. The top (strategic) level of control uses prolog as a rule based language for the specification of the discrete event system (DES) aspects of the mission. Multiple servo controllers are coordinated by the middle (tactical) level software in performing the mission, while the execution level controllers guarantee robust motion stability through multiple sliding modes.

DESCRIPTORS: (U) *COMPUTER PROGRAMS, *UNDERWATER VEHICLES, *AUTONOMOUS NAVIGATION, STABILITY, MANEUVERABILITY, CONTROL SYSTEMS, DECISION MAKING, DEMONSTRATIONS, MINE COUNTERMEASURES, NUMERICAL ANALYSIS, MOTION, SELF OPERATION, HYBRID SYSTEMS, SERVOMECHANISMS, SLIDING.

AD-A322276/JAA

CALSTART
BURBANK, CA

(U) Electric and Hybrid Electric Vehicle Technologies.

DESCRIPTIVE NOTE: Quarterly report 1 JUL-30 SEP 96.
SEP 1996 150 PAGES

DESCRIPTORS: (U) *ELECTRIC AUTOMOBILES, MANAGEMENT PLANNING AND CONTROL, REPORTS, MILITARY RESEARCH, RESEARCH MANAGEMENT, COMPOUND ENGINES.

AD-A320371/JAA

AIR FORCE INST OF TECH
WRIGHT-PATTERSON AFB, OH

(U) Gyrodynamic Effects of an Energy Storage Flywheel on the Handling of a Hybrid-Electric Vehicle.

DESCRIPTIVE NOTE: Master's thesis
9 JAN 1997 145 PAGES
PERSONAL AUTHORS: Greer, James L.

UNCLASSIFIED REPORT

ABSTRACT: (U) This research presents the results of numerical simulation of the handling characteristics of a hybrid-electric vehicle which uses a flywheel for temporary energy storage. The work is presented in an effort to understand the potential interaction of the flywheel and the vehicle, and to predict what positive and negative outcomes may result. The vehicle is modeled with four wheels, and the roll, yaw, and sideslip-angle degrees of freedom. The simulation uses an empirical model of the nonlinear interface between the tire and the road. The results are presented graphically, and are analyzed on both quantitative and qualitative bases. The vehicle parameters used to define the baseline vehicle are based on the broad guidelines set forth by the partnership for a new generation of vehicles. The size and speed range of the flywheel is based on a compilation of results presented in the popular literature. Analyses of the results are based on alignment of the angular momentum vector of the flywheel along the three axes of the vehicle. The speed of the flywheel is varied from -100,000 rpm to +100,000 rpm. Negative speeds represent orientation of the angular momentum vector of the flywheel along the negative axes, and positive speeds represent orientation along the positive axes.

DESCRIPTORS: (U) *ENERGY STORAGE, *ELECTRIC AUTOMOBILES, *FLYWHEELS, ROLL, YAW, NUMERICAL ANALYSIS, THESES, BASE LINES, SIDESLIP, DIGITAL SIMULATION, ANGULAR MOMENTUM.

IDENTIFIERS: (U) HYBRID ELECTRIC VEHICLES

AD-A316209/JAA

HELSINKI UNIV OF TECHNOLOGY
ESPOO, FINLAND

(U) A Study of Concentration and Potential in a Porous Electrode

30 SEP 1995 44 PAGES
PERSONAL AUTHORS: Heikonen, J.; Noponen, T.; Lampinen, M.

UNCLASSIFIED REPORT

ABSTRACT: (U) We find explicit expressions for the concentration and potential as functions of time during discharge in three different models of a cell with a porous metal hydride electrode. The effect of convection is studied and estimates of the convergence rate to the steady state are given. An example of an electric vehicle battery application is presented.

DESCRIPTORS: (U) *HYDRIDES, *ELECTRODES, *CONCENTRATION(CHEMISTRY), *POROUS METALS, STEADY STATE, CELLS, CONVECTION, CONVERGENCE, ELECTRIC PROPULSION, POROUS MATERIALS, FINLAND, ELECTRIC BATTERIES.

IDENTIFIERS: (U) *POTENTIAL, LCGL COLLECTION, GRAY LITERATURE, COPYRIGHTED MATERIALS, FOREIGN REPORTS

AD-A315347/JAA

NATIONAL AEROSPACE LAB
TOKYO, JAPAN

(U) A Preliminary Flight Evaluation of DGPS-INS Hybrid Navigation System

MAR 1995 14 PAGES
PERSONAL AUTHORS: Shingu, Hirokimi; Murata, Masaaki; Harigae, Masatoshi; Tsujii, Toshiaki; Ono, Takatsugu

UNCLASSIFIED REPORT

ABSTRACT: (U) This paper summarizes the flight evaluation of the DGPS-INS hybrid navigation system conducted as a preliminary study for constructing a next-generation navigation system at the National Aerospace Laboratory (NAL). First, the configuration used in the flight experiments, including ground facilities and the measurement systems, is described. Secondly, the design concept for a method of estimating navigation errors using a Kalmann filter is presented. Thirdly, flight profiles employed in the experiments are defined, and the experimental results of GPS, DGPS-INS in both stand-alone and hybrid modes which correspond to each profile are shown. Also, improvement in navigation performance by introducing the DGPS-INS hybrid navigation system was experimentally verified. In conclusion, the design concept of the DGPS-INS hybrid navigation system available for future space vehicles has been successfully completed.

DESCRIPTORS: (U) *GLOBAL POSITIONING SYSTEM, *INERTIAL NAVIGATION, TEST AND EVALUATION, GROUND LEVEL, FLIGHT TESTING, MEASUREMENT, SPACECRAFT, FACILITIES, PROFILES, NAVIGATION, ERRORS, HYBRID SYSTEMS, FLIGHT PATHS.

IDENTIFIERS: (U) COPYRIGHTED MATERIALS, LCGL COLLECTION, GRAY LITERATURE, FOREIGN REPORTS

AD-A313530/JAA

TEXAS UNIV AT AUSTIN

(U) User's Guide for POWERSIM and Associated Programs.

DESCRIPTIVE NOTE: Report for AUG 94-DEC 95
AUG 1996 55 PAGES
PERSONAL AUTHORS: Redding, Eric; Fish, Scott

UNCLASSIFIED REPORT

ABSTRACT: (U) This report provides an overview of the power simulation code developed by the AT for analysis of energy and power flow throughout combat vehicles equipped with electric weapons. The purpose of the code, which has been nicknamed POWERSIM, is to provide an intuitive modeling environment for this analysis under the rather complex mission sequences associated with battlefield operation of these vehicles. The utility of simulating the power flow through the vehicle under these conditions hinges on assessing the impact of all the power system components on the overall vehicle system performance under conditions (movement and firing) which are considered realistic for the application of interest. The UE of this code, can through the appropriate graphical user interfaces, (1) configure complex mobility and firing sequences, (2) configure a hybrid electric combat vehicle with electric weapons, (3) run simulations for mobility loads alone, (4) run simulations with mobility and firepower, and (5) perform some simple analysis of the simulation results. The code described here is the first complete version of the code, and development continues on adding component models and increasing the accuracy and speed of the existing component models.

DESCRIPTORS: (U) *COMPUTER PROGRAMS, *COMPUTERIZED SIMULATION, *COMBAT VEHICLES, *ELECTRIC PROPULSION, *ELECTRIC POWER TRANSMISSION, MOBILITY, ENVIRONMENTS, MODELS, BATTLEFIELDS, PERFORMANCE(ENGINEERING), INTERFACES, ACCURACY, SEQUENCES, CODING, COMPUTER GRAPHICS, HYBRID SYSTEMS, FLOW

IDENTIFIERS: (U) *POWER FLOW, ELECTRIC VEHICLES, HYBRID VEHICLES, POWERSIM COMPUTER PROGRAM, MATLAB PROGRAMMING LANGUAGE

AD-A313505/JAA

FOSTER-MILLER INC
WALTHAM, MA

(U) Low Magnetic Signature Propulsion System.

DESCRIPTIVE NOTE: Final report 27 NOV 95-27 MAY 96
AUG 1996 67 PAGES
PERSONAL AUTHORS: Cope, D.

UNCLASSIFIED REPORT

ABSTRACT: (U) The electric propulsion system of the seal delivery vehicle (SDV) has associated magnetic fields whether operating or not. These fields were measured and documented and the feasibility of a magnetic shielding system was proven during this program. The shielding system was demonstrated on a surrogate electric motor in foster-miller's laboratory and by computer simulation of the battery pack. The substitute motor and battery pack simulation were used due to limited availability of the SDV for actual shield installation and validation. The major magnetic field sources of the SDV were: the battery pack, the ferromagnetic motor mass and the operating motor itself. Detection ranges were calculated for each major field source of the SDV and varied depending upon motor load. Actual detection ranges may be greater or lesser depending upon the actual operating conditions, detection threshold sensitivity, and the ambient magnetic noise environment. The shielding system consisted of active magnetic field cancellation for the ferromagnetic motor mass and simulated conductor rerouting for the battery pack. The results of the magnetic signature reduction were: motor field reduced by 21 dB and the battery pack field reduced by 15 dB. This level of magnetic field reduction decreased the calculated detection ranges by 55 percent.

DESCRIPTORS: (U) *ELECTRIC PROPULSION, *ELECTROMAGNETIC SHIELDING, *MAGNETIC SIGNATURES, SIMULATION, VALIDATION, THRESHOLD EFFECTS, REDUCTION, AMBIENT NOISE, MOTORS, NOISE(ELECTRICAL AND ELECTROMAGNETIC), FERROMAGNETISM, LEGENDRE FUNCTIONS, MAGNETOMETERS, MAGNETIC ANOMALY DETECTION.

IDENTIFIERS: (U) BATTERY PACK, FERROMAGNETIC MASS, COIL FILAMENT, LEAST SQUARE MATRIX METHODS, CONDUCTOR TRANSMISSION LINES, MOTOR DUCTING

AD-A307324/JAA

WRIGHT LAB
WRIGHT-PATTERSON AFB, OH

(U) An Induction Motor Drive Using a Resonant DC Link Inverter.

DESCRIPTIVE NOTE: Final report MAY-DEC 95
FEB 1996 73 PAGES
PERSONAL AUTHORS: Fronista, Gregory L.

UNCLASSIFIED REPORT

ABSTRACT: (U) New initiatives to increase the use of electrical power, such as the electric vehicle and the more electric airplane, have created a need for improved motor drives. The use of adjustable speed drives has recently received more attention in these applications because new circuit topologies and power components have been developed that have enabled improvements in efficiency, power density and response times. This study reports the design and simulation of an actively clamped resonant dc link inverter that will drive an induction motor based blower. The objective of this study is to design, build and test a resonant dc link (RDCL) inverter and compare the performance of a six-step control strategy with a pulse density modulation strategy in an adjustable speed drive. Comparisons are made between a hard switched pulse width modulation converter and an RDCL inverter. Theoretical and experimental power loss calculations of the RDCL inverter are compared and discussed. The performance of constant voltage/ frequency adjustable speed control is presented.

DESCRIPTORS: (U) *AIRCRAFT ENGINES, *INDUCTION MOTORS, THEORY, TOPOLOGY, RESONANCE, DIRECT CURRENT, DRIVES(ELECTRONICS), INVERTERS, ELECTRIC PROPULSION, CIRCUIT ANALYSIS, PULSE MODULATION, SPEED REGULATORS.

IDENTIFIERS: (U) DIRECT CURRENT INVERTERS

AD-A307294/JAA

NAVAL POSTGRADUATE SCHOOL
MONTEREY, CA

(U) Computer Simulation of an Unmanned Aerial Vehicle Electric Propulsion System.

DESCRIPTIVE NOTE: Master's thesis
MAR 1996 122 PAGES
PERSONAL AUTHORS: Yourkoski, Joel

UNCLASSIFIED REPORT

ABSTRACT: (U) There has been a substantial increase in the use of electric propulsion systems in unmanned aerial vehicles (UAVs). However, this area of engineering has lacked the benefits of a dynamic model that could be used to optimize the design. Configurations and flight profiles. The Naval Research Laboratory (NRL) has accurate models for the aerodynamics associated with UAVs. Therefore the proposed electric propulsion model would use the torque and rpm requirements generated by the aerodynamic model and provide an accurate representation of the desired UAV electric propulsion system. This thesis reports on the development of such a model. The model is adaptive in the sense that motor and battery parameters can be altered by the user to reflect systems currently in use or those considered for future systems. Not only will the simulation model accurately reflect the operating conditions of the motor and battery during the mission, but different flight profiles with the same configuration can be evaluated in terms of efficiency based on the percent battery capacity used (PBCU) at the end of the mission.

DESCRIPTORS: (U) *COMPUTERIZED SIMULATION, *SYSTEMS ENGINEERING, *UNMANNED, *AIRCRAFT MODELS, *ELECTRIC PROPULSION, AERODYNAMIC CONFIGURATIONS, SIMULATORS, OPTIMIZATION, MODELS, ACCURACY, EFFICIENCY, FLIGHT PATHS, MOTORS, TORQUE, ELECTRIC BATTERIES.

IDENTIFIERS: (U) UAV(UNMANNED AERIAL VEHICLES), PBCU(PERCENT BATTERY CAPACITY USED)

AD-A303752/JAA

MASSACHUSETTS INST OF TECH
CAMBRIDGE, MA

(U) Applications of the Theory of Distributed and Real Time Systems to the Development of Large-Scale Timing Based Systems.

DESCRIPTIVE NOTE: Status report 1 OCT-31 DEC 95
26 JAN 1996 9 PAGES
PERSONAL AUTHORS: Lynch, Nancy A.

UNCLASSIFIED REPORT

ABSTRACT: (U) This report summarizes the progress of research in the theory of distributed systems group. Members of the group have been active during this period in modeling, designing, and developing applications for concurrent systems. Our main theme is to support highly effective concurrent application designs by providing specification, quantification, and verification tools that capture behavior without limiting performance. We have developed a new ' hybrid automata model' for analyzing the behaviors of systems like industrial robots or computer controlled vehicles. We have made progress in applying our specification and automated verification methods to several complicated test problems in distributed computing. We have introduced a variety of new approaches to evaluating concurrent algorithms, among them 'eventual serializability,' 'linearizability,' and a novel local measure of linearizability for load balancing data structures.

DESCRIPTORS: (U) *DISTRIBUTED DATA PROCESSING, *REAL TIME, *CONCURRENT ENGINEERING, TEST AND EVALUATION, MATHEMATICAL MODELS, ALGORITHMS, AUTOMATION, VERIFICATION, TOOLS, THEORY, ROBOTS, LIMITATIONS, COMMUNICATION AND RADIO SYSTEMS, HYBRID SYSTEMS, BEHAVIOR, TIMING DEVICES, AUTOMATA.

IDENTIFIERS: (U) TRANSIT SYSTEMS

AD-A302298/JAA

BROWN UNIV
PROVIDENCE, RI

(U) Distributed Planning and Control for Applications in Transportation Scheduling.

DESCRIPTIVE NOTE: Research and development status report 1-31 MAY 95
31 MAY 1995 11 PAGES
PERSONAL AUTHORS: Dean, Thomas; Hoebel, Lou

UNCLASSIFIED REPORT

ABSTRACT: (U) The authors have been investigating the use of techniques from statistical mechanics to solve very large optimization problems. There is an interesting phenomenon concerning the difficulty of optimization problems that as the number of relevant entities (aircraft, trucks) increases assumptions of uniformity can play an increasingly important role in reducing complexity. Even in medium-scale problems such as those faced by the military in transportation control and cities in highway traffic control, statistical techniques that rely on aggregation and (quasi) uniform behavior appear to be effective. We are particularly interested in hybrid methods that combine techniques from statistical mechanics and combinatorial optimization techniques that do differentiate with regard to local behavior.

DESCRIPTORS: (U) *TRANSPORTATION, *MANAGEMENT PLANNING AND CONTROL, *SCHEDULING, *TRAFFICABILITY, CONTROL, OPTIMIZATION, AIRCRAFT, TRAFFIC, PLANNING, HYBRID SYSTEMS, BEHAVIOR, COMBINATORIAL ANALYSIS, STATISTICAL PROCESSES, STATISTICAL MECHANICS, HIGHWAYS.

AD-A299738/JAA

NORTH CAROLINA STATE UNIV AT RALEIGH
DEPT OF ELECTRICAL AND COMPUTER ENGINEERI NG

(U) Outdoor Landmark Recognition Using Hybrid Fractal Vision System and Neural Networks.

DESCRIPTIVE NOTE: Quarterly progress report JAN-MAR 95
MAR 1995 9 PAGES
PERSONAL AUTHORS: Luo, Ren C.

UNCLASSIFIED REPORT

ABSTRACT: (U) A hybrid fractal vision system is being developed for landmark detection and recognition in natural scenes. At the current quarter of research, a reconfigurable neural network is being designed to recognize landmarks. The fractal model detected the landmarks for cluttered images, and the neural network would recognize those landmarks. A brief description of the theoretical design of this reconfigurable neural network is given here. Also, some of the initial results obtained by testing the neural network on real image data are included with this report. A new learning method is also being developed and briefly reported here. Automatic recognition systems can be useful in both military and commercial domains. Tasks such as military surveillance, automatic target recognition, automatic vehicle navigation, material handling, inspection, data compression/decompression, autonomous robot navigation, etc are some of the practical issues directly enhanced by automatic and robust vision systems.

DESCRIPTORS: (U) *FRACTALS, *NEURAL NETS, *TARGET RECOGNITION, *LANDFORMS, *OUTDOOR, IMAGE PROCESSING, SPATIAL DISTRIBUTION, ROBOTS, NAVIGATION, RECOGNITION, HYBRID SYSTEMS, VEHICLES, DATA COMPRESSION, SURVEILLANCE, AUTOMATIC PILOTS, DECOMPRESSION, NAVIGATION REFERENCE, MATERIALS HANDLING.

IDENTIFIERS: (U) LANDMARK RECOGNITION

AD-A294615/JAA

NAVAL POSTGRADUATE SCHOOL
MONTEREY, CA

(U) Simulation of a Solar Powered Electric Vehicle Under the Constraints of the World Solar Challenge.

DESCRIPTIVE NOTE: Master's thesis
MAR 1995 102 PAGES
PERSONAL AUTHORS: Roerig, Steven J.

UNCLASSIFIED REPORT

ABSTRACT: (U) Development of an effective method for evaluation of alternative energy sources in the automotive industry has always been a necessity for cost efficient design analysis. One viable alternative energy source is electricity. In the present day environment of shrinking fossil fuel supplies and environmental awareness, electric powered vehicles are becoming a low cost, non- polluting, alternative means of transportation. The analysis of reliable electric propulsion can be expensive without a modeling tool for evaluating design strategies before vehicle construction. This thesis explores electricity as an alternative energy source for the automobile of tomorrow. Under the guidelines of the world solar challenge, a solar powered electric vehicle, using a permanent-magnet brushless dc motor has been modeled and simulated in simulink (dynamic system simulation software). The simulations were performed with the goal of determining the optimum configuration to efficiently utilize the power supplied from the solar array, batteries, and motor.

DESCRIPTORS: (U) *SOLAR ENERGY, *ELECTRIC PROPULSION, *ELECTRIC AUTOMOBILES, VELOCITY, COMPUTER PROGRAMS, COMPUTERIZED SIMULATION, OPTIMIZATION, ENVIRONMENTS, LOW COSTS, COST ANALYSIS, ENERGY, EFFICIENCY, THESES, TERRAIN, RELIABILITY, CONFIGURATIONS, ELECTRICITY, DAY, SUPPLIES, DIRECT CURRENT, AWARENESS, ELECTRIC MOTORS, FOSSIL FUELS, SOLAR PANELS, AUTOMOTIVE INDUSTRY, BRUSHLESS ELECTRICAL EQUIPMENT, PERMANENT MAGNET GENERATORS.

AD-A294318/JAA

SOUTHWEST RESEARCH INST TARDEC FUELS AND LUBRICANTS RESEARCH FACILITY
SAN ANTONIO, TX

(U) Free-Piston Engine Linear Generator for Hybrid Vehicles Modeling Study.

DESCRIPTIVE NOTE: Interim report JAN -AUG 94,
MAY 1995 51 PAGES
PERSONAL AUTHORS: Callahan, T. J.; Ingram, S. K.

UNCLASSIFIED REPORT

ABSTRACT: (U) Development of a free piston engine linear generator was investigated for use as an auxiliary power unit for a hybrid electric vehicle. The main focus of the program was to develop an efficient linear generator concept to convert the piston motion directly into electrical power. Computer modeling techniques were used to evaluate five different designs for linear generators. These designs included permanent magnet generators, reluctance generators, linear dc generators, and two and three-coil induction generators. The efficiency of the linear generator was highly dependent on the design concept. The two-coil induction generator was determined to be the best design, with an efficiency of approximately 90 percent.

DESCRIPTORS: (U) *PISTONS, *PISTON ENGINES, *ELECTRIC AUTOMOBILES, *ENGINE GENERATOR SETS, COMPUTERIZED SIMULATION, LINEAR SYSTEMS, AUXILIARY, MODELS, ENGINE COMPONENTS, MOTION, EFFICIENCY, ELECTRIC POWER, POWER EQUIPMENT, HYBRID SYSTEMS, VEHICLES, GENERATORS, DIRECT CURRENT, ELECTRIC PROPULSION, INDUCTION SYSTEMS, PERMANENT MAGNET GENERATORS.

IDENTIFIERS: (U) *FREE PISTON ENGINES, RELUCTANCE GENERATORS, INDUCTION GENERATORS, HEV(HYBRID ELECTRIC VEHICLES), APU(AUXILIARY POWER UNITS).

AD-A281109/JAA

NAVAL SURFACE WARFARE CENTER
SILVER SPRING, MD

(U) Atomic Structure and Valency of Nickel in Some of its Oxycompounds.

DESCRIPTIVE NOTE: Technical report
28 JUN 1994 11 PAGES
PERSONAL AUTHORS: Mansour, A. N.; Melendres, C. A.; Pankuch, M.; Brizzolare, R. A.

UNCLASSIFIED REPORT

ABSTRACT: (U) The structure of the higher oxide forms of nickel (where Ni has a valency greater than +2) is of great interest from the standpoint, of developing advanced nickel batteries for consumer applications and for electric vehicle propulsion. In spite of the considerable research work that has been published, there is still much uncertainty and confusion as to the stoichiometry and structure of the various oxides (hydroxides) that are formed during the charging (and discharging) of the nickel electrode. The difficulty stems in part from the highly disordered or amorphous nature of the phases formed which makes structural determination by x-ray diffraction difficult. X-ray absorption spectroscopy (XAS) consisting of the x-ray absorption near edge structure (XANES) and the extended x-ray absorption fine structure (EXAFS) is an excellent technique for the characterization of such materials which have no long range order. Preliminary to using the technique for in-situ structural determinations in an electrochemical cell, we have used XAS to study a number of standard samples for subsequent use as reference. We report initial XANES and EXAFS results that give the valency and structure of nickel in some compounds of interest in battery work.

DESCRIPTORS: (U) *NICKEL, *OXIDES, *ATOMIC STRUCTURE, *VALENCE, *CHEMICAL COMPOUNDS, *BATTERY COMPONENTS, ABSORPTION, CELLS, HYDROXIDES, MATERIALS, PHASE, SPECTROSCOPY, STANDARDS, STOICHIOMETRY, STRUCTURES, VEHICLES, X RAY DIFFRACTION, ELECTRIC AUTOMOBILES, ELECTRIC PROPULSION, ELECTRODES, ELECTROCHEMISTRY.

AD-A275413/JAA

AIR FORCE INST OF TECH SCHOOL OF ENGINEERING
WRIGHT-PATTERSON AFB, OH

(U) Orbital Applications of Electrodynamic Propulsion.

DESCRIPTIVE NOTE: Master's thesis

DEC 1993 125 PAGES
PERSONAL AUTHORS: Irwin, Troy

UNCLASSIFIED REPORT

ABSTRACT: (U) Electrodynamic propulsion (EDP) uses forces resulting from electric currents in conductors as a spacecraft travels through a magnetic field. A vehicle-independent expression for the specific power required for any maneuver is derived and used to assess EDP feasibility. Analytical expressions for the accelerations and combined current-conductor vector required to change the orbital plane or the argument of perigee are developed based on Lagrange's planetary equations. Solutions to the forced Clohessy-Wiltshire equations are developed to study iii-plane rendezvous. Results show EDP can change inclination or right ascension of the ascending mode at approximately 0.4 degrees/day with current spacecraft specific power technology. The effects of the earth's oblateness on a 24 hour, 90 degree inclination Molniya orbit can be negated. Rendezvous is possible with EDP, and approaches along the target velocity vector with no attitude change are possible with current spacecraft specific power. Approaches involving altitude changes will be possible when modest spacecraft power improvements are made.

DESCRIPTORS: (U) *ELECTRODYNAMICS, *ORBITS, *PROPULSION SYSTEMS, ACCELERATION, ALTITUDE, DECAY, DOCKS, ELECTRIC CURRENT, ELECTRIC PROPULSION, MAGNETIC FIELDS, MANEUVERS, MOMENTUM, NODES, PERIGEE, PLUMES, SPACECRAFT, TARGETS, THRUSTERS, VEHICLES, VELOCITY, THESES, CONDUCTIVITY, CURRENTS.

IDENTIFIERS: (U) ORBITAL PLANE CHANGE, LAGRANGE'S PLANETARY EQUATIONS, MOLNIYA ORBIT, RENDEZVOUS, INCLINATION, RIGHT ASCENSION, ASCENDING.

AD-A269088/JAA

PHILLIPS LAB
KIRTLAND AFB, NM

(U) Constant-Thrust Orbit-Raising Transfer Charts.

DESCRIPTIVE NOTE: Final report AUG 92-MAY 93
JUL 1993 23 PAGES
PERSONAL AUTHORS: Alfano, Salvatore; Thorne, James D.

UNCLASSIFIED REPORT

ABSTRACT: (U) This report outlines a method to generate minimum-fuel trajectories between coplanar circular orbits for a vehicle with constant thrust. The rocket equation models the effects of continuous fuel expenditure while also serving to recast the solution in terms of accumulated velocity change. These orbit-raising solutions are globally mapped with no restrictions on initial thrust magnitude, intermediate eccentricity, or number of revolutions of the central body. Several examples are presented to verify the transfer charts and familiarize the reader with their use. These charts are useful tools for mission planners and satellite designers to assess preliminary fuel requirements for constant-thrust systems or to compare different propulsion technologies.... Electric propulsion, thrust, thruster, efficiency, orbits, flight maneuvers, trajectories, satellites (artificial).

DESCRIPTORS: (U) *ARTIFICIAL SATELLITES, *FUEL CONSUMPTION, *SPACECRAFT TRAJECTORIES, *ORBITS, *THRUST, CHARTS, SPACE PROPULSION, DESIGN CRITERIA, EQUATIONS OF MOTION, SPACE MISSIONS, ACCELERATION, CIRCULAR ORBITS, ECCENTRICITY, EFFICIENCY, ELECTRIC PROPULSION, FLIGHT MANEUVERS, MODELS, REQUIREMENTS, ROCKETS, THRUSTERS, TRAJECTORIES, TRANSFER, VELOCITY.

IDENTIFIERS: (U) WUPL2181TA01, SBI1, FISCAL YEAR 93, TRANSFER CHARTS.

AD-A263087/JAA

ARGONNE NATIONAL LAB
IL

(U) Dynamics and Controls in Maglev Systems

SEP 1992 75 PAGES
PERSONAL AUTHORS: Cai, Y.; Chen, S. S.; Rote, D. M.

UNCLASSIFIED REPORT

ABSTRACT: (U) The dynamic response of magnetically levitated (MAGLEV) ground transportation systems has important consequences for safety and ride quality, guideway design, and system costs. Ride quality is determined by vehicle response and by environmental factors such as humidity and noise. The dynamic response of the vehicles is the key element in determining ride quality, and vehicle stability is an important safety-related element. To design a proper guideway that provides acceptable ride quality in the stable region, vehicle dynamics must be understood. Furthermore, the trade-off between guideway smoothness and the levitation and control systems must be considered if MAGLEV systems are to be economically feasible. The link between the guideway and the other MAGLEV components is vehicle dynamics. For a commercial MAGLEV system, vehicle dynamics must be analyzed and tested in detail. In this study, the role of dynamics and controls in MAGLEV vehicle/guideway interactions is discussed, and the literature on modeling the dynamic interactions of vehicle/guideway and suspension controls for ground vehicles is reviewed.

DESCRIPTORS: (U) *MASS TRANSPORTATION, *ELECTRIC PROPULSION, LAND TRANSPORTATION, MAGNETIC FORCES, GROUND VEHICLES.

IDENTIFIERS: (U) MAGLEV(MAGNETICALLY LEVIATATED) VEHICLES.

AD-A243349/JAA

AIR FORCE INST OF TECH
WRIGHT-PATTERSON, AFB OH

(U) Control Algorithms for Aerobraking in the Martian Atmosphere.

DESCRIPTIVE NOTE: Doctoral thesis
DEC 1991 187 PAGES
PERSONAL AUTHORS: Shipley, Buford W., Jr.

UNCLASSIFIED REPORT

ABSTRACT: (U) The analytic predictor corrector (APC) and energy controller (EC) atmospheric guidance concepts have been adapted to control an interplanetary vehicle aerobraking in the Martian atmosphere. Modifications are made to the APC to improve its robustness to density variations. These modifications include adaptation of a new exit phase algorithm, an adaptive transition velocity to initiate the exit phase, refinement of the reference dynamic pressure calculation and two hybrid density estimation techniques. The modified controller with the hybrid density estimation technique is called the Mars hybrid predictor corrector (MHPC), while the modified controller with a polynomial density estimator is called the mars predictor corrector (MPC). A Lyapunov steepest descent controller (LSDC) is adapted to control the vehicle. The LSDC lacked robustness, so a Lyapunov tracking exit phase algorithm is developed to guide the vehicle along a reference trajectory. The equilibrium glide entry phase is employed for the first part of the trajectory. This algorithm, when using the hybrid density estimation technique to define the reference path, is called TE Lyapunov hybrid tracking controller (LHTC).

DESCRIPTORS: (U) , ADAPTIVE SYSTEMS, ALGORITHMS, COMPUTATIONS, DENSITY, DYNAMIC PRESSURE, ENERGY, ESTIMATES, EXITS, HYBRID SYSTEMS, LYAPUNOV FUNCTIONS, MARS (PLANET), PLANETARY ATMOSPHERES, POLYNOMIALS, PREDICTIONS, STEEPEST DESCENT METHOD, TRACKING, TRAJECTORIES, VELOCITY.

IDENTIFIERS: (U) *ATMOSPHERE ENTRY, *DESCENT TRAJECTORIES, MARS PROBES, BRAKING, *AEROBRAKING, THESES, APC(ANALYTIC PREDICTION CORRECTOR), MHPC(MARS HYBRID PREDICTION CORRECTOR).

AD-A240865/JAA

CHEMICAL PROPULSION INFORMATION AGENCY
LAUREL MD

(U) JANNAF Propulsion Meeting Held in Anaheim, California on 3-5 October 1990. Volume 2.

DESCRIPTIVE NOTE: Meeting proceedings 26 MAY 89-5 OCT 90,
OCT 1990 482 PAGES
PERSONAL AUTHORS: Brown, Karen L.; Eggleston, Debra S.

UNCLASSIFIED REPORT

ABSTRACT: (U) This volume, the second of six, is a collection of 39 unclassified/unlimited distribution papers which were presented at the 1990 joint army-navy-NASA-air force (JANNAF) propulsion meeting, held 3-5 October 1990. Specific subjects discussed include nondestructive evaluation, launch vehicle propulsion, space shuttle engines, hybrid propulsion technology, liquid rocket engines, attitude control engines, and electric propulsion systems.

DESCRIPTORS: (U) , ATTITUDE CONTROL SYSTEMS, ELECTRIC PROPULSION, ENGINES, HYBRID PROPULSION, LAUNCH VEHICLES, LIQUID PROPELLANT ROCKET ENGINES, NONDESTRUCTIVE TESTING, PROPULSION SYSTEMS, SPACE SHUTTLES.

IDENTIFIERS: (U) *ROCKET ENGINES, *ROCKET PROPELLANTS, ROCKET PROPULSION, SOLID PROPELLANT ROCKET ENGINES, LIQUID PROPELLANT ROCKET ENGINES, *BOOSTER ROCKET ENGINES, CRYOGENIC ENGINES, HYBRID ROCKET ENGINES, GAS GENERATING SYSTEMS, COMBUSTION STABILITY, METALLIZED PROPELLANTS, HYDRAZINES, MONOPROPELLANTS, ARC JET ENGINES, NONDESTRUCTIVE TESTING.

AD-A236938/JAA

NORTHWESTERN UNIV DEPT OF ELECTRICAL ENGINEERING AND COMPUTER SCIENCE EVANSTON IL

(U) Estimation and Control of Nonlinear and Hybrid Systems.

DESCRIPTIVE NOTE: Final report 15 JAN 89-14 OCT 90
14 OCT 1990 82 PAGES
PERSONAL AUTHORS: Haddad, A. H.

UNCLASSIFIED REPORT

ABSTRACT: (U) The research covers several aspects of the basic issues that are needed to develop and implement nonlinear filtering and control of maneuvering vehicles in uncertain environments and nonlinear geometry. The research is involved in modeling maneuvering nonlinear vehicles as switched linear Markov models. The research therefore leads in several directions investigating various aspects of such models which in general are called hybrid systems. Three different aspects are considered: the first involves realization and other generic properties of hybrid systems, including controllability and stability as well as simulation and averaging. The second involves estimation and detection systems for hybrid systems, including various related models and approximate filtering schemes. The third involves the application of switched Markov filtering schemes to the tracking of maneuvering vehicles.

DESCRIPTORS: (U) , CONTROL, DETECTORS, FILTERS, GEOMETRY, HYBRID SYSTEMS, LINEARITY, MANEUVERABILITY, MARKOV PROCESSES, MATHEMATICAL MODELS, NONLINEAR SYSTEMS, SIMULATION, SWITCHING, TRACKING, VEHICLES.

IDENTIFIERS: (U) *NONLINEAR SYSTEMS, *HYBRID SYSTEMS, *ELECTRICAL ENGINEERING.

AD-A229233/JAA

ARMY BALLISTIC RESEARCH LAB ABERDEEN PROVING GROUND, MD

(U) A Technical Assessment of Electromagnetic Propulsion for Small Caliber Weapons Applications.

DESCRIPTIVE NOTE: Technical report
NOV 1990 88 PAGES
PERSONAL AUTHORS: Jamison, Keith A.

UNCLASSIFIED REPORT

ABSTRACT: (U) An assessment of the future potential of electromagnetic propulsion for small caliber weapons has been performed to consider possible benefits, systems configurations, research and development needs, and mission requirements. The assessment consists of a panel evaluation of an existing electromagnetic launcher EML program and comparisons of envisioned point designs for small caliber weapons systems. The general conclusions are that the present research effort is well-founded and that em propulsion has a great deal of potential for a vehicle mounted, crew-served weapon. Although the potential improvements are significant, some risk in maturing the technology to a fielded weapon is accrued from the number and complexity of components in the EML system. Keywords: rail guns; electromagnetic guns; electromagnetic launcher; electromagnetic propulsion. (JHD)

DESCRIPTORS: (U) *ELECTROMAGNETIC GUNS, CONFIGURATIONS, ELECTRIC PROPULSION, ELECTROMAGNETIC DRIVES, ELECTROMAGNETIC RADIATION, ELECTROMAGNETISM, LAUNCHERS, MILITARY REQUIREMENTS, RISK, TEST AND EVALUATION, WEAPON SYSTEMS.

IDENTIFIERS: (U) RAILGUNS, CREW SERVED WEAPONS.

AD-A224201/JAA

ASTRONAUTICS LAB (AFSC)
EDWARDS AFB, CA

(U) Development of the Electric Vehicle Analyzer.

DESCRIPTIVE NOTE: Final report AUG 86-DEC 88
JUN 1990 42 PAGES
PERSONAL AUTHORS: Dickey, Michael R.; Klucz, Raymond S.; Ennix, Kimberly A.; Matuszak, Leo M.

UNCLASSIFIED REPORT

ABSTRACT: (U) The increasing technological maturity of high power (> 20 kw) electric propulsion devices has led to renewed interest in their use as a means of efficiently transferring payloads between earth orbits. Several systems and architecture studies have identified the potential cost benefits of high performance electric orbital transfer vehicles (EOTVs). These studies led to the initiation of the electric insertion transfer experiment (elite) in 1988. Managed by the astronautics laboratory, elite is a flight experiment designed to sufficiently demonstrate key technologies and options to pave the way for the full-scale development of an operational EOTV. An important consideration in the development of the elite program is the capability of available analytical tools to simulate the orbital mechanics of a low thrust, electric propulsion transfer vehicle.

DESCRIPTORS: (U) , ACCURACY, ANALYZERS, ARCHITECTURE, ASTRONAUTICS, BENEFITS, CELESTIAL MECHANICS, COST EFFECTIVENESS, EARTH ORBITS, EFFICIENCY, ELECTRIC PROPULSION, ELECTRICAL EQUIPMENT, FLIGHT TESTING, HIGH POWER, LOW POWER, MATHEMATICAL ANALYSIS, MISSION PROFILES, ORBITS, SPACE TRANSPORTATION, TEST AND EVALUATION, TRANSFER, VEHICLES.

IDENTIFIERS: (U) EVA(ELECTRIC VEHICLE ANALYZER), EOTV(ELECTRIC ORBITAL TRANSFER VEHICLES), EITE(ELECTRIC INSERTION TRANSFER EXPERIMENT).

AD-A218318/JAA

PENNSYLVANIA STATE UNIV STATE COLLEGE

(U) Sea-Water Magnetohydrodynamic Propulsion for Next-Generation Undersea Vehicles.

DESCRIPTIVE NOTE: Annual report 1 FEB 89-31 JAN 90
FEB 1990 49 PAGES
PERSONAL AUTHORS: Lin, T. F.; Gilbert, J. B.; Kossowsky, R.

UNCLASSIFIED REPORT

ABSTRACT: (U) Three tasks were performed in this report period. Their individual abstracts are summarized as follows: (I) thruster performance modelings - the purpose of this work is to analyze underwater vehicle propulsion by applying Lorentz forces to the surrounding sea water. While this propulsion concept involves two different schemes, i.e. the external field method and the internal duct-type method, the current analysis focuses on the internal thruster scheme due to the space limitations and speed considerations. The theories of magnetohydrodynamic (MHD) pump jet propulsion are discussed. A so-called 'dual control volume' analysis to model the MHD thruster, and calculations of vehicle velocity and power efficiency are presented. (ii) sea water conductivity enhancement - this work discusses the mechanisms of enhancing the electric conductivity of sea water. The direct impact of conductivity enhancement of sea water is the improvement of propulsion performances of marine vehicles that use the magnetohydrodynamic thrusts of sea water. The performance improvement can be in energy efficiency or in vehicle speed. Injection of strong electrolytes (acids or bases) into the main sea water flow in the MHD channel appeared to be the most logical way of achieving the purpose.

DESCRIPTORS: (U) *ELECTROLYTES, *JET PROPULSION, *MAGNETOHYDRODYNAMICS, *ELECTRIC PROPULSION, *SEA WATER, *UNDERWATER PROPULSION, ACIDS, CHANNELS, COMPUTATIONS, CURRENT DENSITY, EFFICIENCY, ELECTRICAL CONDUCTIVITY, LORENTZ FORCE, MARINE TRANSPORTATION, OPTIMIZATION, PERFORMANCE(ENGINEERING), PUMPS

IDENTIFIERS: (U) *MAGNETOHYDRODYNAMIC PROPULSION, MAGNETOHYDRODYNAMIC PUMPS, *SEA WATER PROPULSION.

Products and Services Order Form

MAIL Orders:
DTIC-BRR
Defense Technical Information Center
8725 John J. Kingman Rd., Ste 0944
Ft. Belvoir, VA 22060-6218

CALL-IN Orders:
DTIC-BRR
Defense Technical Information Center
(703) 767-8274/(DSN) 427-8274
1-800-225-DTIC (3842)
(Menu selection 1, Option 1)

FAX Orders:
DTIC-BRR
Defense Technical Information Center
(703) 767-9070/(DSN) 427-9070

INTERNET Orders:
msorders@dtic.mil
or
www.dtic.mil/dtic/docorderform.html

Requesting Organization Information

User Code ___|___|___|___|___|___|___

Organization ______________________________

Point of Contact ______________________________

Phone Number ______________________________

Method of Payment
Note: All Credit Card Types Must Be Preregistered

[] Deposit Account Number ___|___|___|___|___|___-___|___

[] VISA [] MasterCard [] American Express

Account Number ______________________________

Cardholder's Name ______________________________

Expiration Date ______________________________

DTIC does not accept cash, checks, or COD.

Service Codes

R - Regular Service
Priority Services (Must be called in or faxed)
P - Picked Up Next Business Day ($10.00 surcharge/document)
M - Mailed Next Business Day
E - Express - Mailed Next Business Day, Guaranteed Delivery in Two Business Days ($20.00 surcharge/document)

Document Orders

Service Code	AD Number	Quantity Hard Copy	Quantity Microfiche
	/JAA		
	/JAA		
	/JAA		
	/JAA		
	/JAA		
	/JAA		
	/JAA		
	/JAA		
	/JAA		
	/JAA		
	/JAA		
	/JAA		
	/JAA		
	/JAA		
	/JAA		